THE UNIVERSITY of ADELAIDE

Climate, humans, fire and megafauna – key drivers of Australian subtropical vegetation change

Haidee R. Cadd

Department of Earth Sciences

School of Physical Sciences

The University of Adelaide

October 2019

Table of Contents

Abstract

The timing and cause of megafauna extinctions across Australian, and indeed around the world, have been strongly debated particularly since Martin (1967) first implicated human agency as a major factor in megafauna disappearances. The cause of the demise of the megafauna has been the focus of many studies, yet no work to date has developed independent environmental and climate reconstructions from a single Australian location in relation to megafauna extinctions. Sedimentary records from wetlands provide a particularly powerful archive to examine terrestrial ecosystem change in response to internal and external drivers across a variety of spatial and temporal scales. The presence of coprophilous fungi spores, such as *Sporormiella*, preserved in wetland sediments can indicate the local presence of large herbivorous, including extinct megafauna. Records of megafauna presence can then be coupled with palaeoecological and palaeoclimatological proxies to disentangle the influence of climate on terrestrial ecosystem change and the timing of megafauna disappearance. Sedimentary records that extend beyond the Holocene in Australia are rare. Rarer still are long, continuous, high-resolution records that extend beyond Marine Isotope Stage 3 (MIS3; 57 – 29 ka), a period of substantial significance in Australia that encompasses human arrival and megafauna extinctions.

In this thesis I integrate a range of proxies from an 80,000 year old, well-dated, continuous sedimentary sequence from Welsby Lagoon, North Stradbroke Island to investigate the climate and environmental variability of subtropical eastern Australia from MIS4 to present. In this thesis I present, for the first time at a single location, records of inferred megafauna presence, local fire occurrence, vegetation change and independent local climate variability. Understanding the development of the wetland system and identification of changes in depositional environment at ca. 28 ka provide a robust basis for interpretation of proxies.

During MIS4 and the Holocene fire is an important component of the surrounding landscape and drives vegetation change, with a more limited influence during MIS3 and MIS2. The largest changes in the vegetation around Welsby Lagoon occur between 55 – 40 ka, in the absence of frequent fire and coincident with the timing of widespread human migration and megafauna extinction. The shifts in vegetation during this period are predominantly driven by changes in climate, as inferred from the $\delta^{13}C$ of bulk sediment and the $\delta^{18}O$ of aquatic cellulose. The climate of this period displays a high level of variability as well as a shift to drier climates at ca. 54 and again at 43 ka. In addition to driving changes in vegetation dynamics, *Sporormiella* disappeared from the record at this time, during a shift to drier climate conditions.

Within chronological uncertainty, the changes in vegetation composition and hydroclimate at ca. 43 ka at Welsby Lagoon are concurrent with abrupt changes in the Darling River region and central Australia as well as five vegetation records from across the central and eastern Australia. The data suggest that climatic change was major contributor to megafauna and vegetation change during Marine Isotope Stage 3.

Declaration

I certify that this work contains no material which has been accepted for the award of any other degree or diploma in my name, in any university or other tertiary institution and, to the best of my knowledge and belief, contains no material previously published or written by another person, except where due reference has been made in the text. In addition, I certify that no part of this work will, in the future, be used in a submission in my name, for any other degree or diploma in any university or other tertiary institution without the prior approval of the University of Adelaide and where applicable, any partner institution responsible for the joint-award of this degree.

I acknowledge that copyright of published works contained within this thesis resides with the copyright holder(s) of those works.

I also give permission for the digital version of my thesis to be made available on the web, via the University's digital research repository, the Library Search and also through web search engines, unless permission has been granted by the University to restrict access for a period of time.

I acknowledge the support I have received for my research through the provision of an Australian Government Research Training Program Scholarship.

Haidee Cadd DATE: 26/09/2019

Acknowledgements

First and foremost I would sincerely like to thank my supervisors John Tibby and Jon Tyler for all of their support over the past 4 years, both academically and personally. Your faith in me and my work has encouraged me to continually strive to achieve more and push my academic boundaries. Your insights and experience has been paramount to all that I have been able to achieve. The research environment you have created is one of collaboration, excellence and fun and I could not think of a better place to have undertaken my PhD and I sincerely thank you for that. You have provided me with so many wonderful opportunities during my time at Adelaide and I feel lucky to have gained such great colleagues.

To the rest of my academic family, Cameron Barr, Melanie Leng, Cesca McInerney, Jeff Baldock, Jon Marshall, Glenn McGregor, Cam Shultz and Michela Mariani, working with you has always been a pleasure and I value both your academic assistance and friendship. This journey, the field trips and the conferences were made better by your presence and I wouldn't have wished to share it with a better group of people.

To Jack, Sheree and Briony, your friendship has meant a lot to me over the past 4 years. Moving to a new city was daunting, but meeting each of you has made the journey worthwhile. I appreciate your unwavering support and friendship, keeping me grounded and helping me through when times got tough.

To my office mates and the Mawson PhD cohort, you made coming to work each day a pleasure. The Friday beers, the morning teas and the BBQs were always a relief from the daily grind and made the past 4 years a (mostly) pleasant experience.

I've been granted many amazing opportunities during this PhD and would like to thank the generous funding I have received to help me present my work at international conferences and pursue my research. Much of the research in this study was funded by Australian Research Council project DP150103875. I am grateful to the Walter Dorothy Duncan Trust, CRC LEME, the Alderman-Kleeman Award, Australian Quaternary Association (AQUA), the Southern Hemisphere Last Glacial Maximum working group (SHeMAX) and the Southern Hemisphere Assessment of Palaeoenvironments working group (SHAPE) for providing funding.

Publications arising from this PhD research

Journal articles

Cadd, H.R., Tibby, J., Barr, C., Tyler, J. Unger, L., Leng, M.J., Marshall, J.C., McGregor, G., Lewis, R., Arnold, L.J., Lewis, T., Baldock, J. (2018). Development of a southern hemisphere subtropical wetland (Welsby Lagoon, south-east Queensland, Australia) through the last glacial cycle. *Quaternary Science Reviews*. 202: 53-65

Cadd, H.R., Tyler, J., Tibby, J., Baldock, J., Hawke, B., Barr, C., Leng, M. (2020) The potential for rapid determination of charcoal from wetland sediments using infrared spectroscopy. *Palaeogeography, Palaeoclimatology, Palaeoecology*. 542: 1-13

Other journal articles produced during PhD

Cadd, HR., Fletcher, MS., Mariani, M., Heijnis, H., Gadd, P. (2019). The role of fire frequency, species composition and topography in determining rainforest recovery: insights from Tasmania. *Journal of Quaternary Science*. 1-8

Tibby, J., Barr, C., Marshall, J.C., Richards, J., Perna, C., Fluin, J., Cadd, H.R. (2019). Assessing the Relative Impacts of Land-use Change and River Regulation on Burdekin River (Australia) Floodplain Wetlands. *Aquatic Conservation: Marine and Freshwater Ecosystems*. 1-14

Conference abstracts

Cadd, HR., Tyler, J., Tibby., J., Barr. C., Leng. M.J., Baldock, J., Lewis, R., Arnold, L., Unger, L., Marshall, J., McGregor, G., Yokoyama, Y., (2019). Climate and vegetation change during Australia's most recent mass extinction. *International Quaternary Association, Dublin, Ireland*

Cadd, HR., Tyler, J., Tibby., J., Barr. C., Leng. M.J., Baldock, J., Lewis, R., Arnold, L., Unger, L., Marshall, J., McGregor, G., Yokoyama, Y., (2019). Climate and vegetation change during Australia's most recent mass extinction. *Palaeo in the Pub, Adelaide, Australia*

Cadd, HR., Tyler, J., Tibby., J., Barr. C., Leng. M.J., Baldock, J., Lewis, R., Arnold, L., Unger, L., Marshall, J., McGregor, G., Yokoyama, Y., (2018). Millennial scale climate and environmental change from Welsby Lagoon, North Stradbroke Island for the past 80,000 years. *Australasian Quaternary Association Biennial Conference, Canberra, Australia*

Cadd, HR., Petherick, L., Tyler, J., Herbert, A., Cohen, T., Barrows, T., Kemp, J., Fulop, R., Sniderman, K., Shulmeister, J., Knight, J. (2018) SHeMax: A regional perspective on the timing of the Last Glacial Maximum in Australia . *Australasian Quaternary Association Biennial Conference, Canberra, Australia*

Cadd, HR., Tyler, J., Tibby., J., Barr. C., Leng. M.J., Baldock, J., Lewis, R., Arnold, L., Unger, L., Marshall, J., McGregor, G., Yokoyama, Y., (2018). A multi-proxy assessment of millennial scale climate variability and environmental change for the past 80,000 years from Welsby Lagoon, North Stradbroke Island. *SHeMax workshop, North Stradbroke Island, Australia.*

Cadd, HR., Tyler, J., Tibby., J., Barr. C., Leng. M.J., Baldock, J., (2018). A multi-proxy assessment of millennial scale climate variability and environmental change in sub-tropical Australia. *GSA Earth Sciences Student Symposium, South Australia, Adelaide.*

Cadd, HR., Tyler, J., Tibby., J., Barr. C., Leng. M.J., Baldock, J., (2017). 100,000 years of environmental change in subtropical Australia, *Past Global Changes Open Science Meeting, Zaragoza, Spain*.

Cadd, HR, Tibby, J., Tyler, J. & Barr, C. (2016) Using Infrared spectroscopy to infer organic carbon, nitrogen and charcoal from sediments. *Australasian Quaternary Association Biennial Conference, Auckland.*

1

Introduction and study site

1 Introduction

The last glacial cycle (defined here as 125,000 calendar years before 1950; 125 ka BP – before present) is a significant period in Australia's environmental history, encompassing the arrival of humans and the extinction of the Australian megafauna (Roberts et al., 2001; Rodríguez-Rey et al., 2016; Clarkson et al., 2017; Tobler et al., 2017). Knowledge of the environment and climates of this most recent geological time period provide context for modern Australian ecological distributions and aid in predictions of future change. The understanding of this period in Australia is limited by the scarcity of continuous terrestrial archives that extend beyond Marine isotope stage 3 (MIS3; ~57-29 ka). Currently only two continuous records of environmental change exist from mainland Australia, Caledonia Fen (Kershaw et al., 2007b; Johnson et al., 2016), a ca. 140 ka record from temperate southern Australia and Lynchs Crater (Turney et al., 2004; Kershaw et al., 2007a; Rule et al., 2012), a ca. 230 ka record from the northern wet tropic. These sedimentary sequences that do extend into MIS3 and 4 typically have poor chronological constraints, restricting the ability to independently examine spatial variations in the timing of environmental and climate changes. This hinders understanding of climate and ecological variability, both spatially and temporally, during one of the most significant periods in Australia's environmental history. Developing high-resolution reconstructions of ecological and climate change throughout the last glacial cycle, with high-precision chronologies, is essential to identifying millennial to centennial scale changes and long term trends in the Australian environment.

Wetland sediments are a particularly powerful archive that can provide long-term information about terrestrial ecosystems at a resolution that is typically an order of magnitude greater than marine archives (Birks & Birks, 2006). Wetlands represent a diverse range of permanent aquatic, palustrine and terrestrial habitats (Junk et al., 2006). Their sedimentary records enable examination of long-term ecological data across a broad spatial and temporal range, enabling reconstructions of climate and ecosystem dynamics (i.e. vegetation and disturbance) at scales from local to global and from annual to millennial (Seppä & Bennett, 2003; Willis & Birks, 2006; Lindbladh et al., 2013). This thesis

presents a palaeoecological and geochemical study of the sediments of Welsby Lagoon, a wetland in subtropical Australia with a sediment sequence that extends through the last glacial cycle (Figure 1B). This thesis aims to improve understanding of climate and environmental change through the last glacial cycle and provides a critical spatial link between the limited number of records extending through this time period, primarily from the northern wet tropics and southern temperate zones (Figure 1; Johnson et al., 2016; Kershaw et al., 2007a, 2007b; Rule et al., 2012; Turney et al., 2004).

1.1. Study Site

North Stradbroke Island is second largest sand island in the world (275 km²) and the southernmost extent of the Great Sandy Region, located offshore of the city of Brisbane, Queensland. The Great Sandy Region is composed of siliceous sands (Pye, 1993; Patton et al., 2019) forming a series of northwest orientated parabolic sand ridges along the east coast of Queensland (Figure 1B). Rocky outcrops rise from a platform of submerged bedrock that acts as an anchor for the Quaternary sand dunes (Leach, 2011; Patton et al., 2019). The dune fields were formed during the Pleistocene and Holocene with the oldest dunes located on the western side of the field and Holocene to modern formations occurring on the eastern side (Walker et al., 2018; Patton et al., 2019). Soils across the sand mass are acidic, heavily leached humic and podzolic soils (Thompson, 1981). Soil depth varies in association with dune age, with huge podzols forming in the oldest Cooloola and Awinya dune morphosequences (Thompson, 1981; Walker et al., 2018; Patton et al., 2019).

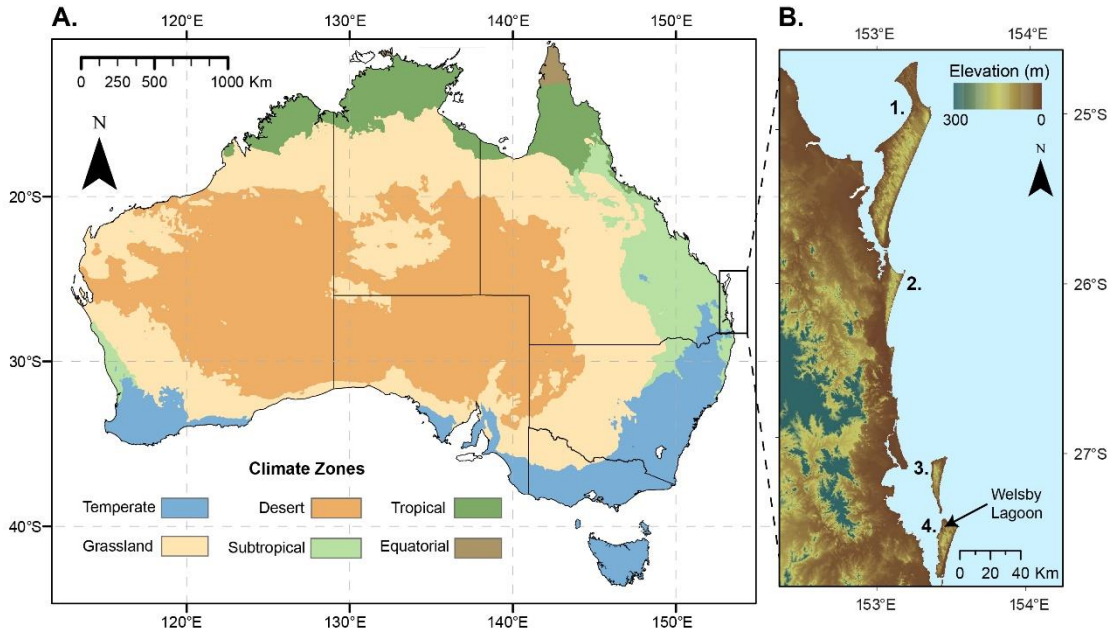

Figure 1. A. Map of Australia showing the major Köppen climate zones (BOM, 2018). B. The Great Sandy Region of southeast Queensland with the four major areas marked; 1. Fraser Island, 2. Cooloola sand mass, 3. Moreton Island, 4. North Stradbroke Island. Welsby Lagoon is indicated on the northern end of NSI. Shading indicates elevation across the region (modified from Gallant et al. 2011).

Vegetation dynamics across the Great Sandy Region are viewed as an important example of successional dynamics across developing soil sequences (Walker et al., 1981, 1983). Early successional vegetation on sand dunes <120,000 years old is typically composed of fast growing species with large quantities of litter that promote decomposition and nutrient turnover (Walker et al., 1981, 2010; Wardle, 2005). As succession succeeds on dunes >120,000 years old, tall closed forests with high vegetation biomass increase, with a relative abundance of available nutrients (Walker et al., 1981, 2010). On dunes >300,000 years old, inaccessible organic matter accumulates in the soil, nutrient availability decreases and nutrient cycling through the ecosystem becomes slower and restricted (Walker et al., 1981; Chen et al., 2015; Bokhorst et al., 2017). The restriction of nutrients results in the development of a retrogressive ecosystem, characterised by slow decomposition rates, reduced vegetation stature, biomass and productivity (Chen et al., 2015; Bokhorst et al., 2017). To fully understand how successional dynamics influence current distributions, composition and structure of vegetation, requires knowledge of vegetation and disturbance changes through time.

The Great Sandy Region provides a perfect opportunity to test the classical theories of successional dynamics due to the high density of wetlands and lakes across the region. The many freshwater lakes and wetlands can be classified as either window lakes (a surface expression of the regional water table) or perched lakes (confined by impermeable layers disconnected from the regional water table) (Figure 2). The accumulation of organic sediments in many of these wetland sites extends almost to the age of the hosting dunes (Tibby et al., 2017).

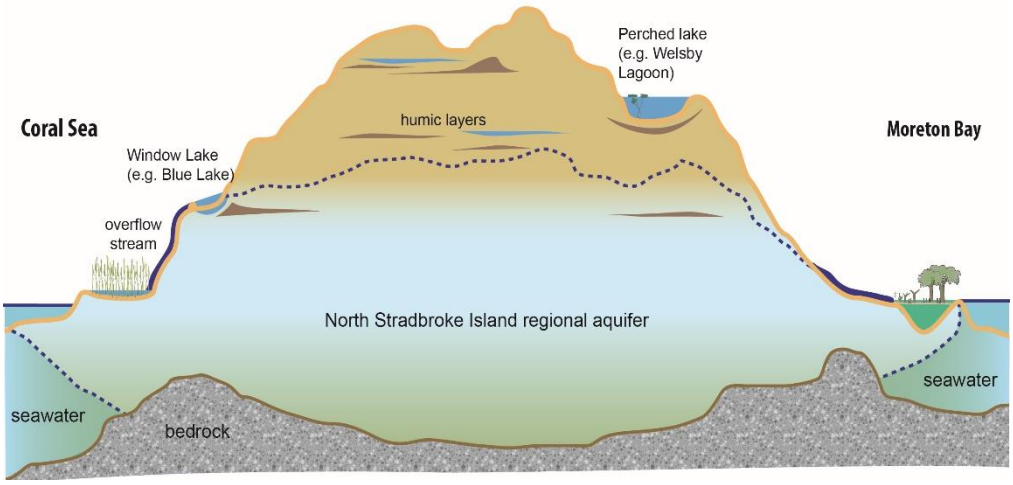

Figure 2. Schematic of lake type and formation common on North Stradbroke Island (modified after McGregor, G. pers.comm).

Welsby Lagoon (27°26'12"S, 153°26'56"E; 29 m.a.s.l) is an ideal location for palaeoenvironmental and palaeoclimatological studies. Welsby Lagoon is a perched, permanent wetland, with a variable water depth between 0 – 1.5m situated at the northwest end of NSI, within the Yankee Jack dune sequence. Welsby Lagoon is an internally draining, closed wetland system, with no inflowing streams. The wetland (0.19 km^2) reflects the perched freshwater aquifer of the Welsby Lagoon catchment, with a

drainage basin of 5.38 km² (~2% of the island; Leach, 2011). The basal sands of the Welsby Lagoon sedimentary sequence have been dated close to the age of emplacement of the Yankee Jack dune system at ca. 130 ka (Tibby et al. 2017; Lewis et al. Accepted).

1.1.1. Existing Chronology

The chronology of the Welsby Lagoon sediment sequence has been developed by Lewis et al. (Accepted). A total of 21 single-grain OSL and 7 macrofossil radiocarbon ages were used to develop a comprehensive Bayesian age-depth model for the composite sediment sequences (WEL 15-2 and WEL 15-1) using OxCal (Lewis et al., Accepted). For further information regarding chronological methods and age-depth modelling the reader is referred to Lewis et al. (Accepted).

1.2. Australian Climate

There is a broad range of climate zones in Australia, from the arid centre to the equatorial north (Figure 1). The highly variable climates of Australia are influenced by several modes of ocean-atmosphere variability, including the El Nino-Southern Oscillation (ENSO), the Southern Annular Mode (SAM), the Indian Ocean Dipole (IOD) and the Inter-decadal Pacific Oscillation (IPO), which in turn affect the positions of the Inter Tropical Convergence Zone (ITCZ) and the subtropical ridge over Australia (Figure 2; King et al., 2014; Marshall, 2003; McGee et al., 2014; Risbey et al., 2009; Ummenhofer et al., 2011). The relative influence of these processes on the variability of Australian rainfall may vary over daily, seasonal, inter-annual and decadal time scales (Kiem, 2004; King et al., 2014) and according to interactions between modes of variability (Gallant et al., 2013).

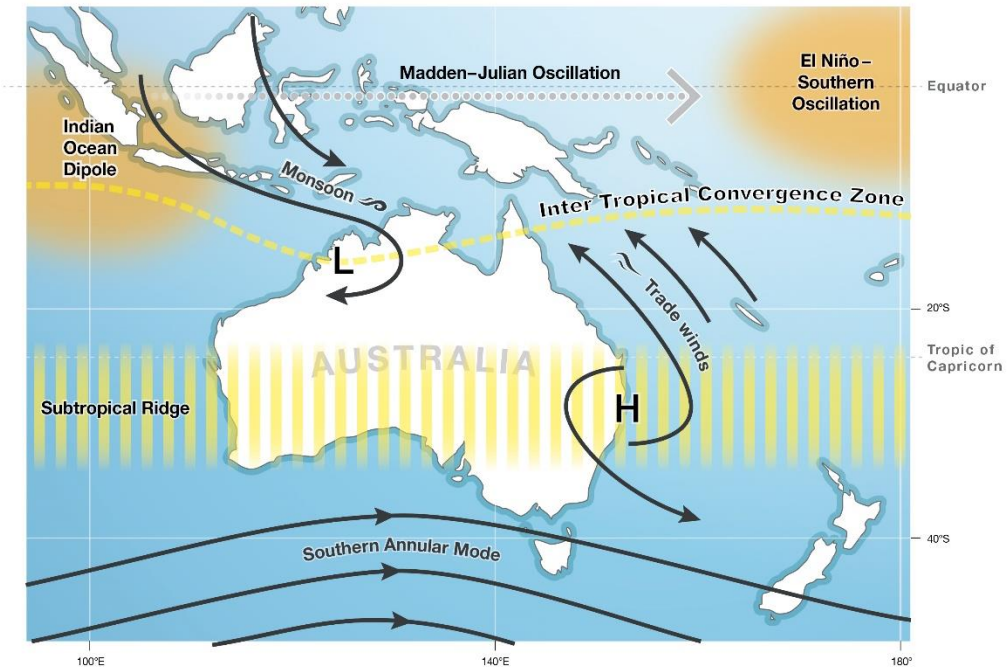

Figure 3. Australian climate drivers. Source; Bureau of Meteorology (2018)

Climate variability through the last glacial cycle in Australia is relatively poorly understood. The substantial influence of the large range of remote climate drivers and the lack of palaeoclimate records of sufficient resolution inhibits examination of key climatic variables, namely rainfall and temperature, across a variety of regions and time periods (Dixon et al., 2017). Importantly, understanding of how past climate change has impacted upon ecosystem dynamics, including fire regimes, has remained elusive due to the lack of palaeoecological records which are coupled with an independent record of local palaeoclimate (Lynch et al., 2007). This problem becomes exacerbated when attempting to test the influence of climate on ecosystem dynamics beyond the Holocene, particularly for one of the biggest controversies about Australia's environment: the extinction of the Australian megafauna ca. 45 ka (Roberts et al., 2001). To accurately constrain the role of climate in the extinction megafauna requires independent and localised records of climate, coupled with information on both catchment vegetation and local megafauna presence.

1.3. Fire and vegetation dynamics

Fire, after climate, is the single greatest control on global vegetation patterns (Bond et al., 2005; Bowman et al., 2009). Fire reduces plant biomass, and depending on the frequency and severity, can result in vegetation shifts from forests to shrub lands to grasslands (Bond et al., 2005). Australia is the most fire prone continent in the world and fire has played an integral role in shaping vegetation patterns since the Miocene (Kershaw et al., 2002; Bond et al., 2005; Keeley et al., 2011). The proliferation of the highly fire-adapted species occurred as a response to an increase in landscape fire in association with drying climates and soil nutrient depletion (Bowman & Murphy, 2010). The most successful fire adapted genus, *Eucalyptus*, occurs across all climate zones of Australia and is composed of more than 800 species. The prolific vegetative recovery via epicormic buds, high incidence of serotiny and germination by heat and smoke, enable *Eucalyptus* species not only to survive fire, but to outcompete fire-sensitive species following fire (Williams & Woinarski, 1997; Bowman & Murphy, 2010; Cadd et al., 2019). Specific adaptations to fire, combined in some instance with flammable and fire promoting foliage, have resulting in the expansion of fire adapted species at the expense of fire-sensitive species over much of the Australian continent (Williams & Woinarski, 1997; Bowman, 2000; Kershaw et al., 2002).

Fire activity is strongly influenced by climate variability (Figure 4). Fire weather, relative humidity, temperature and wind speed, governs the probability of fire occurrence on daily to weekly timescales (Cary et al., 2006). Climate, on monthly to decadal timescales, fuel load and topography predict how fire behaves across the landscape (Cary et al., 2006; Bowman & Murphy, 2010; Wood et al., 2011; Cadd et al., 2019). The spread and frequency of fire is also influenced by the vegetation type. The rapid accumulation of fine fuels and litter in grassy ecosystems promotes the frequent occurrence of fire, while dense rainforest rarely supports fire due to rapid decomposition of litter and maintenance of moist fuels by humid microclimates (Bowman et al., 2009; Pausas & Paula, 2012; Pausas & Ribeiro, 2013).

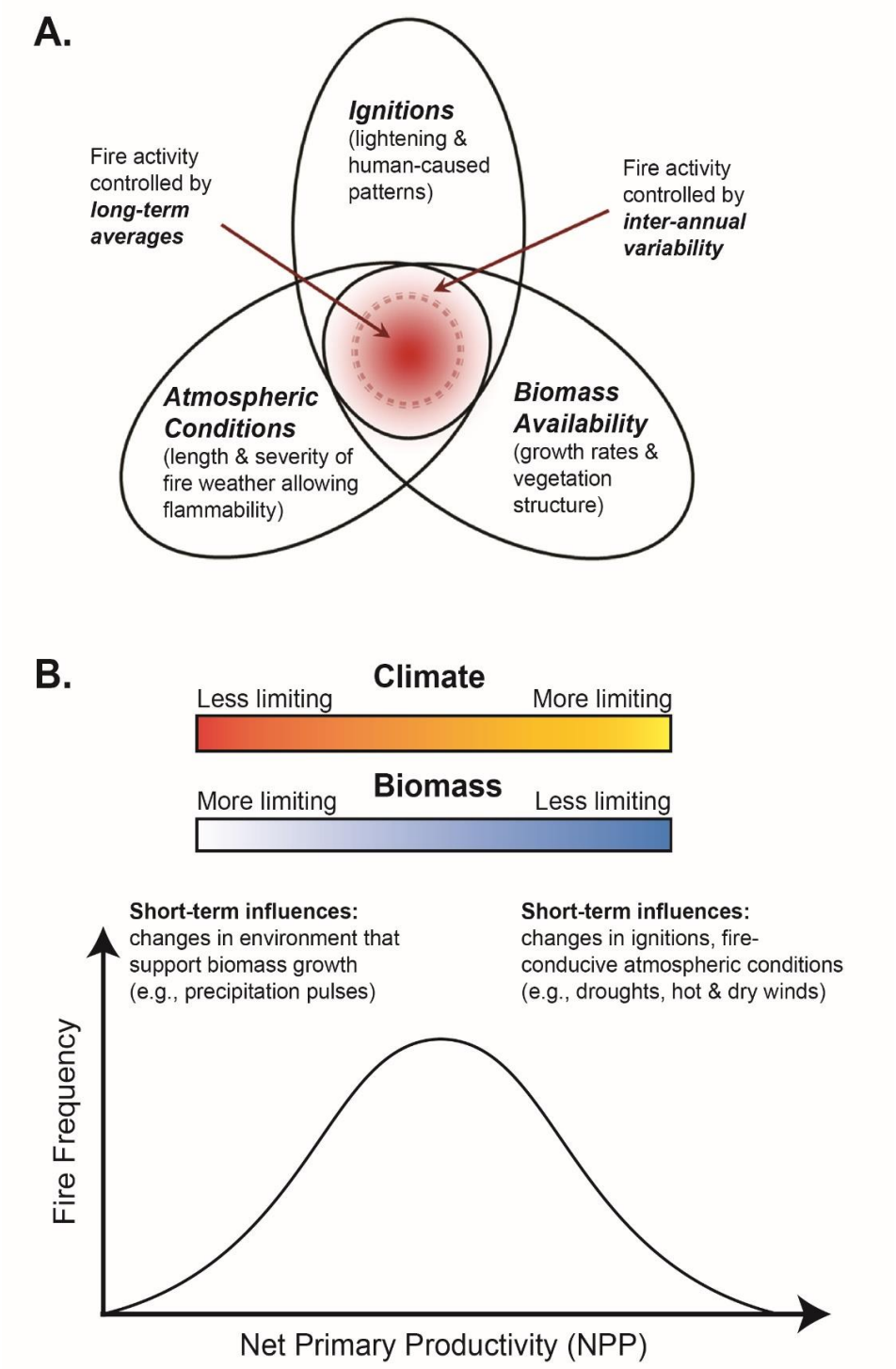

Figure 4. Conceptual diagram of controls on fire activity adapted from Moritz et al. (2012). **A**. Reflects the three main controls on fire activity – ignititions, vegetation characteristics and fire weather – across different spatial and temporal scales. The dark shading in the centre represents core probability of fire activity controlled by long-term environmental conditions. The light shading of the out circle represents additional variability controlled by short-term environmental conditions. **B**. Areas characterised by fuel limitation are likely to experience increased fire in response to precipitation increases, while areas characterised by abundant biomass will experience increased fire due to ignition pulses and episodic drought conditions.

Fire activity over longer timescales is influenced by annual to inter-annual climate variability (Mariani and Fletcher, 2016). In general, moist rainforests are susceptible to severe fires only after extended periods of precipitation deficit, while fire activity and severity increases in arid areas in response to build-up of fuels after wet periods (Cochrane, 2003; Pausas & Ribeiro, 2013).

The pattern of timing, intensity, size, frequency and severity of fire occurrence is collectively classified as the fire regime (Figure 4; Bond et al., 2005; Bowman et al., 2009). The infrequent nature of fire in many ecosystems, with fire return intervals in the order of centuries to millennia, inhibits the use of modern ecology to accurately characterise natural fire regimes in many ecosystems (Cochrane, 2003; Haberle et al., 2006; Lindbladh et al., 2013; Fletcher et al., 2014). Fire activity is projected to increase under global climate change, and the ability to characterise baseline conditions and understand the full variability of fire regimes is critical to establish adequate management practices (Moritz et al., 2012; Bowman et al., 2017). In addition, the legacy of changing fire regimes in influencing vegetation dynamics through time requires data spanning time periods considerably longer than observational records.

Palaeoecology can provide data spanning a sufficient temporal extent to understand the full range of fire regimes and to determine the climatic controls on fire over centuries to millennia (Lynch et al., 2007). Sedimentary charcoal is a common proxy used to determine past fire occurrence. Charcoal is produced by the incomplete combustion of organic material and subsequent deposition in wetland sediments provides evidence for past fire activity (Whitlock & Larsen, 2001; Mooney & Tinner, 2011). The ability for charcoal particles to be carried aloft and transported large distance means that charcoal source area can range from local to regional scales. Macroscopic charcoal (particles >125 μm) s with a high volume to surface area ratio tend to travel shorter distances from source fires (Whitlock & Larsen, 2001; Peters & Higuera, 2007). Whilst this size determined measure of local fire provide some understanding of local fire occurrence, variations in charcoal size and morphology are also closely linked to source vegetation type, fire intensity and subsequent transport mechanisms (Crawford & Belcher, 2014, 2016). Understanding the different components of sedimentary charcoal and determining the source of sedimentary charcoal variations is necessary to elucidate a more thorough understand of past fire activity in response to changes in vegetation type, climate and fire intensity.

1.4. Megafauna

The term megafauna generally refers to species weighing >45 kg and includes species from all the major animal groups (Martin & Klein, 1989; Barnosky, 2008). Megafauna were a dominant component of Pleistocene faunal communities, with a diverse range of megafauna species inhabiting all continents except Antarctica (Barnosky et al., 2004). Global extinctions of the Pleistocene megafauna occur during distinct time periods around the world. European, Asian and African megafauna suffered a steady decline from approximately 50 ka (Stuart, 1999), Australian megafauna had seemingly disappeared

from the fossil record by ~45 ka (Roberts et al., 2001; Rodríguez-Rey et al., 2016), while the megafauna species of the Americas survived until ~10 ka (Haynes, 2009; Owen-Smith, 2013). The extended extinction windows of Eurasia (consistent extinctions from 50 – 3 ka) and Africa (50 – 10 ka) and the rapid cluster of extinctions in the Americas (11.5 ka – 10 ka) and Australia (51 – 40 ka) have led to a variety of causal drivers being implicated on each continent (Johnson et al., 2016; Lorenzen et al., 2011; Miller et al., 2016; Stuart, 1999; van der Kaars et al., 2017). A global review of evidence by Barnosky (2004) concluded that humans were the primary driver of extinctions in North America and Australia, while climate was the main driver of extinctions in Eurasia. Subsequent analysis by Sandom et al. (2014) reported that the severity of megafauna extinctions across the globe is closely tied to the palaeo-biogeography of modern *Homo sapiens*. They conclude the climates of Australia, South America and areas of North America were relatively stable during the periods of highest extinctions, implying the arrival of *Homo sapiens* instigated the demise of the megafauna in these regions. The milder and more extended extinction windows of Eurasia and Africa were also predominantly driven by *Homo sapiens*, but the patterns of extinction can be attributed to the length of megafauna-hominin co-occurrence and combined extinction drivers in these regions (Sandom et al., 2014; Cooper et al., 2015).

The causes of the extinction of megafauna have been no more contested than in Australia. Since Martin (1963) implicated human agency in the disappearance of the megafauna, the debate has centred around two competing hypotheses; that the megafauna were driven to extinction by early human populations, or that changing climate resulted in conditions inhospitable for megafauna survival. The climate change hypothesis invokes increasing climate variability and aridity during the late Pleistocene as a cause for widespread megafauna population declines and ultimate extinction (Wroe & Field, 2006; Webb & Webb, 2008; Field & Wroe, 2012; Wroe et al., 2013; Cohen et al., 2015a). The human mediated hypothesis states hunting and habitat modification, particularly through the use of fire, by *Homo sapiens* drove megafauna populations to extinction (Sandom et al., 2014; Bartlett et al., 2016; Miller et al., 2016b; Saltré et al., 2016; van der Kaars et al., 2017). The role of climate has been dismissed as irrelevant or unimportant based on the relatively benign climate trends of MIS3 identified from Antarctica and Greenland (Wroe & Field, 2006; Wroe et al., 2013). The persistence of many species of megafauna through the oscillating glacial-interglacial cycles of the late Quaternary has been suggested to demonstrate their ability to withstand substantial climate changes (Miller, 2005; Brook et al., 2013; Sandom et al., 2014; Johnson et al., 2016b). Whilst there is limited evidence for substantial change in Antarctic ice volume during MIS3 (Jouzel et al., 2007; Wolff et al., 2010; Laepple et al., 2011), there are very few high quality palaeoclimate records from across Australia at this time (Kemp et al., 2019). The records that do exist during this period display a high level of spatial variability (Kemp et al., 2019), with evidence for substantial declines in freshwater availability evident across much of the continent (Bowler et al., 2003; Cohen et al., 2011, 2015a)

In addition to understanding the drivers of megafauna extinction, there is very little direct evidence to understand how the removal of a range of giant herbivores may have resulted

in changing ecosystem dynamics (Barnosky et al., 2016; Johnson et al., 2016; Rule et al., 2012). Impacts of megafauna on ecosystem structure can range from their direct influence on physical vegetation structure (Bakker et al., 2016), changes from top-down to bottom up or fire driven ecosystem regulation (Burney et al., 2003; Robinson et al., 2005; Gill et al., 2009, 2012), and spatial variation in landscape structure (Hopcraft et al., 2010; Bakker et al., 2016; Malhi et al., 2016). Longer term changes in vegetation composition, diversity and distribution (Guimarães et al., 2008; Bakker et al., 2016) and nutrient cycling (Doughty et al., 2013) may occur for centuries or millennia after megafauna extinctions (Barnosky et al., 2016). Despite the increased understanding of ecological services provided by megafauna in Eurasia, Africa and the Americas, relatively little is known about the role of Australia's megafauna species in ecosystem dynamics. By incorporating records of megafauna abundances with changes in fire frequency and vegetation composition and structure, we can examine how the removal of megafauna influenced ecosystem structure and function (Johnson et al., 2016; Johnson et al., 2015; Rule et al., 2012).

The preservation of certain species of coprophilous fungi spores, such as *Sporormiella*, in lake sediments has become a widely used proxy for the local presence of large herbivorous animals (Davis & Shafer, 2006; Baker et al., 2013; Johnson et al., 2015; Dodson & Field, 2018). *Sporormiella* is a coprophilous fungi that is ingested by large herbivores and germinate in their dung (Baker et al., 2013). The fruiting bodies produced within the dung release their spores into the environment to recommence the life cycle (Baker et al., 2013). The thick organic-walled fungal spores of *Sporormiella* preserve well in sedimentary archives and alongside their limited dispersal abilities (<2 m) provide a reliable indicator of the local presence and distribution of large herbivores (Davis & Shafer, 2006). This proxy for mega-herbivore occurrence can be directly compared to environmental proxies from the same sediment core, allowing the sequence of ecological changes both preceding and following megafauna extinctions to be examined.

The limited number of terrestrial archives of climate and environmental change extending into the last glacial cycle have made it difficult to create accurate chronologies of species loss relative to major climatic or environmental changes (Rodríguez-Rey et al., 2016). This thesis aims to increase understanding of climate and environmental change from MIS4 to present from subtropical eastern Australia. This subtropical record provides a critical link between the climate and ecological trends reported in northern wet tropics and southern temperate zone (Johnson et al., 2016; Kershaw et al., 2007a, 2007b; Rule et al., 2012; Turney et al., 2004).

2 Thesis outline

This PhD thesis is focussed on developing high-resolution reconstructions of climate and environmental variability throughout the last glacial cycle from Welsby Lagoon, North Stradbroke Island. The independent environmental and climate records developed from

Welsby Lagoon permits robust assessments of centennial to millennial scale climate and ecological variability through the last glacial cycle.

Chapter 2

In order to determine how wetland systems responded to climatic and environmental changes, we first need to understand how their depositional environment changed through time. The second chapter of this thesis details a model for the development of the Welsby Lagoon wetland that documents its transition from open water lacustrine conditions to a shallow palustrine state (Published as Cadd et al. 2018, *Quaternary Science Reviews*). This chapter incorporates a series of proxies; including photosynthetic pigments, plant macrofossils, aquatic pollen, carbon and nitrogen isotopes and sedimentary lignin to identify the source of sedimentary carbon and the changing nature of the wetland.

This foundational study forms the basis for ongoing work which includes the exploration of centennial scale climate and environmental variability (Chapters 3 – 6 this thesis) and the application of novel climate proxies (Barr et al., in prep).

Chapter 3

The third chapter explores the use of infrared spectroscopy for the determination of charcoal content from lacustrine sediments. The charcoal content of lacustrine sediments is important for understanding past fire regimes, as well as the role recalcitrant carbon plays in the global carbon cycle. Methodologies commonly used to determine charcoal concentrations of sediments have limitations in their ability to quantify the full charcoal particle size continuum from macroscopic charcoal to sub-micron particles and degradation products. Infrared spectroscopy provides a rapid, non-destructive and cost effective method for simultaneously determining charcoal concentration alongside multiple sediment properties.

Partial least squares regression models are developed to predict the charcoal content and total organic carbon using infrared spectroscopic analysis of Welsby Lagoon sediments. Two measures of charcoal content were used as targets for model development: traditional palaeoecological charcoal area measures ($cm^2\ g^{-1}$) and solid state ^{13}C nuclear magnetic resonance of poly-aryl structures. The study provides encouraging results for using infrared to determine the charcoal content of lacustrine sediment. Future method development incorporating calibration samples from multiple sites could provide a reliable and rapid technique for the investigation of fire histories across a variety of spatial and temporal scales.

Chapter 4

Long-term dynamics of vegetation change in response to climate, fire and succession are important components of understanding modern vegetation composition and distribution. Chapter four details the high-resolution fire and vegetation record developed from Welsby Lagoon from MIS4 to present. The vegetation record shows dynamic

responses to changes in fire regime, with fire driving declines in rainforest taxa and contributing to increases in Asteraceae, Poaceae and Casuarinaceae pollen types throughout the record. Charcoal abundance and fire activity increases during the Holocene, likely in response to higher biomass availability driven by warming and an increase in effective moisture. Notably, a change in the dominant canopy species occurs after ca. 43 ka, a result of the combined increase in fire occurrence, continued leaching of nutrients from the ageing dune system and as a response to a drying climate.

We propose that increased climate variability and fire activity accelerated successional dynamics on the already nutrient poor sand dune systems of NSI. The evolution of the Welsby Lagoon catchment vegetation can be explained by a combination of succession, fire and climate. The combination of factors, including local changes in fire occurrence and climate can help explain the divergent vegetation types found on the same dune units across the Cooloola dune field.

Chapter 5

Understanding Australia's climate during the last glacial period, a key time period in the environmental and cultural history of the continent, is important when considering how climate may have influenced vegetation, fire regimes and the potential influence of climate on the extinction of Australia's megafauna. Chapter 5 of this thesis presents a palaeoclimate reconstruction from Welsby Lagoon using high resolution $\delta^{13}C$ analysis of bulk sediments during MIS4 and MIS3 (80 – 30 ka). Variations in $\delta^{13}C$ occur in concert with orbitally forced Antarctic δD and global CO_2 variation. Superimposed upon the long-term trend are fluctuations in $\delta^{13}C$ which corresponds to local hydroclimate inferred from oxygen isotopes preserved in aquatic cellulose ($\delta^{18}O$ lake water; Barr et al. in prep). These trends resemble the shape and timing of Antarctic Isotope Maxima (AIM) warming events. This finding indicates a link between Pacific climates and the Southern Hemisphere high-latitudes.

Chapter 6

Records such as those from Welsby Lagoon are critical to debates about the relative roles of people, climate and the extinction of megafauna in shaping Australia's environment during the last glacial cycle. The palaeoclimate reconstruction presented in chapter 5 coupled with the high-resolution vegetation and fire records from chapter 4 allows an examination of the relative role of climate in driving changes in vegetation, fire and megafauna abundance, as inferred from *Sporormiella* fungal spores. The timing of disappearance of *Sporormiella* occurs during a shift to drier climates after ca. 55 ka, evident in both $\delta^{13}C$ and $\delta^{18}O$ record from aquatic cellulose (Barr et al. in prep). A shift in vegetation dominance to Casuarinaceae woodland at ca. 43 ka occurs in response to drying climates. The data from Welsby Lagoon are then compared with other Australian records of environmental change through MIS3 to identify whether similar changes occurred synchronously (within age uncertainty) across the continent. A coincident timing of ecosystem changes recorded at several sites, in conjunction with the extinction

of megafauna, occurs during a shift to drier climate across the continent. We therefore concur with previous studies which have concluded that climatic change may have played a role in the extinction of Australian megafauna.

Chapter 7

The final chapter of this thesis provides some concluding statements regarding the current state of research at Welsby Lagoon and the key findings of this thesis. Recommendations for further research are included in this chapter.

References

Baker, A.G., Bhagwat, S.A., & Willis, K.J. (2013) Do dung fungal spores make a good proxy for past distribution of large herbivores? *Quaternary Science Reviews*, **62**, 21–31.

Bakker, E.S., Gill, J.L., Johnson, C.N., Vera, F.W.M., Sandom, C.J., Asner, G.P., & Svenning, J.-C. (2016) Combining paleo-data and modern exclosure experiments to assess the impact of megafauna extinctions on woody vegetation. *Proceedings of the National Academy of Sciences*, **113**, 847–855.

Barnosky, A.D. (2008) Megafauna biomass tradeoff as a driver of Quaternary and future extinctions. *Proceedings of the National Academy of Sciences*, **105**, 11543–11548.

Barnosky, A.D., Koch, P.L., Feranec, R.S., Wing, S.L., & Shaberl, A.B. (2004) Assessing the Causes of Late Pleistocene Extinctions on the Continents. *Science*, **306**, 70–75.

Barnosky, A.D., Lindsey, E.L., Villavicencio, N.A., Bostelmann, E., Hadly, E.A., Wanket, J., & Marshall, C.R. (2016) Variable impact of late-Quaternary megafaunal extinction in causing ecological state shifts in North and South America. *Proceedings of the National Academy of Sciences*, **113**, 856–861.

Barr, C., Cadd, H.R., Tibby, J., Leng, M.J., Tyler, J.J., McInerney, F.A., Henderson, A.C.G., Arnold, L.J., Marshall, J.C., & McGregor, G.B. Hydrological change in subtropical Australia from 80 - 40 ka. .

Bartlett, L.J., Williams, D.R., Prescott, G.W., Balmford, A., Green, R.E., Eriksson, A., Valdes, P.J., Singarayer, J.S., & Manica, A. (2016) Robustness despite uncertainty: Regional climate data reveal the dominant role of humans in explaining global extinctions of Late Quaternary megafauna. *Ecography*, **39**, 152–161.

Birks, H.H. & Birks, H.J.B. (2006) Multi-proxy studies in palaeolimnology. *Vegetation History and Archaeobotany*, **15**, 235–251.

Bokhorst, S., Kardol, P., Bellingham, P.J., Kooyman, R.M., Richardson, S.J., Schmidt, S., & Wardle, D.A. (2017) Responses of communities of soil organisms and plants to soil aging at two contrasting long-term chronosequences. *Soil Biology and Biochemistry*, **106**, 69–79.

Bond, W.J., Woodward, F.I., & Midgley, G.F. (2005) The global distribution of ecosystems in a world without fire. *New Phytologist*, **165**, 525–538.

Bowler, J.M., Johnston, H., Olley, J.M., Prescott, J.R., Roberts, R.G., Shawcross, W., & Spooner, N.A. (2003) New ages for human occupation and climatic change at Lake Mungo, Australia. *Nature*, **421**, 837–840.

Bowman, D.M.J.S. (2000) *Australian Rainforests: Islands of Green in a Land of Fire.* Cambridge University Press, New York.

Bowman, D.M.J.S., Balch, J.K., Artaxo, P., et al. (2009) Fire in the Earth System. *Science*, **324**, 481–484.

Bowman, D.M.J.S. & Murphy, B.P. (2010) Fire and biodiversity. *Conservation Biology for All* (ed. by N.S. Sodhi and P.R. Ehrlich), pp. 163–180. Oxford University Press, Oxford.

Bowman, D.M.J.S., Williamson, G.J., Abatzoglou, J.T., Kolden, C.A., Cochrane, M.A., & Smith, A.M.S.

(2017) Human exposure and sensitivity to globally extreme wildfire events. *Nature Ecology and Evolution*, **1**, 1–6.

Brook, B.W., Bradshaw, C.J.A., Cooper, A., Johnson, C.N., Worthy, T.H., Bird, M., Gillespie, R., & Roberts, R.G. (2013) Lack of chronological support for stepwise prehuman extinctions of Australian megafauna. *Proceedings of the National Academy of Sciences*, **110**, 3368–3368.

Burney, D.A., Robinson, G.S., & Burney, L.P. (2003) Sporormiella and the late Holocene extinctions in Madagascar. *Proceedings of the National Academy of Sciences*, **100**, 10800–10805.

Cadd, H.R., Fletcher, M.-S., Mariani, M., Heijnis, H., & Gadd, P.S. (2019) The influence of fine-scale topography on the impacts of Holocene fire in a Tasmanian montane landscape. *Journal of Quaternary Science*, 1–8.

Cary, G.J., Keane, R.E., Gardner, R.H., Lavorel, S., Flannigan, M.D., Davies, I.D., Li, C., Lenihan, J.M., Rupp, T.S., & Mouillot, F. (2006) Comparison of the Sensitivity of Landscape-fire-succession Models to Variation in Terrain, Fuel Pattern, Climate and Weather. *Landscape Ecology*, **21**, 121–137.

Chen, C.R., Hou, E.Q., Condron, L.M., Bacon, G., Esfandbod, M., Olley, J., & Turner, B.L. (2015) Soil phosphorus fractionation and nutrient dynamics along the Cooloola coastal dune chronosequence, southern Queensland, Australia. *Geoderma*, **257–258**, 4–13.

Clarkson, C., Jacobs, Z., Marwick, B., et al. (2017) Human occupation of northern Australia by 65,000 years ago. *Nature*, **547**, 306–310.

Cochrane, M.A. (2003) Fire science for rainforests. *Nature*, **421**, 913–919.

Cohen, T.J., Jansen, J.D., Gliganic, L.A., Larsen, J.R., Nanson, G.C., May, J.-H., Jones, B.G., & Price, D.M. (2015) Hydrological transformation coincided with megafaunal extinction in central Australia. *Geology*, **43**, 195–198.

Cohen, T.J., Nanson, G.C., Jansen, J.D., Jones, B.G., Jacobs, Z., Treble, P., Price, D.M., May, J.H., Smith, A.M., Ayliffe, L.K., & Hellstrom, J.C. (2011) Continental aridification and the vanishing of Australia's megalakes. *Geology*, **39**, 167–170.

Crawford, A.J. & Belcher, C.M. (2014) Charcoal morphometry for paleoecological analysis: The effects of fuel type and transportation on morphological parameters. *Applications in Plant Sciences*, **2**, 1–10.

Crawford, A.J. & Belcher, C.M. (2016) Area–volume relationships for fossil charcoal and their relevance for fire history reconstruction. *Holocene*, **26**, 822–826.

Davis, O.K. & Shafer, D.S. (2006) Sporormiella fungal spores, a palynological means of detecting herbivore density. *Palaeogeography, Palaeoclimatology, Palaeoecology*, **237**, 40–50.

Dixon, B.C., Tyler, J.J., Lorrey, A.M., Goodwin, I.D., Gergis, J., & Drysdale, R.N. (2017) Low-resolution Australasian palaeoclimate records of the last 2000 years. *Climate of the Past*, **13**, 1403–1433.

Dodson, J. & Field, J.H. (2018) What does the occurrence of Sporormiella (Preussia) spores mean in Australian fossil sequences? *Journal of Quaternary Science*, **33**, 380–392.

Doughty, C.E., Wolf, A., & Malhi, Y. (2013) The legacy of the Pleistocene megafauna extinctions on nutrient availability in Amazonia. *Nature Geoscience*, **6**, 761–764.

EPICA community members (2004) Eight glacial cycles from an Antarctic ice core. *Nature*, **429**, 623–628.

EPICA Community Members, Barbante, C., Barnola, J.M., et al. (2006) One-to-one coupling of glacial climate variability in Greenland and Antarctica. *Nature*, **444**, 195–198.

Field, J. & Wroe, S. (2012) Aridity, faunal adaptations and Australian Late Pleistocene extinctions. *World Archaeology*, **44**, 56–74.

Fletcher, M.S., Wolfe, B.B., Whitlock, C., Pompeani, D.P., Heijnis, H., Haberle, S.G., Gadd, P.S., & Bowman, D.M.J.S. (2014) The legacy of mid-holocene fire on a Tasmanian montane landscape.

Journal of Biogeography, **41**, 476–488.

Gallant, A.J.E.E., Phipps, S.J., Karoly, D.J., Mullan, A.B., & Lorrey, A.M. (2013) Nonstationary Australasian teleconnections and implications for paleoclimate reconstructions. *Journal of Climate*, **26**, 8827–8849.

Gill, J.L., Williams, J.W., Jackson, S.T., Donnelly, J.P., & Schellinger, G.C. (2012) Climatic and megaherbivory controls on late-glacial vegetation dynamics: A new, high-resolution, multi-proxy record from Silver Lake, Ohio. *Quaternary Science Reviews*, **34**, 66–80.

Gill, J.L., Williams, J.W., Jackson, S.T., Lininger, K.B., & Robinson, G.S. (2009) SI Pleistocene Megafaunal Collapse, Novel Plant Communities, and Enhanced Fire Regimes in North America. *Science*, **326**, 1100–1103.

Guimarães, P.R., Galetti, M., & Jordano, P. (2008) Seed Dispersal Anachronisms: Rethinking the Fruits Extinct Megafauna Ate. *PLoS ONE*, **3**, 1–13.

Haberle, S.G., Tibby, J., Dimitriadis, S., & Heijnis, H. (2006) The impact of European occupation on terrestrial and aquatic ecosystem dynamics in an Australian tropical rain forest. *Journal of Ecology*, **94**, 987–1002.

Haynes, G. (2009) *American megafaunal extinctions at the end of the Pleistocene.* Springer,

Hopcraft, J.G.C., Olff, H., & Sinclair, A.R.E.E. (2010) Herbivores, resources and risks: alternating regulation along primary environmental gradients in savannas. *Trends in Ecology and Evolution*, **25**, 119–128.

Johnson, C., Rule, S., Haberle, S.G., Kershaw, A.P., McKenzie, G.M., & Brook, B.W. (2016a) Geographic variation in the ecological effects of extinction of Australia's Pleistocene megafauna. *Ecography*, **39**, 109–116.

Johnson, C.N., Alroy, J., Beeton, N.J., Bird, M.I., Brook, B.W., Cooper, A., Gillespie, R., Herrando-PÉrez, S., Jacobs, Z., Miller, G.H., Prideaux, G.J., Roberts, R.G., Rodríguez-Rey, M., SaltrÉ, F., Turney, C.S.M., & Bradshaw, C.J.A. (2016b) What caused extinction of the pleistocene megafauna of sahul? *Proceedings of the Royal Society B: Biological Sciences*, **283**, 1–8.

Johnson, C.N., Rule, S., Haberle, S.G., Turney, C.S.M., Kershaw, A.P., & Brook, B.W. (2015) Using dung fungi to interpret decline and extinction ofmegaherbivores: Problems and solutions. *Quaternary Science Reviews*, **110**, 107–113.

Jouzel, A.J., Cattani, O., Dreyfus, G., et al. (2007) Orbital and Millennial Antarctic Climate Variability of the Past 800,000 Yeasr. *Science*, **317**, 793–796.

Junk, W.J., Brown, M., Campbell, I.C., Finlayson, M., Gopal, B., Ramberg, L., & Warner, B.G. (2006) The comparative biodiversity of seven globally important wetlands: A synthesis. *Aquatic Sciences*, **68**, 400–414.

van der Kaars, S., Miller, G.H., Turney, C.S.M., Cook, E.J., Nürnberg, D., Schönfeld, J., Kershaw, A.P., & Lehman, S.J. (2017) Humans rather than climate the primary cause of Pleistocene megafaunal extinction in Australia. *Nature Communications*, **8**, 1–6.

Keeley, J.E., Pausas, J.G., Rundel, P.W., Bond, W.J., & Bradstock, R.A. (2011) Fire as an evolutionary pressure shaping plant traits. *Trends in Plant Science*, **16**, 406–411.

Kemp, C.W., Tibby, J., Arnold, L.J., & Barr, C. (2019) Australian hydroclimate during Marine Isotope Stage 3: A synthesis and review. *Quaternary Science Reviews*, **204**, 94–104.

Kershaw, A.P., Bretherton, S.C., & van der Kaars, S. (2007a) A complete pollen record of the last 230 ka from Lynch's Crater, north-eastern Australia. *Palaeogeography, Palaeoclimatology, Palaeoecology*, **251**, 23–45.

Kershaw, A.P., Clark, J.S., Gill, A.M., & D'Costa, D.M. (2002) A history of fire in Australia. *Flammable Australia: The fire regimes and biodiversity of a continent* pp. 3–25. Cambridge University Press,

Kershaw, A.P., McKenzie, G.M., Porch, N., Roberts, R.G., Brown, J., Heijnis, H., & Orr, M.. (2007b) A

high-resolution record of vegetation and climate through the last glacial cycle from Caledonia Fen, southeastern highlands of Australia. *Journal of Quaternary Science*, **22**, 801–815.

Kiem, A.S. (2004) Multi-decadal variability of drought risk, eastern Australia. *Hydrological Processes*, **18**, 2039–2050.

King, A.D., Klingaman, N.P., Alexander, L. V., Donat, M.G., Jourdain, N.C., & Maher, P. (2014) Extreme rainfall variability in Australia: Patterns, drivers, and predictability. *Journal of Climate*, **27**, 6035–6050.

Laepple, T., Werner, M., & Lohmann, G. (2011) Synchronicity of Antarctic temperatures and local solar insolation on orbital timescales. *Nature*, **471**, 91–94.

Leach, L.M. (2011) Hydrological and physical setting of North Stradbroke Island. *Proceedings of the Royal Society of Queensland*, **117**, 21–46.

Lewis, R., Tibby, J., Arnold, L.J., Gadd, P.S., Marshall, J.C., Barr, C., & Yokoyama, Y. (Accepted) Bayesian deposition model of the Welsby Lagoon sediment sequence. *Quaternary Science Reviews.*

Lindbladh, M., Fraver, S., Edvardsson, J., & Felton, A. (2013) Past forest composition, structures and processes - How paleoecology can contribute to forest conservation. *Biological Conservation*, **168**, 116–127.

Lorenzen, E.D., Nogués-Bravo, D., Orlando, L., et al. (2011) Species-specific responses of Late Quaternary megafauna to climate and humans. *Nature*, **479**, 359–364.

Lynch, A.H., Beringer, J., Kershaw, P., Marshall, A., Mooney, S., Tapper, N., Turney, C., & Van Der Kaars, S. (2007) Using the Paleorecord to Evaluate Climate and Fire Interactions in Australia. *Annual Review of Earth and Planetary Sciences*, **35**, 215–239.

Malhi, Y., Doughty, C.E., Galetti, M., Smith, F.A., Svenning, J.-C., & Terborgh, J.W. (2016) Megafauna and ecosystem function from the Pleistocene to the Anthropocene. *Proceedings of the National Academy of Sciences*, **113**, 838–846.

Mariani, M. & Fletcher, M.S. (2016) The Southern Annular Mode determines interannual and centennial-scale fire activity in temperate southwest Tasmania, Australia. *Geophysical Research Letters*, **43**, 1702–1709.

Marshall, G.J. (2003) Trends in the Southern Annular Mode from observations and reanalyses. *Journal of Climate*, **16**, 4134–4143.

Martin, P.S. (1963) Prehistoric overkill. *Pleistocene extinctions: The search for a cause* (ed. by P.S. Martin and H.E. Wright), pp. 75–120. Yale University Press,

Martin, P.S. & Klein, R.G. (1989) *Quaternary extinctions: a prehistoric revolution.* University of Arizona Press,

McGee, D., Donohoe, A., Marshall, J., & Ferreira, D. (2014) Changes in ITCZ location and cross-equatorial heat transport at the Last Glacial Maximum, Heinrich Stadial 1, and the mid-Holocene. *Earth and Planetary Science Letters*, **390**, 69–79.

Miller, G.H. (2005) Ecosystem Collapse in Pleistocene Australia and a Human Role in Megafaunal Extinction. *Science*, **309**, 287–290.

Miller, G.H., Magee, J., Smith, M., Spooner, N., Baynes, A., Lehman, S., Fogel, M., Johnston, H., Williams, D., Clark, P., Florian, C., Holst, R., & DeVogel, S. (2016) Human predation contributed to the extinction of the Australian megafaunal bird Genyornis newtoni ~47 ka. *Nature Communications*, **7**, 1–7.

Mooney, S. & Tinner, W. (2011) The analysis of charcoal in peat and organic sediments. *Mires and Peat*, **7**, 1–18.

Moritz, M.A., Parisien, M.-A., Batllori, E., Krawchuk, M.A., Van Dorn, J., Ganz, D.J., & Hayhoe, K. (2012) Climate change and disruptions to global fire activity. *Ecosphere*, **3**, 1–22.

Owen-Smith, N. (2013) Contrasts in the large herbivore faunas of the southern continents in the late Pleistocene and the ecological implications for human origins. *Journal of Biogeography*, **40**, 1215–1224.

Patton, N.R., Ellerton, D., & Shulmeister, J. (2019) High-resolution remapping of the coastal dune fields of south east Queensland, Australia: a morphometric approach. *Journal of Maps*, **15**, 578–589.

Pausas, J.G. & Paula, S. (2012) Fuel shapes the fire-climate relationship: Evidence from Mediterranean ecosystems. *Global Ecology and Biogeography*, **21**, 1074–1082.

Pausas, J.G. & Ribeiro, E. (2013) The global fire-productivity relationship. *Global Ecology and Biogeography*, **22**, 728–736.

Peters, M.E. & Higuera, P.E. (2007) Quantifying the source area of macroscopic charcoal with a particle dispersal model. *Quaternary Research*, **67**, 304–310.

Pye, K. (1993) Late Quaternary development of coastal parabolic megadune complexes in northeastern Australia. *Aeolian sediments : Ancient and modern* (ed. by K. Pye and N. Lancaster), pp. 167. Blackwell Scientific Publications,

Risbey, J.S., Pook, M.J., McIntosh, P.C., Wheeler, M.C., & Hendon, H.H. (2009) On the Remote Drivers of Rainfall Variability in Australia. *Monthly Weather Review*, **137**, 3233–3253.

Roberts, R.G., Flannery, T.F., Ayliffe, L.K., Yoshida, H., Olley, J.M., Prideaux, G.J., Laslett, G.M., Baynes, A., Smith, M.A., Jones, R., & Smith, B.L. (2001) New ages for the last Australian megafauna: continent-wide extinction about 46,000 years ago. *Science*, **292**, 1888–1892.

Robinson, G.S., Burney, L.P., & Burney, D.A. (2005) Landscape Paleoecology and Megafaunal Extinction in Southeastern New York State. *Ecological Monographs*, **75**, 295–315.

Rodríguez-Rey, M., Herrando-Pérez, S., Brook, B.W., et al. (2016) A comprehensive database of quality-rated fossil ages for Sahul's Quaternary vertebrates. *Scientific Data*, **3**, 1–7.

Rule, S., Brook, B.W., Haberle, S.G., Turney, C.S.M., Kershaw, A.P., & Johnson, C.N. (2012) The Aftermath of Megafaunal Extinction: Ecosystem Transformation in Pleistocene Australia. *Science*, **335**, 1483–1486.

Saltré, F., Rodríguez-Rey, M., Brook, B.W., Johnson, C.N., Turney, C.S.M., Alroy, J., Cooper, A., Beeton, N., Bird, M.I., Fordham, D.A., Gillespie, R., Herrando-Pérez, S., Jacobs, Z., Miller, G.H., Nogués-Bravo, D., Prideaux, G.J., Roberts, R.G., & Bradshaw, C.J.A. (2016) Climate change not to blame for late Quaternary megafauna extinctions in Australia. *Nature Communications*, **7**, 1–7.

Sandom, C., Faurby, S., Sandel, B., & Svenning, J.-C. (2014) Global late Quaternary megafauna extinctions linked to humans, not climate change. *Proceedings of the Royal Society B: Biological Sciences*, **281**, 1–9.

Seppä, H. & Bennett, K.D. (2003) Quaternary pollen analysis: recent progress in palaeoecology and palaeoclimatology. *Progress in Physical Geography*, **27**, 548–579.

Stuart, A.J. (1999) Late Pleistocene megafaunal extinctions. *Extinctions in near time* pp. 257–269. Springer,

Thompson, C.H. (1981) Podzol chronosequences on coastal dunes of eastern Australia. *Nature*, **291**, 59–61.

Tibby, J., Barr, C., Marshall, J.C., McGregor, G.B., Moss, P.T., Arnold, L.J., Page, T.J., Questiaux, D., Olley, J., Kemp, J., Spooner, N., Petherick, L., Penny, D., Mooney, S., & Moss, E. (2017) Persistence of wetlands on North Stradbroke Island (south-east Queensland, Australia) during the last glacial cycle: implications for Quaternary science and biogeography. *Journal of Quaternary Science*, **32**, 770–781.

Tobler, R., Rohrlach, A., Soubrier, J., et al. (2017) Aboriginal mitogenomes reveal 50,000 years of regionalism in Australia. *Nature*, **544**, 180–184.

Turney, C.S.M., Kershaw, a P., Clemens, S.C., Branch, N., Moss, P.T., & Fifield, L.K. (2004) Millennial

and orbital variations of El Niño/Southern Oscillation and high-latitude climate in the last glacial period. *Nature*, **428**, 306–10.

Ummenhofer, C.C., Gupta, A. Sen, Briggs, P.R., England, M.H., McIntosh, P.C., Meyers, G.A., Pook, M.J., Raupach, M.R., & Risbey, J.S. (2011) Indian and Pacific Ocean influences on southeast Australian drought and soil moisture. *Journal of Climate*, **24**, 1313–1336.

Walker, J., Lees, B., Olley, J., & Thompson, C. (2018) Dating the Cooloola coastal dunes of South-Eastern Queensland, Australia. *Marine Geology*, **398**, 73–85.

Walker, J., Thompson, C.H., Fergus, I.F., & Tunstall, B.R. (1981) Plant Succession and Soil Development in Coastal Sand Dunes of Subtropical Eastern Australia. *Forest Succession: concepts and application* (ed. by D.C. West, H.H. Shugart, and D.F. Botkin), pp. 107–131. Springer, New York.

Walker, J., Thompson, C.H., & Jehne, W. (1983) Soil Weathering Stage, Vegetation Succession, and Canopy Dieback. *Pacific Science*, **37**, 471–481.

Walker, L.R., Wardle, D.A., Bardgett, R.D., & Clarkson, B.D. (2010) The use of chronosequences in studies of ecological succession and soil development. *Journal of Ecology*, **98**, 725–736.

Wardle, D.A. (2005) How plant communities influence decomposer communities. *Biological Diversity and Function in Soils* (ed. by R. Bardgett, M. Usher, and D. Hopkins), pp. 119–138. Cambridge University Press,

Webb, S. & Webb, S. (2008) Megafauna demography and late Quaternary climatic change in Australia : A predisposition to extinction. **2008**, .

Whitlock, C. & Larsen, C. (2001) Charcoal as a Fire Proxy. *Tracking Environmental Change Using Lake Sediments: Terrestrial, Algal, and Siliceous Indicators* (ed. by J.P. Smol, H.J.B. Birks, W.M. Last, R.S. Bradley, and K. Alverson), pp. 75–97. Springer Netherlands, Dordrecht.

Williams, J.E. & Woinarski, J. (1997) *Eucalypt ecology : individuals to ecosystems.* Cambridge University Press,

Willis, K.J. & Birks, H.J.B. (2006) What is natural? The need for a long-term perspective in biodiversity conservation. *Science*, **314**, 1261–1265.

Wolff, E.W., Chappellaz, J., Blunier, T., Rasmussen, S.O., & Svensson, A. (2010) Millennial-scale variability during the last glacial: The ice core record. *Quaternary Science Reviews*, **29**, 2828–2838.

Wood, S.W., Murphy, B.P., & Bowman, D.M.J.S. (2011) Firescape ecology: How topography determines the contrasting distribution of fire and rain forest in the south-west of the Tasmanian Wilderness World Heritage Area. *Journal of Biogeography*, **38**, 1807–1820.

Wroe, S. & Field, J. (2006) A review of the evidence for a human role in the extinction of Australian megafauna and an alternative interpretation. *Quaternary Science Reviews*, **25**, 2692–2703.

Wroe, S., Field, J.H., Archer, M., Grayson, D.K., Price, G.J., Louys, J., Faith, J.T., Webb, G.E., Davidson, I., & Mooney, S.D. (2013) Climate change frames debate over the extinction of megafauna in Sahul (Pleistocene australia-new guinea). *Proceedings of the National Academy of Sciences of the United States of America*, **110**, 8777–8781.

Statement of Authorship

Title of Paper	Late Quaternary development of a Southern Hemisphere sub-tropical wetland (Welsby Lagoon, south-east Queensland, Australia)
Publication Status	☑ Published ☐ Accepted for Publication ☐ Submitted for Publication ☐ Unpublished and Unsubmitted work written in manuscript style
Publication Details	Published in the Quaternary Science Reviews as: Cadd, H.R., Tibby, J., Barr, C., Tyler, J. Unger, L., Leng, M.J., Marshall, J.C., McGregor, G., Lewis, R., Arnold, L.J., Lewis, T., Baldock, J. 2018. Development of a southern hemisphere subtropical wetland (Welsby Lagoon, south-east Queensland, Australia) through the last glacial cycle. Quaternary Science Reviews. 202: 53-65

Principal Author

Name of Principal Author	Haidee Cadd		
Contribution to the Paper	Conceptualisation of the work, development of ideas and conclusions, carried out analytical work for palynology, isotopes, nuclear magnetic resonance, assisted with acquisition of macrofossil and pigment data, carried out statistical analysis, interpretation of the data, wrote manuscript.		
Overall percentage (%)	75		
Certification:	This paper reports on original research I conducted during the period of my Higher Degree by Research candidature and is not subject to any obligations or contractual agreements with a third party that would its inclusion in this thesis. I am the primary author of this paper.		
Signature		Date	26/09/19

Co-Author Contributions

By signing the Statement of Authorship, each author certifies that:

i. the candidate's stated contribution to the publication is accurate (as detailed above);
ii. permission is granted for the candidate in include the publication in the thesis; and
iii. the sum of all co-author contributions is equal to 100% less the candidate's stated contribution.

Name of Co-Author	John Tibby		
Contribution to the Paper	Conducted fieldwork, provided conceptual and interpretation guidance, edited manuscript		
Signature		Date	12/09/19

Name of Co-Author	Cameron Barr		
Contribution to the Paper	Conducted fieldwork, provided conceptual and interpretation guidance, edited manuscript		
Signature		Date	12/09/19

Name of Co-Author	Jonathan Tyler		
Contribution to the Paper	Provided conceptual and interpretation guidance, edited manuscript		
Signature		Date	12/09/19

Name of Co-Author	Lilian Unger		
Contribution to the Paper	Collected macrofossil data and aided with interpretation of macrofossil data.		
Signature		Date	20/09/2019

Name of Co-Author	Melanie Leng		
Contribution to the Paper	Assisted with acquisition and processing of modern stable isotope data, provided conceptual guidance, edited manuscript.		
Signature		Date	12/09/19

Name of Co-Author	Jonathan Marshall		
Contribution to the Paper	Conducted fieldwork, assisted with acquisition and processing of pigment data, edited manuscript.		
Signature		Date	12/09/19

Name of Co-Author	Glenn McGregor		
Contribution to the Paper	Conducted fieldwork, assisted with acquisition and processing of pigment data, edited manuscript.		
Signature		Date	20/09/19

Name of Co-Author	Richard Lewis		
Contribution to the Paper	Conducted fieldwork, processed, aided with interpretation and wrote text pertaining to OSL data.		
Signature		Date	12/09/19

Name of Co-Author	Lee Arnold		
Contribution to the Paper	Assisted with acquisition and interpretation of optically stimulated luminescence data.		
Signature		Date	16/09/19

Name of Co-Author	Tara Lewis		
Contribution to the Paper	Assisted with acquisition and interpretation of macrofossil data		
Signature		Date	26/09/19

Name of Co-Author	Jeff Baldock		
Contribution to the Paper	Assisted with acquisition and interpretation of nuclear magnetic resonance data.		
Signature		Date	20/09/19

2

Development of a Southern Hemisphere subtropical wetland (Welsby Lagoon, south-east Queensland, Australia) through the last glacial cycle

Published as:

Cadd, H.R., Tibby, J., Barr, C., Tyler, J. Unger, L., Leng, M.J., Marshall, J.C., McGregor, G., Lewis, R., Arnold, L.J., Lewis, T., Baldock, J. 2018. Development of a southern hemisphere subtropical wetland (Welsby Lagoon, south-east Queensland, Australia) through the last glacial cycle. *Quaternary Science Reviews.* 202: 53-65

https://doi.org/10.1016/j.quascirev.2018.09.010

Abstract

Continuous records of terrestrial environmental and climatic variability that extend beyond the Last Glacial Maximum (LGM) in Australia are rare. Furthermore, where long records do exist, interpretations of climate and ecological change can be hampered by marked changes in sedimentary environment which, in turn, affect the taphonomy of palaeoecological remains. As a consequence, in order to determine how wetland systems responded to climatic and environmental changes, we first need to understand how their depositional environment changed through time. Here we document the development of freshwater Welsby Lagoon, south-east Queensland, from a 12.7 m sediment sequence with a basal age of ca. 130,000 years. We present a variety of proxies reflecting change within the wetland. Carbon and nitrogen concentrations and carbon and nitrogen isotope ratios are used to infer the source of organic matter. However, the nitrogen limited nature of the catchment soils and presence of the colonial algae *Botryococcus* meant that organic material with C:N ≥20 is likely to be derived from autochthonous sources rather than terrestrial sources. A combination of photosynthetic pigments, plant macrofossils, aquatic pollen and sedimentary lignin was used to identify the sources of organic matter and the changing nature of this wetland. Since its formation, Welsby Lagoon has undergone a progressive change from an open-water, algae and cyanobacteria dominated, freshwater lacustrine system, to an aquatic macrophyte-dominated palustrine swamp after ca. 40 ka. It did not revert to lacustrine conditions during the Holocene, despite what is widely viewed as an increase in the regional moisture balance, most likely due to continual infilling of the wetland with sediment. With so few records of terrestrial change throughout MIS3 and MIS4, adequately understanding the development of sites like Welsby Lagoon is imperative to advancing our knowledge of this important environmental and cultural period in Australia's history, which encompasses events such as the extinction of megafauna and human colonisation of the continent.

1 Introduction

The last glacial cycle (from ca. 123,000 years before present; 123 ka) is a period of substantial environmental and cultural importance in Australia, encompassing the arrival of humans and the mass extinction of the Australian megafauna (Roberts et al., 2001; Hamm et al., 2016; Clarkson et al., 2017). The main terrestrial environmental and climate information for this period originate from the interpretation of proxies preserved in wetland sediments. However, the scarcity of continuous wetland sedimentary sequences extending beyond the Last Glacial Maximum (LGM; previously defined as 22–18 ka, Reeves et al., 2013), through MIS3 (57–29 ka) and MIS4 (71–57 ka), hampers efforts to robustly investigate environmental and climatic changes. The majority of Australian sedimentary records of substantial antiquity suffer from depositional hiatuses or sedimentary deflation, commonly during the period of cold and arid climates characteristic of the LGM (Singh et al., 1981; D'Costa et al., 1993; Longmore, 1997; Harle et

al., 2002; Black et al., 2006). Thus, spatially diverse interpretations of continental climate and Australian landscape change are lacking during the important time periods of MIS3 and MIS4 (Turney et al., 2006).

Welsby Lagoon provides a regionally important sedimentary record of changes in sub-tropical, eastern Australia during MIS3 and MIS4. Optically stimulated luminescence (OSL) ages from the basal sands of Welsby Lagoon indicate that the wetland formed during MIS5, with a basal age of ca. 130 ka (Tibby et al., 2017). The two other continuous wetland sedimentary sequences that extend through MIS3 and MIS4 (Figure 1), Caledonia Fen in the cool-temperate south (Kershaw et al., 2007b) and Lynch's Crater in the wet tropics (Kershaw et al., 2007a), have become the focus of a substantial number of studies (e.g. Johnson et al., 2016; Kershaw et al., 2007a, 2007b; Rule et al., 2012; Turney et al., 2004). These spatially isolated records provide the basis for many interpretations of terrestrial climate and environmental change for continental Australia. However, as highlighted by Reeves et al. (2013a), Australian climate variability during the last glacial period was spatially complex. The wide diversity of topography, large latitudinal range, extensive low-relief interior and fringing mountainous areas, has led to asynchronous, and often contradictory, responses from wetland, vegetation and ocean records. Welsby Lagoon is a lowland, sub-tropical site that fills a large spatial gap between the previously documented continuous terrestrial MIS4 and MIS3 records from tropical and temperate eastern Australia (Figure 1).

Understanding the depositional nature of wetland sedimentary sequences is a fundamental requirement for their use in robust reconstructions of external environmental and climatic conditions (Birks & Birks, 2006). Furthermore, knowledge of the origin and fate of organic matter is essential for robust palaeoclimate interpretations based on organic proxies. Sedimentary organic matter in wetlands may be derived from terrestrial production within their catchments or be produced by autotrophs within wetlands. Autochthonous primary producers in wetlands typically consist of algae and cyanobacteria, as phytoplankton, periphyton or metaphyton and submerged, floating or emergent vascular macrophytes (Finlay & Kendall, 2008). In macrophyte-dominated wetlands, phytoplankton production is typically low, and the dominant source of sedimented organic matter is macrophytes (Blindow, 1992). The importance of emergent macrophytes diminishes with increasing wetland water depth, such that in deep lakes, primary production and hence organic matter deposition, tends to be dominated by unicellular photoautotrophs (Schlesinger & Bernhardt, 2013). These varying sources of organic matter are charactered by different concentrations and isotopic ratios of carbon and nitrogen (Meyers & Teranes, 2001).

In order to understand the history of wetland formation and variability in the sources of organic matter at Welsby Lagoon, we analysed carbon and nitrogen isotope ratios ($\delta^{13}C$ and $\delta^{15}N$) of organic matter and total organic carbon (TOC), total nitrogen (TN), macrofossil remains, autotroph pigments, sediment lignin content and pollen composition categorised into plant habitat from a 12.7 m sediment core. This multi-proxy

approach provides a reconstruction of the depositional environment of Welsby Lagoon from which we infer its evolving nature, particularly its progression from a lacustrine to palustrine wetland. This foundation study provides vital information to support future research into the climate and environmental history of this region.

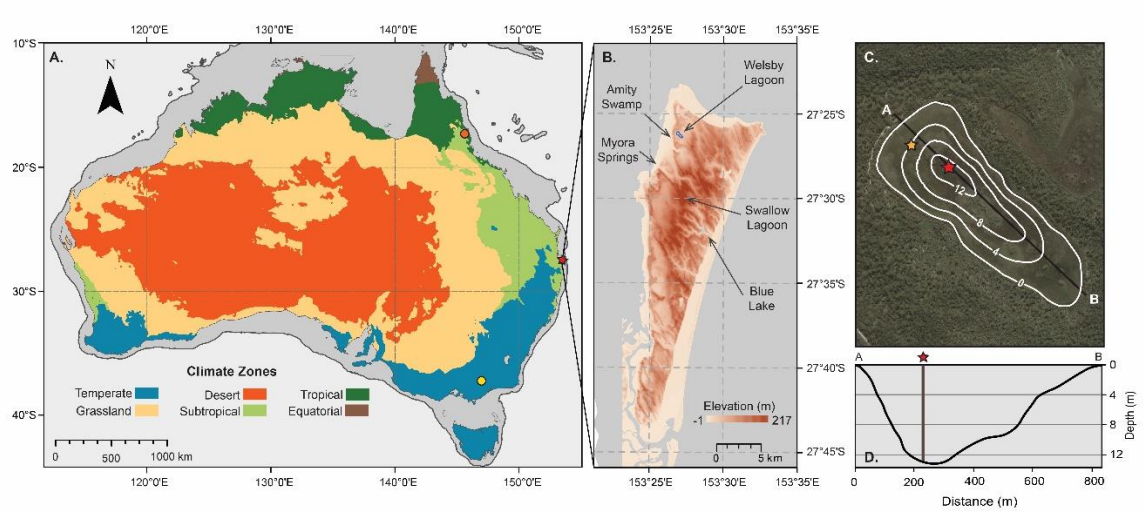

Figure 3. Map of Australia showing the major Köppen climate zones (BOM, 2018b) and maximum extent of exposed continental shelf (dark grey) during the last glacial maximum. Orange circle indicates location of Lynch's Crater, yellow circle indicates location of Caledonia Fen. **B.** Location of North Stradbroke Island, Welsby Lagoon and other sites named in the text. Shading shows sand dune elevation on the Island (Gallant et al., 2011). **C.** Satellite image of Welsby Lagoon (source: Google Earth). Contours denote basin sediment depth (m) determined from a series of probing transects and interpolated in ArcMap 10.3.1 using the IDW kriging tool. Red star denotes coring location of this study, orange star denotes coring location from Barr et al., 2017. **D.** Depth profile of the Welsby Lagoon basin between points A and B in panel C.

1.1. Regional setting

North Stradbroke Island (NSI; 27°27'S, 153°28'E), south-eastern Queensland, is situated in the sub-tropical climate zone of south-eastern Australia (Figure 1A). The ocean proximity moderates temperatures, with the island experiencing warm, humid summers (mean 26°C) and mild, dry winters (mean 19°C) (BOM & BOM, 2018). The majority of annual precipitation (1500 mm) occurs during Austral summer and autumn months, with only 15% of rainfall occurring from July to October (BOM & BOM, 2018).

The key synoptic drivers of southeast Queensland rainfall variability on annual timescales are the south-easterly trade winds, cut-off lows and extra-tropical cyclones. Regional climate is modulated on inter-annual to decadal timescales by the Inter-Tropical Convergence Zone (ITCZ), the El Niño-Southern Oscillation (ENSO) and the Inter-decadal Pacific Oscillation (IPO) (Barr et al., 2017; Moss et al., 2013 and references therein).

NSI is part of the larger regional Cooloola sand mass and is the second largest sand island

in the world (285 km²; Figure 1B). NSI last became isolated from mainland Australia by the flooding of Moreton Bay during the mid-Holocene, ca. 6000 years ago (Pye, 1993). Topographically, NSI is, for the most part, composed of a series of north-west to south-east orientated parabolic sand dunes, although Welsby Lagoon is bounded by a north – south oriented dune on the western side (Figure 1b). The Cooloola sand mass consists of a series of stabilised sand dunes formed over a number of dune-building phases from ca. 500 ka. The dunes were formed predominantly during glacial periods from the aeolian transport of continental and exposed marine sands (Walker et al., 1981; Lees, 2006; Miot da Silva & Shulmeister, 2016).

Soils on the quartz-rich sand dunes show progressive development with age, with the depth of podzol development varying in relation to dune age (Thompson, 1981). The low-nutrient capital of the quartz-dominated dunes results in relatively low soil productivity with low soil carbon contents (<2% C) (Walker et al., 1981; Stephens & Sharp, 2009; Chen et al., 2015). Dry sclerophyll forest, Casuarinaceae woodland and heath communities dominate the majority of the island, with mangrove forests found on the coastal fringes of the western side. Rainforest vegetation is restricted to a single patch on the north-west side of the island at Myora Springs (Stephens & Sharp, 2009; Moss et al., 2011).

On NSI, precipitation percolates rapidly through the sand regolith into a predominantly subterraneous, regional, freshwater aquifer (Leach, 2011). Freshwater springs and groundwater-fed lakes and wetlands occur mostly along the coastal fringe, forming where surface topography intersects the regional aquifer. The regional groundwater-regulated wetlands of NSI demonstrate remarkable stability and resilience to environmental perturbations such as fire and drought (Mettam et al., 2011; Specht & Stubbs, 2011; Barr et al., 2013; Tibby et al., 2017). Other wetlands are associated with perched aquif that occur across the island where indurating layers of organic and/or inorganic material have developed in dune hollows (Timms, 1986). Perched wetlands can occur high above the regional aquifer, while others have developed at lower altitudes due to interactions between the perched and regional aquifers (Leach, 2011). Many NSI freshwater wetlands are palustrine, waterlogged, oligotrophic environments, dominated by sedges *Baumea* spp., *Gahnia sieberiana*, *Lepironia articulata* and *Baloskion pallens* (syn. *Restio pallens*) and open *Melaleuca quinquenervia* forest (Marshall & McGregor, 2011).

Today Welsby Lagoon (27°26'12"S, 153°26'56"E; 29 m.a.s.l; Figure 1C, 1D) is a perched, palustrine wetland, with a variable water depth of 0 – 1.5 m. During periods when there is no surface water present, the peaty organic sediments remain waterlogged close to the surface by the perched aquifer. Welsby Lagoon has an internally draining catchment of 5.38 km² (~2% of the island) and is hydrologically closed with no fluvial input. The wetland water is generally well-mixed, acidic (pH 4.3 – 6.8), soft (hardness as $CaCO_3$ 15 mg/l), nutrient deficient, and fresh (37.3 – 50 µS/cm), with very low turbidity (<2 NTU) and strongly tannin-stained waters (true colour 1370 Hazen units) (Queensland Government, unpublished data). The wetland surface is dominated by emergent sedges and reeds (*Baumea* spp. being dominant), while fringing terrestrial vegetation is

dominated by Eucalypt woodland with a predominantly heathy understory of *Banksia* and Casuarinaceae (Moss et al., 2013).

2 Methods

2.1. Sediment coring

The thickest sedimentary sequence, and hence the location of core collection, was identified by a systematic sediment probing survey (Figure 1C, D). Coring was undertaken in approximately 0.5 m of water depth from a Kawhaw coring platform. Sediments were extracted as two, 0.5 m offset, parallel cores (WL15-1 and WL15-2) extending to 12.78 m and 12.72 m depth respectively. In this study only WL15-2 is discussed. The coring process minimised sediment exposure to light by using black PVC tubing coupled to a modified Bolivia corer (Myrbo & Wright, 2008). Once raised, the 1 m core sections were wrapped in black plastic to maintain the integrity of the natural luminescence signal for OSL dating. Core sections remained wrapped and sealed until being split under filtered and subdued red LED light conditions at the University of Adelaide.

2.2. Single-grain Optically Stimulated Luminescence (OSL) dating

Two 20 cm sediment samples from the WL15-2 core were dated using optically stimulated luminescence (OSL) at the University of Adelaide. OSL dating of Welsby Lagoon basal sands has previously been reported by Tibby et al. (2017). All sample extraction was conducted under filtered and subdued red LED lighting. Approximately 30 g of bulk sediment (dry weight) was retained from each sample for dose rate determination. Water and bulk density analysis was conducted on sediment samples collected at 10 cm intervals through the 12.7 m core sequence.

Preparations for equivalent dose (D_e) estimation on refined quartz fractions (180–250 μm) were conducted using standard procedures outlined in Aitken (1998), including a 48% hydrofluoric acid etch (40 minutes). Single-grain D_e measurements were made using the instrumentation and experimental procedures described by Arnold et al. (2016, 2013). Single-grain analysis was performed using a Risø TL/OSL DA-20 reader equipped with an EMI9235QA photomultiplier tube, a mounted $^{90}Sr/^{90}Y$ β source for irradiation, and a 10 mW Nd:YVO_4 single-grain laser attachment emitting at 532 nm.

Individual D_e measurements were determined using the single-grain SAR protocol (Murray and Wintle, 2000; Table S1) and D_e values were only accepted for burial dose evaluation if they satisfied a series of routine quality assurance criteria (Arnold et al., 2007; Table S2). The final burial dose estimates of samples WL15-2(3) and WL15-2(6) have been calculated using the four-parameter unlogged minimum age model (MAM-4UL; Arnold et al., 2009) and the central age model (CAM; Galbraith et al., 1999), respectively

(see Supplementary Information for further details).

The sedimentological components of the environmental dose rate were calculated using a combination of inductively coupled plasma mass spectrometry (ICP-MS) and inductively coupled plasma optical emission spectrometry (ICP-OES). Elemental concentrations were converted to beta and gamma dose rates using the conversion factors of Guérin et al. (2011), with allowances for beta-dose attenuation and moisture content (Mejdahl, 1979; Table 1). The cosmic ray contribution to the total environmental dose rate was determined using the approach of Prescott and Hutton (1994), assuming a steady post-depositional overburden accumulation and a constant lake depth (equivalent to present-day conditions).

2.3. Geochemical Analysis

Total organic carbon (TOC) and total nitrogen (TN) concentrations, carbon and nitrogen isotope ratios ($^{13}C/^{12}C$ and $^{15}N/^{14}N$ respectively) were determined from fifty sub-samples throughout the Welsby Lagoon core. Approximately 2 cm^3 of bulk sediment was freeze dried and ground to a homogeneous consistency using a Retsch ball mill prior to analysis. Samples were combusted in a EuroVector EuroEA elemental analyser, in-line with a Nu Instruments Nu Horizon continuous flow Isotope Ratio Mass Spectrometer at the University of Adelaide. Samples were calibrated against internal glycine, glutamic acid and triphenylamine standards through USGS40, USGS41, IAEA CH6, NBS22 and NBS24 for $^{13}C/^{12}C$ and IAEAN1, IAEAN2, IAEANO3, USGS25, USGS32, USGS40 and USGS41 for $^{15}N/^{14}N$. All carbon and nitrogen isotope ratios reported here are expressed on the delta scale ($\delta^{13}C$ and $\delta^{15}N$) to per mille (‰) relative to VPDB and AIR, respectively. Carbon to nitrogen ratios (C:N) are expressed as weight ratios. Analytical precision for replicate measurement of standards was ±0.06‰. Standards were used to calculate a drift and peak size correction that was then applied to sediment samples.

Constrained incremental sum of squares (CONISS) was conducted in the rioja package (Juggins, 2015) in R (R Core Team, 2017) on organic geochemical data (TOC, $\delta^{13}C$, $\delta^{15}N$, C:N) to determine major groupings within the sediment core (Figure S3).

Modern algae and cyanobacteria (herein referred to as algae), emergent macrophyte, terrestrial vegetation and soil samples were collected from NSI in February 2017 (Table S3). Phytoplankton was collected by towing a 20 cm diameter plankton net with a 10 µm mesh at 0.3 m from the surface of the lake for approximately 3 minutes. Mats, crusts and other epiphytic and metaphytic algal material was collected by hand. All samples were kept chilled until observed in the laboratory. Live material was examined using bright-field, phase contrast, and differential interference contrast illumination systems with an Olympus BX53 compound microscope to a maximum magnification of 1000x. Terrestrial vegetation samples consisted of leaves and fine stem material. Emergent aquatic samples are an average of measurements taken from the tip, stem and root of each plant. Samples

were freeze-dried and finely ground before being transported for analysis at the British Geological Survey. For the modern samples, $\delta^{13}C$, $\delta^{15}N$ and TOC and TN were analysed by combustion via an online Costech ECS4010 Elemental Analyser and evolved gas was transferred to a VG TripleTrap and Optima dual-inlet mass spectrometer. Samples were calibrated against in house standards (BROC and SOIL) through NBS18, NBS-19 and NBS22. Analytical precision for replicate measurement of standards was <0.1‰.

2.4. Sediment Nuclear Magnetic Resonance (NMR)

The relative proportion of lignin in sediment was estimated using solid-state ^{13}C nuclear magnetic resonance (NMR) spectroscopy on the same 50 samples analysed for stable isotopes. All spectra were acquired at the CSIRO Waite campus on a Bruker 200 Avance spectrometer equipped with a 4.7 T wide-bore superconducting magnet operating at a resonance frequency of 50.33 MHz. Weighed samples (150-600 mg) were packed into 7 mm diameter zirconia rotors with Kel-F end caps and spun at 5 kHz. Chemical shift values were calibrated to the methyl resonance of hexamethylbenzene at 17.36 ppm and a 50 Hz Lorentzian line broadening was applied. A cross polarisation (CP) pulse sequence as used with a delay between pulses set to the longer of 1 s or five times sample specific T1H values determined by inversion recovery analysis. A 3.2 µs and 195 w 90° pulse with a 1 ms contact time was used, with between 10,000 and 20,000 transient collected for each sample. All spectral processing was completed using the Bruker TopSpin 3.2 software. After phasing and baseline corrections were applied, the absolute NMR signal intensities acquired for each sample were divided by the number of transients collected and corrected for the empty rotor background signal intensity. The resultant spectral intensities were integrated over a series of chemical shift limits and used to estimate the lignin content of the samples according to the calculations described by Baldock et al (2013).

2.5. Palynology

Pollen samples were processed using a modified version of the standard protocols outlined in Faegri and Iverson (1989). Sixty x 0.5 cm^3 sediment samples were taken at ~20 cm intervals along the length of the core. A total of 250 grains of terrestrial origin (excluding fern spores) form the base pollen sum. Percentages of aquatic taxa are based on a super-sum inclusive of both terrestrial and aquatic taxa. Terrestrial taxa are grouped according to morphology and habitat types.

2.6. Macrofossils

Macrofossil analysis was undertaken on 19 samples, with sampling effort focussed on the depths from 380 – 790 cm. Macrofossil samples were processed using the methods outlined in Birks (2002). Sediment (30 cm^3, 3 cm of core depth) was extracted for each sample and measured using volume displacement in 50 mL of water. Samples were gently

rinsed through nested sieves to separate the >250 µm and >125 µm size fractions. All material retained in the 250 µm sieve was examined and 10 mL sub-samples of the >125 µm fraction were examined. Material was identified using a combination of online and print identification guides, modern samples and a macrofossil reference collection and database (Lewis, 2012). The abundance of material of unknown taxonomic origin (dominated by stem material) was estimated using a point count method (after Clark, 1982). In this method, 5 ml aliquots of the >250 µm material were taken from a 200 ml suspension of material and added to a gridded petri dish with 60 intersections or "points." The number of times plant material fell on these points was then recorded and expressed as a percentage.

2.7. Sedimentary pigments

Pigments were extracted from 14 sediment samples. Pigment analysis was performed at the Queensland Government's Department of Environment and Science's Chemistry Centre laboratories using a modified HPLC method. Sediment samples (~0.4 g) were combined with 3 ml of acetone and homogenised using a ceramic mortar and pestle. An additional 2 ml of acetone was added and solution was refrigerated at -20ºC for 2 hours before being filtered using a 0.22 µm nylon syringe filter. Samples were dried under N_2 gas and reconstituted with 200 µl of 7 mM tetrabutyl ammonium acetate and methanol. HPLC analyses were performed on a Dionex Ultimate 3000 U-HPLC system with a Dionex DAD 3000 diode array detector. 10 µl of each sample and an intermediate standard (containing lutein, β-carotene, zeaxanthin, alloxanthin, fucoxanthin, chl α and peridinin) were injected onto a Phenomenex chromatographic system with an inline 0.2 µm filter. Pigment data was calibrated using response factors of certified mixed pigment standards. Chromatograms were integrated using Chromeleon 7.2 acquisition software with pigments identified using a combination of their retention times and absorbance spectra. Pigment concentrations are expressed as ng/g of carbon based on measured TOC. Taxonomic affinities of identified pigments were determined from Leavitt and Hodgson (2002) and Roy et al. (2011).

3 Results

The modern plant and algae samples all have $\delta^{13}C$ values consistent with those of C_3 plants (–24 to –34 ‰, Figure 2, Supplementary Table 1; Meyers and Teranes, 2001). Terrestrial plants have the lowest $\delta^{13}C$ values of all samples, from –30.4 to –31.6 ‰ (Figure 2A, 2C). Algae exhibited the largest range of $\delta^{13}C$, from –27.2 to –31.7 ‰ (mean –29.2 ‰) (Figure 2A, 2C). Emergent aquatic plants have the highest $\delta^{13}C$, from –23.1 to –29.3 ‰, however these still fall within the global C_3 plant range (Figure 2A). All modern samples (including the algae) have C:N ratios above 18. Algae samples have the lowest C:N ratios ranging from 18 to 46. All terrestrial and emergent aquatic vascular plants have C:N ratios above 40 except for *Eucalyptus* leaves, with a value of 29 (Figure 2A, 2D).

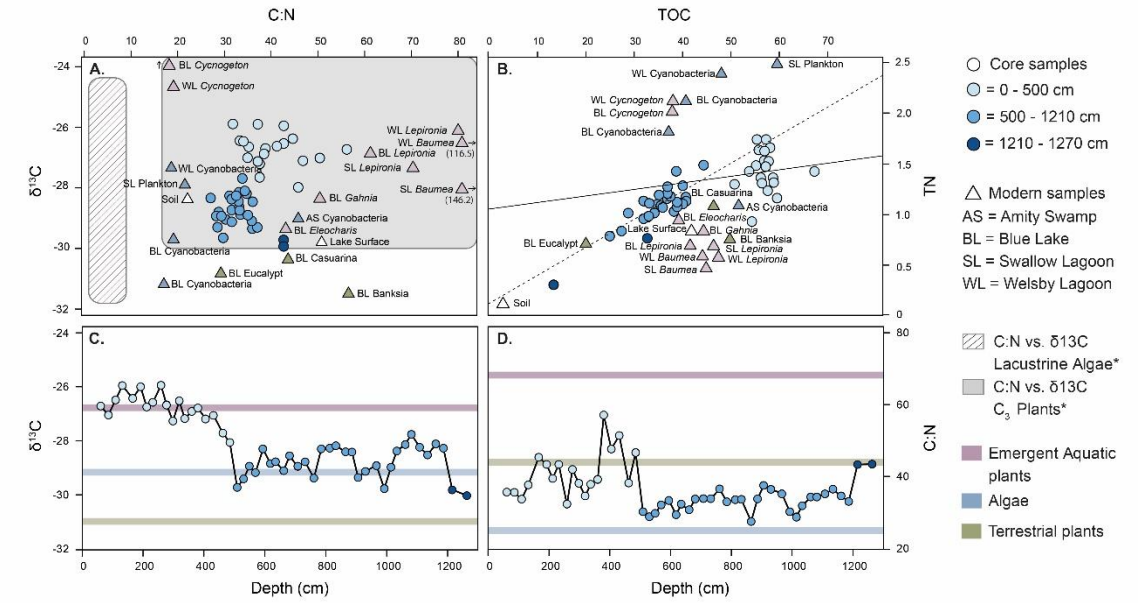

Figure 4. A. Carbon isotopes vs. carbon:nitrogen (C:N) ratio of core samples (circles) and modern samples (triangles). B. Total organic carbon (TOC) vs. Total nitrogen (TN) of core samples (circles) and modern samples (triangles). Regression line for samples from 0 – 500 cm is show as a solid line and regression line for samples from 500 – 1210 cm is shown as a dashed line. Assuming a linear relationship between TOC and TN, the amount on inorganic nitrogen (IN) is defined as the y-axis intercept (0 – 500 cm IN = 1.0%; 500 – 1210 cm IN = 0.05%) C. Sediment δ13C plotted by depth with averages of modern sample shown in A and B. D. Sediment C:N plotted by depth with modern sample averages. Colours of modern samples in all panels correspond to designation as emergent aquatic plants, lacustrine algae and terrestrial plants. *adapted from Meyers and Terranes 2001.

The 12.7 m sediment core recovered from Welsby Lagoon consists of highly organic, dark coloured sediment (Figure 3). CONISS, conducted on organic geochemical data (TOC, $\delta^{13}C$, C:N; Figure S3), in conjunction with lithology (i.e. changes in sediment type), was used to separate the sediment core into three phases. Three OSL and radiocarbon ages were used to infer the broad timing of major changes in sediment deposition. OSL samples WL15(2)-3 and WL15(2)-6 were analysed for this study (Table 3; Sup info Table S1, S2, Figure S1) and OSL sample GU5.1 from the basal sands of the wetland from Tibby et al., (2017). Radiocarbon ages from a core taken from the edge of Welsby Lagoon (Moss et al., 2013; Chang et al., 2015; Barr et al., 2017) were correlated to the upper sediments of the core used in this study (Supplementary Figure S2). Based on changes in sedimentology and the preliminary OSL and ^{14}C ages, we cautiously infer three main phases corresponding broadly to early marine isotope stage 5 (MIS5), MIS5 – MIS3 and MIS2 – present.

Table 1. Dose rate data, equivalent doses (D_e), overdispersion values, and OSL ages for lacustrine samples from Welsby Lagoon, North Stradbroke Island. The final OSL age of each sample has been calculated by dividing the D_e value by the total dose rate.

Sample (core)	Depth (cm)	Grain size (μm)	Water Content (% Dry) [a]	Environmental dose rate (Gy/ka) [b,c,d,e,f]					Equivalent dose (D_e) data				D_e (Gy) [f]	Final age (ka) [f,k]
				Beta dose rate	Gamma dose rate	Internal dose rate	Cosmic dose rate	Total dose rate	D_e type [g]	No. of grains [h]	Overdis-persion (σ_b) (%) [i]	Age Model [g]		
WL15-2(3) (2015)	380	180-250	505/629/923	0.01±0.001	0.01±0.001	0.02±0.007	0.02±0.002	0.05±0.008	SG OSL	82	117	MAM-4_{UL}	0.94±0.15	18.6±4.1
WL15-2(6) (2015)	510	180-250	575/620/945	0.04±0.01	0.05±0.001	0.02±0.007	0.01±0.002	0.12±0.01	SG OSL	113	34	CAM	5.46±0.22	43.7±5.4
GU5.1 (2011)	1268	180-212	247/247/761	0.06±0.009	0.08±0.005	0.03±0.01	0.01±0.001	0.19±0.02	SG OSL	64	15	CAM	24.5±0.6	130±15.3

[a] Long-term water contents used for beta / gamma / cosmic-ray dose rate attenuation, expressed as % of dry mass of mineral fraction, with an assigned relative uncertainty of ±5% (WL15 samples) or ±10% (GU5.1). The final beta dose rates have been adjusted for moisture attenuation using the measured water contents determined from the midpoint of each OSL sample depth. The final gamma dose rates have been adjusted using the average water content measured from each OSL sample midpoint, as well as from 1 cm^3 bulk sediment samples collected 10 cm above and 10 cm below the OSL sample midpoint. The final cosmic-ray dose rates have been adjusted using the average water content measured from 1 cm^3 bulk sediment samples collected at 10 cm intervals throughout the overlying core sequence.

[b] Beta, gamma and internal dose rates have been calculated on dried and powdered sediment samples using ICP-MS and ICP-OES (WL15 samples) or high-resolution gamma spectrometry (GU5.1).

[c] Radionuclide concentrations have been converted to alpha, beta and gamma dose rates using the published conversion factors of , allowing for beta-dose attenuation (Mejdahl, 1979; Brennan, 2003) and long-term water content correction (Aitken, 1985).

[d] An internal dose rate of 0.02 ± 0.01 Gy / ka has been included in the final dose rate calculations of samples WL15-2(3) and WL15-2(6), based on ICP-MS U and Th measurements made on etched quartz grains from associated aeolian deposits at Welsby Lagoon (Lewis et al., Accepted) and an alpha efficiency factor (*a* value) of 0.04 ± 0.01 (Rees-Jones, 1995; Rees-Jones & Tite, 1997). Tibby et al. (2017) assigned an assumed internal dose rate of 0.03 ± 0.01 Gy/ka to sample GU5.1, following Bowler et al. (2003).

[e] Cosmic-ray dose rates were calculated using the approach of Prescott & Hutton (1994), and assigned a relative uncertainty of ±10%.

[f] Mean ± total uncertainty (68% confidence interval), calculated as the quadratic sum of the random and systematic uncertainties.

[g] SG OSL = single-grain optically stimulated luminescence; MAM-4_{UL} = Unlogged four-parameter minimum age model (Arnold et al., 2009) ; CAM = Central age model (Galbraith et al., 1999).

[h] Number of D_e measurements that passed the SAR quality assurance criteria and were used for D_e determination.

[i] The relative spread in the D_e dataset beyond that associated with the measurement uncertainties for individual D_e values, calculated using the CAM (WL15-2(6)) or CAM_{UL} (WL15-2(3)).

[j] Total uncertainty includes a systematic component of ±2% associated with laboratory beta-source calibration.

Phase 1 comprises the sediments below 1210 cm and consists of a thick sand layer at the base and intermixed sandy organic lake muds from 1266 – 1210 cm (Figure 3). The basal sands of Welsby Lagoon were OSL dated to 130 ± 15.3 ka (Tibby et al., 2017). Phase 2 occurs from 1210 – 500 cm and is comprised of homogenous, elastic, fine grained, dark organic sediments. The top 500 cm of the core is designated as phase 3 and is composed of poorly decomposed, sub-fibrous, organic sediments. Phase 1, comprising only 60 cm of the core, is represented by few analysed samples. This section is characterised by low TOC, $\delta^{13}C$, $\delta^{15}N$ values and high C:N ratios. Phase 2 and 3 comprise the remainder of the record and are clearly distinct in their geochemical properties, with no overlap in either the $\delta^{13}C$ vs. C:N and TN vs. TOC space (Figure 2). This shift in organic composition coincides with a change in sedimentology, from fine consolidated sediments to decomposed sub-fibrous peat (Figure 3). The shift in sedimentology and organic geochemistry occurs in the middle of a drive (4.5 – 5.5 m) in the WEL15-2 core and is therefore not an artefact of coring.

TOC concentrations are high throughout the record (25.3 – 67.1 %), with a 25 % increase in TOC occurring between 530 and 485 cm. In contrast, TN concentrations are low throughout the record (0.77 – 1.72 %), with a slight long-term increasing trend. The C:N ratios are lowest and least variable in phase 2, yet are consistently above 27. The highest C:N values (46.6 – 57.1) occur between 485 and 360 cm. The proportion of lignin exhibits similar trends to the C:N ratio, with lower values (11.6 – 35.6%) in phase 2, a marked increase in values between 509 – 360 cm (43.0 – 56.7 %) and maintenance of high values from 360 – 0 cm (32.2 – 45.3 %; Figure 3). Phase 2 has the highest $\delta^{15}N$ values of 1.52 – 2.8 ‰, which declined substantially between 509 – 405 cm (–1.81 to –0.87 ‰). A brief return to positive values occurs between 380 and 320 cm (0.22 to 0.52 ‰) until a decrease in $\delta^{15}N$ values from 319 – 0 cm (–0.47 to –2.23‰; Figure 3). The $\delta^{13}C$ record exhibits an inverse relationship to $\delta^{15}N$, with the lowest values (–29.8 to –27.8 ‰) occurring in phase 2 and highest values (–27.7 to –25.9 ‰) occurring in phase 3 (Figure 3).

Changes in macrofossil relative abundances display similarities with both the isotope and pollen data (Figure 4). The basal part of the record, from 1210 – 780 cm, is characterised by low concentrations of macrofossil remains, with those present being dominated by fern sporangia (cf. Polypodiaceae). After 750 cm, there is an increase in the percentage of overall plant macrofossil remains, as well as an increase in the presence of *Selaginella uliginosa*, a small perennial herb common in swampy locations, and *Lepironia articulata*, an emergent aquatic sedge which can grow in water depths ranging from no standing water to over 3 m (Marshall & McGregor, 2011). *S. uliginosa* is rare in the record above 625 cm. After the decline in *S. uliginosa*, there is a period of dominance by the charophyte macroalgae *Nitella* and emergent rush *Typha orientalis*. The dominance of *Nitella* is short lived and it is largely replaced at 505 cm by *L. articulata*, Casuarinaceae anthers and a variety of swamp adapted terrestrial herbs. In concert with the changes in the $\delta^{15}N$, C:N, lignin and emergent aquatic pollen records, the relative representation by terrestrial taxa declines above 380 cm. Macrofossil remains of *L. articulata* and Casuarinaceae anthers still occur in the upper portion of the record, however are present at much lower concentrations.

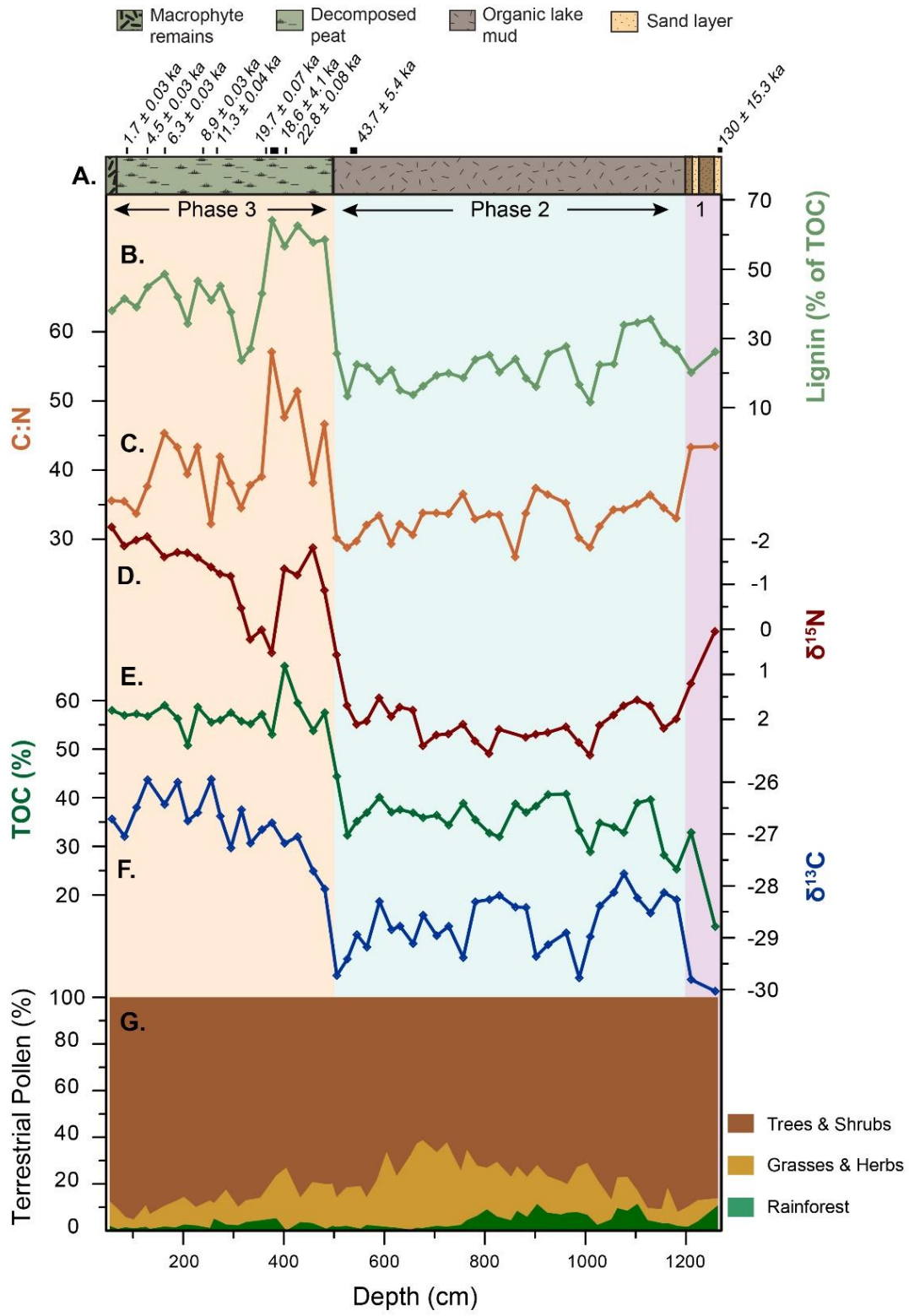

Figure 5. Summary plot of Welsby Lagoon data **A.** stratigraphic profile of 12.7 m Welsby Lagoon sedimentary sequence with description of the lithological units indicated above. Location of radiocarbon (^{14}C) and optically stimulated luminescence (OSL) dates from this study and basal date from Tibby et al. (2017) shown above the stratigraphic profile. **B**. Proportion of TOC identified as lignin from ^{13}C NMR. **C**. C:N ratio. **D**. δ^{15}N (note inverted scale). **E**. TOC %. **F.** δ^{13}C. **G**. Summed terrestrial pollen of sclerophyllous trees and shrubs, grass and herb pollen and rainforest pollen percentages. Shading denotes the three broad phases identified in the wetland record; purple = Phase 1, blue = Phase 2, orange = Phase 3.

Sedimentary pigment concentrations are generally higher at the base of the sediment core, with the highest concentrations occurring at 1081 and 566 cm (Figure 5). Chlorophyll α is undetectable in all samples, however Chlorophyll α derivatives (Pheophytin α, Pyropheophytin α and Pheophorbide α) are present in all samples with an overall declining trend towards the top of the core (Figure 5). Carotenoid pigments are abundant in all samples, with pigments indicative of green algae (Lutein and Astaxanthin) being the most abundant in samples from 1150 – 681 cm and pigments indicative of cyanobacteria (Myxoxanthophyll, Echinenone and Zeaxanthin) and colonial cyanobacteria (Canthaxanthin) being most abundant in samples from 566 – 96 cm. Although pigment concentrations were lowest in the top part of the core, they were well above the limit of detection.

4 Discussion

The modern terrestrial, algae and emergent aquatic plant samples indicate that organic material with C:N >20 may be indicative of either lacustrine algae, emergent aquatic or terrestrial plant sources. In general, terrestrial and aquatic vascular plants contain large proportions of nitrogen poor structural carbon, such as lignin, leading to high C:N ratios. Non-vascular, unicellular algae contain minimal structural carbon and are relatively nitrogen rich due to their high protein content, leading to lower C:N ratios (Meyers & Teranes, 2001; Talbot, 2001). Modern algae samples collected from NSI have C:N ratios in excess of 18, values considered in other settings to be indicative of terrestrial plants (Figure 2; Meyers and Teranes, 2001). High C:N values have previously been reported from the colonial green alga *Botryococcus* (Heyng et al., 2012) and from algal-dominated organic matter in N-limited systems (Hecky et al., 1993; Mayr et al., 2009). High C:N ratios in *Botryococcus* result from high lipid and hydrocarbon contents (Huang et al., 1999; Heyng et al., 2012). Algal growth under N-limited conditions can result in cell material with a C:N ratio as high as 20 (Hecky et al., 1993; Talbot & Lærdal, 2000; Healey & Hendzel, 2008).

Water quality data from NSI lakes show evidence for nitrogen limitation. Brown Lake, a large perched lake, has 7 years of nutrient (N and P) monitoring data. Using the Redfield ratio of 16:1 N:P as a threshold, Brown Lake was N limited for over half the monitoring period. (Supplementary Figure S4). Soil nutrient concentrations in the Cooloola dune system show that nitrogen limitation is common on younger dunes (<130 – 170 ka), with phosphorus becoming increasingly limiting on older dunes (Chen et al., 2015). In summary, nitrogen limitation may help to explain the relatively high C:N ratios of modern North Stradbroke Island algal samples.

Nitrogen limitation is inferred during phase 2 of the sedimentary record from the high levels of astaxanthin, a pigment found in green algae in nitrogen limited waters (Lee, 2008; Roy et al., 2011; Figure 5). The presence of pigments indicative of N-fixing cyanobacteria (Myxoxanthophyll, Echinenone, Canthaxanthin and Zeaxanthin) also contribute to the interpretation of N-limitation within the system, as these taxa have a competitive advantage

during times of low nitrogen availability (Vitousek et al., 2002). Low levels of inorganic nitrogen are further indicated during phase 2 by the TOC vs. TN plot that indicates the majority of nitrogen is bound with organic carbon (Figure 2B). The intercept of the regression line at 0.05% on the TN axis suggests that at the time of deposition almost all nitrogen within the system was organically bound (Talbot, 2001). Based on the change in TOC vs. TN and the presence of N-limited green algae and cyanobacterial pigments in sediments from 500 – 1200 cm, it is very likely that Welsby Lagoon has been nitrogen limited for the entirety of is existence.

Modern samples from NSI highlight the need for caution when interpreting C:N ratios. Algal organic matter produced in N-limited waters as well as colonies of the green algae *Botryococcus* have been previously been observed to produce C:N ratios greater than 20 (Hecky et al., 1993; Huang et al., 1999; Talbot & Lærdal, 2000; Heyng et al., 2012). Based on this, and the C:N ratios of modern algal samples from NSI, we conclude that the C:N ratio indicative of allochthonous material from these systems will be ≥ 20. Therefore, the C:N ratios ≥ 20 during phase 2 are interpreted here to derive from autochthonous primary productivity, namely lacustrine algae, due to continued N-limitation within the system and/or the presence of the colonial green algae *Botryococcus* (Figure 4).

4.1. Phase 1

The basal sands from Welsby Lagoon have previously been dated with OSL, returning an age of 130 ± 15.3 ka for the initial formation of the wetland (Tibby et al., 2017). From 1260 – 1210 cm sand layers are intermixed with organic lake sediments. This section of the core extends through MIS5, but it is unlikely to be continuous, as indicated by the presence of sand layers that probably represent depositional unconformities.

4.2. Phase 2

The Welsby Lagoon record from 1210 – 500 cm is comprised of 7 m of continuous, homogenous lake muds. This section of the core, to ca. 40 ka likely represents part of MIS5, the entirety of MIS4 and the majority of MIS3. It is characterised by high organic carbon inputs, and relatively low C:N and lignin values (Figure 3). We infer that the bulk of organic carbon deposition during this time was dominated by autochthonous algal primary productivity. This interpretation is supported by low $\delta^{13}C$, low macrofossil concentrations and high concentrations of algal sedimentary pigments. Sedimentary pigments in this phase are dominated by astaxanthin, a pigment produced by green algae in nitrogen-limited environments (Figure 5). The carotenoid pigments fucoxanthin, diatoxanthin and diadinoxanthin are also found in this phase and can be derived from both diatoms and dinoflagellates (Leavitt & Hodgson, 2002; Roy et al., 2011). Low but consistent inputs of echinenone and zeaxanthin and high levels of canthaxanthin, indicate the presence of N-fixing phototrophic cyanobacteria. Combined, the autotrophic pigment composition, high TOC, low TN, low C:N, and low lignin values indicate a nutrient poor, but relatively

productive, open water environment dominated by autochthonous algal organic carbon production throughout phase 2.

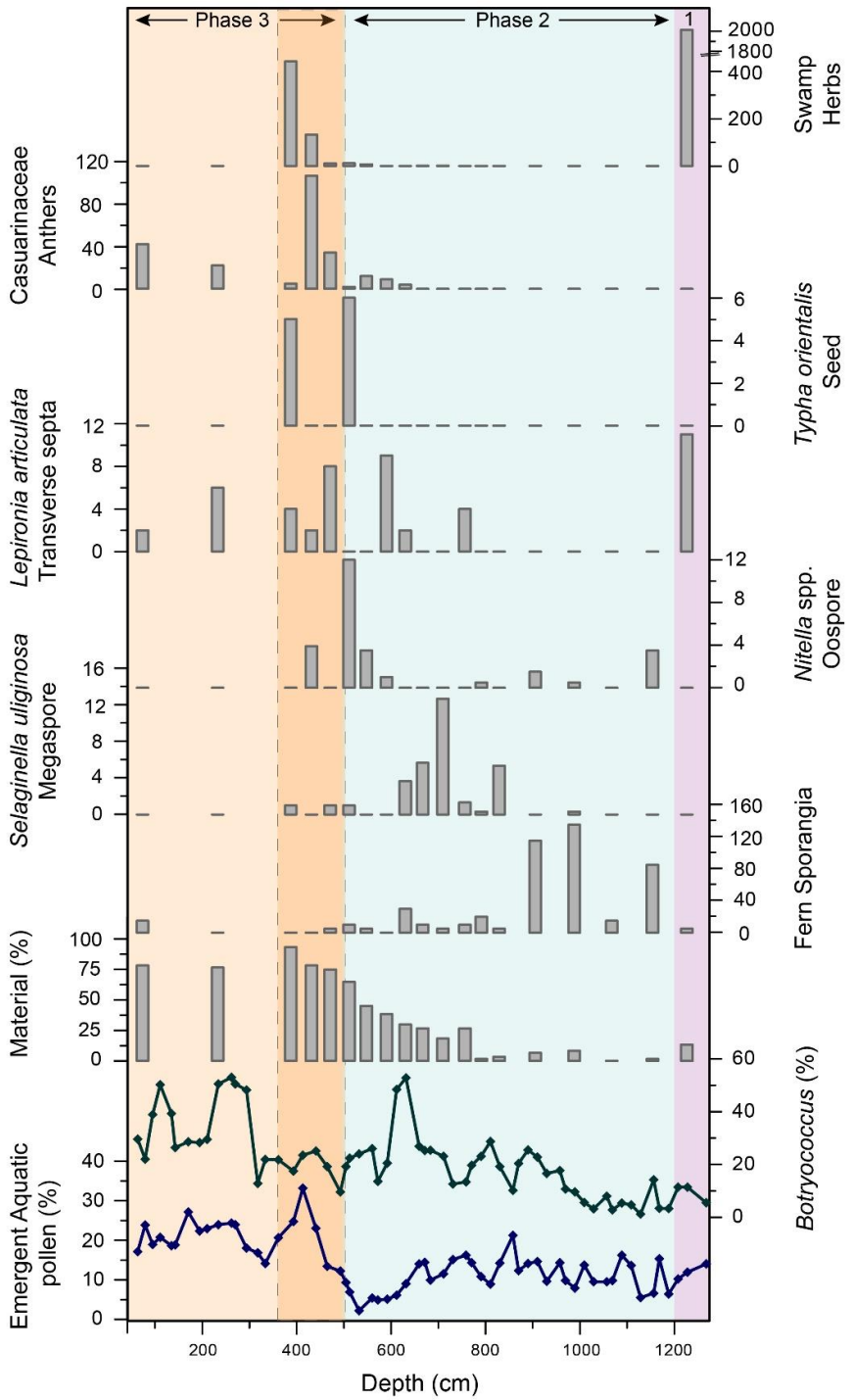

Figure 6. Macrofossil and aquatic pollen summary plot. Macrofossil count data includes all material >125 µm. Emergent aquatic pollen percentage is based on a super sum of all terrestrial and aquatic pollen taxa. *Botryococcus* percentage is based on a super sum of all terrestrial, aquatic and algal taxa. Macrofossil % material is calculated from a 5 mL aliquot of the >250 µm macrofossil sample. Swamp herbs include *Goodenia paniculata (*seed), Cyperaceae (nut), *Gonocarpus* cf. *micranthus* sub sp. *ramosissimus* (seed), cf. *Drosera* (seed), *Utricularia* (seed), *Cyperus polystachyos var. polystachyos* (nut), *Lobelia anceps* (seed) and *Hydrocotyle verticillata* (mericarp). Shading denotes the three broad phases identified in the wetland record; purple = Phase 1, blue = Phase 2, orange = Phase 3.

Sedimentary $\delta^{13}C$ generally reflects the $\delta^{13}C$ of the dominant source of organic matter entering a wetland system (Meyers & Teranes, 2001). Within the sediments of phase 2, $\delta^{13}C$ is most similar to modern algal samples from the island, though could also be derived from an approximately equal contribution of organic matter from aquatic (higher $\delta^{13}C$) and terrestrial (lower $\delta^{13}C$) vascular plant end members. However, the absence of terrestrial and emergent plant macrofossils, and low C:N and lignin values indicate that terrestrial material is unlikely to be a major contributor to sedimentary carbon, and hence that autochthonous algae is the most likely source of organic matter. During periods of enhanced algal productivity, the preferential uptake of ^{12}C depletes the carbon pool and the $\delta^{13}C$ of the dissolved inorganic carbon (DIC), and hence sedimentary carbon, becomes enriched in ^{13}C (Leng & Marshall, 2004; Leng, 2006). In addition, an increase in algal growth rate reduces the DIC-organic carbon fractionation factor during photosynthesis, resulting in higher $\delta^{13}C$ values in the organic carbon (Laws et al., 1995). Thus, isotope changes of algal-dominated sedimentary organic material are indicative of changes in lake productivity (Mayr et al., 2009). The $\delta^{13}C$ during this phase exhibits fluctuations that are therefore likely reflecting changes algal productivity. Changes in lake productivity may reflect changes in nutrient availability or depositional processes, with an increase in nutrient supply or concentration driving an increase in $\delta^{13}C$.

The $\delta^{15}N$ of sedimentary organic matter reflects multiple biogeochemical processes, including uptake of dissolved inorganic nitrogen (DIN) by primary producers, denitrification, nitrogen fixation and organic matter degradation during sedimentation (Talbot, 2001). In N-limited systems all DIN is consumed and discrimination against ^{15}N is small, resulting in $\delta^{15}N$ of organic matter that reflects the DIN pool in which it formed (Leng, 2006). Nitrogen fixing cyanobacteria have a competitive advantage in N-limited systems, and deposit organic matter with $\delta^{15}N$ which is slightly lower than that of atmospheric N (0 to –1‰). If DIN is not fully utilised, preferential uptake of ^{14}N results in organic matter that is isotopically lighter than the substrate. The $\delta^{15}N$ values through phase 2 maintains consistent positive values (Figure 3) suggesting that isotopic discrimination is small.

Whilst the geochemical signatures of organic material implies the persistence of lacustrine conditions at Welsby Lagoon during phase 2, the macrofossil record indicates a gradual shallowing and shift to drier conditions after 825 cm (Figure 4). In addition, the decline in rainforest pollen after 800 cm implies drier conditions more broadly across the island. This progressive drying is consistent with a transition to increasingly more arid climates through MIS4 and MIS3 seen in both pollen records from eastern Australia (Kershaw & Nanson, 1993; Moss & Kershaw, 2000; Kershaw et al., 2007b, 2007a) and fluvial archives that exhibit reduced activity across central and northern Australia (Chen & Barton, 1991; Nanson et al., 2008; Cohen et al., 2012, 2015b).

4.3. Late MIS3 and LGM

The second phase of the record commences at 500 cm (ca. 40 ka) with a large and permanent shift in both the amount and isotope signature of sedimentary carbon, along with a number of other of proxies ($\delta^{15}N$, C:N, lignin, autotroph pigments and macrofossil composition; Figure 3 & 4). This distinct change is not apparent in the terrestrial vegetation, suggesting that the $\delta^{13}C$, $\delta^{15}N$, TOC, C:N, lignin, autotroph pigments and macrofossil composition records primarily reflect within-wetland conditions.

The higher organic carbon input from 500 cm to present could have been driven by a reduction in water depth at the centre of the basin that prompted an increase in the dominance of emergent aquatic vegetation (Figure 3 & 4). An increase in rooted macrophytes leads to higher rates of carbon burial in sediments, as well high C:N and lignin concentrations (Saunders et al., 2014). In macrophyte dominated wetlands, the primary source of sedimentary organic matter is emergent aquatic plants that typically possess higher $\delta^{13}C$ than algae because they utilise both dissolved and atmospheric CO_2 (Gu et al., 1996). This is also the case for the modern samples from NSI that show that emergent aquatic plants tend to have higher $\delta^{13}C$ than algae (Figure 2A). A transition to an emergent macrophyte dominated wetland also explains the shift to lower $\delta^{15}N$ values. Rooted macrophytes often have negative $\delta^{15}N$ values due to their ability to utilise nitrogen both from the water column and recycled from decomposing sediments (Barko et al., 1991; Drew et al., 2008; Chang et al., 2009).

The transition to an emergent macrophyte dominated system is also reflected in the macrofossil and aquatic pollen records, with an increase in aquatic plant remains and aquatic pollen occurring above 505 and 460 cm respectively (Figure 5). The decrease in total concentration of sedimentary pigments from 500 cm could be a result of reduced algal productivity, dilution by pigment-poor lithic material and/or shallowing water. Photosynthetic pigments are highly labile and degradation can occur with increases in light, oxygen and temperature (Sanger, 1988), conditions associated with shallowing water.

The transition of Welsby Lagoon from a lake to an emergent macrophyte dominated swamp may have resulted from a shift in climate or by crossing a threshold of basin infilling, or a combination of the two. A return to deeper water following this transition is indicative of a climate control, rather than a threshold of basin infilling being reached. A hypothesised hydrological driver, is supported by proxy changes (i.e. reduction in lignin, C:N, macrophyte macrofossils and pollen and $\delta^{15}N$) after 380 cm (ca. 18 ka), indicating a return to less terrestrial, deeper water conditions similar to phase 2 of the record. The timing of this increase in moisture is consistent with locally inferred wetter conditions (Moss et al., 2013; Barr et al., 2017; Petherick et al., 2017), as well as broader regional conditions that indicate increased precipitation during the early deglacial (18 – 15 ka; Kershaw et al., 2007b; Petherick et al., 2008, 2011, Reeves et al., 2013a, 2013b).

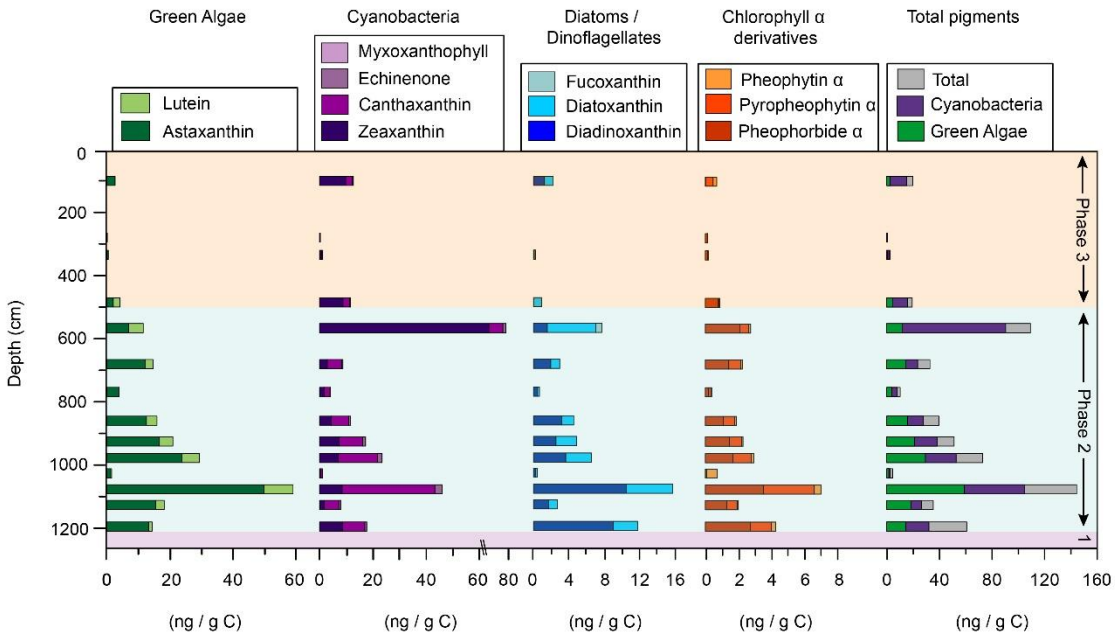

Figure 7. Sedimentary pigment concentration data grouped according to most likely major sources determined from Leavitt and Hodgson (2002) and Roy et al. (2011). All pigment concentrations are expressed as a portion of TOC. Shading denotes the three broad phases identified in the wetland record; purple = Phase 1, blue = Phase 2, orange = Phase 3. Leavitt and Hodgson (2002) and Roy et al. (2011).

The desiccation of sediments from an edge core from of Welsby Lagoon (Figure 1C) at ca. 22 ka (Chang et al., 2015; Barr et al., 2017) indicates that the standing water of the wetland had contracted towards the middle of the site during this time. The proxy records (TOC, $\delta^{13}C$, lignin, C:N, macrofossils, pollen and $\delta^{15}N$) suggest a shallowing of the wetland between 500 – 360 cm, however continued deposition of organic wetland sediments at the centre of the lagoon indicates there was still sufficient moisture to sustain the Welsby Lagoon wetland. In addition to the positive moisture balance inferred from the aquatic proxies, the terrestrial pollen record suggests that arboreal vegetation persisted throughout this period, in contrast to the dominance of grass and herb vegetation in other parts of Australia (van der Kaars & De Deckker, 2002; Kershaw et al., 2007b, 2007a). The absence of sand layers and the persistence of arboreal pollen taxa indicates that the landscape of NSI was relatively stable from MIS5 to present. An island-wide landscape stability is supported by pollen records from Native Companion Lagoon and Tortoise Lagoon, and the absence of sand layers in other NSI wetland records (Moss et al., 2013; Barr et al., 2017; Tibby et al., 2017). There are three potential hypotheses that could lead to the persistence of a shallow wetland during the LGM: 1. Connection of the site to a perched aquifer of sufficient size (volume) to buffer rainfall deficits; or 2. Climate along the lower east coast of Australia were not significantly drier than today; or 3. Despite a reduction in precipitation, lower temperatures reduce the evaporative effect across the wetland.

Welsby Lagoon is predominantly supported by a perched aquifer that extends beyond the surface expression of the wetland (Figure 6). Contemporary observations have shown that the surface water can be lost during annual and inter-annual drought periods; however,

during these events the wetland sediments remain inundated by the perched aquifer. Therefore, the buffering effect of the perched aquifer may have contributed to creating a positive moisture balance at this site during dry periods.

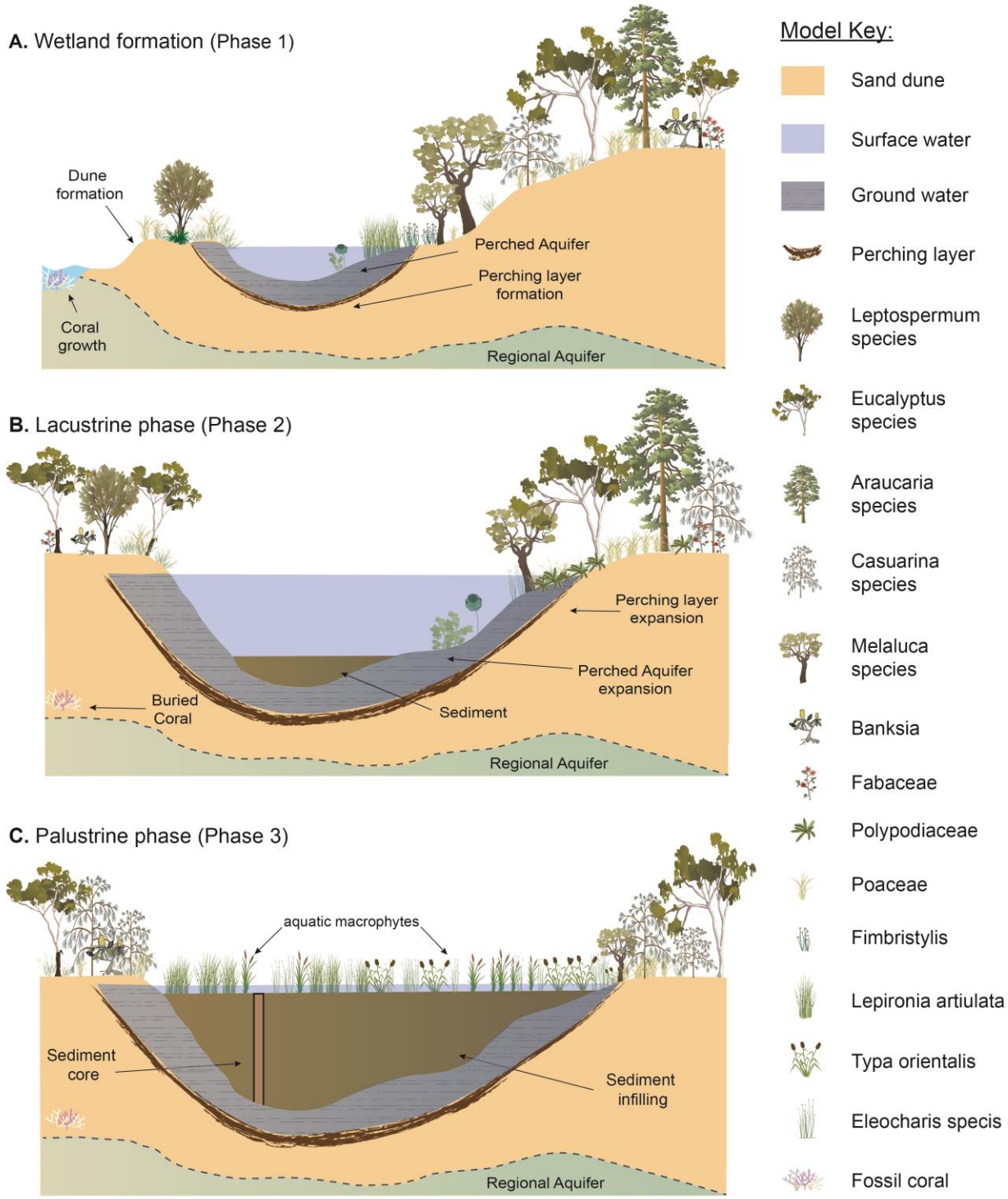

Figure 8. Welsby Lagoon development conceptual model of the A. development of the wetland, B. evolution through an algal dominated lacustrine system, and C. macrophyte dominated shallow swamp phase. Basin morphology defined from basin profile determined in Figure 1. Vegetation images from Integration and Application Network (2018).

NSI would have maintained a relatively coastal position, even during the lowest sea level stands of the LGM, due to its location close to the edge of the continental shelf (Figure 1A). An increasing body of evidence has emerged in the last two decades indicating that regions of Australia were not as arid during the LGM as previously thought (Nanson et al., 2008; Petherick et al., 2008; Cohen et al., 2012; Reeves et al., 2013a; Tibby et al., 2017). The maintenance of a maritime climate during this period may have tempered the effects of a more arid climate seen across other regions of Australia, allowing Welsby Lagoon, and other sites on the island (Moss et al., 2013; Petherick et al., 2017; Tibby et al., 2017), to maintain a positive moisture balance. An increase in water availability may be driven by increased rainfall or reduced evaporation rates resulting from depressed temperatures. The maintenance of organic deposition in the centre of Welsby Lagoon during the LGM indicates a positive moisture was maintained for the entirety of this record. The persistence of a number of wetland sites across NSI during the LGM and presence of arboreal pollen suggest that changes in precipitation were not sufficiently large to cause these wetlands to dry or shift the local vegetation from an open woodland to non-arboreal vegetation system (Moss et al., 2013; Petherick et al., 2017).

4.4. Deglacial and Holocene

The recommencement of peat accumulation after ca. 19 ka on the Welsby Lagoon fringe indicates inundation of the wetland margin and increased moisture balance at the site (Barr et al., 2017). A shift to more moist conditions is also suggested in the centre of the wetland at this time. Terrestrial indicators (swamp herbs and Casuarinaceae anthers) and emergent macrophyte fossils decline after 380 cm (Figure 4). These indicators are closely followed by a decline in sedimentary lignin and an increase in $\delta^{15}N$, implying a reduction in the dominance of aquatic macrophytes (Figure 3). Together these data suggest that our core site at the centre of the wetland reverted to a deeper water system at the beginning of the deglacial.

A permanent palustrine wetland developed during the Holocene (above 260 cm) and is characterised by higher mean lignin, TOC, $\delta^{13}C$ and lower $\delta^{15}N$. It is possible that after the period of increased inputs of organic carbon, driven by the dominance of emergent macrophytes, the wetland crossed a critical threshold of basin infilling. If the level of sediment surface (due to infilling) surpasses the highest level of the perched aquifer (i.e. the perching layer), the water-holding capacity of the site would prevent the development of deep water as any excess would 'overflow' through the sandy regolith. Therefore, the surface expression of the Welsby Lagoon aquifer is dependent on the limit of the perched water table, the morphology of the basin and the depth of sediment surface. The current Welsby Lagoon wetland contains 12.7 m of sediment and is presently a palustrine wetland dominated by emergent sedges (Figure 6). Sediment has largely filled the basin and the present water depth varies seasonally, ranging between 0 and 1.5 m. In conjunction with the palaeolimnological information garnered in this study, it is clear that the Welsby Lagoon basin is approaching the terminal stage of lake succession.

5 Conclusions

We have inferred the evolution of Welsby Lagoon and its interactions with broad scale prevailing climate for the last ca. 130,000 years by considering patterns in the variability of multiple proxies preserved in the 12.7 m sediment sequence of Welsby Lagoon. The formation of a perching layer in the basin that now supports Welsby Lagoon occurred at ca.130 ka during MIS5e. Continuous sediment deposition began sometime after this and has persisted until present.

The Welsby Lagoon sediments from 1210 cm to 500 cm indicate an open-water lake environment dominated by aquatic algae. Gradual shallowing of the wetland after 825 cm was associated with an increased dominance of emergent aquatic macrophytes and terrestrial swamp herbs. Progressive climatic drying after 800 cm led to a decline in regional rainforest vegetation. After 500 cm the wetland transitioned to a shallower, emergent macrophyte dominated swamp environment.

The interval between 500 and 360 cm was the driest in the history of the site, yet the centre of Welsby Lagoon maintained a positive moisture balance, as indicated by the continued deposition of organic peat. Between 360 – 300 cm there is an indication the site had more areas of open water. Shallow palustrine swamp conditions occur after 300 cm that persist until present.

The understanding garnered from this foundation study provides a strong basis for using this site for further investigations into Australian palaeoclimate and palaeoecology. The development of a robust age model to tightly constrain the record is a key research priority to identify key Quaternary events, such as arrival of humans and extinction of megafauna. The Welsby Lagoon sedimentary record offers an opportunity to become a key Australian sedimentary archive to contribute to an enhanced global understanding of Quaternary climate and ecosystem responses.

Acknowledgments

We acknowledge Minjerribah (NSI) and the surrounding waters as Quandamooka Country. The study was funded by Australian Research Council project DP150103875. We thank Jie Chang, Jacinta Greer, Matthew Jones, Patrick Moss and Cameron Schulz for assistance in the field. We sincerely thank Fred Oudyn for analysis and data processing of pigment samples with such efficiency and Janine McGowan (CSIRO Agriculture and Food) for assistance with NMR sample analysis and data processing. We thank Adriana Garcia for assistance with macrofossil identification. Discussions with Carl Sayer, Tim Page and Paul Smith improved our understanding.

References

Aitken, M.J. (1985) *Thermoluminescence dating.*

Aitken, M.J. (1998) *An introduction to optical dating: The dating of Quaternary sediments by the use of photon-stimulated luminescence.*

Arnold, L.J., Bailey, R.M., & Tucker, G.E. (2007) Statistical treatment of fluvial dose distributions from southern Colorado arroyo deposits. *Quaternary Geochronology*, **2**, 162–167.

Arnold, L.J., Demuro, M., Navazo, M., Benito-Calvo, A., & Pérez-González, A. (2013) OSL dating of the Middle Palaeolithic Hotel California site, Sierra de Atapuerca, north-central Spain. *Boreas*, **42**, 285–305.

Arnold, L.J., Duval, M., Demuro, M., Spooner, N.A., Santonja, M., & Pérez-González, A. (2016) OSL dating of individual quartz 'supergrains' from the Ancient Middle Palaeolithic site of Cuesta de la Bajada, Spain. *Quaternary Geochronology*, **36**, 78–101.

Arnold, L.J., Roberts, R.G., Galbraith, R.F., & DeLong, S.B. (2009) A revised burial dose estimation procedure for optical dating of youngand modern-age sediments. *Quaternary Geochronology*, **4**, 306–325.

Baldock, J.A., Sanderman, J., Macdonald, L.M., Puccini, A., Hawke, B., Szarvas, S., & McGowan, J. (2013) Quantifying the allocation of soil organic carbon to biologically significant fractions. *Soil Research*, **51**, 561.

Barko, J.W., Gunnison, D., & Carpenter, S.R. (1991) Sediment interactions with submersed macrophyte growth and community dynamics. *Aquatic Botany*, **41**, 41–65.

Barr, C., Tibby, J., Marshall, J.C., Mcgregor, G.B., Moss, P.T., Halverson, G.P., & Fluin, J. (2013) Combining monitoring, models and palaeolimnology to assess ecosystem response to environmental change at monthly to millennial timescales: The stability of Blue Lake, North Stradbroke Island, Australia. *Freshwater Biology*, **58**, 1614–1630.

Barr, C., Tibby, J., Moss, P.T., Halverson, G.P., Marshall, J.C., McGregor, G.B., & Stirling, E. (2017) A 25,000-year record of environmental change from Welsby Lagoon, North Stradbroke Island, in the Australian subtropics. *Quaternary International*, **449**, 106–118.

Birks, H.H. (2002) Plant Macrofossils. *Tracking Environmental Change Using Lake Sediments: Terrestrial, Algal, and Siliceous Indicators* (ed. by J.P. Smol, H.J.B. Birks, W.M. Last, R.S. Bradley, and K. Alverson), pp. 49–74. Springer Netherlands, Dordrecht.

Birks, H.H. & Birks, H.J.B. (2006) Multi-proxy studies in palaeolimnology. *Vegetation History and Archaeobotany*, **15**, 235–251.

Black, M.P., Mooney, S.D., & Martin, H.A. (2006) A 43,000-year vegetation and fire history from Lake Baraba, New South Wales, Australia. *Quaternary Science Reviews*, **25**, 3003–3016.

Blindow, I. (1992) Long- and short-term dynamics of submerged macrophytes in two shallow eutrophic lakes. *Freshwater Biology*, **28**, 15–27.

BOM & BOM, (Australian Bureau of Meterology) (2018) Available at: http://www.bom.gov.au/climate/averages/tables/cw_040209.shtml.

Brennan, B.J. (2003) Beta doses to spherical grains. *Radiation Measurements*, **37**, 299–303.

Chang, C.C.Y., McCormick, P. V., Newman, S., & Elliott, E.M. (2009) Isotopic indicators of environmental change in a subtropical wetland. *Ecological Indicators*, **9**, 825–836.

Chang, J.C., Shulmeister, J., Woodward, C., Steinberger, L., Tibby, J., & Barr, C. (2015) A chironomid-inferred summer temperature reconstruction from subtropical Australia during the last glacial maximum (LGM) and the last deglaciation. *Quaternary Science Reviews*, **122**, 282–292.

Chen, C.R., Hou, E.Q., Condron, L.M., Bacon, G., Esfandbod, M., Olley, J., & Turner, B.L. (2015) Soil phosphorus fractionation and nutrient dynamics along the Cooloola coastal dune chronosequence,

southern Queensland, Australia. *Geoderma*, **257–258**, 4–13.

Chen, X.Y. & Barton, C.E. (1991) Onset of aridity and dune-building in central Australia: sedimentological and magnetostratigraphic evidence from Lake Amadeus. *Palaeogeography, Palaeoclimatology, Palaeoecology*, **84**, 55–73.

Clark, R.L. (1982) Point Count Estimation of Charcoal in Pollen Preparation and Thin Sections of Sediments. *Pollen et Spores*, **24**, 523–535.

Clarkson, C., Jacobs, Z., Marwick, B., et al. (2017) Human occupation of northern Australia by 65,000 years ago. *Nature*, **547**, 306–310.

Cohen, T.J., Jansen, J.D., Jansen, J.D., & Larsen, J.R. (2015) Drying inland seas probably helped kill Australia's megafauna. *The Conversation*, 1–3.

Cohen, T.J., Nanson, G.C., Jansen, J.D., Jones, B.G., Jacobs, Z., Larsen, J.R., May, J.H., Treble, P., Price, D.M., & Smith, A.M. (2012) Late Quaternary mega-lakes fed by the northern and southern river systems of central Australia: Varying moisture sources and increased continental aridity. *Palaeogeography, Palaeoclimatology, Palaeoecology*, **356–357**, 89–108.

D'Costa, D.M., Grindrod, J., & Ogden, R. (1993) Preliminary environmental reconstructions from late Quaternary pollen and mollusc assemblages at Egg Lagoon, King Island, Bass Strait. *Australian Journal of Ecology*, **18**, 351–366.

Drew, S., Flett, I., Wilson, J., Heijnis, H., & Skilbeck, C.G. (2008) The trophic history of Myall Lakes, New South Wales, Australia: Interpretations using δ13C and δ15N of the sedimentary record. *Hydrobiologia*, **608**, 35–47.

Finlay, J.C. & Kendall, C. (2008) Stable isotope tracing of temporal and spatial variability in organic matter sources to freshwater ecosystems. *Stable Isotopes in Ecology and Environmental Science* (ed. by R. Michener and K. Lajtha), pp. 283–333. Blackwell Publishing Ltd, Oxford.

Galbraith, R.F., Roberts, R.G., Laslett, G.M., Yoshida, H., Olley, J.M., Galbraith, R.F., Olley, J.M., Yoshida, H., & Laslett, G.M. (1999) Optical dating of single and multiple grains of quartz from Jinmium rock shelter, Northern Australia: Part I, Experimetal design and statistical models. *Archaeometry*, **41**, 339–364.

Gallant, J.C., Dowling, T.I., Read, A.M., Wilson, N., Tickle, P., & Inskeep, C. (2011) 1 second SRTM Derived Digital Elevation Models User Guide. .

Gu, B., Schelske, C.L., & Brenner, M. (1996) Relationship between sediment and plankton isotope ratios (δ13C and δ15N) and primary productivity in Florida lakes. *Canadian Journal of Fisheries and Aquatic Sciences*, **53**, 875–883.

Guérin, G., Mercier, N., & Adamiec, G. (2011) Dose-rate conversion factors: update. *Ancient TL*, **29**, 5–8.

Hamm, G., Mitchell, P., Arnold, L.J., Prideaux, G.J., Questiaux, D., Spooner, N.A., Levchenko, V.A., Foley, E.C., Worthy, T.H., Stephenson, B., Coulthard, V., Coulthard, C., Wilton, S., & Johnston, D. (2016) Cultural innovation and megafauna interaction in the early settlement of arid Australia. *Nature*, **539**, 280–283.

Harle, K.J., Heijnis, H., Chisari, R., Kershaw, A.P., Zoppi, U., & Jacobsen, G. (2002) A chronology for the long pollen record from Lake Wangoom, western Victoria (Australia) as derived from uranium/thorium disequilibrium dating. *Journal of Quaternary Science*, **17**, 707–720.

Healey, F.P. & Hendzel, L.L. (2008) Physiological Indicators of Nutrient Deficiency in Lake Phytoplankton. *Canadian Journal of Fisheries and Aquatic Sciences*, **37**, 442–453.

Hecky, R.E., Campbell, P., & Hendzel, L.L. (1993) The stoichiometry of carbon, nitrogen, and phosphorus in particulate matter of lakes and oceans. *Limnology and Oceanography*, **38**, 709–724.

Heyng, A.M., Mayr, C., Lücke, A., Striewski, B., Wastegård, S., & Wissel, H. (2012) Environmental changes in northern New Zealand since the Middle Holocene inferred from stable isotope records (δ15N, δ13C) of Lake Pupuke. *Journal of Paleolimnology*, **48**, 351–366.

Huang, Y., Street-Perrott, F.A., Perrott, R.A., Metzger, P., & Eglinton, G. (1999) Glacial-interglacial environmental changes inferred from molecular and compound-specific δ13C analyses of sediments from Sacred Lake, Mt. Kenya. *Geochimica et Cosmochimica Acta*, **63**, 1383–1404.

Johnson, C., Rule, S., Haberle, S.G., Kershaw, A.P., McKenzie, G.M., & Brook, B.W. (2016) Geographic variation in the ecological effects of extinction of Australia's Pleistocene megafauna. *Ecography*, **39**, 109–116.

Juggins, S. (2015) rioja: Anlaysis of Quaternary science data. *R package ver. 0.9-5*, 1–58.

van der Kaars, S. & De Deckker, P. (2002) A late quaternary pollen record from deep-sea core Fr10/95, GC17 offshore Cape Range Peninsula, northwestern Western Australia. *Review of Palaeobotany and Palynology*, **120**, 17–39.

Kershaw, A.P., Bretherton, S.C., & van der Kaars, S. (2007a) A complete pollen record of the last 230 ka from Lynch's Crater, north-eastern Australia. *Palaeogeography, Palaeoclimatology, Palaeoecology*, **251**, 23–45.

Kershaw, A.P., McKenzie, G.M., Porch, N., Roberts, R.G., Brown, J., Heijnis, H., & Orr, M.. (2007b) A high-resolution record of vegetation and climate through the last glacial cycle from Caledonia Fen, southeastern highlands of Australia. *Journal of Quaternary Science*, **22**, 801–815.

Kershaw, A.P. & Nanson, G.C. (1993) The last full glacial cycle in the Australian region. *Global and Planetary Change*, **7**, 1–9.

Laws, E.A., Popp, B.N., Bidigare, R.R., Kennicutt, M.C., & Macko, S.A. (1995) Dependence of phytoplankton carbon isotopic composition on growth rate and [CO2)aq: Theoretical considerations and experimental results. *Geochimica et Cosmochimica Acta*, **59**, 1131–1138.

Leach, L.M. (2011) Hydrological and physical setting of North Stradbroke Island. *Proceedings of the Royal Society of Queensland*, **117**, 21–46.

Leavitt, P.R. & Hodgson, D.A. (2002) Sedimentary Pigments. *Tracking Environmental Change Using Lake Sediments* pp. 295–325.

Lee, R.E. (2008) *Phycology.* Cambridge University Press, New York.

Lees, B. (2006) Timing and Formation of Coastal Dunes in Northern and Eastern Australia. *Journal of Coastal Research*, **221**, 78–89.

Leng, M.J. (2006) *Isotopes in Palaeoenvironmental Research.* Kluwer Academic Publishers, Dordrecht.

Leng, M.J. & Marshall, J.D. (2004) Palaeoclimate interpretation of stable isotope data from lake sediment archives. *Quaternary Science Reviews*, **23**, 811–831.

Lewis, T. (2012) A plant macrofossil identification tool for south-west Victoria. *The Artefact*, **35**, 88–98.

Longmore, M.E. (1997) Quaternary palynological records from perched lake sediments, Fraser Island, Queensland, Australia: Rainforest, forest history and climatic control. *Australian Journal of Botany*, **45**, 507–526.

Marshall, J.C. & McGregor, G.B. (2011) The influence of water depth on the distribution of the emergent sedge Lepironia articulata (Cyperaceae) in two dune lakes of southern Queensland Coastal Wallum Wetlands. *The Proceedings of the Royal Society of Queensland*, **117**, 193–199.

Mayr, C., Lücke, A., Maidana, N.I., Wille, M., Haberzettl, T., Corbella, H., Ohlendorf, C., Schäbitz, F., Fey, M., Janssen, S., & Zolitschka, B. (2009) Isotopic fingerprints on lacustrine organic matter from Laguna Potrok Aike (southern Patagonia, Argentina) reflect environmental changes during the last 16,000 years. *Journal of Paleolimnology*, **42**, 81–102.

Mejdahl, V. (1979) Thermoluminescence Dating: Beta-Dose Attenuation in Quartz Grains. *Archaeometry*, **21**, 61–72.

Mettam, P., Tibby, J., Barr, C., & Marshall, J.C. (2011) Development of Eighteen Mile Swamp, North Stradbroke Island: a palaeolimnological study. *Proceedings of the Royal Society of Queensland*, **117**, 119–131.

Meyers, P.A. & Teranes, J.L. (2001) Sediment Organic Matter. *Tracking Environmental Change Using Lake Sediments: Physical and Geochemical Methods* (ed. by W.M. Last and J.P. Smol), pp. 239–269. Springer Netherlands, Dordrecht.

Miot da Silva, G. & Shulmeister, J. (2016) A Review of Coastal Dunefield Evolution in Southeastern Queensland. *Journal of Coastal Research*, **75**, 308–312.

Mosisch, T.D. & Arthington, A.H. (2001) Polycyclic aromatic hydrocarbon residues in the sediments of a dune lake as a result of power boating. *Lakes and Reservoirs: Research and Management*, **6**, 21–32.

Moss, P.T. & Kershaw, A.P. (2000) The last glacial cycle from the humid tropics of northeastern Australia: Comparison of a terrestrial and a marine record. *Palaeogeography, Palaeoclimatology, Palaeoecology*, **155**, 155–176.

Moss, P.T., Petherick, L., & Neil, D. (2011) Environmental Change at Myora Springs, North Stradbroke Island Over the Last Millenium. *Proceedings of the Royal Society of Queensland*, **117**, 113–140.

Moss, P.T., Tibby, J., Petherick, L., McGowan, H., & Barr, C. (2013) Late Quaternary vegetation history of North Stradbroke Island, Queensland, eastern Australia. *Quaternary Science Reviews*, **74**, 257–272.

Murray, A.S. & Wintle, A.G. (2000) Luminescence dating of quartz using an improved single-aliquot regenerative-dose protocol. *Radiation Measurements*, **32**, 57–73.

Myrbo, A. & Wright, H.E. (2008) SOP: Livingstone-bolivia. .

Nanson, G.C., Price, D.M., Jones, B.G., Maroulis, J.C., Coleman, M., Bowman, H., Cohen, T.J., Pietsch, T.J., & Larsen, J.R. (2008) Alluvial evidence for major climate and flow regime changes during the middle and late Quaternary in eastern central Australia. *Geomorphology*, **101**, 109–129.

Petherick, L., McGowan, H., & Moss, P. (2008) Climate variability during the Last Glacial Maximum in eastern Australia: Evidence of two stadials? *Journal of Quaternary Science*, **23**, 787–802.

Petherick, L.M., Moss, P.T., & McGowan, H.A. (2011) Climatic and environmental variability during the termination of the Last Glacial Stage in coastal eastern Australia: a review. *Australian Journal of Earth Sciences*, **58**, 563–577.

Petherick, L.M., Moss, P.T., & McGowan, H.A. (2017) An extended Last Glacial Maximum in subtropical Australia. *Quaternary International*, **432**, 1–12.

Prescott, J.R. & Hutton, J.T. (1994) Cosmic ray contributions to dose rates for luminescence and ESR dating: Large depths and long-term time variations. *Radiation Measurements*, **23**, 497–500.

Pye, K. (1993) Late Quaternary development of coastal parabolic megadune complexes in northeastern Australia. *Aeolian sediments : Ancient and modern* (ed. by K. Pye and N. Lancaster), pp. 167. Blackwell Scientific Publications,

R Core Team (2017) R: A Language and Environment for Statistical Computing. *R Foundation for Statistical Computing, Vienna, Austria*, **0**, {ISBN} 3-900051-07-0.

Rees-Jones, J. (1995) Optical dating of young sediments using fine-grain quartz. *Ancient TL*, **13**, 9–14.

Rees-Jones, J. & Tite, M.S. (1997) Optical Dating Results for British Archaeological Sediments. *Archaeometry*, **39**, 177–187.

Reeves, J.M., Barrows, T.T., Cohen, T.J., et al. (2013a) Climate variability over the last 35,000 years recorded in marine and terrestrial archives in the Australian region: An OZ-INTIMATE compilation. *Quaternary Science Reviews*, **74**, 21–34.

Reeves, J.M., Bostock, H.C., Ayliffe, L.K., et al. (2013b) Palaeoenvironmental change in tropical Australasia over the last 30,000 years - a synthesis by the OZ-INTIMATE group. *Quaternary Science Reviews*, **74**, 97–114.

Roberts, R.G., Flannery, T.F., Ayliffe, L.K., Yoshida, H., Olley, J.M., Prideaux, G.J., Laslett, G.M., Baynes, A., Smith, M.A., Jones, R., & Smith, B.L. (2001) New ages for the last Australian megafauna: continent-wide extinction about 46,000 years ago. *Science*, **292**, 1888–1892.

Roy, S., Llewellyn, C., Egeland, E.S., & Johnsen, G. (2011) *Phytoplankton Pigments: Characterization,*

Chemotaxonomy and Applications in Oceanography. Cambridge University Press, Cambridge.

Rule, S., Brook, B.W., Haberle, S.G., Turney, C.S.M., Kershaw, A.P., & Johnson, C.N. (2012) The Aftermath of Megafaunal Extinction: Ecosystem Transformation in Pleistocene Australia. *Science*, **335**, 1483–1486.

Sanger, J.E. (1988) Fossil pigments in paleoecology and paleolimnology. *Palaeogeography, Palaeoclimatology, Palaeoecology*, **62**, 343–359.

Saunders, M.J., Kansiime, F., & Jones, M.B. (2014) Reviewing the carbon cycle dynamics and carbon sequestration potential of Cyperus papyrus L. wetlands in tropical Africa. *Wetlands Ecology and Management*, **22**, 143–155.

Schlesinger, W.H. & Bernhardt, E.S. (2013) *Biogeochemistry: An Analysis of Global Change.* Academic Press,

Singh, G., Opdyke, N.D., & Bowler, J.M. (1981) Late Cainozoic stratigraphy, palaeomagnetic chronology and vegetational history from Lake George, N.S.W. *Journal of the Geological Society of Australia*, **28**, 435–452.

Specht, A. & Stubbs, B.J. (2011) Long-term monitoring of a coastal sandy freshwater wetland: Eighteen Mile Swamp, North Stradbroke Island, Queensland. *Proceedings of the Royal Society of Queensland*, **December**, 201–223.

Stephens, K.M. & Sharp, D. (2009) *The flora of North Stradbroke Island.* State of Queensland, Environmental Protection Agency,

Talbot, M.R. (2001) Nitrogen Isotopes in Palaeolimnology. *Tracking Environmental Change Using Lake Sediments* pp. 401–439.

Talbot, M.R. & Lærdal, T. (2000) The Late Pleistocene - Holocene palaeolimnology of Lake Victoria, East Africa, based upon elemental and isotopic analyses of sedimentary organic matter. *Journal of Paleolimnology*, **23**, 141–164.

Thompson, C.H. (1981) Podzol chronosequences on coastal dunes of eastern Australia. *Nature*, **291**, 59–61.

Tibby, J., Barr, C., Marshall, J.C., McGregor, G.B., Moss, P.T., Arnold, L.J., Page, T.J., Questiaux, D., Olley, J., Kemp, J., Spooner, N., Petherick, L., Penny, D., Mooney, S., & Moss, E. (2017) Persistence of wetlands on North Stradbroke Island (south-east Queensland, Australia) during the last glacial cycle: implications for Quaternary science and biogeography. *Journal of Quaternary Science*, **32**, 770–781.

Timms, B. (1986) The coastal dune lakes of eastern Australia. *Limnology in Australia* (ed. by P. Deckker and W.D. Williams), pp. 688. Springer Netherlands,

Turney, C.S.M., Haberle, S.G., Fink, D., Kershaw, A.P., Barbetti, M., Barrows, T.T., Black, M., Cohen, T.J., Correge, N.J., Zhao, J. xin, D'Costa, D.M., Feng, Y. xing, Gagan, M.K., Mooney, S.D., & Xia, Q. (2006) Integration of ice-core, marine and terrestrial records for the Australian Last Glacial Maximum and Termination: a contribution from the OZ INTIMATE group. *Journal of Quaternary Science*, **21**, 751–761.

Turney, C.S.M., Kershaw, a P., Clemens, S.C., Branch, N., Moss, P.T., & Fifield, L.K. (2004) Millennial and orbital variations of El Niño/Southern Oscillation and high-latitude climate in the last glacial period. *Nature*, **428**, 306–10.

Vitousek, P.M., Cassman, K., Cleveland, C., Crews, T., Field, C.B., Grimm, N.B., Howarth, R.W., Marino, R., Martinelli, L., Rastetter, E.B., & Sprent, J.I. (2002) Towards an ecological understanding of biological nitrogen fixation. *Biogeochemistry*, .

Walker, J., Thompson, C.H., Fergus, I.F., & Tunstall, B.R. (1981) Plant Succession and Soil Development in Coastal Sand Dunes of Subtropical Eastern Australia. *Forest Succession: concepts and application* (ed. by D.C. West, H.H. Shugart, and D.F. Botkin), pp. 107–131. Springer, New York. .

6 Supplementary Information

Single grain OSL dating

A total of 500 individual quartz grains from each sample were analysed for equivalent dose (De) determination using the single-aliquot regenerative-dose (SAR) method outlined in Table S1. In total, 16 % of measured grains from sample WL15-2(3) and 23 % of measured grains from sample WL15-2(6) were considered suitable for single grain OSL dating after applying the quality assurance criteria outlined in Table S2.

The De dataset of sample WL15-2(6) exhibits moderate overdispersion of 34% (Table S3, Figure S1b), which is consistent at 2σ with the overdispersion values obtained for well-bleached and unmixed aeolian deposits at Welsby Lagoon (Lewis et al., Accepted). The final burial dose of this sample has therefore been calculated using the central age model (CAM) (Galbraith et al., 1999). The De dataset of sample WL15-2(3) is characterised by enhanced inter-grain scatter and a much higher overdispersion value of 117% (Table S3, Figure S1a). These De distribution characteristics are interpreted as reflecting insufficient bleaching of some grains prior to deposition and burial (e.g., (Olley et al., 2004, Bailey and Arnold, 2006). This sample also contains a significant number of grains with near-zero Gy De values; 34% of accepted grains having individual De values consistent with 0 Gy at 2σ. The final burial dose of this sample has therefore been calculated using the four-parameter unlogged minimum age model of Arnold et al. (2009).

Table S1: Single-aliquot regenerative-dose (SAR) procedures used for D_e determination. L_x = regenerative-dose OSL signal response; L_n = natural dose OSL signal response; T_x = test dose OSL signal response for a laboratory dose cycle T_n = test dose OSL signal response for the natural dose cycle.

OSL SAR procedure		
Step	Treatment	Signal
1	Give dose (natural or laboratory)	
2[a]	IRSL stimulation (50°C for 60 s)	
3	Preheat 1 (PH_1 = 260°C for 10 s)	
4	Single grain OSL stimulation (125°C for 2 s)	L_n or L_x
5	Test dose (9-10 Gy)	
6	Preheat 2 (PH_2 = 160°C for 10 s)	
7	Single grain OSL stimulation (125°C for 2 s)	T_n or T_x
8	Repeat cycle for different regenerative doses	

[a] Step 2 is only included in the single-grain OSL SAR procedure when measuring the OSL IR depletion ratio (Duller 2003).

Table S2: Single grain OSL classification statistics for the Welsby Lagoon sequence samples, following the quality assurance criteria of Arnold (2007). The proportion of grains that were rejected from the final D_e estimation after applying the various quality assurance criteria are shown in rows 7-13.

Sample name	WL15-2(3)	WL15-2(6)
Depth (cm)	380	510
SAR protocol	SG OSL	SG OSL
Total measured grains	500	500
Reason for rejecting grains from De analysis		
Standard SAR rejection criteria:	%	%
Tn <3σ background	60.6	44.6
Dose recycling ratio ≠ 1 at ±2σ	8	14.6
OSL-IR depletion ratios <1 at ±2σ	3	4.8
0 Gy L_x/T_x >5% L_n/T_n	0.8	0.0
Additional rejection criteria:		
Saturated grains (Ln/Tn ≥ dose response curve Imax at ±2σ)	0.4	0.0
Anomalous dose response / unable to perform Monte Carlo fit	10.8	13.2
Sum of rejected grains (%)	83.6	77.2
Sum of accepted grains (%)	16.4	22.8

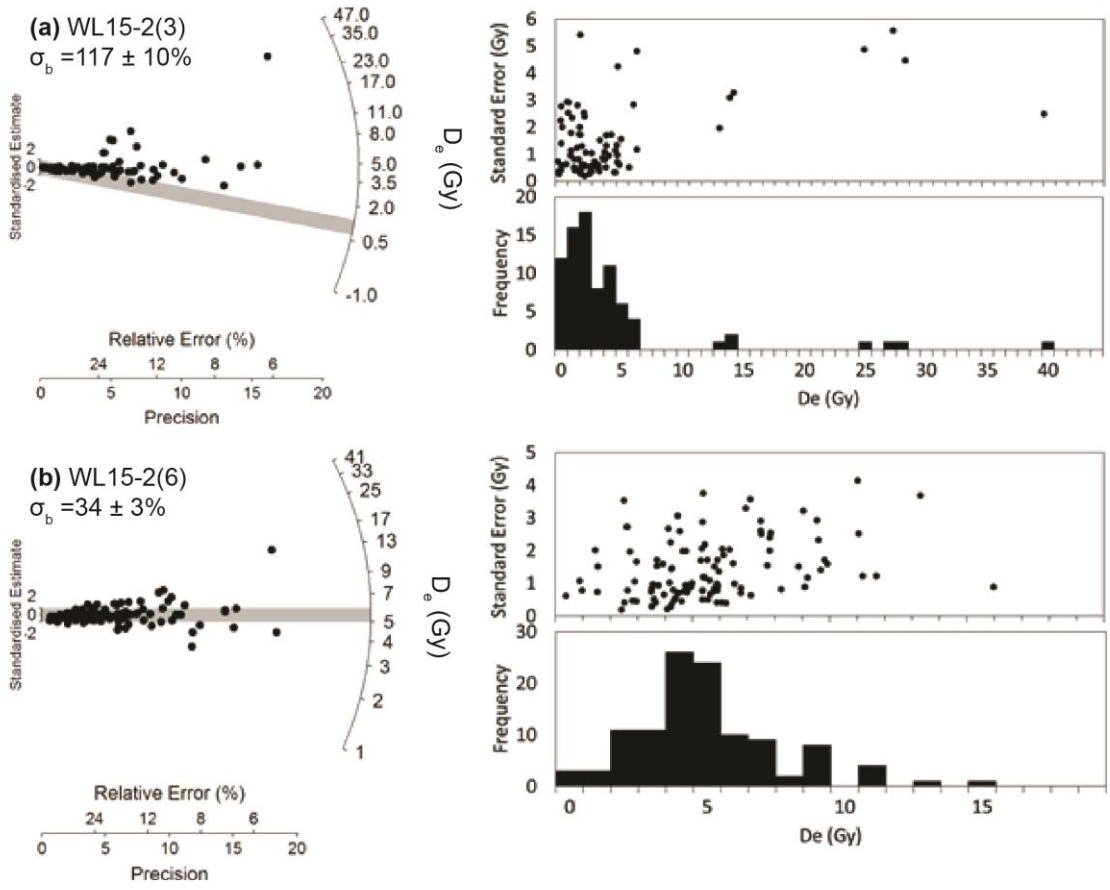

Figure S1: Single-grain De distributions for samples (a) WL15-2(3) and (b) WL15-2(6) shown as radial plots and frequency histograms with ranked plots of De versus standard error. The grey bars on the radial plots are centred on the De values used to derive the final burial dose estimate for each sample (i.e., MAM-4UL for WL2(3) and CAM for WL2(6); (Galbraith et al., 1999, Arnold et al., 2009).

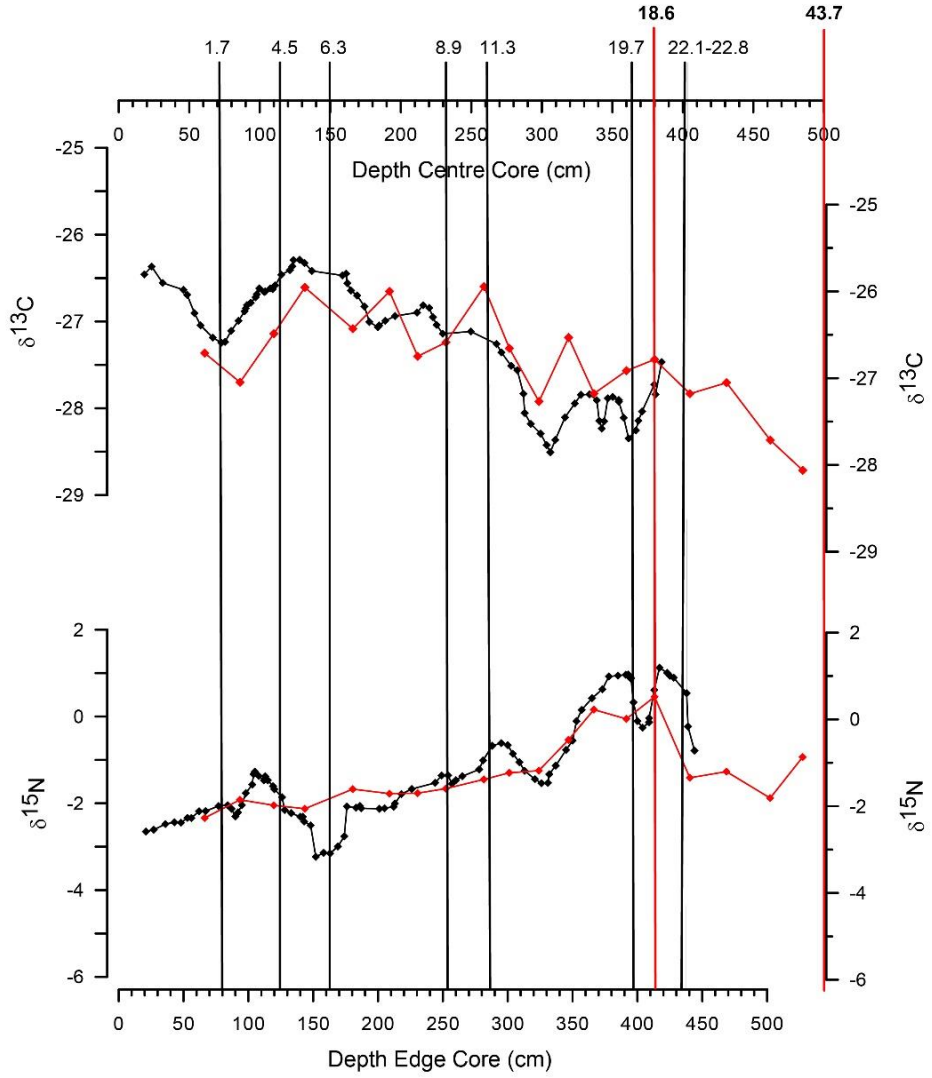

Figure S2. Sediment δ13C and δ15N from this study (red) compared with sediment δ13C and δ15N from a core taken from the edge of the Welsby Lagoon wetland (black; Barr et al., 2017). Radiocarbon ages from the wetland edge core were recalibrated from Moss et al. (2013) and are shown with vertical black lines with calibrated ages (ka) shown above. Red lines indicate the OSL samples from this study with ages (ka) shown in bold above.

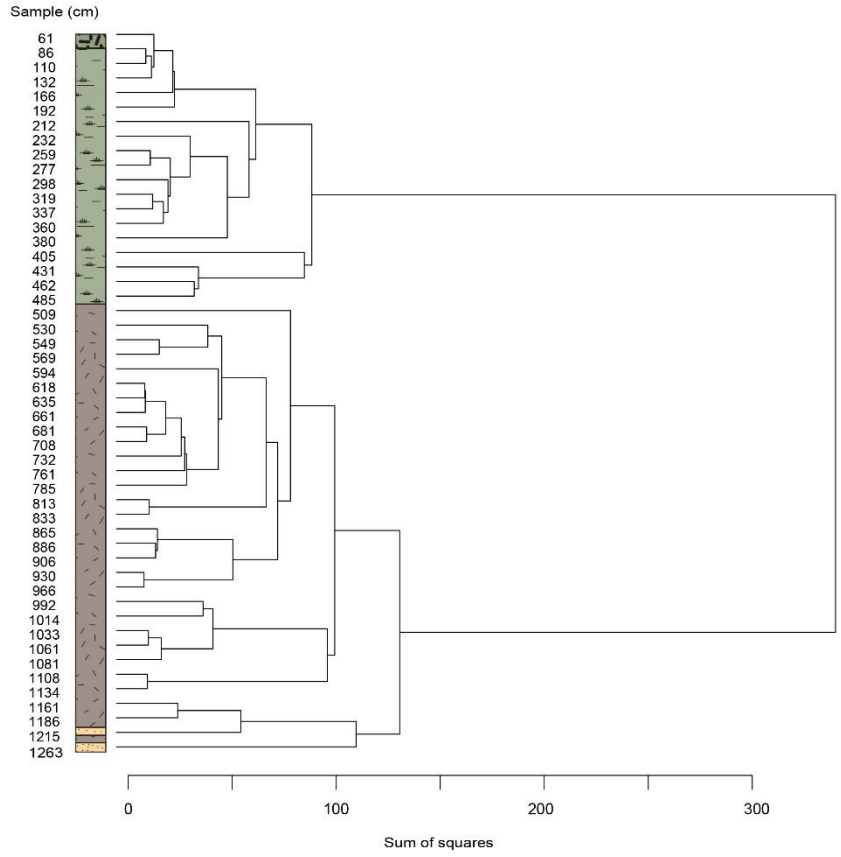

Figure S3: Constrained incremental sum of squares (CONISS) of geochemical data (TOC, TN, δ13C, δ15N). Dendrogram denotes zones according to heirarchical clustering of data based on similarities of samples. Sediment lithology is used in accordance with the CONISS analysis to determine the major periods of change in the record.

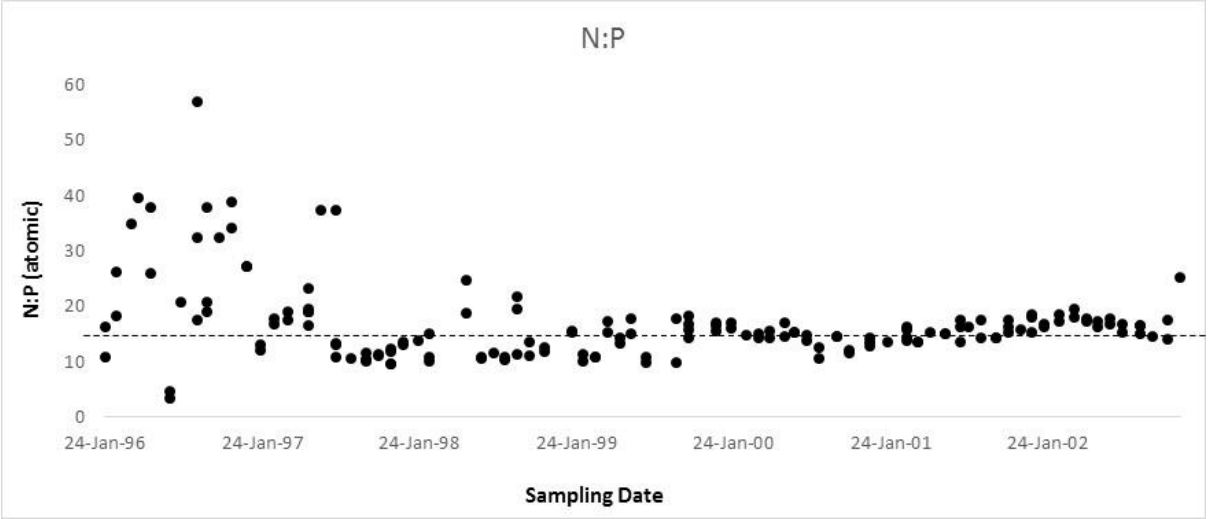

Figure S4: Nitrogen and Phosphorus data from Brown Lake NSI from the period January 1996 to November 2002. Dashed line indicates Redfield ratio of 16:1 N:P as a threshold of N limitation. Data from Mosisch & Arthington (2001).

Table S3. Isotope values of modern plant and algae samples from North Stradbroke Island.

Site	Species	δ13C	%C	%N	C:N
Welsby Lagoon	*Leperonia articulata*	-26.2	47.0	0.6	81.7
Blue Lake	*Leperonia articulata*	-26.8	42.5	0.7	62.8
Swallow Lagoon	*Leperonia articulata*	-27.4	46.1	0.7	72.8
Welsby Lagoon	*Baumea* spp.	-26.7	44.7	0.6	116.5
Swallow Lagoon	*Baumea* spp.	-28.0	45.1	0.5	146.2
Blue Lake	*Gahnia* spp.	-28.4	44.3	0.8	52.1
Welsby Lagoon	*Cycnogeton procerus*	-24.6	38.0	2.2	19.4
Blue Lake	*Triglochin* spp.	-23.0	37.8	2.1	18.0
Blue Lake	*Eleocharis* spp.	-29.4	40.2	0.9	44.2
Blue Lake	*Casuarina*	-30.4	48.3	1.1	44.2
Blue Lake	*Eucalyptus*	-31.0	20.4	0.7	29.4
Blue Lake	*Banksia*	-31.6	49.0	0.8	58.1
Blue Lake	Lake Surface	-29.8	42.1	0.8	51.5
Blue Lake	Soil sample	-28.4	2.7	0.1	22.3
Blue Lake	Cyanobacteria	-29.8	36.7	1.9	19.1
Blue Lake	*Hapalosiphon spp.*	-31.7	38.3	2.1	18.1
Welsby Lagoon	Cyanobacteria	-27.2	45.9	2.5	18.6
Amity Swamp	Cyanobacteria	-29.3	50.8	1.1	46.8
Swallow Lagoon	Plankton	-27.9	57.0	2.6	22.0

Group totals	δ13C	%C	%N	C/N
Aquatic Algae	-29.1	45.7	2.1	24.8
Submerged Plants	-26.2	39.0	1.5	31.1
Terrestrial Plants	-31.0	39.2	0.9	43.9
Emergent Plants	-26.8	43.2	1.0	68.6

Statement of Authorship

Title of Paper	The potential for rapid determination of charcoal from wetland sediments using infrared spectroscopy
Publication Status	☑ Published ☐ Accepted for Publication ☐ Submitted for Publication ☐ Unpublished and Unsubmitted work written in manuscript style
Publication Details	Cadd, H.R., Tyler, J., Tibby, J., Baldock, J., Hawke, B., Barr, C., Leng, M.J. (2019) Rapid determination of charcoal from wetland sediments using infrared spectroscopy.

Principal Author

Name of Principal Author	Haidee Cadd		
Contribution to the Paper	Conceptualisation of the work, development of ideas and conclusions, carried out analytical work, carried out statistical analysis, interpretation of the data, wrote manuscript.		
Overall percentage (%)	85		
Certification:	This paper reports on original research I conducted during the period of my Higher Degree by Research candidature and is not subject to any obligations or contractual agreements with a third party that would n its inclusion in this thesis. I am the primary author of this paper.		
Signature		Date	26/09/19

Co-Author Contributions

By signing the Statement of Authorship, each author certifies that:

i. the candidate's stated contribution to the publication is accurate (as detailed above);
ii. permission is granted for the candidate in include the publication in the thesis; and
iii. the sum of all co-author contributions is equal to 100% less the candidate's stated contribution.

Name of Co-Author	Jonathan Tyler		
Contribution to the Paper	Provided conceptual and interpretation guidance, edited manuscript		
Signature		Date	12/09/19

Name of Co-Author	John Tibby		
Contribution to the Paper	Conducted fieldwork, provided conceptual and interpretation guidance, edited manuscript		
Signature		Date	12/09/19

Name of Co-Author	Jeff Baldock		
Contribution to the Paper	Assisted with acquisition and interpretation of nuclear magnetic resonance data.		
Signature		Date	20/09/19

Name of Co-Author	Bruce Hawke		
Contribution to the Paper	Assisted with acquisition and interpretation of nuclear magnetic resonance data.		
Signature		Date	29/09/19

Name of Co-Author	Cameron Barr		
Contribution to the Paper	Conducted fieldwork, provided conceptual and interpretation guidance, edited manuscript		
Signature		Date	12/09/19

Name of Co-Author	Melanie Leng		
Contribution to the Paper	Assisted with acquisition and processing of modern stable isotope data, provided conceptual guidance, edited manuscript.		
Signature		Date	12/09/19

3

The potential for rapid determination of charcoal from wetland sediments using infrared spectroscopy

Published as:

Cadd, H.R., Tyler, J., Tibby, J., Baldock, J., Hawke, B., Barr, C., Leng, M., (2020). The potential for rapid determination of charcoal from wetland sediments using infrared spectroscopy. *Palaeogeography, Palaeoclimatology, Palaeoecology* . 542: 1-13

Abstract

Wetland sediments archive information about past terrestrial ecosystem change including variations in fire occurrence and terrestrial carbon fluxes. The charcoal content of sediments is important for understanding past fire regimes, as well as the role this recalcitrant carbon plays in the global carbon cycle. Infrared (IR) spectroscopy provides a rapid, non-destructive and cost effective method for simultaneously analysing numerous organic and inorganic sediment properties. The use of IR spectroscopy is well developed for determining concentrations of total organic carbon (TOC), total nitrogen (TN), biogenic silica and carbonate in lacustrine sediments. In soil science IR spectroscopy is also routinely used to determine charcoal content, however the potential for analysing charcoal content from lacustrine sediments has yet to be investigated. Here we develop IR spectroscopy and partial least squares regressions (PLSR) to predict the charcoal and TOC content of an organic, 130,000 year old sediment sequence from North Stradbroke Island (Minjerribah), Australia. Charcoal concentrations used for model development were derived using both traditional palaeoecological area measures ($cm^2\ g^{-1}$) and solid state ^{13}C nuclear magnetic resonance (^{13}C-NMR) of poly-aryl structures. The IR PLSR models yielded significant correlations for the two charcoal methodologies (area measurements, $R^2 = 0.57$, $p<0.05$; ^{13}C-NMR, $R^2 = 0.70$, $p<0.05$). We additionally find a very strong, significant, correlation for TOC ($R^2 = 0.92$, $p<0.05$), consistent with previous studies. Hence, IR is a promising tool for determining the charcoal content of lacustrine sediments, particularly for first-order sample screening, as part of a multi-proxy framework. IR spectroscopy can therefore provide a reliable and rapid technique for the initial investigation of fire histories and organic constituents of sedimentary sequences.

1 Introduction

Charcoal and black carbon, defined as carbonaceous substances of pyrogenic origin (Masiello, 2004; Preston and Schmidt, 2006) and herein generically referred to as charcoal, represent a significant sink in the global carbon cycle (Forbes et al., 2006). Due to its polycyclic structure, charcoal is relatively chemically and microbially inert and can persist in the environment for millions of years (Schmidt and Noack, 2000; Preston and Schmidt, 2006). The products of combustion exist as a continuum, ranging from particles > 1 µm of charred biomass (commonly termed charcoal), to sub-micron particles (30 – 40 nm) produced from the condensation of gas phase intermediates (Masiello, 2004; Hammes et al., 2007). Charcoal is abundant in the biosphere, with global estimates of charcoal produced from biomass burning ranging from 40 – 270 Tg $year^{-1}$ (Kuhlbusch and Crutzen, 1996; Forbes et al., 2006). The major charcoal stores are ocean sediments (480 – 145 Pg) and soils (54 – 109 Pg), with an unquantified pool in terrestrial wetland sediments (Bird et al., 2015). Estimating global charcoal stocks and fluxes is hampered by the lack of reliable and consistent analytical techniques for identifying and quantifying charcoal (Forbes et al., 2006; Hammes et al., 2007; Wiedemeier et al., 2014). Different methods of

charcoal quantification assess different components of the charcoal continuum and therefore result in widely variable estimates (Hammes et al., 2007).

In addition to its potential to act as a sink for carbon, the charcoal content of lake and ocean sediments is an important indicator of past fire regimes (Patterson et al., 1987; Whitlock and Larsen, 2001). In fire prone landscapes, such as Australia, fire is an important biological agent and indicator of ancient cultural activity (Bowman, 2000; Bliege Bird et al., 2008; Williams et al., 2015). Despite its importance in understanding past vegetation change and as an indicator of human impacts upon landscapes, charcoal analyses in palaeoecological studies are often performed at coarse resolution which may not provide meaningful ecological and cultural data. The amount of time and sediment required for high-resolution and multi-proxy studies (Birks and Birks, 2006) can make these analyses labour and cost intensive, increasing with the greater number of analyses required.

Infrared spectroscopy is a non-destructive, rapid and cost effective method for measuring multiple organic and inorganic properties of sediment (Korsman et al., 2002). IR spectroscopy is based on the unique vibrations emitted by molecular bonds exposed to infra-red wavelengths (Colthup et al., 1990). Information on multiple biogeochemical and sediment properties can be extracted from a single infrared spectrum without chemical pre-treatment or complex sample preparation (Viscarra Rossel et al., 2006). Infrared spectroscopy has been shown to be an effective method to improve the resolution and efficiency of organic carbon, nitrogen, biogenic silica and carbonate analyses of lake and ocean sediments (Malley et al., 1999; Chang et al., 2005; Vogel et al., 2008; Rosén et al., 2010; Meyer-Jacob et al., 2014; Pearson et al., 2014; Cunningham et al., 2016; Van de Broek and Govers, 2019). In addition, infrared spectroscopy has been identified as a robust method for characterising charcoal carbon in soils (Janik et al., 1995, 2007; Bornemann et al., 2008; Baldock et al., 2013b, 2013a; Yao et al., 2014; Hardy et al., 2017) and the pyrolysis temperature of charcoal (Guo and Bustin, 1998; Kwon et al., 2013; Gosling et al., 2019), since the aromatic bands present in charcoal carbon respond directly to IR wavelengths (Colthup et al., 1990). However, the potential for using IR spectroscopy to quantify the charcoal content of wetland sediments has yet to be explored.

The application of IR spectroscopy to sediment samples is complicated by the complex nature of the sediment matrix, with IR spectral signatures often obscured or superimposed by a multitude of organic and inorganic compounds. Multivariate calibration models relating IR spectra to conventionally measured sediment properties (e.g. Total organic carbon and biogenic silica) can be used to quantitatively predict those properties (Naes et al., 2002; Viscarra Rossel and Behrens, 2010). The ability of IR spectroscopy to quantitatively measure sediment properties is partly dependent on the calibration method used and the quality of reference samples. The ability of any model to accurately predict input data is only as good as the input data it is being regressed against. Therefore, calibration samples must be able to accurately capture the properties of interest across the full range of variation. In addition, model performance and prediction

error is influenced by the number of calibration samples used for model development (Pearson et al., 2014).

Solid state ^{13}C nuclear magnetic resonance (^{13}C-NMR) spectroscopy is commonly used to quantify the amount polycyclic carbon compounds, which are dominated by charcoal in soils, termed resistant organic carbon (ROC) (Skjemstad et al., 1999; Hammes et al., 2007; Janik et al., 2007; Baldock et al., 2013b). ^{13}C-NMR directly measures the proportion of aromatic C compounds within a sample, and therefore provides values for all components of the charcoal continuum, including high temperature charcoals from a variety of materials (i.e. wood and grass chars) (Wiedemeier et al., 2014). In contrast, methods for identifying charcoal in palaeoecological studies have largely been limited to optical techniques that estimate the number of charcoal particles within a sediment matrix. These methods are unable to accurately detect charcoal particles with a diameter less than 10 µm (Clark, 1988), and thus fail to quantify small charcoal particles and charcoal degradation products. The inability to identify all components of the charcoal continuum can result in incomplete records of biomass burning. This may be particularly problematic for records of regional biomass burning, reconstructions from ancient sediments or within landscapes that possess biomass that is fully combusted or easily macerated (Graetz and Skjemstad, 2003; Masiello, 2004; Bird et al., 2015; Sawyer et al., 2018). Knowledge of the full suite of charcoal components in sediment sequences also provides an opportunity to gain an understanding of the role of recalcitrant charcoal carbon contents from wetlands in the global carbon cycle and long term carbon sequestration (Bird et al., 2015).

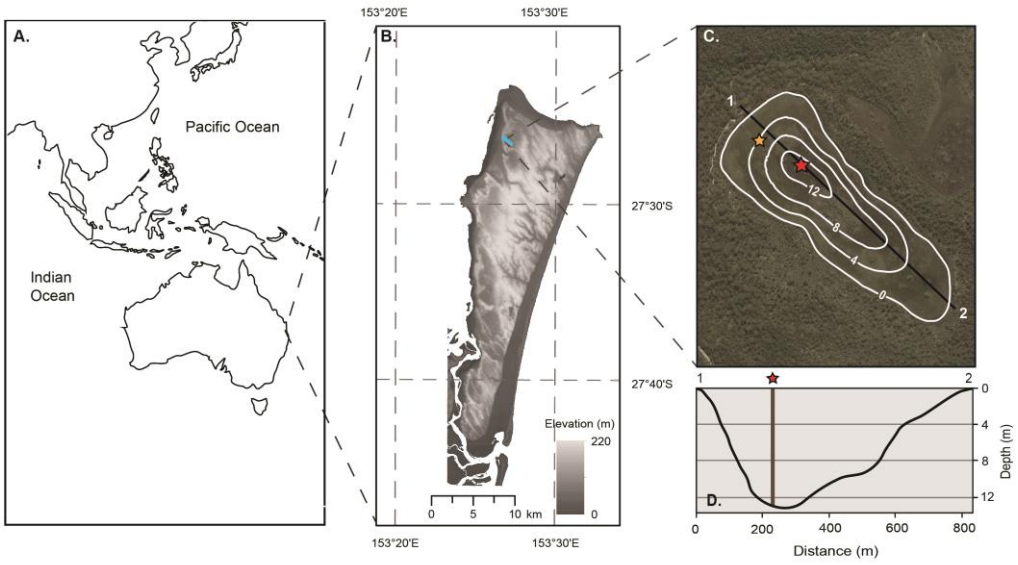

Figure 1. A. Location map of North Stradbroke Island, Queensland, Australia. B. Location of Welsby Lagoon on North Stradbroke Island. C. Aerial image of Welsby Lagoon with contours indicates sediment depth determined by systematic probing of sediment depth. Red star indicates coring location used in this study and yellow star represents location of core studied by Barr et al. (2017). D. cross section of sediment depth of the Welsby Lagoon basin from 1 – 2 line in C.

Here we test for the first time the viability of infrared spectroscopy to determine the content of charcoal carbon within lacustrine sediments. We develop calibration models for charcoal C and TOC content from the ca. 130,000 year old highly organic sediments of Welsby Lagoon, North Stradbroke Island, Australia (Cadd et al. 2018). We calibrate IR data against two established methods for charcoal determination; the traditional area quantification method of macroscopic (> 125µm) charcoal and solid state ^{13}C nuclear magnetic resonance to determine if alternate methods of charcoal quantification influence model performance

2 Methods

2.1. Field Sampling

A 12.7 m sediment sequence was extracted from Welsby Lagoon, a permanent, perched wetland located on North Stradbroke Island (NSI; 27°27'12"S, 153°28'56"E), south-east Queensland, Australia (Fig. 1B). Welsby Lagoon is currently shallow (<1 m water depth) and heavily vegetated, and its sediments are predominantly comprised of organic peats. For further information regarding the Welsby Lagoon site and coring methodology see Cadd et al. (2018).

2.2. Geochemical analysis

Fifty sediment samples, sub-sampled along the 12.7 m sediment core, were analysed for infrared (IR) spectroscopy, total organic carbon (TOC), optical charcoal and solid state ^{13}C nuclear magnetic resonance (^{13}C-NMR). Approximately 2 cm^2 of sediment was freeze dried and ground using a ball mill prior to IR, TOC and ^{13}C-NMR analysis. TOC concentrations (%) of bulk sediment samples were weighed into tin capsules and combusted in a EuroVector EuroEA elemental analyser at the University of Adelaide. Sample carbon concentrations were calibrated against glycine, glutamic acid and triphenylamine standards. Analytical precision for replicate measurement of standards was ±0.06 %.

An additional 1 cm^3 of sediment from the same 50 depth locations was sub-sampled to determine the organic content of different size fractions. These samples were immersed in distilled water for 24 hours to disaggregate sediments. Each sample was then rinsed gently through 125 and 250 µm nested sieves. The material from the three size fractions, <125 µm, 125 – 250 µm and >250 µm was retained, transferred to vials, freeze dried and homogenised using a mortar and pestle. Samples of the three homogenised size fractions of sediment were weighed into tin capsules and analysed for TOC concentration (%) at the British Geological Survey, Keyworth. TOC concentration were determined using a Costech ECS4010 Elemental Analyser. Samples were calibrated against in house standards (BROC and SOIL) through NBS18, NBS-19 and NBS22. Analytical precision for replicate measurement of standards was <0.1%.

2.3. Infrared spectroscopy

Diffuse reflectance infrared spectra of the Welsby Lagoon sediments were measured using a Nicolet 6700 Fourier Transform Infrared (FTIR) spectrometer (Thermo Fisher Scientific Inc., Waltham, MA, USA) fitted with a KBr beam-splitter and DTGS detector. Homogenised sediment samples (approximately 100 mg dry weight) were loaded into 9 mm stainless steel cups before being loaded onto a Pike AutoDiff-Automated diffuse reflectance accessory (Pike Technologies, Madison, WI, USA). A silicon carbide disk was scanned prior to analysis of each group of samples to determine background spectra. Samples were placed in the same laboratory as the FTIR instrument for 2 hours prior to analysis to avoid variations induced by measurement conditions. Spectra were acquired at 8 cm^{-1} intervals from an average of 60 scans for wavenumbers ranging from 8000 cm^{-1} to 400 cm^{1}. Each of the 50 sediment samples were re-loaded, analysed 3 times and spectra averaged to remove potential biases from the small point sample size. Reflectance spectra were converted to absorbance spectra using Omnic software (V.8).

2.4. Nuclear Magnetic Resonance (NMR)

The concentration of resistant organic carbon (ROC) was estimated using solid-state ^{13}C nuclear magnetic resonance (^{13}C-NMR) spectroscopy on a Bruker 200 Avance spectrometer equipped with a 4.7 T wide-bore superconducting magnet operating at a resonance frequency of 50.33 MHz. Between 150 – 600 mg of each of the 50 homogenised sediments was loaded into 7 mm diameter zirconia rotors with Kel-F end caps and spun at 5 kHz. Chemical shift values were calibrated to the methyl resonance of hexa-methyl benzene at 17.36 ppm and a 50 Hz Lorentzian line broadening was applied. A cross polarisation (CP) pulse sequence was used with either a one second delay between pulses or a delay equivalent to five times sample specific T1H values determined by inversion recovery analysis when this value was >1 s. Scans (10,000 - 20,000) were collected for each sample with a 3.2 µs and 90° pulse with a 1 mille second contact time.

Cross polarisation analyses were also completed on size fractionated material (<125 µm, 125 – 250 µm and >250 µm) of two depths (300 and 800 cm). Direct polarisation (DP) experiments were performed on both the bulk sediment and size fractionated material of the two depths (300 and 800 cm) to aid in the quantification of charcoal carbon (Skjemstad et al., 1999). The DP pulse sequence was used with a 90 second delay between pulses, a 4 µs and 90° pulse, and a 1 mille second contact time. Phasing and baseline corrections of ^{13}C-NMR spectra were conducted using Bruker TopSpin 3.2 software. Absolute ^{13}C-NMR signal intensities were divided by the number of transients collected and corrected against the background signal intensity of the empty rotor. Resultant spectral intensities were integrated over a series of known chemical shifts as outlined in Baldock et al. (2013b).

The resistant organic carbon fraction of each sediment sample was estimated as the

amount of carbon existing as poly-aryl compounds in addition to regions of aryl carbon not defined as lignin, i.e. chemical signatures consistent with charcoal. The two component model of Baldock et al. (2013) was used to allocate the proportion of carbon to the ROC fraction from the acquired ^{13}C-NMR spectra. This modelling approach assumed that charcoal and lignin were the two dominant sources of aryl and O-aryl carbon present in the samples. The proportion of aryl and O-aryl carbon attributed to the ROC component was determined from averages of ^{13}C NMR spectra of a variety of charcoals (Baldock et al., 2004, 2013b) The ROC fraction derived from the ^{13}C-NMR spectra may potentially include the presence of poly-aryl structures created via chemical reactions within the wetland or surrounding soil and thus cannot be ruled out as a minor additional contributor to the ROC fraction (Tan, 2014). However, it is likely that charcoal carbon contributes the bulk of the carbon existing as poly-aryl compounds, particularly in fire-prone regions (Hammes et al., 2007; Mcbeath and Smernik, 2009; Baldock et al., 2013b; Wiedemeier et al., 2014), thus ROC is considered to primarily represent charcoal and hereafter will be considered as such.

The ^{13}C-NMR signal intensity in the aryl and O-aryl spectra regions was compared in the CP and DP ^{13}C-NMR spectra. The fraction of ROC not observed by the CP analysis was determined using the calculation described by Baldock et al. (2013b). The ROC observed by CP analysis (f_{ROC}CP) and ROC observed by DP analysis (f_{ROC}True) were used to determine the CP observability (ϕ_{CP}) of ROC.

$$f_{ROC}\,\text{True} = \frac{\frac{f_{ROC}\,CP}{\phi_{CP}}}{\frac{f_{ROC}\,CP}{\phi_{CP}} + (1 - f_{ROC}\,CP)} \quad (1)$$

The proportion of ROC not detected by the CP spectra was corrected with equation 1 (Baldock et al., 2013b).

Table 2. Spectra wavenumbers (cm^{-1}) associated with organic functional groups and chemical properties of charcoal.

Wavenumber (cm^{-1})[a]	Assignments	Contribution to ROC & Charcoal PLSR models
2933	Asymmetric Aliphatic CH stretching	Positive
2850	Symmetric Aliphatic CH stretching	Positive
1715	Aromatic Carbonyl / Carboxyl C=O stretching	-
1600 – 1610	Aromatic C=C / C=N ring stretching	Positive
1510	Aromatic C=C ring stretching	Positive
1450	Aliphatic CH deformation / C=C ring stretching	Positive
1430 – 1420	Aromatic C=C ring stretching	-
1270 – 1250	Aromatic CO^{-} and phenolic $^{-}$OH stretching	Positive
1170 – 650	C-OH stretching of polysaccharides	-
1060 – 1030	Aliphatic ether C-O^{-} and alcohol C-O stretching	-

[a.] Wavenumber groups determined from Guo and Bustin (1998), Hardy et al. (2017) and Nocentini et al. (2010)

2.5. Quantification of charcoal by optical microscopy

An additional 2.0 cm^2 of sediment was sub-sampled from the same depth location for optical charcoal analysis following Mooney and Tinner (2011). Charcoal samples were weighed and submerged in 5% hydrogen peroxide (H_2O_2) for 24 hours before being rinsed through 125 µm and 250 µm nested sieves. The two size fractions were rinsed into petri dishes and photographed for charcoal analysis. Measurements of the area of photographed charcoal particles were calculated in ImageJ software using the method outlined by Mooney and Black (2003) for the different size fractions. The total area of charcoal was expressed as cm^2 per gram of dry sediment ($cm^2\ g^{-1}$). Calculations based on >125 µm size fraction are a combined value of particles in both size fractions.

The use of area measurements of charcoal concentration neglects the potential for variability in the 3-dimensional volume and density of charcoal particles. Fragmentation of particles and variations in charcoal particles related to fuel source mean that area measurements may underestimate the true variation in total charcoal volume (Belcher et al., 2013; Crawford and Belcher, 2014). Hence, we converted charcoal area measurements to volume in an attempt to facilitate a better comparison between the optical charcoal values and ^{13}C-NMR and IR data. To translate areal measurements to their approximate volumes of charcoal in each sample we applied equation 2 (Weng 2005).

$$V_t = C \sum_{i=1}^{N} A_i^{\frac{3}{2}} \qquad (2)$$

where V_t is the volume of the charcoal within the sample, C is a constant related to particle morphology and A_i the projected area of the charcoal particle. Variations in particle morphology were accounted for by calculating a mean estimate for the C based on the mean circularity of all charcoal particles within each sample in ImageJ. TOC content (% TOC) was used in conjunction with the volume measurements of charcoal, by assuming a constant charcoal density, to calculate the amount of carbon existing as charcoal within each of the size fractionated samples. The derivation of four optical charcoal measures could theoretically result in underestimation of the prediction errors (as a result of multiple comparisons). However, we developed models for both the >125 µm and >250 µm size fractions (both area and volume) as these are regularly used in palaeoecological studies.

2.6. Scanning Electron Microscopy (SEM)

Charcoal fragments from seven samples from the length of the core were isolated under a binocular microscope at 25x magnification. Fragments from each of the seven samples were mounted and carbon coated prior to imaging on a FEI Quanta 450 FEG Scanning Electron Microscope at Adelaide Microscopy, University of Adelaide. Secondary electron images were captured using 10 kV beam voltage and spot size of three.

2.7. Data analysis

Prior to model development, IR spectra were truncated to 4000 – 600 cm^{-1} and baseline corrected using the baseline offset transformation in Unscrambler V10.5 (Camo Software, AS, Oslo, Norway). A principle component analysis (PCA) of the IR spectra was conducted in the vegan package (Oksanen et al., 2013) for R (R Core Team, 2017).

Partial least squares regression (PLSR) was used to develop calibration models between the IR spectra and TOC, optical charcoal and ^{13}C-NMR in the PLS package (Mevik and Wehrens, 2007) in R (R Core Team, 2017). PLSR defines the orthogonal latent variables (scores and loadings) to compress the information contained in the IR spectra whilst simultaneously removing the irrelevant material, maximising the covariance between X and Y. PLSR models conducted on untransformed ROC and optical charcoal data produced predictive models with significant curvature and non-uniformed variance of residuals (Baldock et al., 2013a). Thus, a log transformation of the ROC and charcoal variable data was applied before derivation of the predictive PLSR models to remove curvature, improve the homogeneity of residuals and achieve the greatest linearity of PLSR models (supplementary Fig. 3).

A cross-validation model was derived for each measured variable. Five random samples were excluded from the prediction dataset with a regression model built using the remaining 44 samples. This was repeated until each group of samples in turn, was set aside. Root mean square error of prediction (RMSEP) was used as an estimate of prediction error of each model. The number of components retained for each PLSR model was determined using the one-sigma heuristic, whereby the model with the fewest components that was still one standard error from the 'optimal' model was chosen (supplementary Fig. 1; Mevik and Wehrens, 2007).

Possible temporal autocorrelation between samples (samples closer together down core will influence neighbouring samples) can result in overestimation of regression models in temporal sequences, however there were insufficient degrees of freedom to use consecutive samples for the PLSR model development, exemplified by the small number of samples available for calibration. Furthermore, the presence of two distinct populations of data occurring as a result of a marked change in sediment characteristics at 500 cm (Cadd et al., 2018) resulted in an uneven distribution of data. It is therefore possible that the PLSR models developed for each predictor variable may have an overinflated R^2 and predictive power and, as such, are interpreted with caution.

3 Results

3.1. Geochemical analysis

Concentrations of TOC were >13.5% throughout the 12.7 m sediment core, however values

increase from 34.9% (range of 13.5 – 44.4%) in the deeper (500 – 1270 cm) section of the core to an average of 60.0 % (range of 50.7 – 67.1%) in the upper (0 – 500 cm) sections. Size fractionated TOC revealed that in sediments between 500 – 1270 cm, over 90% of the TOC was in the <125 μm fraction. Samples between 0 – 500 cm were also dominated by TOC in the <125 μm fraction (89 – 43%) but displayed higher variability and greater contributions from the >125 μm and >250 μm size fractions, ranging from 56 – 11% of TOC in these samples. Correlations between bulk geochemical analyses and ^{13}C-NMR derived ROC (% TOC) and Lignin (% TOC) are included in supplementary information (Supplementary Fig 6).

3.2. Infrared spectroscopy

Averaged, baseline corrected and truncated IR spectra for all samples are shown in Fig. 2a. Principle components analysis (PCA) was applied to all transformed IR spectra to examine the degree of sediment clustering according to sediment depth. Comparison of PCA axis 1 and 2 scores (explaining 67.8% and 12.9% of variance respectively; both significant in broken stick test) shows that there was no major clustering of IR spectra (Fig. 3). PC1 axis displays the greatest variation in spectra from 0 – 500 cm of the core, while PC2 provides some, but not complete, differentiation between the IR spectra acquired from the upper and lower (500 - 1250 cm) sections of the core. Key spectral regions previously associated with aromatic carbon are indicated in Table 1. The spectra from the Welsby Lagoon sediment samples display many of these features associated with poly-aromatic charcoal carbon (Table 1, Fig. 2a).

3.3. Nuclear Magnetic Resonance (^{13}C NMR)

Cross-polarised ^{13}C-NMR spectra for the 50 sediment samples are shown in Figure. 2b. A comparison of the CP and DP spectra acquired for the size fractionated samples at 300 and 800 cm displayed a relative enrichment in the aromatic spectral region (110 – 145 ppm; Fig.4) in the DP analysis. This confirmed the unsaturation of the resonance at 130 ppm with regards to hydrogen, suggesting that this resonance was associated with carbon more than three bonds away from a hydrogen, consistent with the presence of polycyclic aromatic compounds, the chemical signal consistent with charcoal. Following Baldock et al. (2013b) we solved equation 1 for the optimum value of ϕ_{CP}. The size fractionated samples combined with samples analysed for DP spectra by Baldock et al. (2013b) provided an optimum ϕ_{CP} value of 0.55. An optimal ϕ_{CP} value of 0.55 indicates that approximately 55% of the aromatic carbon within these samples was being detected by the CP spectra (Fig. 5). The observability correction (ϕ_{CP} = 0.55) was applied to all ^{13}C-NMR spectra prior to PLS model development.

The proportion of ROC identified by ^{13}C-NMR spectra sediments was on average 30.6%, ranging from 21.8 – 47.7%. When adjusted for TOC content of the sediment, ROC

contents ranged from 4.67 – 26.6% (46.7 – 266.0 mg ROC g^{-1} TOC. Sedimentary lignin (as % TOC) values range from 2.38 – 34.17%. Lower lignin concentrations (2.38 – 6.63%) were measured from the deeper sediments from 500 – 1200 cm, with a marked increase in lignin between 485 – 380 cm (10.88 – 34.17%). There was no significant correlation between the down-core values of ROC (% TOC) and Lignin (% TOC) (P>0.5).

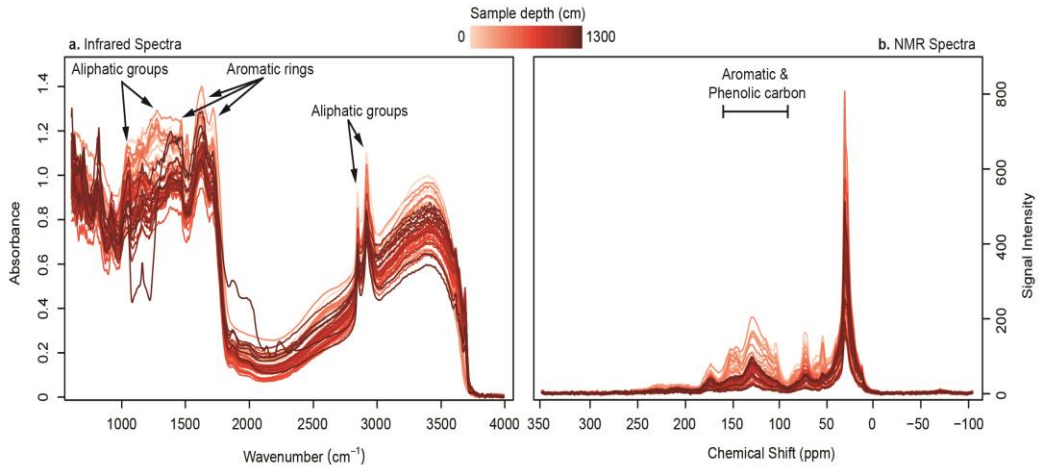

Figure 2. a. Baseline corrected and truncated (600 – 4000 cm-1) infrared spectra. Key wavelengths associated with charcoal carbon (Table 1) are indicated by arrows b. NMR spectra for the 50 Welsby Lagoon whole sediment samples. The key 13C NMR spectral region (160 – 110) for aromatic carbon is indicated. The basal sample (1263 cm) exhibits different spectral properties to the remainder of the core. This is likely due to its deposition during the formation of the wetland (Cadd et al. 2018)..

3.4. Conventional charcoal measurements

Area based charcoal measurements ($cm^2\ g^{-1}$) range between 0 – 32.1 $cm^2\ g^{-1}$ from 500 – 1270 cm for the 125 – 250 µm and >250 µm size fractions. Charcoal from 0 – 500 cm was dominated by the 125 – 250 µm (5.6 – 172.6 $cm^2\ g^{-1}$) and >250 µm (2.0 – 126.8 $cm^2\ g^{-1}$) size fractions. The charcoal content of the >250 µm and 125 - 250 µm size fraction were highly correlated (R^2=0.84, p<0.005).

Charcoal volumes ($cm^3\ g^{-1}$) between 500 – 1270 cm range from 0.0 – 73.6 $cm^3 g^{-1}$ for the 125 - 250 µm size fraction and 0.0 – 106.3 $cm^3 g^{-1}$ >250 µm size fraction. Between 0 – 500 cm the charcoal volume from the 125 - 250 µm ranged from 5.9 – 947.0 $cm^3\ g^{-1}$ and the >250 µm size fraction from 2.0 – 924.0 $cm^3\ g^{-1}$. Charcoal volume measurements expressed as a portion of total organic carbon (mg CHAR C / g TOC) were highest for the > 250 µm size fraction, ranging from 0.0 – 255.2 (mg CHAR C / g TOC), while the 125 - 250 µm size fraction ranged from 0.0 – 195.7 (mg CHAR C / g TOC).

3.5. Scanning Electron Microscopy (SEM)

SEM images of charcoal fragments indicate that in most cases the original features of the plant tissue are recognizable (Fig. 6). The majority of fragments appear morphologically

intact and display no clear trends in preservation throughout the core.

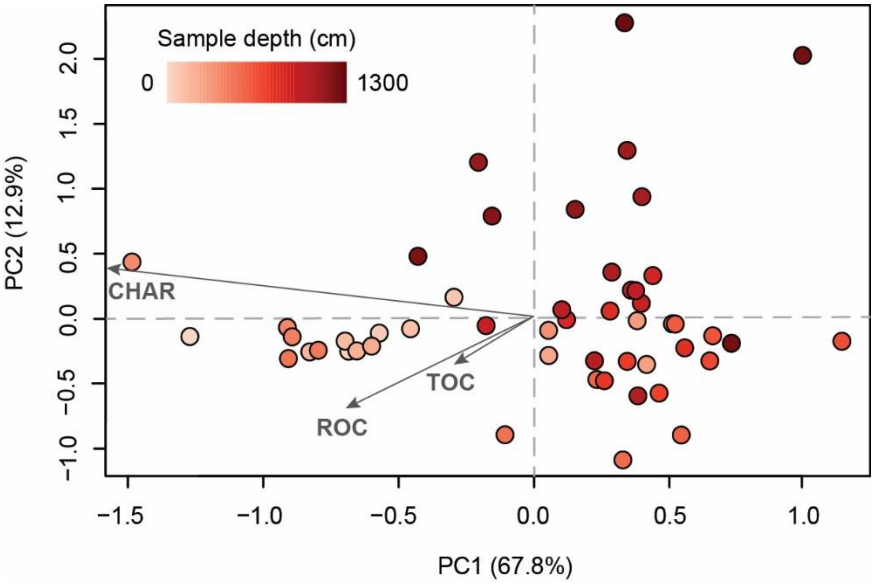

Figure 3. Principle component analysis of the infrared spectra obtained for the 50 Welsby Lagoon whole sediment samples. Measured variables plotted as passive vectors on PCA biplot

3.6. Data analysis

Partial Least Squares Regression (PLSR) calibration models between IR spectra and conventionally measured concentrations of TOC, ROC and optical charcoal measurements were developed (Fig. 7). Coefficients of determination were robust for a PLSR model between TOC and IR (5 comp; R^2=0.92; RMSEP=3.1, 13.4% of the range) and between ROC and IR (3 comp; R^2=0.70; RMSEP=0.07, 7.9% of the range). PLSR models of different optically based calculations and size fractions of charcoal content were less robust with higher prediction errors and variable model results (Table 2).

Calibration models using the >125 µm size fractions performed best for all optical measurements. The best model performance for optical charcoal measurements was determined based on the coefficient of determination as well as homogeneity of residuals and linearity of the prediction model. The best performing model for all criteria was obtained for the area measurement ($cm^2\ g^{-1}$) of the >125 µm size fractions (four component; R^2=0.56, RMSEP =0.33; 6.4% of the range). We used this model for all further analysis and discussion, as it had the best statistical performance and this measurement technique is the most common in palaeoecological studies.

The IR spectral features that contributed to the PLSR models for TOC, ROC and optical charcoal are shown in Figure.8. The beta coefficients show similar spectral patterns for all models. The covariance of the beta coefficients is not surprising, as TOC and charcoal are correlated in the original dataset, and indeed, in most natural systems (Supplementary Fig. 2; 6). Although the first PC1 loadings of the models co-vary, the subsequent model loadings are distinct between the two charcoal measures and TOC (Fig. 9). Several deviations exist between the β coefficients and spectral peaks identified for charcoal and TOC match those of previous studies (Fig. 8, Table 1).

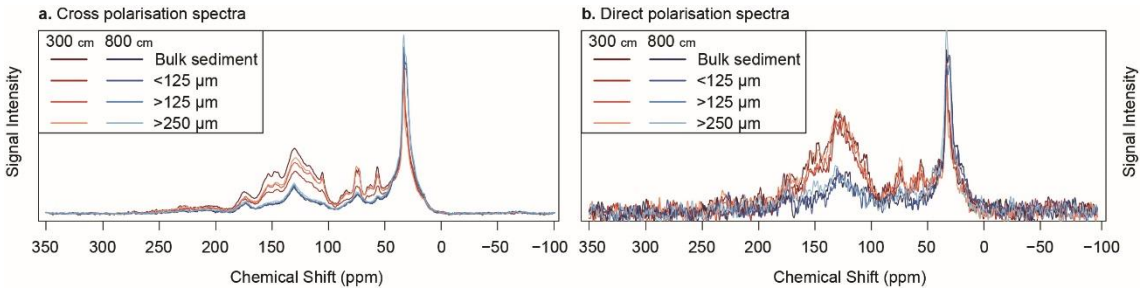

Figure 4. Cross polarisation **(a)** and direct polarisation **(b)** spectra for the 300 (orange) and 800 (blue) cm depth samples.

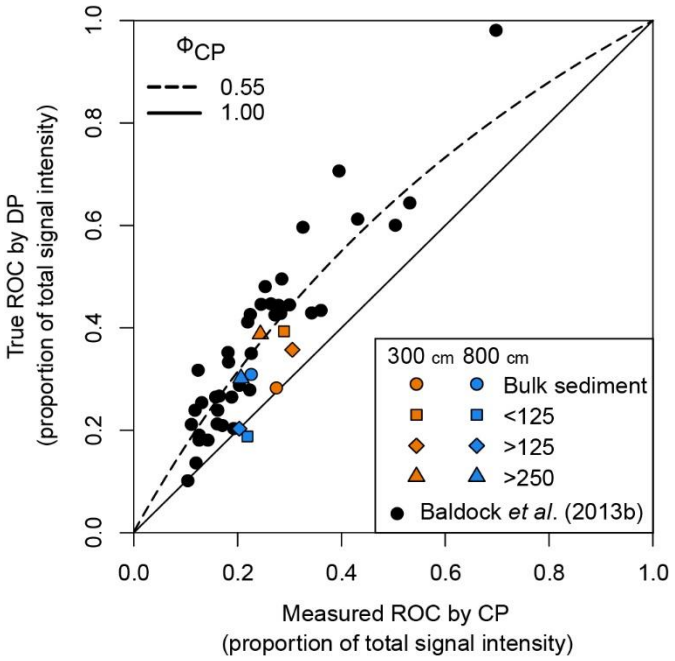

← Figure 5. Relationship between the proportion of resistant organic carbon (ROC) obtained from cross polarisation and direct polarisation of samples from 300 cm (orange) and 800 cm (blue) depth for the three different size fractions and bulk sediment samples. Solid and dashed lines show the theoretical relationship obtained for the optimised value of ROC observability under CP (ϕCP) using equation 1. Samples analysed by DP spectra acquired for this study were combined with DP spectra obtained by Baldock et al. (2013a) to determine ROC observability (ϕCP = 0.55).

4 Discussion

4.1. Model performance

Our analysis indicates that IR spectroscopy provides a useful and cost effective method for the rapid determination of charcoal and TOC, in support of previous studies (Vogel et al., 2008; Rosén et al., 2010, 2011; Baldock et al., 2013a; Pearson et al., 2014). The predictive error associated with the limited number of calibration samples in our study is likely compounded by changes in sediment lithology over the ca. 130,000-year history of Welsby Lagoon (Cadd et al. 2018). Nevertheless, the ability to achieve robust predictive models for TOC with a small and variable calibration dataset highlights the applicability of IR spectroscopy to studies of organic sediment properties.

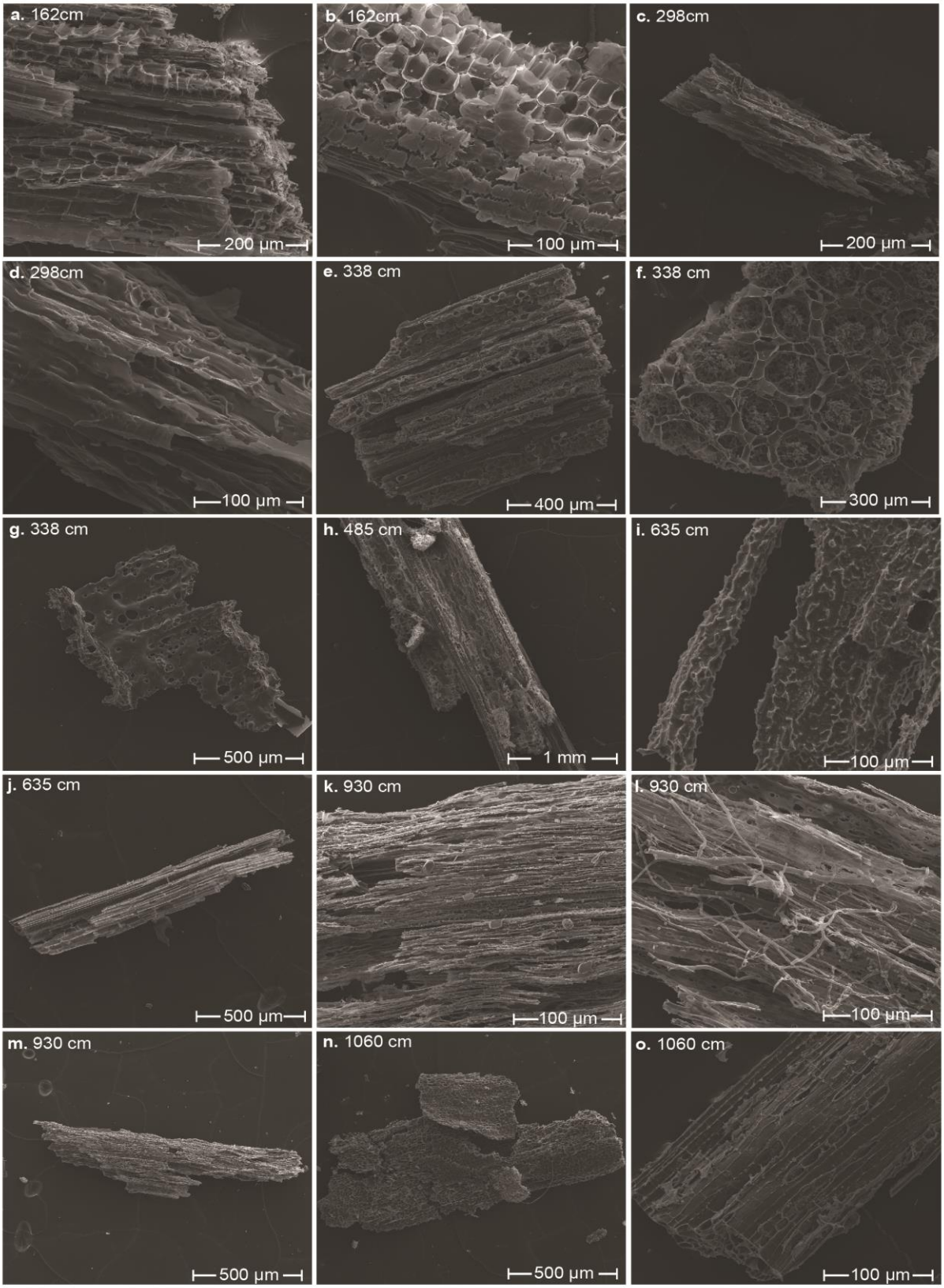

Figure 6. . SEM images of isolated charcoal fragments from the Welsby Lagoon sediment sequence. . Core depth of charcoal sample are shown in top left corner of each images. The original features, such as the cellular structure, of most fragments are still recognizable..

The analysis of charcoal in wetland sediments is an important proxy used to reconstruct fire histories (Power et al., 2008; Conedera et al., 2009). Understanding past fire regimes is crucial to develop appropriate modern management and conservation practices, provide information on past drivers of fire and the response of ecosystems to various fire regimes (Bowman et al., 2009; Conedera et al., 2009). Current methods to quantify fossil charcoal have been developed to be both time and cost effective; however, these methods don't explicitly account for variations in charcoal density and structure (Belcher et al., 2013). In addition, these methods have limited ability to adequately quantify small (<10 μm) charcoal fragments. IR spectroscopy can provide an equally time and cost effective method to quantify the whole spectrum of charcoal components (Skjemstad et al., 1999; Janik et al., 2007; Bornemann et al., 2008; Baldock et al., 2013a; Yao et al., 2014), however this method has hitherto not been validated for wetland sediments.

IR spectroscopy, coupled with ^{13}C-NMR spectroscopy, can accurately predict the concentration of compounds consistent with charcoal from soils (Skjemstad et al., 1999; Janik et al., 2007; Bornemann et al., 2008; Baldock et al., 2013a; Yao et al., 2014). Results from Welsby Lagoon show that IR spectroscopy also has potential for predicting charcoal from wetland sediments. The cross validated PLSR model provides a good first order estimation of the large-scale changes in down core charcoal concentration (Fig. 10). The predictive PLSR model between ^{13}C-NMR derived ROC contents and IR spectra displays a slightly lower (typically R^2<0.2) predictive power than seen using the same techniques in soil studies. The lower precision of the PLS models may be largely due to the limited number of samples in the calibration dataset, a consequence of the costliness of ^{13}C-NMR analysis. Pearson et al. (2014) highlight the need for large calibration datasets in IR PLS studies, suggesting a minimum of 120 calibration samples to achieve accurate model results. In addition, the presence of two distinct populations of TOC, ROC and charcoal values occurring as a result of the change in depositional setting of the wetland (Cadd et al. 2018), may have overestimated the predictive power of PLSR models. Although the PLSR model was able to provide broad scale estimates of changes in mean charcoal abundance, the ability to predict extreme variations in charcoal concentration was more limited (Fig. 10). The reduced ability of the model to accurately predict the extreme values may be driven by calibration sample concentrations not being uniformly distributed over the full concentration range. The unequal distribution of calibration samples is likely to have resulted in lower predictive power of the PLSR models.

Developing a more comprehensive calibration dataset, that more uniformly covers the full range of ROC variability may provide more accurate and precise models. Currently, the application of this model to a single sediment sequence limits our ability to assess its applicability across a variety of sites. The addition of calibration samples from other wetlands and inclusion of additional calibration samples would likely improve the predictive power of the PLSR models. The high costs associated with ^{13}C-NMR spectroscopy prohibits the development of extensive calibration or multi-site datasets. In addition, the ability of this method to be applied to inorganic sediment sequences (TOC

<1%) has yet to be examined and may be hindered by low carbon concentrations. In low organic carbon sediments, extraction and concentration of OC from mineral material may be necessary. Extensive pre-treatments and increased sediment material required may reduce the applicability of this method to sedimentary sequences with low organic carbon content (Fox et al., 2017). However, the potential for this method to develop ultra-high-resolution fire records, or the development of inter-site calibration sets and applications, may render this approach worthwhile. An integrated calibration dataset of Australian soils has proved to be successful (Baldock et al., 2013a) and a similar approach with lake and wetland sediments in Australia and overseas could result in a wide range of new insights into terrestrial and aquatic ecosystem change.

Table 3. Partial Least Squares model results for the different measures of optical charcoal for two different size fractions

Area ($cm^2 g^{-1}$) [a]	***n* comp [b]**	**RMSEP [c]**	**% Gradient [d]**	**R^2**
>125 µm	4	0.33	6.4	0.57
>250 µm	3	0.53	14.3	0.17
Volume ($cm^3 g^{-1}$)	***n* comp**	**RMSEP**	**% Gradient**	**R^2**
>125 µm	4	0.49	9.9	0.55
>250 µm	3	0.77	14.1	0.17
CHAR C (mg CHAR C/mg TOC)	***n* comp**	**RMSEP**	**% Gradient**	**R^2**
>125 µm	6	0.52	13.1	0.44
>250 µm	1	0.90	16.8	0.02

[a].All data was log transformed prior to model development.
[b]. RMSE = Root mean square error of prediction.
[c] .*n* comp = number of model components used for model predictions.
[d].% Gradient = the RSMEP/gradient length of the original dataset.

The Welsby Lagoon sequence is composed of highly organic sediment with high concentrations of TOC (>25%) and charcoal, a combination not often encountered in mineral agricultural soils from which charcoal-IR calibrations have been derived (Baldock et al. 2013a; Supplementary Fig. 4). The IR spectral features of the first component used to build the PLSR predictive models for TOC and both measures of charcoal concentration show strong covariance (Fig. 9). The covariance of these sediment properties is not unexpected, as charcoal is a major component of the organic carbon content of Welsby Lagoon sediments (accounting for 4.6– 26.6% of TOC). Whilst the first component of the loading spectra for each model shows strong covariance, loadings of TOC components 2 – 5 relate to different spectral features compared to the loading components 2 – 4 of the charcoal and ROC models (Fig. 9). As a consequence, the two models are deemed to be sufficiently different for the independent identification of charcoal from other components of bulk organic matter.

4.2. Comparison of charcoal methods

The different calibration models derived using ^{13}C-NMR and optical charcoal estimates highlight an important challenge in determining the optimal approach for charcoal determination in sediments. The two methods of charcoal determination used in this study measure different components of the full suite of charcoal components. Predictions of optical charcoal show variable, but consistently lower, correlations than the ROC model, depending on the measure of charcoal used (Table 2; Fig. 7). Visual area-based methods of charcoal determination, techniques which use photography coupled with particle area measurements, are only able to reliably measure particles >125 µm (Hawthorne and Mitchell, 2016) and are thus biased towards identifying the coarse fraction or 'macroscopic' charcoal. Optical microscopy based techniques using point counting (without area measurements) generally restrict confident identification to particles >10 µm. Both methods fail to detect particles <10 µm and charcoal degradation products. ^{13}C-NMR has the potential to quantify all poly-aromatic carbon compounds with a chemical composition consistent with charcoal from a bulk sediment sample. This method, whilst having the ability to quantify all fractions of the charcoal continuum, may be confounded by the presence of biosynthetic polycyclic compounds produced within the wetland or surrounding landscape (Lee et al., 1981; Tan, 2014).

Through the deeper part of the Welsby Lagoon core (1200 – 500 cm), the ^{13}C-NMR ROC measurements show consistently higher values than the optical charcoal measurements (Fig. 10). Scanning electron microscopy of charcoal fragments (Fig. 6) show no systematic preservation bias, indicating that degradation or breakdown of particles in older samples is unlikely to be influencing the offset between the charcoal measurements. The inability of the optical method to identify particles <10µm, which contribute to the charcoal budget of ^{13}C-NMR, may account for the offset between the two methods. In the deeper part of the Welsby Lagoon sediment sequence, the TOC content of the sediments is dominated by material in the <125 µm fraction (average 92.4% TOC <125 µm). The higher mean values obtained by the ^{13}C-NMR method may indicate the presence of poly-aryl structures other than charcoal, however these higher mean values are suspected to result from unquantified <125 µm charcoal particles in the optical method.

The two methods of charcoal determination, ^{13}C-NMR based ROC and optical area >125µm, are correlated (R^2=0.77) and show similar broad trends (Fig. 10). The similarities seen between the different methods of charcoal determination, especially in the upper part of the sediment sequence, may be due to the greater contribution of larger macroscopic (>125 µm) charcoal particles to the overall charcoal concentrations. The differences seen between the two methodologies, thus, become less important when sediments are dominated by macroscopic charcoal fragments that are measureable by both methods.

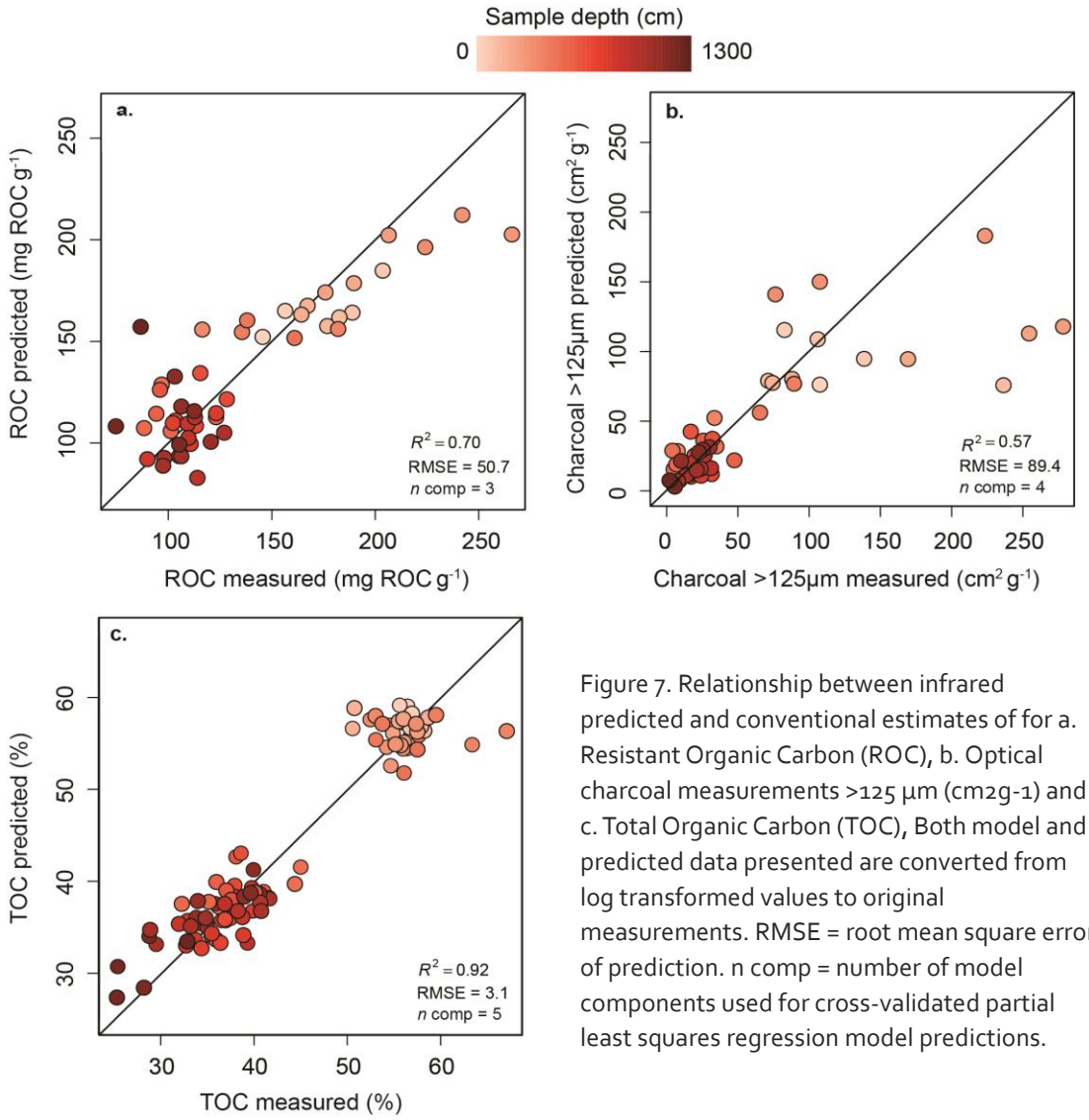

Figure 7. Relationship between infrared predicted and conventional estimates of for a. Resistant Organic Carbon (ROC), b. Optical charcoal measurements >125 µm (cm2g-1) and c. Total Organic Carbon (TOC), Both model and predicted data presented are converted from log transformed values to original measurements. RMSE = root mean square error of prediction. n comp = number of model components used for cross-validated partial least squares regression model predictions.

The comparison between conventional optical and ^{13}C-NMR based total charcoal raises important questions about the overall aim of palaeoecological charcoal studies. Traditional palaeoecological optical methods are able to determine the number or area of coarse macroscopic charcoal particles (>125 µm), but have limited ability to detect smaller charcoal fragments (<125 µm) and are unable to detect sub-micron particles. The use of optical charcoal methods is generally motivated by ease of analysis and the dispersal bias of large particles (>125 µm) towards short distances (Peters and Higuera, 2007). The modelled dispersal range (m to km) of macroscopic charcoal indicates that this charcoal fraction is a reliable indicator of local fire events (Higuera et al., 2007; Peters and Higuera, 2007). However, the theoretical assumptions of local macroscopic charcoal deposition is often countered by empirical studies that indicate that particle size alone is not a reliable predictor of transport distance (Whitlock and Millspaugh, 1996; Pitkänen et al., 1999; Asselin and Payette, 2005; Tinner et al., 2006). Hence in order to fully characterise charcoal produced from local fires, alternative techniques that characterise the sub 125 µm fraction such as those outlined herein.

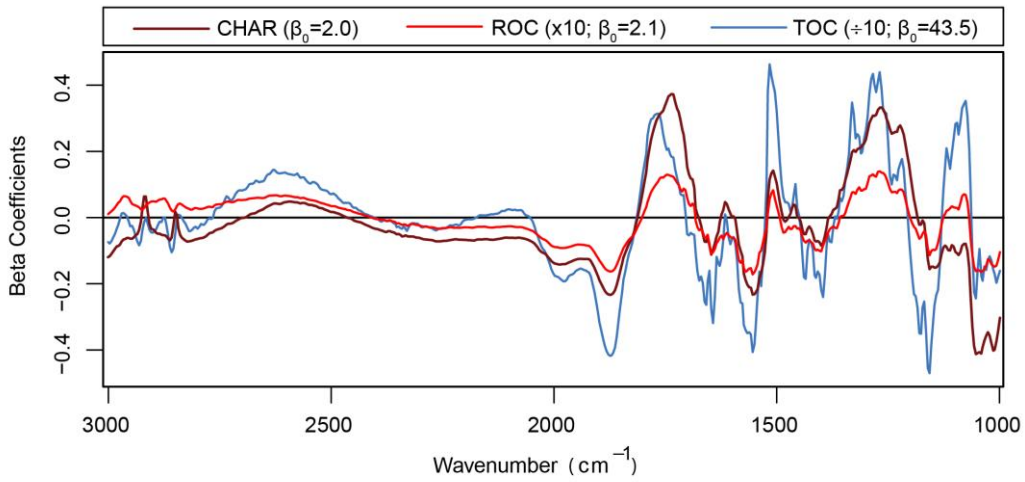

Figure 8. Beta coefficients of the Infrared spectra used to the build the partial least squares model for CHAR (optical charcoal >125 µm (cm^2 g^{-1})), ROC (resistant organic carbon) and TOC (total organic carbon).

The production of the various components of the charcoal continuum is influenced by the plant type (fuel) consumed and the degree and temperature of combustion. In addition, differential fragmentation and sorting of charcoal particles during transportation and deposition, from both physical and chemical processes, may lead to size biases that are not easily identifiable. Thus, the production and preservation of macroscopic and/or microscopic charcoal is closely related to the type of biomass consumed, combustion temperature and degree of degradation, factors largely unrelated to frequency of burning (Bird et al., 2015). For example, grasslands experience frequent wildfire, yet the rapid combustion of fine fuels and subsequent maceration of delicate particles by wind and water can result in limited deposition of macroscopic charcoal particles (Graetz and Skjemstad, 2003). Optical methods may therefore be unable to detect the products of high temperature combustion, easily macerated fuel types, radiative effects of biomass burning and regional biomass burning histories (Graetz and Skjemstad, 2003; Masiello, 2004).

The complex relationship between macroscopic charcoal production, fine fuels and fire intensity may mask certain signals of fire occurrence. The potential biases associated with macroscopic charcoal analysis may restrict identification of low intensity fire events, in particular those associated with human management of landscapes. The estimation of the full suite of charcoal compounds of a bulk sediment sample via ^{13}C-NMR and IR spectroscopy can provide an estimation of total charcoal concentrations, regardless of particle size or morphology (Preston and Schmidt, 2006; McBeath et al., 2011). ^{13}C-NMR methods may provide a less nuanced representation of local burning history, however may provide the potential to identify previously undetectable fire events. Uncertainties associated with biomass type and transport bias (Belcher et al., 2013; Crawford and

Belcher, 2014) may render this method a more robust technique in regions where vegetation type has changed dramatically or there is a predominance of non-woody, fine textured or volatile fuels.

This method displays the potential for create ultra high resolution fire histories, on annual to decadal scales, via IR calibrations (Rosén et al., 2010). In order to place current fire activity in to the context of historical fire requires analysis of fire histories on a scale relevent to management and mitigation (Conedera et al., 2009). The ability to examine changes in fire regimes on annual to decadal scale may also enable examination of subtle changes in fire regime in response to climate or landuse change.

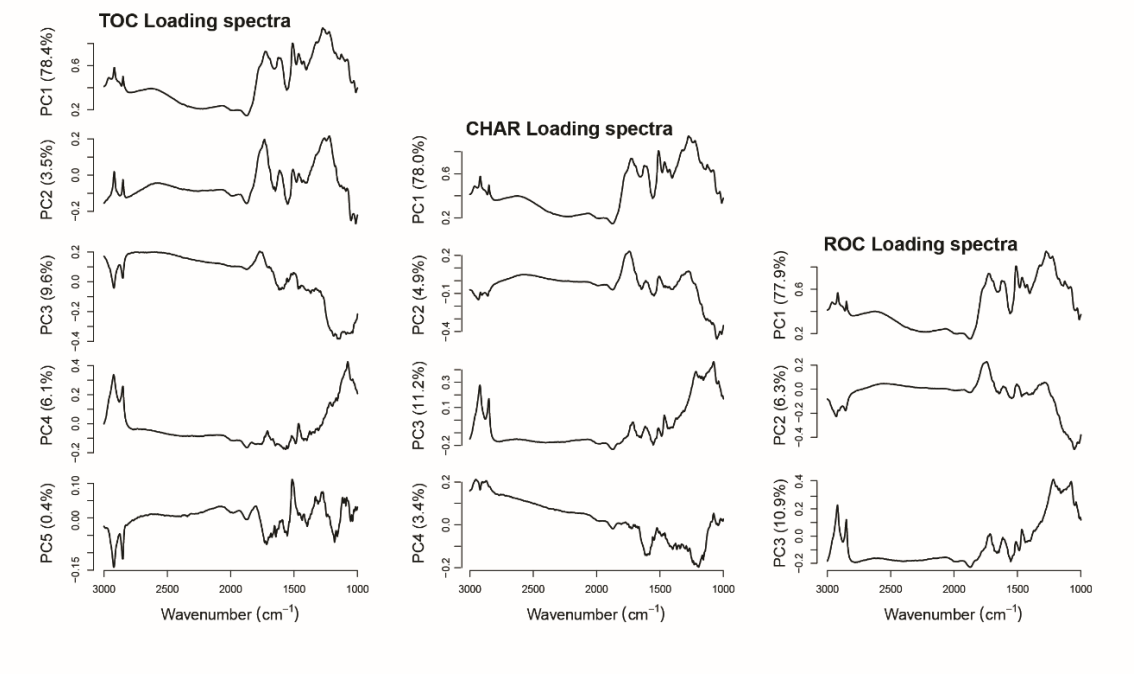

Figure 9. Loading spectra for TOC, ROC and charcoal PLSR models. Percent of total variance explained by each principle component is included in the y-axis label.

4.3. Carbon cycling and palaeoecological implications

^{13}C-NMR and IR spectroscopy provide the ability to determine quantitative estimates of the total charcoal content of sediments. Quantitative estimates of charcoal concentrations can be utilised for budgeting the carbon sequestration potential of wetlands. This presently unquantified pool of charcoal carbon may be a large contributor to global carbon storage (Bird et al., 2015). Movement of stored soil charcoal via soil erosion can result in burial of large amounts of charcoal at sites of terrestrial sediment accumulation, such as wetlands. The ability to account for this charcoal carbon pool will provide greater understanding of the role this slow-cycling carbon component plays in the global carbon cycle, as well as its potential for providing long-term carbon sequestration.

Quantifying the contribution of black carbon to the total organic carbon content of

sediments can also provide more accurate interpretations of other organic sedimentary analyses. TOC, carbon: nitrogen ratio (C: N), and both carbon and nitrogen isotope ($\delta^{13}C$ and $\delta^{15}N$) signatures of bulk sediment are commonly used to infer the source of organic carbon and the palaeoproductivity of past ecosystems (Leng, 2006). Combustion of biomass can alter the $\delta^{13}C$ of source material and inflate C:N ratios (Ferrio et al., 2006; Bird and Ascough, 2012). In sediments where charcoal or black carbon contributes to the overall TOC content, this charcoal may considerably influence the resulting geochemical signatures (Wiechmann et al., 2015). Ratios of C:N are commonly used in palaeolimnological studies to infer the relative contribution of terrestrial or algal carbon to the sedimentary record (Meyers, 1994; Meyers and Teranes, 2001). Low C:N ratios (C:N ≤ 10) are indicative of protein rich and lignin poor organic material sourced from autochonous algal production. In contrast, high C:N ratios (C:N ≥ 20) are commonly interpreted as being dominated by protein poor, lignin rich, terrestrial organic material (Meyers and Teranes, 2001). Addition of small amounts of carbon rich charcoal may inflate C:N ratios, leading to incorrect interpretation of the major sources of sedimentary carbon. Within the Welsby Lagoon sediments peak C:N values occur concurrently with peak lignin values, suggesting the high C:N values between 380 – 485 cm are driven by the input of carbon rich terrestrial material (Cadd et al., 2018). The C:N and lignin records display some correlation (R^2=0.56; Figure S6), however the C:N ratio remains elevated even during periods when the proportion of lignin is low, indicating there are additional influences on the sedimentary C:N ratios (Cadd et al., 2018). Determining the total charcoal content of sediments is thus an important goal for a variety of palaeoecological and carbon budgeting studies. Consequently, the choice of charcoal method should be based on an informed decision of the desired knowledge outcome. If users are interested in the total charcoal concentration of sediments, ^{13}C-NMR and IR spectroscopy may provide a reliable and cost effective option.

Our results demonstrate that IR spectroscopy can provide a viable and low labour technique for accurate determination of charcoal concentrations from wetland sediments. The ability to predict sediment charcoal concentration whilst concurrently estimating the concentrations of TOC, total nitrogen, total inorganic carbon, biogenic silica and mineralogical properties (Vogel et al., 2008; Rosén et al., 2010), emphasises the potential for IR spectroscopy. The ability to predict an array of sediment properties alongside charcoal content highlights the prospect for this method to become, at least, a standard preliminary screening tool for a variety of palaeoenvironmental studies and, at best, an approach to quantify poly-aromatic ROC. If used in conjunction with a multi-proxy vegetation and geochemical data, this information would allow the elucidation of both local and regional scale biomass burning across the continuum of fuel types, pyrolysis temperatures and degradation products.

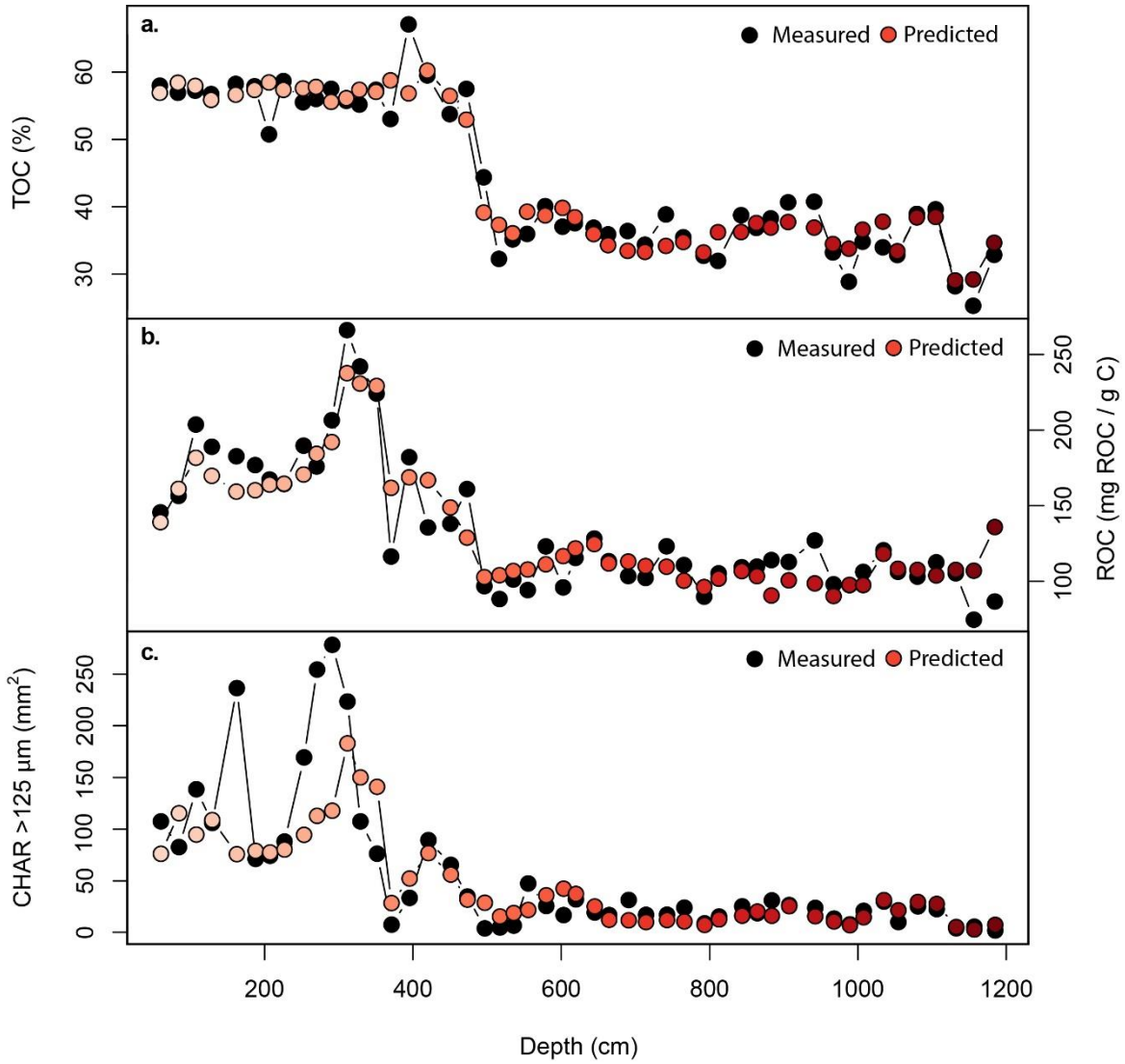

Figure 10. Conventionally measured (black circles) vs. infrared predicted (coloured circles) a. Total organic carbon (TOC), b. Resistant organic carbon (ROC) and c. Optical charcoal >125 µm (cm2 g-1). Both model and predicted data presented are converted from log transformed values to original measurements. All series are plotted via core depth (cm). Predicted symbol colours indicate core depth for each sample.

5 Conclusions

We presented the first attempt to use infrared spectroscopy to predict charcoal content of wetland sediments. Predictive models developed with ^{13}C-NMR-based recalcitrant organic carbon concentrations provide promising results for predicting the entire continuum of combustion materials in sedimentary sequences. PLSR models developed from conventionally measured charcoal using optical microscopy were similar, but less accurate. The lower accuracy of the model for inferring conventionally determined charcoal is likely due to the inability of those methods to quantify small charcoal particles, which can account for a large proportion of sedimentary charcoal. Our work raises important questions regarding which fractions of the continuum of charcoal

compounds will provide the ecological information desired. Future research should consider this in the context of research questions and environmental settings when deciding on methodologies. The continued expansion of this technique and incorporation of a greater number of calibration samples, particularly from additional wetland sites, would likely improve both the predictive power and accuracy of PLSR models for charcoal concentration.

IR spectroscopy is also able to predict TOC concentrations of a highly organic sediment sequence spanning the last 130,000 years. Given the proven ability of IR to quantify a range of sediment properties, the addition of charcoal estimates to that suite, even with a relatively low level of precision, highlights considerable value of IR spectroscopy as a low cost, initial sediment screening tool.

Acknowledgments.

We acknowledge Minjerribah (NSI) and the surrounding waters as Quandamooka Country. The study was funded by Australian Research Council project DP150103875. We thank Jie Chang, Jacinta Greer, Matthew Jones, Richard Lewis, Jonathan Marshall, Glenn McGregor, Patrick Moss and Cameron Schulz for assistance in the field. We thank Janine McGowan (CSIRO Agriculture and Food) for assistance with ^{13}C-NMR sample analysis and data processing and Martin Ankor for assistance with photography equipment and set-up.

References

Asselin, H., Payette, S., 2005. Detecting local-scale fire episodes on pollen slides. Rev. Palaeobot. Palynol. 137, 31–40. https://doi.org/10.1016/j.revpalbo.2005.08.002

Baldock, J.A., Hawke, B., Sanderman, J., Macdonald, L.M., 2013a. Predicting contents of carbon and its component fractions in Australian soils from diffuse reflectance mid-infrared spectra. Soil Res. 51, 577. https://doi.org/10.1071/SR13077

Baldock, J.A., Masiello, C.A., Gélinas, Y., Hedges, J.I., 2004. Cycling and composition of organic matter in terrestrial and marine ecosystems. Mar. Chem. 92, 39–64. https://doi.org/10.1016/j.marchem.2004.06.016

Baldock, J.A., Sanderman, J., Macdonald, L.M., Puccini, A., Hawke, B., Szarvas, S., McGowan, J., 2013b. Quantifying the allocation of soil organic carbon to biologically significant fractions. Soil Res. 51, 561. https://doi.org/10.1071/SR12374

Belcher, C.M., Punyasena, S.W., Sivaguru, M., 2013. Novel Application of Confocal Laser Scanning Microscopy and 3D Volume Rendering toward Improving the Resolution of the Fossil Record of Charcoal. PLoS One 8, e72265. https://doi.org/10.1371/journal.pone.0072265

Bird, M.I., Ascough, P.L., 2012. Isotopes in pyrogenic carbon: A review. Org. Geochem. 42, 1529–1539. https://doi.org/10.1016/j.orggeochem.2010.09.005

Bird, M.I., Wynn, J.G., Saiz, G., Wurster, C.M., McBeath, A., 2015. The Pyrogenic Carbon Cycle. Annu. Rev. Earth Planet. Sci. 43, 273–298. https://doi.org/10.1146/annurev-earth-060614-105038

Birks, H.H., Birks, H.J.B., 2006. Multi-proxy studies in palaeolimnology. Veg. Hist. Archaeobot. 15, 235–251. https://doi.org/10.1007/s00334-006-0066-6

Bliege Bird, R., Bird, D.W., Codding, B.F., Parker, C.H., Jones, J.H., 2008. The "fire stick farming" hypothesis: Australian Aboriginal foraging strategies, biodiversity, and anthropogenic fire mosaics. Proc. Natl. Acad. Sci. 105, 14796–14801. https://doi.org/10.1073/pnas.0804757105

Bornemann, L., Welp, G., Brodowski, S., Rodionov, A., Amelung, W., 2008. Rapid assessment of black carbon in soil organic matter using mid-infrared spectroscopy. Org. Geochem. 39, 1537–1544. https://doi.org/10.1016/j.orggeochem.2008.07.012

Bowman, D.M.J.S., 2000. Australian Rainforests: Islands of Green in a Land of Fire. Cambridge University Press, New York. https://doi.org/10.1111/j.1745-7939.2001.tb01610.x

Bowman, D.M.J.S., Balch, J.K., Artaxo, P., Bond, W.J., Carlson, J.M., Cochrane, M.A., D'Antonio, C.M., DeFries, R.S., Doyle, J.C., Harrison, S.P., Johnston, F.H., Keeley, J.E., Krawchuk, M.A., Kull, C.A., Marston, J.B., Moritz, M.A., Prentice, I.C., Roos, C.I., Scott, A.C., Swetnam, T.W., van der Werf, G.R., Pyne, S.J., 2009. Fire in the Earth System. Science (80-.). 324, 481–484. https://doi.org/10.1126/science.1163886

Cadd, H.R., Fletcher, M.-S., Mariani, M., Heijnis, H., Gadd, P.S., 2019. The influence of fine-scale topography on the impacts of Holocene fire in a Tasmanian montane landscape. J. Quat. Sci. 1–8. https://doi.org/10.1002/jqs.3114

Cadd, H.R., Tibby, J., Barr, C., Tyler, J., Unger, L., Leng, M.J., Marshall, J.C., McGregor, G., Lewis, R., Arnold, L.J., Lewis, T., Baldock, J., 2018. Development of a southern hemisphere subtropical wetland (Welsby Lagoon, south-east Queensland, Australia) through the last glacial cycle. Quat. Sci. Rev. 202, 53–65. https://doi.org/10.1016/j.quascirev.2018.09.010

Chang, C.-W., You, C.-F., Huang, C.-Y., Lee, T.-Q., 2005. Rapid determination of chemical and physical properties in marine sediments using a near-infrared reflectance spectroscopic technique. Appl. Geochemistry 20, 1637–1647. https://doi.org/10.1016/j.apgeochem.2005.04.011

Clark, J.S., 1988. Particle Motion and the Thoery of Charcoal Analysis: Source Area, Transport, Deposition, and Sampling. Quat. Res. 30, 67–80.

Colthup, N.B., Daly, L.H., Wiberley, S.E., 1990. Introduction to Infrared and Raman Spectroscopy, Introduction to Infrared and Raman Spectroscopy. https://doi.org/10.1016/B978-0-08-091740-5.50004-1

Conedera, M., Tinner, W., Neff, C., Meurer, M., Dickens, A.F., Krebs, P., 2009. Reconstructing past fire regimes: methods, applications, and relevance to fire management and conservation. Quat. Sci. Rev. 28, 555–576. https://doi.org/10.1016/j.quascirev.2008.11.005

Crawford, A.J., Belcher, C.M., 2014. Charcoal morphometry for paleoecological analysis: The effects of fuel type and transportation on morphological parameters. Appl. Plant Sci. 2, 1–10. https://doi.org/10.3732/apps.1400004

Cunningham, L., Tibby, J., Forrester, S., Barr, C., Skjemstad, J., 2016. Mid-Infrared Spectroscopy as a Potential Tool for Reconstructing Lake Salinity. Water (Switzerland) 8, 1–17. https://doi.org/10.3390/w8110479

Ferrio, J.P., Alonso, N., López, J.B., Araus, J.L., Voltas, J., 2006. Carbon isotope composition of fossil charcoal reveals aridity changes in the NW Mediterranean Basin. Glob. Chang. Biol. 12, 1253–1266. https://doi.org/10.1111/j.1365-2486.2006.01170.x

Forbes, M.S., Raison, R.J., Skjemstad, J.O., 2006. Formation, transformation and transport of black carbon (charcoal) in terrestrial and aquatic ecosystems. Sci. Total Environ. 370, 190–206. https://doi.org/10.1016/j.scitotenv.2006.06.007

Fox, P.M., Nico, P.S., Tfaily, M.M., Heckman, K., Davis, J.A., 2017. Organic Geochemistry Characterization of natural organic matter in low-carbon sediments : Extraction and analytical approaches. Org. Geochem. 114, 12–22. https://doi.org/10.1016/j.orggeochem.2017.08.009

Gosling, W.D., Cornelissen, H.L., McMichael, C.N.H., 2019. Reconstructing past fire temperatures from ancient charcoal material. Palaeogeogr. Palaeoclimatol. Palaeoecol. 520, 128–137. https://doi.org/10.1016/j.palaeo.2019.01.029

Graetz, R.D., Skjemstad, J.O., 2003. The charcoal sink of biomass burning on the Australian continent. CSIRO Atmos. Res. 64, 1–69.

Guo, Y., Bustin, R.M., 1998. FTIR spectroscopy and reflectance of modern charcoals and fungal decayed woods: implications for studies of inertinite in coals. Int. J. Coal Geol. 37, 29–53. https://doi.org/10.1016/S0166-5162(98)00019-6

Hammes, K., Schmidt, M.W.I., Smernik, R.J., Currie, L.A., Ball, W.P., Nguyen, T.H., Louchouarn, P., Houel, S., Gustafsson, Ö., Elmquist, M., Cornelissen, G., Skjemstad, J.O., Masiello, C.A., Song, J., Peng, P., Mitra, S., Dunn, J.C., Hatcher, P.G., Hockaday, W.C., Smith, D.M., Hartkopf-Fröder, C., Böhmer, A., Lüer, B., Huebert, B.J., Amelung, W., Brodowski, S., Huang, L., Zhang, W., Gschwend, P.M., Flores-Cervantes, D.X., Largeau, C., Rouzaud, J.-N., Rumpel, C., Guggenberger, G., Kaiser, K., Rodionov, A., Gonzalez-Vila, F.J., Gonzalez-Perez, J.A., de la Rosa, J.M., Manning, D.A.C., López-Capél, E., Ding, L., 2007. Comparison of quantification methods to measure fire-derived (black/elemental) carbon in soils and sediments using reference materials from soil, water, sediment and the atmosphere. Global Biogeochem. Cycles 21, n/a-n/a. https://doi.org/10.1029/2006GB002914

Hardy, B., Leifeld, J., Knicker, H., Dufey, J.E., Deforce, K., Cornélis, J.T., 2017. Long term change in chemical properties of preindustrial charcoal particles aged in forest and agricultural temperate soil. Org. Geochem. 107, 33–45. https://doi.org/10.1016/j.orggeochem.2017.02.008

Hawthorne, D., Mitchell, F.J.G., 2016. Identifying past fire regimes throughout the Holocene in Ireland using new and established methods of charcoal analysis. Quat. Sci. Rev. 137, 45–53. https://doi.org/10.1016/j.quascirev.2016.01.027

Higuera, P.E., Peters, M.E., Brubaker, L.B., Gavin, D.G., 2007. Understanding the origin and analysis of sediment-charcoal records with a simulation model. Quat. Sci. Rev. 26, 1790–1809.

https://doi.org/10.1016/j.quascirev.2007.03.010
Janik, L., Skjemstad, J., Raven, M., 1995. Characterization and analysis of soils using mid-infrared partial least-squares .1. Correlations with XRF-determined major-element composition. Aust. J. Soil Res. 33, 621. https://doi.org/10.1071/SR9950621
Janik, L.J., Skjemstad, J.O., Shepherd, K.D., Spouncer, L.R., 2007. The prediction of soil carbon fractions using mid-infrared-partial. Aust. J. Soil Res. 45, 73–81. https://doi.org/10.1071/sr06083
Korsman, T., Renberg, I., DÅBakk, E., Nilsson, M.B., 2002. Near-Infrared Spectrometry (Nirs) in Palaeolimnology, in: Tracking Environmental Change Using Lake Sediments. Kluwer Academic Publishers, Dordrecht, pp. 299–317. https://doi.org/10.1007/0-306-47670-3_11
Kuhlbusch, T.A., Crutzen, P.J., 1996. Black carbon, the global carbon cycle and atmospheric carbon dioxide, in: J., L. (Ed.), Biomass Burning and Global Change. MIT Press, pp. 161–169.
Kwon, S.M., Jang, J.H., Lee, S.H., Park, S.B., Kim, N.H., 2013. Change of heating value, pH and FT-IR spectra of charcoal at different carbonization temperatures. J. Korean Wood Sci. Technol. 41, 440–446. https://doi.org/10.5658/WOOD.2013.41.5.440
Lee, M., Novotny, M. V., Bartle, K.D., 1981. Analytical Chemistry of Polycyclic Aromatic Compounds. Elsevier Science, New York.
Leng, M.J., 2006. Isotopes in Palaeoenvironmental Research, Developments in Paleoenvironmental Research. Kluwer Academic Publishers, Dordrecht. https://doi.org/10.1007/1-4020-2504-1
Malley, D.F., Rönicke, H., Findlay, D.L., Zippel, B., Region, A., 1999. Feasibility of using near-infrared reflectance spectroscopy for the analysis of C, N, P, and diatoms in lake sediments. J. Paleolimnol. 21, 295–306. https://doi.org/10.1023/A:1008013427084
Masiello, C.A., 2004. New directions in black carbon organic geochemistry. Mar. Chem. 92, 201–213. https://doi.org/10.1016/j.marchem.2004.06.043
McBeath, A. V., Smernik, R.J., Schneider, M.P.W., Schmidt, M.W.I., Plant, E.L., 2011. Determination of the aromaticity and the degree of aromatic condensation of a thermosequence of wood charcoal using NMR. Org. Geochem. 42, 1194–1202. https://doi.org/10.1016/j.orggeochem.2011.08.008
Mcbeath, A. V, Smernik, R.J., 2009. Organic Geochemistry Variation in the degree of aromatic condensation of chars. Org. Geochem. 40, 1161–1168. https://doi.org/10.1016/j.orggeochem.2009.09.006
Mevik, B.-H., Wehrens, R., 2007. The pls Package: Principle Component and Partial Least Squares Regression in R. J. Stat. Softw. 18, 1–24. https://doi.org/10.1002/wics.10
Meyer-Jacob, C., Vogel, H., Gebhardt, A.C., Wennrich, V., Melles, M., Rosen, P., 2014. Biogeochemical variability during the past 3.6 million years recorded by FTIR spectroscopy in the sediment record of Lake El'gygytgyn, Far East Russian Arctic. Clim. Past 10, 209–220. https://doi.org/10.5194/cp-10-209-2014
Meyers, P.A., 1994. Preservation of elemental and isotopic source identification of sedimentary organic matter. Chem. Geol. 114, 289–302. https://doi.org/10.1016/0009-2541(94)90059-0
Meyers, P.A., Teranes, J.L., 2001. Sediment Organic Matter, in: Last, W.M., Smol, J.P. (Eds.), Tracking Environmental Change Using Lake Sediments: Physical and Geochemical Methods. Springer Netherlands, Dordrecht, pp. 239–269. https://doi.org/10.1007/0-306-47670-3_9
Mooney, S., Tinner, W., 2011. The analysis of charcoal in peat and organic sediments. Mires Peat 7, 1–18.
Mooney, S.D., Black, M., 2003. A simple and fast method for calculating the area of macroscopic charcoal isolated from sediments. Quat. Australas. 21, 18–21.
Naes, T., Isaksson, T., Fearn, T., Davis, T., 2002. A user friendly guide to multivariate calibration and classification. NIR publications, Chichester.
Nocentini, C., Certini, G., Knicker, H., Francioso, O., Rumpel, C., 2010. Nature and reactivity of charcoal

produced and added to soil during wildfire are particle-size dependent. Org. Geochem. 41, 682–689. https://doi.org/10.1016/j.orggeochem.2010.03.010

Oksanen, J., Blanchet, F.G., Kindt, R., Legendre, P., Minchin, P.R., O'Hara, R.B., Simpson, G.L., Solymos, P., Stevens, M.H.H., Wagner, H., 2013. Package 'vegan.' R Packag. ver. 2.0–8 254. https://doi.org/10.4135/9781412971874.n145

Patterson, W.A., Edwards, K.J., Maguire, D.J., 1987. Microscopic charcoal as a fossil indicator of fire. Quat. Sci. Rev. 6, 3–23. https://doi.org/10.1016/0277-3791(87)90012-6

Pearson, E.J., Juggins, S., Tyler, J., 2014. Ultrahigh resolution total organic carbon analysis using Fourier Transform Near Infrarred Reflectance Spectroscopy (FT-NIRS). Geochemistry, Geophys. Geosystems 15, 292–301. https://doi.org/10.1002/2013GC004928

Peters, M.E., Higuera, P.E., 2007. Quantifying the source area of macroscopic charcoal with a particle dispersal model. Quat. Res. 67, 304–310. https://doi.org/10.1016/j.yqres.2006.10.004

Pitkänen, A., Lehtonen, H., Huttunen, P., 1999. Comparison of sedimentary microscopic charcoal particle records in a small lake with dendrochronological data: Evidence for the local origin of microscopic charcoal produced by forest fires of low intensity in eastern Finland. Holocene 9, 559–567. https://doi.org/10.1191/095968399670319510

Power, M.J., Marlon, J., Ortiz, N., Bartlein, P.J., Harrison, S.P., Mayle, F.E., Ballouche, A., Bradshaw, R.H.W.W., Carcaillet, C., Cordova, C., Mooney, S., Moreno, P.I., Prentice, I.C., Thonicke, K., Tinner, W., Whitlock, C., Zhang, Y., Zhao, Y., Ali, A.A., Anderson, R.S., Beer, R., Behling, H., Briles, C., Brown, K.J., Brunelle, A., Bush, M., Camill, P., Chu, G.Q., Clark, J., Colombaroli, D., Connor, S., Daniau, A.L., Daniels, M., Dodson, J., Doughty, E., Edwards, M.E., Finsinger, W., Foster, D., Frechette, J., Gaillard, M.J., Gavin, D.G., Gobet, E., Haberle, S., Hallett, D.J., Higuera, P., Hope, G., Horn, S., Inoue, J., Kaltenrieder, P., Kennedy, L., Kong, Z.C., Larsen, C., Long, C.J., Lynch, J., Lynch, E.A., McGlone, M., Meeks, S., Mensing, S., Meyer, G., Minckley, T., Mohr, J., Nelson, D.M., New, J., Newnham, R., Noti, R., Oswald, W., Pierce, J., Richard, P.J.H.H., Rowe, C., Sanchez Goñi, M.F., Shuman, B.N., Takahara, H., Toney, J., Turney, C., Urrego-Sanchez, D.H., Umbanhowar, C., Vandergoes, M., Vanniere, B., Vescovi, E., Walsh, M., Wang, X., Williams, N., Wilmshurst, J., Zhang, J.H., Sanchez Go??i, M.F., Shuman, B.N., Takahara, H., Toney, J., Turney, C., Urrego-Sanchez, D.H., Umbanhowar, C., Vandergoes, M., Vanniere, B., Vescovi, E., Walsh, M., Wang, X., Williams, N., Wilmshurst, J., Zhang, J.H., Sanchez Goñi, M.F., Shuman, B.N., Takahara, H., Toney, J., Turney, C., Urrego-Sanchez, D.H., Umbanhowar, C., Vandergoes, M., Vanniere, B., Vescovi, E., Walsh, M., Wang, X., Williams, N., Wilmshurst, J., Zhang, J.H., 2008. Changes in fire regimes since the last glacial maximum: An assessment based on a global synthesis and analysis of charcoal data. Clim. Dyn. 30, 887–907. https://doi.org/10.1007/s00382-007-0334-x

Preston, C.M., Schmidt, M.W.I., 2006. Black (pyrogenic) carbon: a synthesis of current knowledge and uncertainties with special consideration of boreal regions. Biogeosciences 3, 397–420. https://doi.org/10.5194/bg-3-397-2006

R Core Team, 2017. R: A Language and Environment for Statistical Computing. R Found. Stat. Comput. Vienna, Austria. https://doi.org/http://www.R-project.org/

Rosén, P., Vogel, H., Cunningham, L., Hahn, A., Hausmann, S., Pienitz, R., Zolitschka, B., Wagner, B., Persson, P., 2011. Universally Applicable Model for the Quantitative Determination of Lake Sediment Composition Using Fourier Transform Infrared Spectroscopy. Environ. Sci. Technol. 45, 8858–8865. https://doi.org/10.1021/es200203z

Rosén, P., Vogel, H., Cunningham, L., Reuss, N., Conley, D.J., Persson, P., 2010. Fourier transform infrared spectroscopy, a new method for rapid determination of total organic and inorganic carbon and biogenic silica concentration in lake sediments. J. Paleolimnol. 43, 247–259.

https://doi.org/10.1007/s10933-009-9329-4
Sawyer, R., Bradstock, R., Bedward, M., Morrison, R.J., 2018. Fire intensity drives post-fire temporal pattern of soil carbon accumulation in Australian fire-prone forests. Sci. Total Environ. 610–611, 1113–1124. https://doi.org/10.1016/j.scitotenv.2017.08.165
Schmidt, M.W.I., Noack, A.G., 2000. Black carbon in soils and sediments: Analysis, distribution, implications, and current challenges. Global Biogeochem. Cycles 14, 777–793.
Skjemstad, J.O., Taylor, J. a., Smernik, R.J., 1999. Estimation of charcoal (char) in soils. Commun. Soil Sci. Plant Anal. 30, 2283–2298. https://doi.org/10.1080/00103629909370372
Tan, K.H., 2014. Humic Matter in Soil and the Environment: Principles and controversies, CRC Press.
Tinner, W., Hofstetter, S., Zeugin, F., Conedera, M., Wohlgemuth, T., Zimmermann, L., Zweifel, R., 2006. Long-distance transport of macroscopic charcoal by an intensive crown fire in the Swiss Alps - implications for fire history reconstruction. The Holocene 16, 287–292. https://doi.org/10.1191/0959683606hl925rr
Van de Broek, M., Govers, G., 2019. Quantification of organic carbon concentrations and stocks of tidal marsh sediments via mid-infrared spectroscopy. Geoderma 337, 555–564. https://doi.org/10.1016/j.geoderma.2018.09.051
Viscarra Rossel, R.A., Behrens, T., 2010. Using data mining to model and interpret soil diffuse reflectance spectra. Geoderma 158, 46–54. https://doi.org/10.1016/j.geoderma.2009.12.025
Viscarra Rossel, R.A., Walvoort, D.J.J., McBratney, A.B., Janik, L.J., Skjemstad, J.O., 2006. Visible, near infrared, mid infrared or combined diffuse reflectance spectroscopy for simultaneous assessment of various soil properties. Geoderma 131, 59–75. https://doi.org/10.1016/j.geoderma.2005.03.007
Vogel, H., Rosén, P., Wagner, B., Melles, M., Persson, P., 2008. Fourier transform infrared spectroscopy, a new cost-effective tool for quantitative analysis of biogeochemical properties in long sediment records. J. Paleolimnol. 40, 689–702. https://doi.org/10.1007/s10933-008-9193-7
Weng, C.Y., 2005. An improved method for quantifying sedimentary charcoal via a volume proxy. Holocene 15, 298–301. https://doi.org/10.1191/0959683605hl795rr
Whitlock, C., Larsen, C., 2001. Charcoal as a Fire Proxy, in: Smol, J.P., Birks, H.J.B., Last, W.M., Bradley, R.S., Alverson, K. (Eds.), Tracking Environmental Change Using Lake Sediments: Terrestrial, Algal, and Siliceous Indicators. Springer Netherlands, Dordrecht, pp. 75–97. https://doi.org/10.1007/0-306-47668-1_5
Whitlock, C., Millspaugh, S.H., 1996. Testing the assumptions of fire-history studies: an examination of modern charcoal accumulation in Yellowstone National Park, USA. The Holocene 6, 7–15. https://doi.org/10.1177/095968369600600102
Wiechmann, M.L., Hurteau, M.D., Kaye, J.P., Miesel, J.R., 2015. Macro-particle charcoal C content following prescribed burning in a mixed-conifer forest, Sierra Nevada, California. PLoS One 10, 1–17. https://doi.org/10.1371/journal.pone.0135014
Wiedemeier, D.B., Abiven, S., Hockaday, W.C., Keiluweit, M., Kleber, M., Masiello, C.A., Mcbeath, A. V, Nico, P.S., Pyle, L.A., Schneider, M.P.W., Smernik, R.J., Wiesenberg, G.L.B., Schmidt, M.W.I., 2014. Organic Geochemistry Aromaticity and degree of aromatic condensation of char. Org. Geochem. 78, 135–143. https://doi.org/10.1016/j.orggeochem.2014.10.002
Williams, A.N., Mooney, S.D., Sisson, S.A., Marlon, J., 2015. Exploring the relationship between Aboriginal population indices and fire in Australia over the last 20,000years. Palaeogeogr. Palaeoclimatol. Palaeoecol. 432, 49–57. https://doi.org/10.1016/j.palaeo.2015.04.030
Yao, J., Hockaday, W.C., Murray, D.B., White, J.D., 2014. Changes in fire-derived soil black carbon storage in a subhumid woodland. J. Geophys. Res. Biogeosciences 119, 1807–1819. https://doi.org/10.1002/2014JG002619

6 Supplementary Information

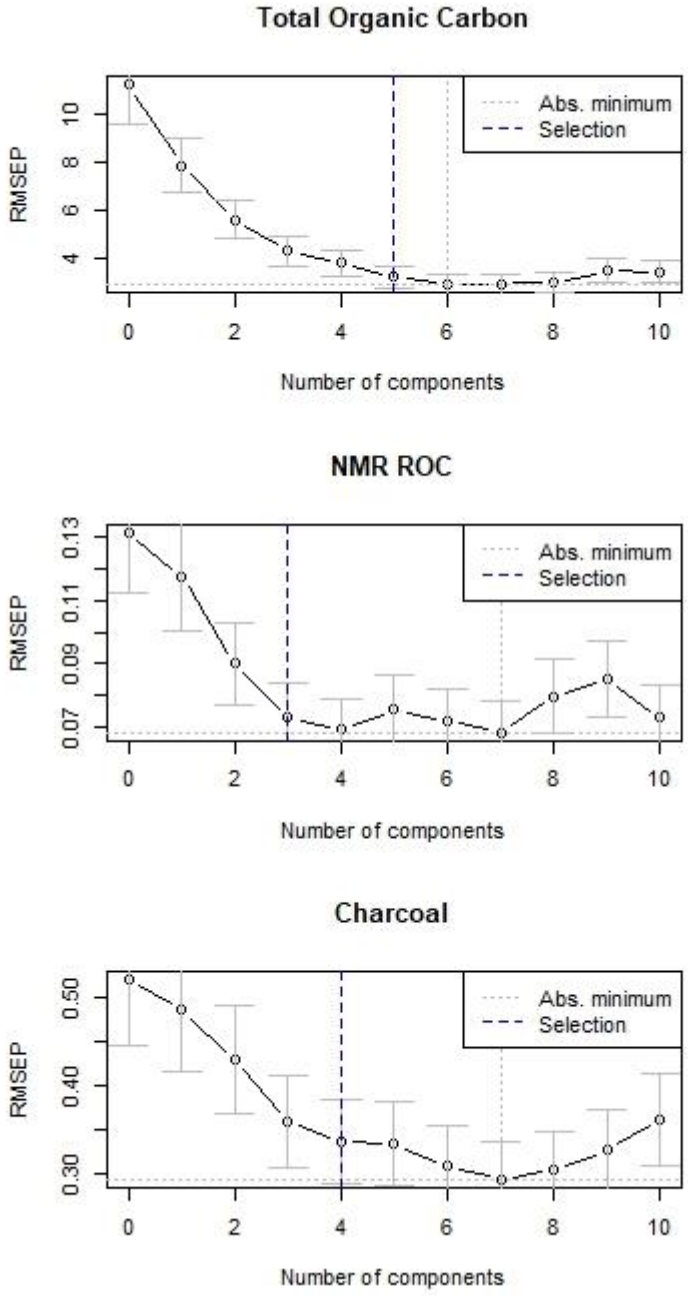

Figure S1. Standard error of the cross-validated (CV) residuals for each modelled variable. The number of components of first partial least squares regression (PLSR) model returned for each variable where the optimal cross validated model is within one standard deviation of the optimal model was used.

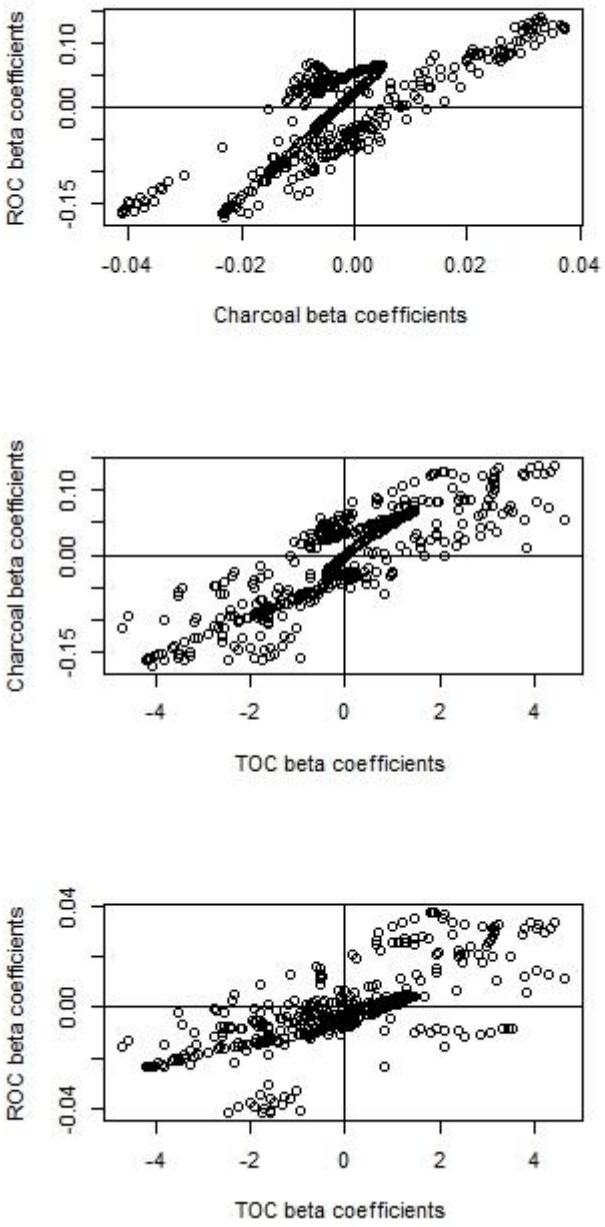

Figure S2. Correlation of the Beta Coefficients between different PLSR models.

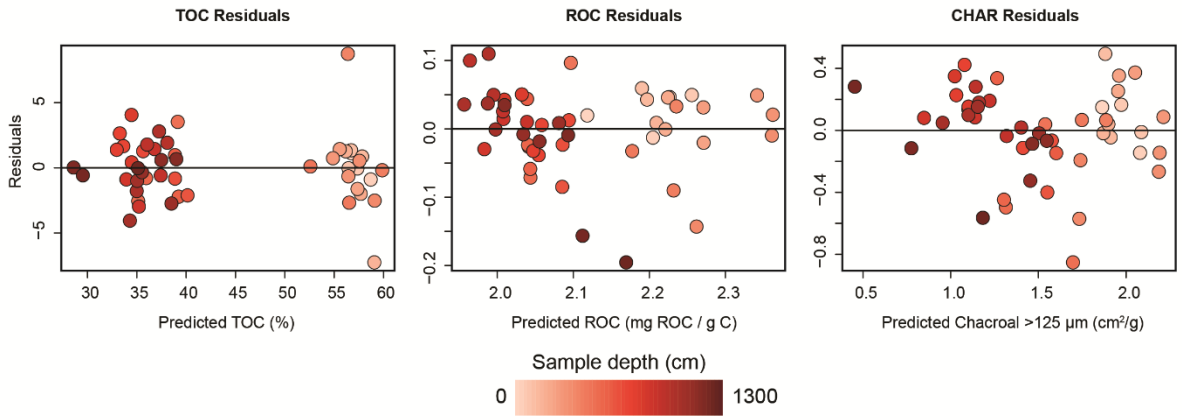

Figure S3. The residuals (yi – yi) as a function of predicted values of Y associated with the prediction models for TOC, ROC and Charcoal.

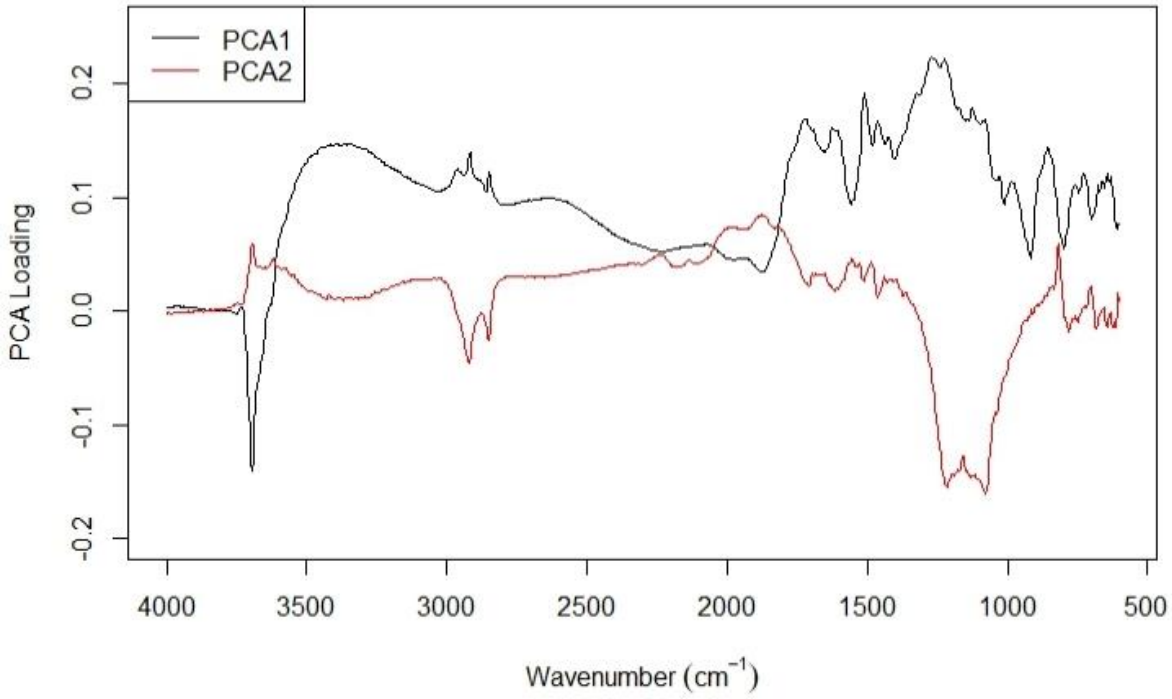

Figure S4. Loading spectra for Principle Component Analysis (PCA) of Infrared spectra. PCA1 and PCA2. PCA axis 1 explains 67.8 % of the variance, while PCA2 explains 12.9% of the variance within the dataset.

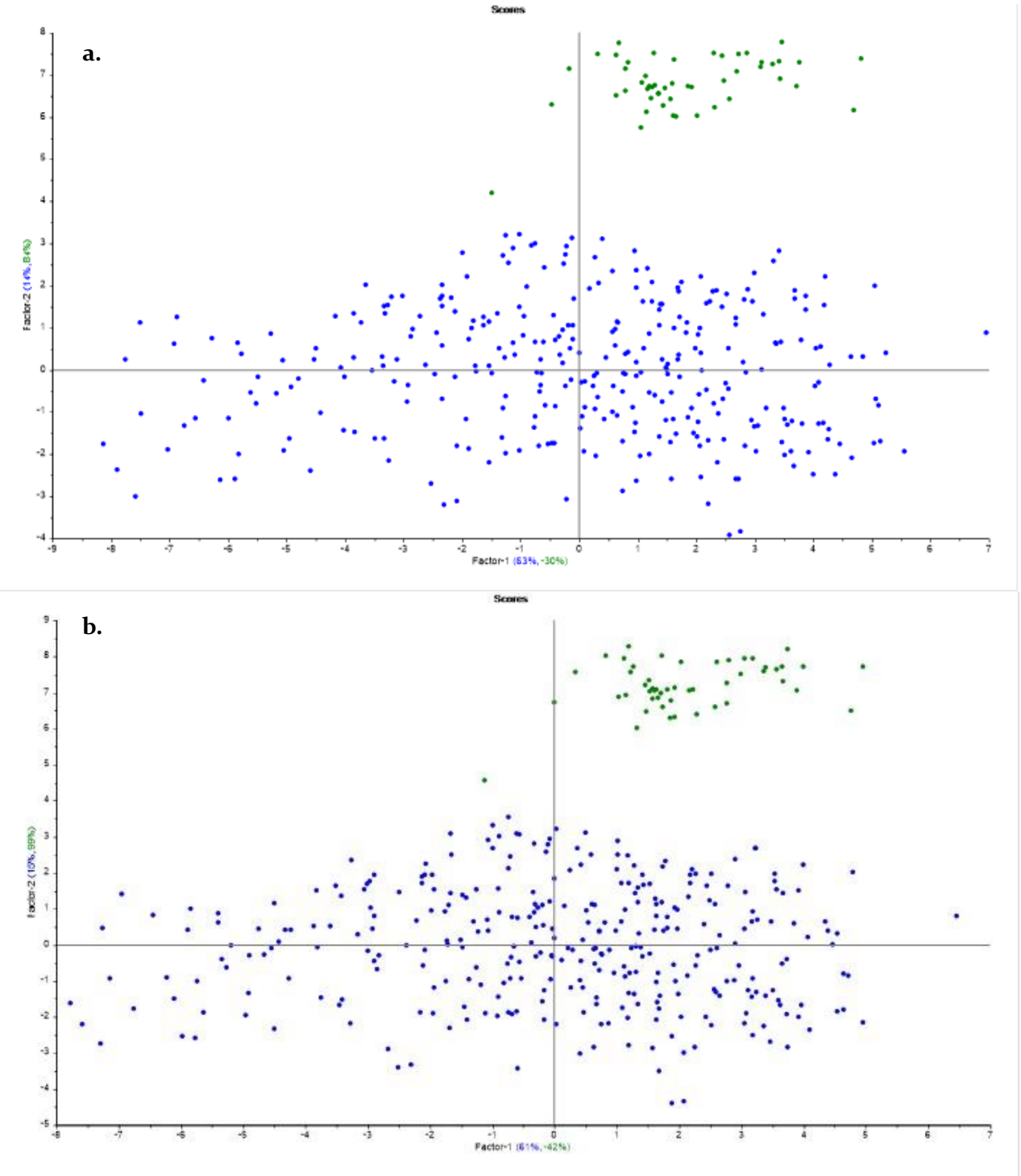

Figure S5 Principle component analysis (PCA) biplot of the infrared spectra and organic carbon data from the mineral agricultural soil database used by Baldock et al. 2013 (blue) and the infrared spectra and organic carbon values from this study (green). **b.** Principle component analysis (PCA) biplot of the infrared spectra and resistant organic carbon (ROC) data from the mineral agricultural soil database used by Baldock et al. 2013 (blue) and the infrared spectra and resistant organic carbon (ROC) values from this study (green).

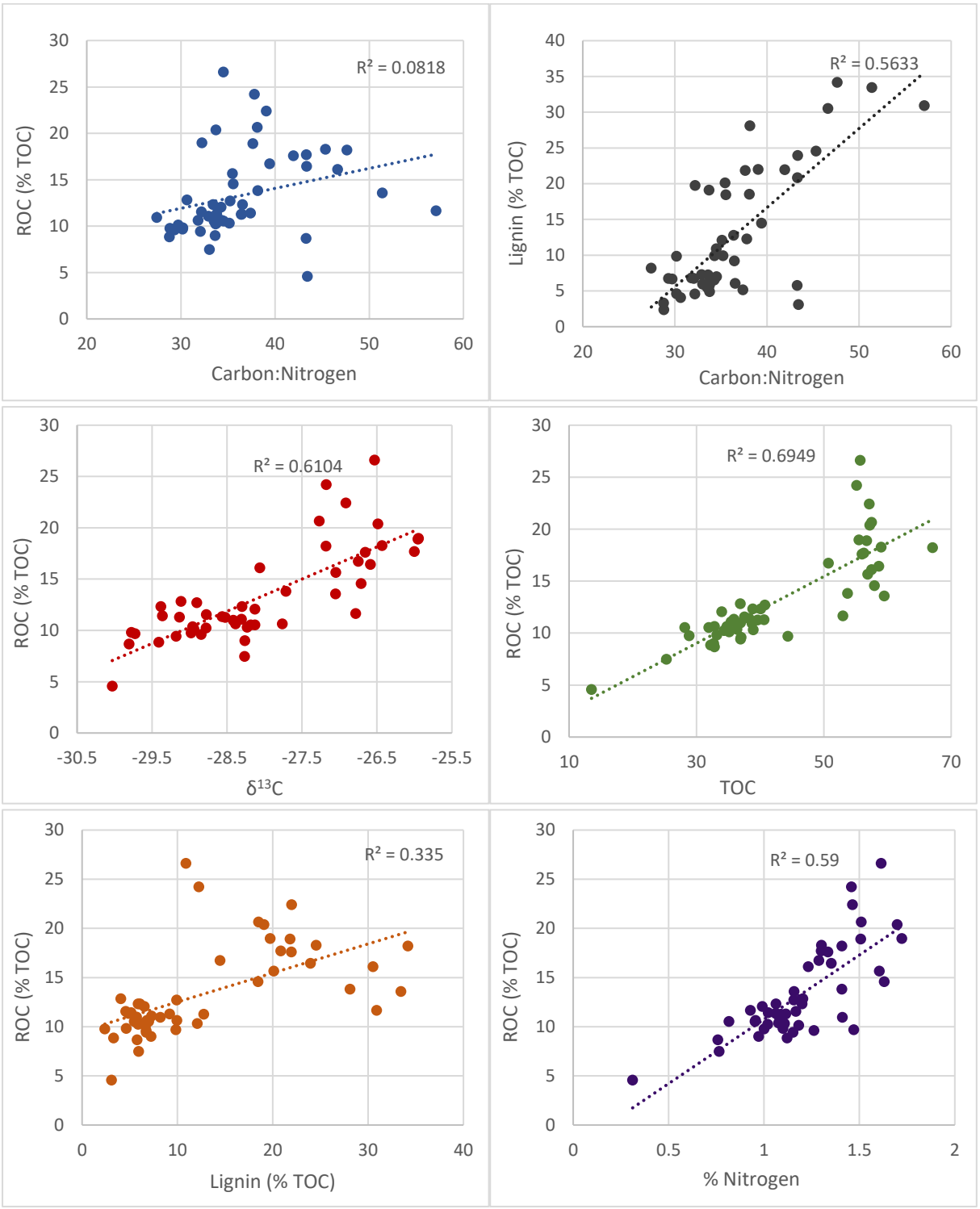

Figure S6. Scatter plots of 13C NMR derived ROC (% TOC) and Lignin (% TOC) with organic carbon and nitrogen proxies.

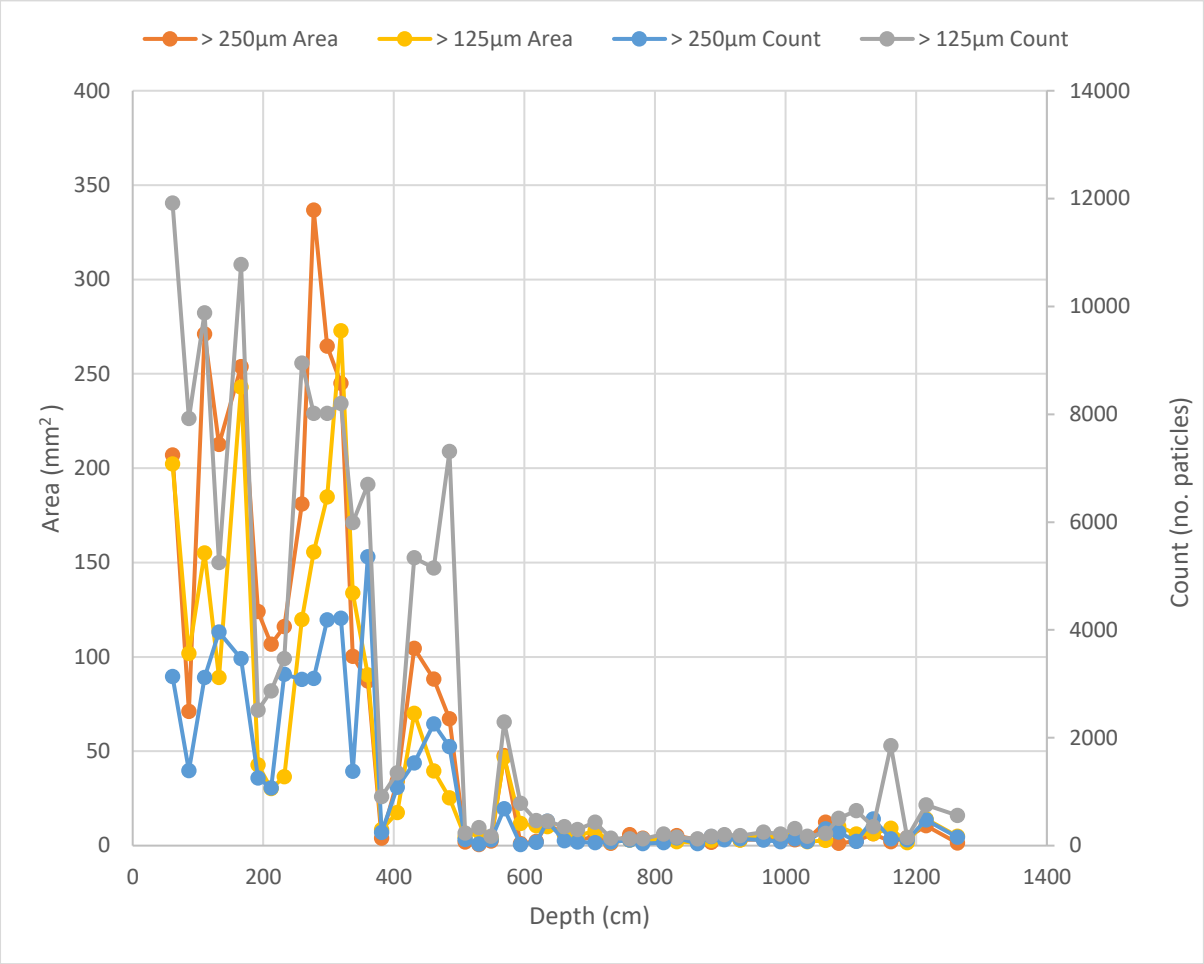

Figure 7. Comparison of charcoal Area measurements (mm^2) and particle counts obtained for the two different size fractions from ImageJ imaging software.

Statement of Authorship

Title of Paper	Vegetation succession accelerated by climate and fire on nutrient poor substrates
Publication Status	☐ Published ☐ Accepted for Publication ☐ Submitted for Publication ☑ Unpublished and Unsubmitted work written in manuscript style
Publication Details	Cadd, H.R.., Tyler, J., Tibby, (2019) Vegetation succession accelerated by climate and fire on nutrient poor substrates

Principal Author

Name of Principal Author	Haidee Cadd		
Contribution to the Paper	Conceptualisation of the work, development of ideas and conclusions, carried out analytical work, carried out statistical analysis, interpretation of the data, wrote manuscript.		
Overall percentage (%)	90		
Certification:	This paper reports on original research I conducted during the period of my Higher Degree by Research candidature and is not subject to any obligations or contractual agreements with a third party that would constrain its inclusion in this thesis. I am the primary author of this paper.		
Signature		Date	26/09/19

Co-Author Contributions

By signing the Statement of Authorship, each author certifies that:

i. the candidate's stated contribution to the publication is accurate (as detailed above);
ii. permission is granted for the candidate in include the publication in the thesis; and
iii. the sum of all co-author contributions is equal to 100% less the candidate's stated contribution.

Name of Co-Author	Jonathan Tyler		
Contribution to the Paper	Provided conceptual and interpretation guidance, edited manuscript		
Signature		Date	12/09/19

Name of Co-Author	John Tibby		
Contribution to the Paper	Conducted fieldwork, provided conceptual and interpretation guidance, edited manuscript		
Signature		Date	12/09/19

4

Vegetation succession accelerated by climate and fire on nutrient poor substrates

In preparation as:

Cadd, H. R., Tibby, J., Tyler, J., In Prep., Vegetation succession accelerated by climate and fire on nutrient poor substrates *Quaternary Science Reviews*

Abstract

Modern vegetation composition and distribution is a product of present-day forces, as well as a combination of processes operating over centuries to millennia. The long-term dynamics of vegetation communities, in response to internal and external forcing, is therefore an important component of understanding present day vegetation distributions. The resilience and recovery of ecosystems is crucial to predicting how ecosystems may respond to climate and environmental perturbations in the future. This paper presents an 80,000 year fire and vegetation record from Welsby Lagoon on North Stradbroke Island (NSI) to examine how subtropical vegetation communities responded to internal and external forcing from Marine Isotope Stage 4 (MIS4) to present. The pollen spectra from Welsby Lagoon display greater variability and rate of change during MIS4 and MIS3 than during MIS2 and the Holocene. The vegetation record shows limited systematic change during glacial periods (MIS4 and MIS2) possibly indicating that this region acted as a biodiversity refugium during glacial periods. Fire occurrence increased during the Holocene, interpreted as a response to increased biomass availability resulting from an increase in precipitation and density of human populations. This record demonstrates the dynamic and variable nature of vegetation and fire over the last 80,000 years and the importance of external drivers in accelerating successional vegetation changes.

1 Introduction

Understanding the present day distribution and composition of vegetation communities, as well as how those communities will respond to future climate and land use changes requires knowledge of historical change (Gillson, 2009). Legacies of vegetation dynamics in response to external (i.e. climate, disturbance, land availability) and internal (i.e. competition, nutrient availability, succession) forces can operate over timescales of centuries to millennia, influencing present day structure and function of ecosystems (Scheffer et al., 2001; Williams et al., 2011; Seddon et al., 2016). The response of vegetation communities to past forcing, in conjunction with changes in resilience and recovery, can help identify tipping points and threats to present day ecosystems (Scheffer et al., 2001; Gillson, 2009; Seddon et al., 2016).

In Australia, since the Miocene, fire has become an increasingly important external vegetation driver (Kershaw et al., 2002; Lynch et al., 2007). Fire imparts a strong impact on vegetation distribution, structure and composition. Whilst many Australian species are pyrophytic (fire promoting), much of the vegetation is pyrophobic (fire-sensitive), and suffers mortality and reduced recruitment following fire (Bowman, 2000). The distribution of vegetation types in Australia tends to reflect this relationship, with fire-sensitive vegetation communities often found in regions where climate is not conducive to fire ignition or spread and topographic locations protected from fire (Bradstock et al., 2010; Wood et al., 2011; Krawchuk et al., 2016). Fire occurrence is modulated by three main

factors: available oxygen, fuel availability and ignition sources (Bowman et al., 2009). Fuel availability is primarily a function of climate, with dry regions otherwise conducive to regular fire, often having insufficient biomass to support frequent fires. In contrast, in regions of wetter climates with ample fuel availability (high biomass), the frequently moist conditions and high humidity inhibits fire ignition and spread (Pausas & Ribeiro, 2013). Short-term climate fluctuations, pulses in precipitation enhancing biomass growth and drought conditions, are therefore important drivers of fire occurrence. Transitions between climate states is an important driver of long-term changes in fire regimes (Harrison & Sanchez Goñi, 2010; Daniau et al., 2012).

Fire activity during the Holocene has been extensively studied from eastern Australia, however records of fire activity extending beyond the LGM are rare (Mooney et al., 2011). The Holocene bias of available fire histories makes inferences about how fire regimes changed during the previous glacial cycle difficult (Mooney et al., 2011). In order to place the human use of fire and transformation of ecosystems in the context of natural fire regimes requires an understanding of fire regimes throughout the entire last glacial cycle across a variety of ecosystems. The relative stability of Holocene climates reduces the ability to examine the resilience of ecosystems in response to fire under a variety of climate regimes (Daniau et al., 2010). The geographically sparse records that currently exist have not permitted close examination of how vegetation responds to long term changes in fire frequency and how fire activity changes in response to changing climate.

Recent evidence from northern Australia has extended the time of human occupation in Australia to between 60 – 70 ka (Clarkson et al., 2017), indicating that humans may have arrived in Australia during MIS4. Whilst this extended occupation window has been challenged, it is generally accepted that widespread occupation of Australia occurred by ca. 50 ka (Hamm et al., 2016; Tobler et al., 2017). Indigenous management of landscapes, particularly by fire, has been commonly invoked as a driver of vegetation change (Bliege Bird et al., 2008). However, it is difficult to determine the extent of early human landscape management due to the lack of records that extend through this period that have macroscopic charcoal and vegetation reconstructions of sufficient resolution to examine ecological changes in association with burning practices. To attempt to untangle the role of early humans populations may have had on altering fire regimes and vegetation dynamics, requires geographically diverse records of local fire and vegetation.

North Stradbroke Island (NSI) is the southernmost part of the Great Sandy Region of south east Queensland that forms a series of sand masses along the subtropical east coast of Australia from 27.5°S to 25.5°S (Figure 1). The Great Sandy Region was formed during a series of Pleistocene and late Holocene dune building phases (Ward, 2016; Walker et al., 2018; Patton et al., 2019) and incorporates North Stradbroke, Moreton and Fraser Islands as well as the continental Cooloola sand mass. Whilst the extensive dune fields presently experience a similar climate regime (Figure 1) and are composed of the same siliceous parent material (quartz), there are major vegetation differences between the southern and northern components of the Great Sandy Region (Figure 7). The southern sand masses,

NSI and Moreton Island are dominated by open eucalypt woodlands and heathland, while the northern regions, Cooloola sand mass and Fraser Island, contain relatively large areas of intact rainforest and wet eucalypt forest. The dry rainforest communities of the Cooloola sand mass and Fraser Island, with an emergent canopy of Araucaria conifers, were also found on NSI during MIS3, becoming locally extinct in most areas during the LGM and deglacial (Moss et al., 2013). The Great Sandy Region chronosequence has previously been studied as a space for time substation to examine processes of succession on nutrient poor substrates. The vegetation structure and composition of the Cooloola sand mass indicated that each dune sequence supports different vegetation communities, with dwarf woodlands and grass forests found on young dune morphosequences transitioning to dense, tall woodlands and forests as nutrient accumulation proceeds (Walker et al., 1981). Retrogressive vegetation communities on the oldest dune sequences form dwarf shrubby woodlands in response to the highly weathered dune systems (Walker et al., 1981, 2010).

This paper describes a newly developed high resolution pollen record from Welsby Lagoon, NSI (Figure 1), to examine changes in vegetation distribution, composition and structure through the last glacial cycle. This vegetation record is coupled with high resolution microscopic and macroscopic charcoal records to understand the changing nature of fire from MIS4, MIS3, MIS2 and the Holocene to determine the influence of fire on vegetation dynamics across this extended time window. In addition, changes in the charcoal record are examined in context of an earlier human arrival. The Welsby Lagoon record provides a unique opportunity to examine the long term dynamic interplay of fire and vegetation from an understudied region bordering the subtropical and temperate climate regions.

1.1. Site description

North Stradbroke Island or Minjerribah (NSI; 27°27'S, 153°28'E) is the second largest sand Island in the world (275 km^2) and the southernmost extent of the Great Sandy Region off the coast of southeast Queensland, Australia (~27°S to 25°S; Figure 1). The parabolic coastal dunes were formed during a series of successive dune-building phases from the mid-Pleistocene to present from aeolian derived siliceous metasediments from eastern New South Wales (Thompson, 1981; Ward, 2016; Patton et al., 2019). Soil development on the predominantly quartz substrates range from weakly developed podzols to giant podzols (Thompson, 1992). Variations in soil properties and depth of podzol development are related to the temporal sequence of the dunes, with thick A2 and B horizons concentrated in older dune sequences (Thompson, 1981; Patton et al., 2019).

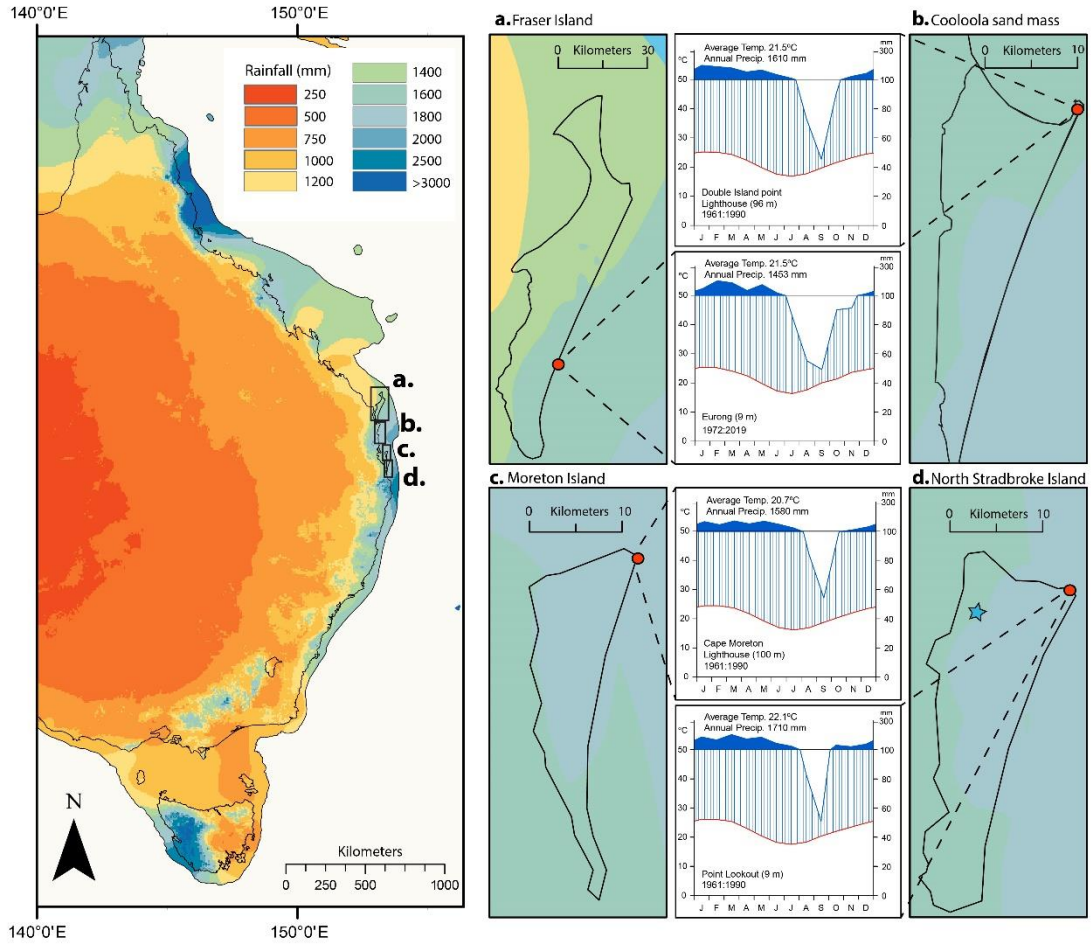

Figure 1. Location map of the Great Sandy Region. Left hand panel. Shading shows the mean annual rainfall of eastern Australia (BOM, 2018). Individual regions of the Great Sandy Region are outlined by black boxes. Right hand panel shows enlargements of boxes from the left panel Shading represents mean annual precipitation from left hand panel. Insets on right hand side are Walter-Leith diagrams of discrete climate stations with record of daily climate from 1961 – 1990 except Eurong which only began recording data in 1992. Blue bars indicate average monthly precipitation with red line indicating average monthly temperature. Blue shading indicates months with rainfall greater than 100 mm.

The vegetation across the Great Sandy Region can be broadly separated into seven communities (Table 1). Dry sclerophyll forest, woodland and heath communities predominate over the majority of the dune fields. The widespread heath vegetation of the region is commonly known as 'Wallum Heath', characteristic of low nutrient substrates. Mangrove forest develop on the western sides of each of the islands. The northern extent of the dune fields (Cooloola sand mass and Fraser Island) contain extensive areas of notophyllopus vine dry rainforest and wet eucalypt forest in the swales of the inland dunes (Gontz et al., 2015). These dense notophyllopus vine forests are almost entirely absent from the southern sand masses (Moreton and NSI), with small isolated pockets of rainforest and wet eucalypt forest occurring on NSI (Stephens & Sharp, 2009).

The range of permanent and ephemeral lacustrine, palustrine and riverine wetlands across the dune fields can generally be grouped as either perched or water table wetlands. The decomposition of organic material, weathering of minerals and water table fluctuations leads to the formation of an impermeable layer, which facilitates the development of perched wetland in the highly permeable dune system (Timms, 1986; Hofmann et al., 2019). Freshwater wetlands are consistent with waterlogged, oligotrophic environments, ranging from closed sedgeland dominated by *Ghania sieberana, Lepironia articulata* and *Restio pallens* to *Melaleuca quinquenervia* open forest.

Situated at the northwest end of NSI, in the Yankee Jack dune morphosequence, Welsby Lagoon (27°26'12"S, 153°26'56"E; 29 m.a.s.l; Figure 1) is a perched, permanent wetland. Welsby Lagoon is an internally draining, closed wetland system, with no fluvial input. The wetland surface is dominated by emergent aquatic sedges, with *Melaleuca* trees fringing the lagoon. The broader vegetation of the area is composed of open woodlands dominated by a canopy of *Eucalyptus sensu lato* and Casuarinaceae with a heathy mid-understory (Stephens & Sharp, 2009; Moss et al., 2013).

2 Methods

2.1. Sediment coring and chronology

Two complete sediment profiles were extracted from Welsby Lagoon in 2015 (WL15-1 and WL15-2). The two, 0.5 m offset, parallel sediment sequences were extracted from the deepest point of the sediment basin (Cadd et al., 2018). Sediment cores were extracted in 1 m core sections from a Kawhaw coring platform using a modified Bolivia corer.

2.2. Palynology

Pollen, microscopic charcoal and spore samples were processed using a modified version of protocols outlined in Fægri and Iverson (1989). In summary, 0.5 cm^3 of sediment was treated with 10% potassium hydroxide and rinsed through a 100 µm sieve. *Lycopodium* spore tablets were dissolved in 10% hydrochloric acid before silicates were separated using sodium polytungstate with a specific density of 1.9 – 2.0 g^1 cm^{-1}. Float material was then subjected to acetolysis before samples were mounted in glycerol and sealed with nail varnish. Pollen, microscopic charcoal and spore identification and counting was undertaken on a Nikon Eclipse E600 light microscope at 400x magnification. A total of 250 pollen grains of terrestrial origin form the base pollen sum. Percentages of aquatic taxa are based on an aquatic sum including both aquatic and terrestrial pollen taxa. A super sum of all taxa forms the basis for percentages of algal and spore taxa. Microscopic charcoal data are expressed as charcoal accumulation rate, CHAR (particles cm^2 yr^{-1}).

Table 1. Vegetation communities of the Cooloola sand mass depicted in figure 6. Key species of each vegetation type and brief description composition. BVG = Broad Vegetation Group. Information and data compiled from Clifford and Specht (1979), Leiper et al. (2008), Nelder et al. (2019), Stephens and Sharp (2009).

Vegetation Community	**BVG 1:5m Number**	**Key taxa**	**Description**
Rainforest	1	*Archontophoenix cunninghamiana, Melicope elleryana, Acronychia imperforata, Araucaria* spp.	Found on moist valley floors and lower fire protected slopes. Small areas of rainforest occur on NSI, but predominantly found on Fraser Island and Cooloola sand mass.
Wet eucalypt Forest	2	*Eucalyptus grandis, Eucalyptus pilularis, Eucalyptus saligna, Eucalyptus resinifera, Corymbia torelliana*	Wet to moist tall open forest dominated by *Eucalyptus* species, often with a rainforest understory.
Eucalypt Forest / woodland	3	*Eucalyptus racemosa, Eucalyptus pilularis, Eucalyptus planchoniana, Banksia aemula, Callitris columellaris, Acacia* spp.	Predominant vegetation of the island. Occurs on a variety of inland areas. Mallee forms occur on low nutrient, deeply leached sandy soils.
Melaleuca woodlands	8	*Melaleuca quinquenervia*	Open forests and woodlands dominated by *Melaleuca quinquenervia* in intermittently inundated swamps and coastal areas.
Heathlands	12	*Casuarina* sp., *Banksia aemula, Banksia serrata,* Ericaceae spp., Myrtaceae sp., Poaceae spp., *Xanthorrhoea johnsonii, Acacia* spp.	An endangered regional ecosystem. High species richness with a variety of colourful wildflower shrubs.
Wetlands	15	*Lepironia articula, Baloskion pallens, Baumea rubiginosa, Xanthorrhoea fulva, Melaleuca* spp., *Banksia robur, Boronia falcifolia*	Includes perched and window lakes, forest swamps and closed wet heath. Contains many rare, threatened and endemic species.
Mangroves / tidal wetlands	16	*Avicennia marina, Sporobolus virginicus, Sarcocornia quinqueflora, Casurina glauca*	Found on the western side of the islands, forming a protective fringe along the shoreline. Includes mangrove shrublands and saltpan vegetation. Important as fisheries habitat.
Rocky Headlands / sand		*Lophostemon confertus, Acacia* spp., *Banksia oblongifolia, Casurina equisetifolia, Pandanus tectorius*	Found on igneous rocky headlands. Species are adapted to withstand harsh exposed environments. Areas of severe weed infestation.

2.3. Macroscopic charcoal

Macroscopic charcoal analysis was conducted on core WL15-2, subsampled at contiguous 1 cm intervals from core depths between 1250 – 450 cm and at 2 cm intervals between 450 – 50 cm. Approximately 2 cm^3 of sediment, sub-sampled from 1 cm intervals, was weighed and submerged in 10% hydrogen peroxide (H_2O_2) for 7 days before being rinsed through a 125 µm sieve. Particles retained in the sieve were rinsed into a petri dish and tallied under a binocular microscope. Charcoal counts are expressed as number of particles per gram of dry sediment (particles g^{-1}). Dry sediment weight was calculated from water content measurements conducted on additional sub-samples from each sample depth.

2.4. Statistical Analysis

Zonation of terrestrial pollen spectra was conducted using a COnstrained Incremental Sum of Squares (CONISS) cluster analysis with Euclidean distance measure in the rioja package (Juggins, 2015) in R (R Core Team, 2017). Principle Component Analysis (PCA) was conducted on untransformed terrestrial pollen spectra in order to summarise the main patterns of change in the vegan package (Oksanen et al., 2013) in R (R Core Team, 2017). Broken stick analysis was used to determine the significance of stratigraphic pollen zones and principle components (Bennett, 1996).

To determine the single largest pattern of vegetation community change, a principal curve (PrC) was fitted to untransformed percentage pollen data in the analogue package (Simpson & Oksanen, 2019) in R (R Core Team, 2017). The PrC is a one-dimensional curve fitted through the pollen data that minimizes the distance between the curve and the response values of each species observation (Simpson & Oksanen, 2019). Rate-of-Change (ROC) analysis was conducted on the PrC of terrestrial pollen spectra using squared chord dissimilarity distance standardised by the time interval between each sample (Simpson & Oksanen, 2019). This method detects both deviations of the data from mean state and the time taken to return to "equilibrium" state. It simultaneously allows major changes in the record and recovery time to be interrogated without the need for regular sampling intervals or interpolation between samples.

Time series analysis of macroscopic charcoal was conducted using CHARanalysis (Higuera et al., 2009, 2010). Due to the changing resolution of the sedimentary sequence, CHARanalysis was run separately on two sections of core for Holocene and pre-Holocene samples. Normalised charcoal counts (particles g^{-1}) were interpolated to the median sample resolution of each of the two section runs. The background charcoal component, representing regional charcoal input, long term catchment inwash and/or secondary deposition, was determined using a locally fitted Gaussian model to identify the 95^{th} percentile threshold of noise distribution. Charcoal peaks were then calculated as the ratio between charcoal accumulation rates and background charcoal (Higuera et al.,2010).

3 Results

The lithology of the sequence represents three distinct sedimentary phases discussed in further detail in Cadd et al. (2018). The timing of the phases identified by Cadd et al. (2018) are refined herein following the development of the full chronology (Lewis et al., Accepted). Phase 1 (1270 – 1248 cm; ca. 126,000 – 83,000 calendar years before 1950, 126 – 83 ka) at the base of the sediment sequence is dated to MIS5. This section is discontinuous and represents the period of induration of the Welsby Lagoon site and formation of the perched aquifer (Lewis et al., Accepted). No samples from Phase 1 were analysed in this study due to the discontinuous nature of sediment accumulation. Phase 2 (1248 – 500 cm; ca. 83 – 28 ka) represents continuous deposition throughout MIS4 and MIS3. Phase 1 (500 – 0 cm; ca. 28 ka– Present) has the highest accumulation rates and represents the period from MIS2 through to present.

A total of 198 samples from Welsby Lagoon were analysed for pollen, spore and microscopic charcoal. Fossil pollen preservation was good throughout the sediment sequence. Identification of pollen grains was predominantly restricted to family or genus level, using a combination of online, print and reference material (APSA Members, 2007).

Species and taxa included in rainforest, heath and wetland pollen groups were determined based on their most common occurrence in modern vegetation communities determined from Clifford and Specht (1979), Leiper et al. (2008), Nelder et al. (2019), Stephens and Sharp (2009). Individual species and families included in each vegetation group is included in the supplementary info (Figures S3-S7). Five significant pollen zones were identified from all terrestrial pollen taxa identified in the Welsby Lagoon record using CONISS (Figure 2; supplimentary information Figure S1; Grimm, 1987, Bennett, 1996)

Zone 1 (ca. 83 – 71 ka) is characterised by high levels of rainforest pollen (1.8 – 12%) composed primarily of Araucariaceae (including *Agathis*) and *Podocarpus* This zone also records the highest levels of *Eucalyptus* (25.8 – 49.8%) and high proportions of *Leptospermum* (0.4 – 6.4%) and heath species (7 – 24.3%).

Zone 2 (ca. 71 – 54 ka) is characterised by alternating dominance of Asteraceae (1.2 – 13.6%) and rainforest pollen (1.5 – 13.7%). High *Eucalyptus* (18.4 – 47.3%), *Leptospermum* (0.7 – 10.7%) and heath (9.2 – 23.9%) taxa continue through this zone.

Zone 3 (ca. 54 – 43 ka) is marked by a substantial increase in Poaceae (7.4 – 18.6%) and Haloragaceae (0.8 – 14.6%) pollen types. Poaceae remains an important component of the pollen spectra for the remainder of Zone 3. This zone is characterised by declines in rainforest (0.3 – 5.8%), *Leptospermum* (0 – 4.8%), *Eucalyptus* (14.7 – 31.9%) and heath (5.6 – 23.5%) pollen, with many of these types becoming minor components of the pollen spectra by the end of Zone 3.

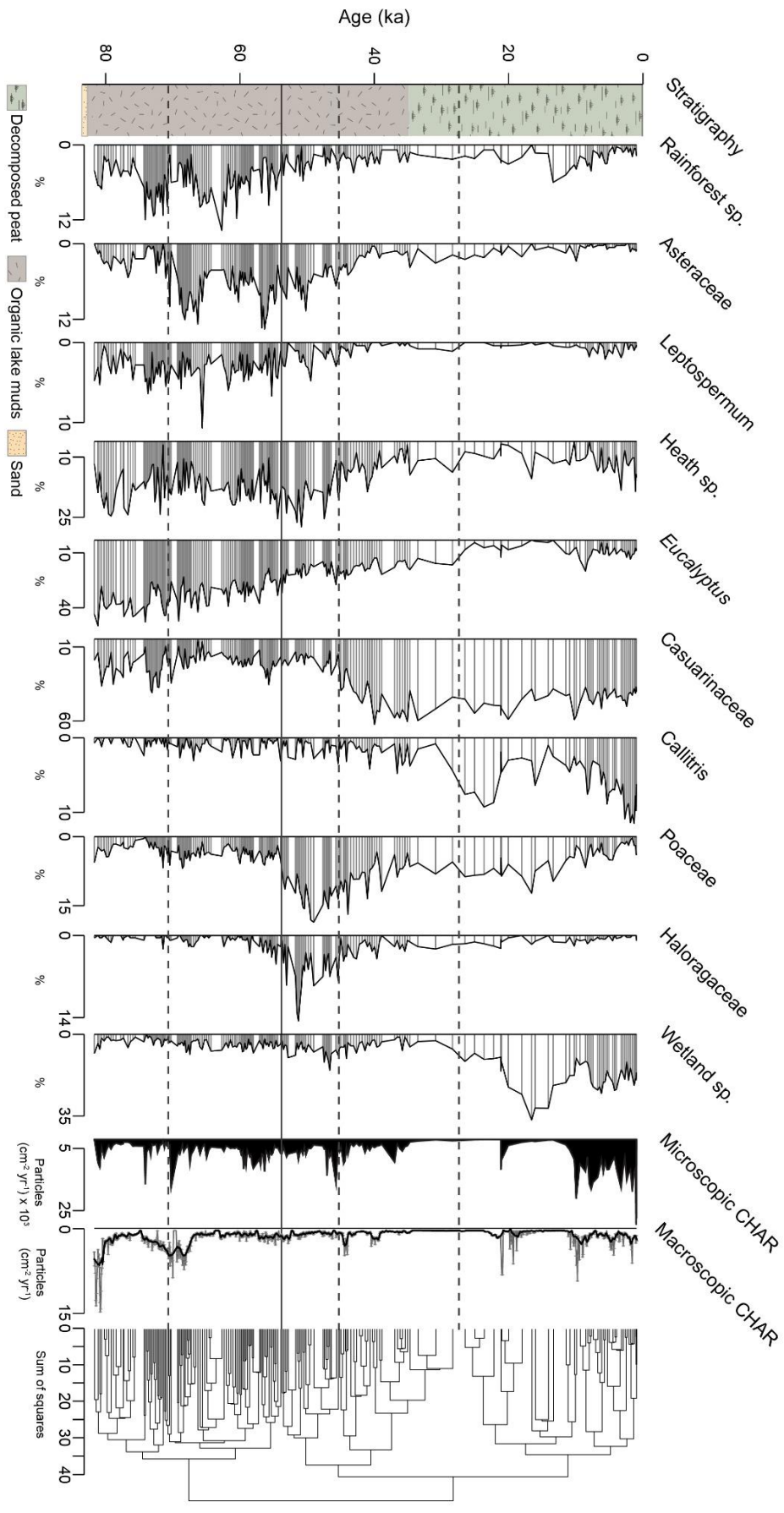

Figure 2. Diagram showing pollen relative abundance of key taxa. Macroscopic and microscopic charcoal accumulation rates (particles cm^{-2} yr^{-1}) are also shown. CONISS cluster analysis represents the significant cluster groups and subzones of the terrestrial pollen types. Solid line represents the largest change within the record. Chronology from Lewis et al. (submitted). Refer to Table 1 and supplimentary information for species included in vegetation groups.

In zone 4 (ca. 43 – 28 ka) Casuarinaceae (14.7 – 62.5%) become the sole dominant pollen type. Declines in Poaceae (3.3 – 16.9%) and Haloragaceae (0 – 7.7%) occurred at the beginning of Zone 4 as well as continued declines in *Eucalyptus* (12.7 – 24.4%) and heath species (8.8 – 23.5%). *Leptospermum* (0 – 2.1%), Asteraceae (0.4 – 5.2%) and rainforest (0.3 – 5.8%) taxa continue as minor components in zone 4.

Zone 5 (ca. 28 – present) is the period of lowest sediment deposition rate throughout the sequence. Zone 5 continues to be dominated by Casuarinaceae (37.1 – 59.2%), with lower values of Poaceae (0.3 – 12.3%). Cupressaceae (1 – 11.5%) pollen (likely *Callitris* species and herein referred to as *Callitris*) begins to contribute greater proportion to the pollen spectra in Zone 5 while rainforest (0 – 6%), Asteraceae (0 – 2.8%) and *Leptospermum* (0 – 0.7%) all become minor components. Zone 3 sees the first increase of wetland pollen types (8.1 – 36.7%), predominantly cyperaceous taxa, through the middle of this zone. Charcoal increases substantially at the top of this zone.

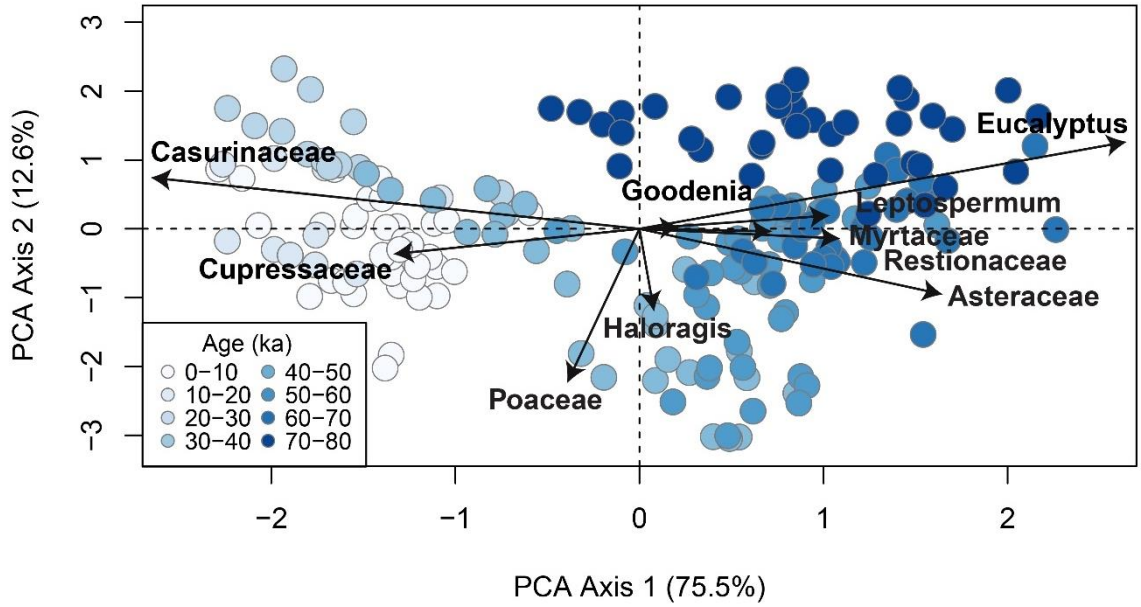

Figure 3. Principle Components Analysis (PCA) of terrestrial pollen taxa. Black arrows highlight taxa with a correlation with the PCA axes larger than r = 0.5. Variance of eigenvalue axis 1 = 75.5%, axis 2 = 12.6%. A broken stick analysis identified the first two principal components as significant.

The broken stick test identified the first two principle components as significant (supplementary information Figure S2; Bennett, 1996). PCA axis 1 accounts for 75.5% of the variance in the terrestrial pollen dataset. Samples corresponding to positive values on PCA axis 1 are composed entirely of samples older than 43 ka (Figure 3). Taxa with a positive association with axis 1 include *Eucalyptus*, *Leptospermum*, Myrtaceae and Asteraceae. Negative values on PCA axis 1 are weighted towards Casuarinaceae and *Callitris* and include samples younger than 43 ka (Figure 3). PCA axis 2 accounts for 12.6% of the variance with Poaceae and Haloragaceae negatively correlated with this axis.

The Principle Curve (PrC) analysis displays a large shift in vegetation occurring at ca. 43 ka (Figure 4). Rate-of-change (ROC) analysis indicates the greatest variability in the pollen spectra occurred between ca. 83 – 54 ka, corresponding to stratigraphic zones 1 and 2. It is important to note that some of the variance seen in the ROC analysis through this portion of the record could be a function of the higher sampling density and lower average time between samples. However, pollen samples between ca. 55 – 35 ka and 10 ka – present have similar temporal resolution and do not record the same magnitude of change (Figure 3).

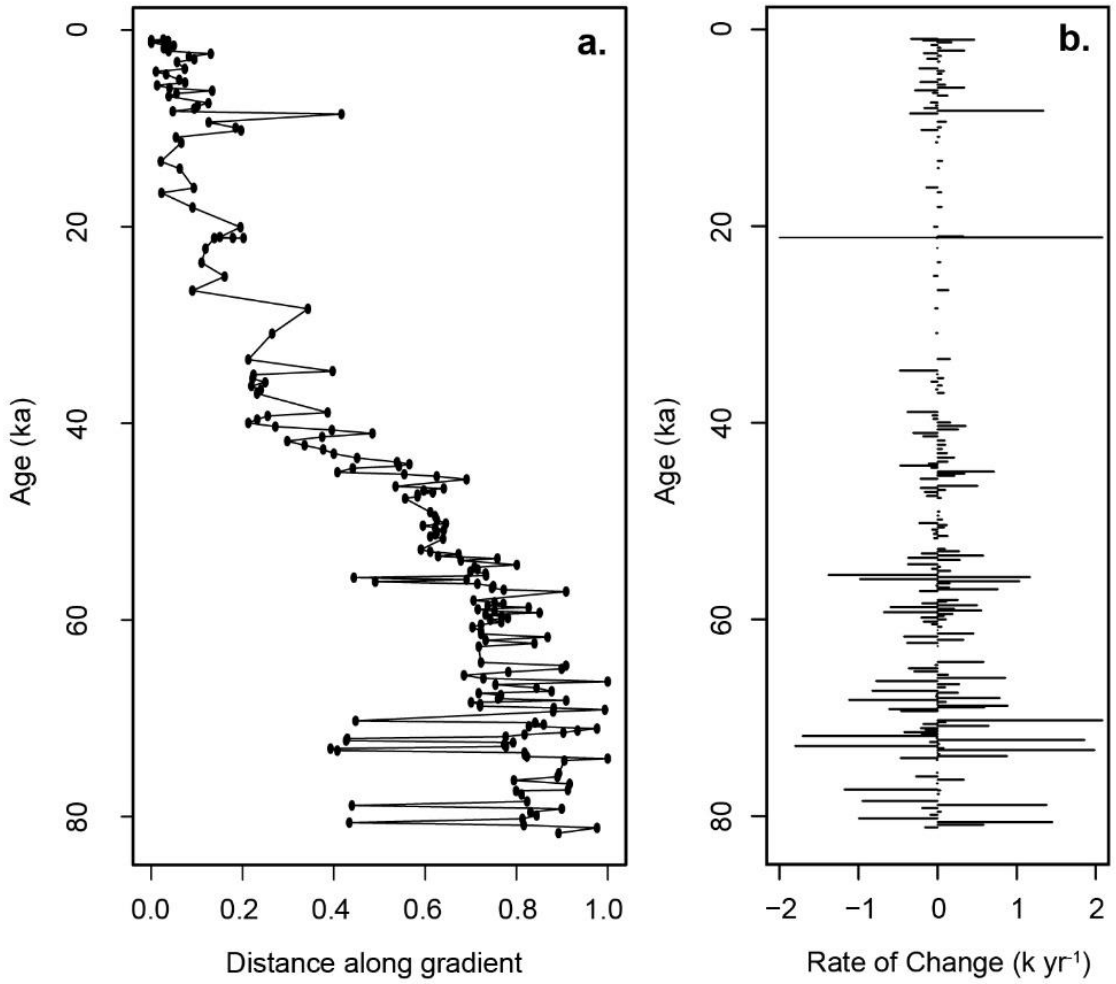

Figure 4. a. Terrestrial pollen Principle Curve (PrC) and b. Rate-of-Change (ROC) analysis was conducted on the PrC of terrestrial pollen spectra. Chronology from Lewis et al. (Accepted)

The macroscopic charcoal concentration from ca. 83 – 30 ka is generally low, with distinct peaks of increased charcoal abundance occurring throughout this period (Figure 2). There is a sharp increase in charcoal abundance between ca. 22 – 18 ka, coinciding with the global last glacial maximum (LGM; ca. 23 – 19 ka). Macroscopic charcoal content increases again at the beginning of the Holocene (ca. 11.8 ka) and remains at high concentrations throughout the remainder of the record.

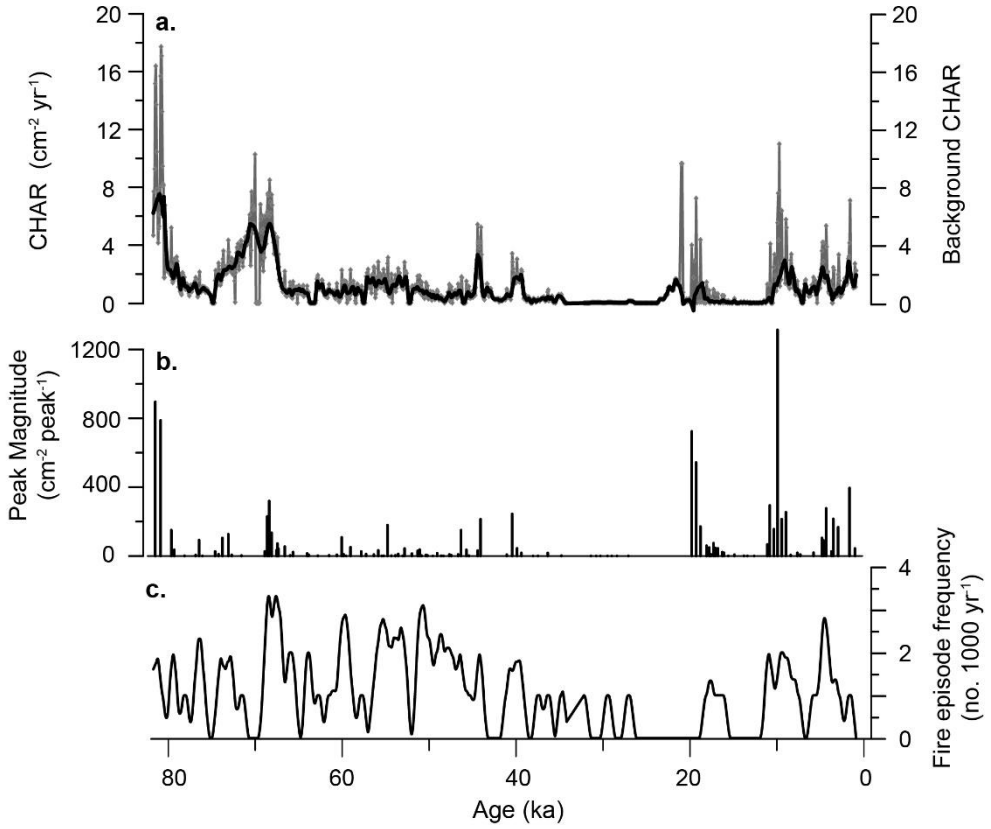

Figure 5. **a**. Charcoal accumulation rate (CHAR). Background chacroal indicated by solid black line in panel, **b**. Macroscopic charcoal peaks (cm^2 $peak^{-1}$) calculated as the ratio between charcoal accumulation rates and background charcoal, **c**. The fire-episode frequency is the number of peaks 1000 yr^{-1}, based on a 500-year smoothing window. Chronology from Lewis et al. (Accepted).

4 Discussion

4.1. Succession and changes in soil nutrient concentration

The Principle Component Analysis and Principle Curve of the Welsby Lagoon terrestrial pollen spectra exhibit a strong unidirectional change throughout the record (Figure 3, 4). This strong trend is evidenced by the long-term decline of rainforest taxa, *Eucalyptus, Leptospermum,* Asteraceae and heath species. After ca. 54 ka, the relative abundance of Poaceae, Haloragaceae and Casuarinaceae pollen increase, with limited reappearance of previously abundant taxa for the remainder of the record. The unidirectional shift seen in our results suggest a linear, one-way forcing. The strong unidirectional shift observed across MIS3, MIS2, the late glacial and the Holocene removes the likelihood of forcing such as global climate, sea level or greenhouse gas concentrations. These global forcings have undergone marked multi-directional changes from MIS3 to present. The persistence of a more open woodland environment from ca. 54 ka to present indicates that this pattern of vegetation change is responding most strongly to a clear one-way forcing, such as succession. The unidirectional, non-climate controlled changes in vegetation provides

strong evidence for a succession based driver of vegetation composition of the Welsby Lagoon catchment for the past 80,000 years.

The beginning of the Welsby Lagoon record is characterised by the highest values of rainforest and *Eucalyptus* pollen in the sequence. The wide ecological, climatological and geographical distributions and inability to differentiate pollen from the genus *Eucalyptus* means that it is difficult to be precise about the climatic and ecological inferences from this pollen taxa (Kershaw et al., 2007a). The high *Eucalyptus* values, in conjunction with high values of rainforest taxa may indicate that the majority of *Eucalyptus* pollen identified during this period was derived from species common in tall wet eucalypt forests. The presence of a small patch of wet eucalypt forest west of Welsby Lagoon, in addition to the common association of wet eucalypt forest and rainforest on Fraser Island and the Cooloola sand mass (Figure 6), provide support for this interpretation. The increased presence of rainforest species during the early part of the Welsby Lagoon record suggests the presence of bioavailable nutrients and sufficiently wet climates during late MIS5 and MIS4 to permit the development of closed forest communities.

A shift in dominance of arboreal species from rainforest taxa and *Eucalyptus* to Casuarinaceae occurs at ca. 43 ka. Dominance of lowland forest and woodland pollen spectra by Casuarinaceae during late MIS3, the LGM and early Holocene is a common feature of many eastern Australia pollen records (Black et al., 2006; Williams et al., 2006), including those from Fraser Island (Longmore & Heijnis, 1999; Donders et al., 2006; Atahan et al., 2014; Moss et al., 2016) and NSI (Petherick et al., 2011; Moss et al., 2013). However, in many of these records a decline in Casuarinaceae and increase in *Eucalyptus* values occurs after the mid-Holocene (after 8.5 ka) (Kershaw et al., 1991; D'Costa et al., 1993; Harle et al., 1999; Black et al., 2006; Donders et al., 2006; Builth et al., 2008; Atahan et al., 2014). Competitive exclusion, increased moisture or temperature, and altered fire regimes have all been suggested to explain the rise in *Eucalyptus* at the expense of Casuarinaceae during the Holocene. This widespread trend of replacement of Casuarinaceae by *Eucalyptus* is not seen in other records from NSI (Moss et al., 2013), including Welsby Lagoon (Figure 3). The switch between dominant arboreal canopy species from rainforest and *Eucalyptus* to Casuarinaceae persists from ca. 43 ka until present. Whilst it is possible that variable climates across the geographical range of these records has resulted in varying vegetation responses, a mid-Holocene decline in Casuarinaceae is seen in other east coast sites such as Redhead Lagoon (Williams et al., 2006) and Lake Baraba (Black et al., 2006), which likely have broadly similar climate histories.

A continued decline in nutrient availability across an already nutrient-poor dunal landscape may provide an alternate explanation for the unusual trend seen on NSI. As primary succession progresses, the loss of nutrients through permeable substrates and accumulation of inaccessible organic matter in the soil reduces the availability of nutrients, slowing nutrient cycling through the ecosystem (Bokhorst et al., 2017). A number of species of Casuarinaceae can fix nitrogen via a symbiotic relationships with

mycorrhizae and the presence of proteoid cluster roots that improve the absorption of nutrients from soils (Diem et al., 2000). The increased capacity for Casuarinaceae to access nutrients can increase their competitive advantage on nutrient poor sand substrates (Diem et al., 2000). The dominance of Casuarinaceae species from other late Quaternary records from NSI (Moss et al., 2013) suggest that the infertile sand substrates of NSI may have inhibited the expansion of *Eucalyptus* during the Holocene which has been observed in other eastern Australian pollen records (Kershaw et al., 1991; D'Costa et al., 1993; Harle et al., 1999; Black et al., 2006; Builth et al., 2008).

The current presence of Casuarinaceae dominated heath on the Pleistocene aged Yankee Jack dune morphosequence on both NSI and Moreton Islands provides additional evidence that the loss of nutrients in the aged dunes has contributed to the dominance of this vegetation type (Figure 7). However, the presence of rainforest and wet eucalypt forest on the same aged dune morphosequence on both Fraser Island and the Cooloola sand mass indicates that dune age alone is not an adequate explanation for the continued dominance of Casuarinaceae (Figure 7). Variations in vegetation types across the broader Great Sandy Region have commonly been attributed to succession, with a relationship existing between vegetation structure and foliage cover with different dune morphosequences of the Cooloola sand mass (Walker et al., 1981; Thompson, 1992). The progress of vegetation succession, from dwarf woodlands through to tall dense forests returning to retrogressive dwarf woodlands and heath, is interpreted to reflect the overall trend towards nutrient limitation in the oldest dune morphosequences (Walker et al., 1983).However, the current vegetation composition of NSI and Moreton Island, and pollen records indicate the local loss of rainforest taxa and dominance of Casuarinaceae on NSI from mid MIS3 (Figure 3, 6; Moss et al., 2013), indicate that factors other than succession alone need to be invoked to explain the divergent vegetation communities of the Great Sandy Region.

4.2. Fire and climate

Fire occurs through the entire Welsby Lagoon record at varying frequencies (Figure 2). The increase in fire activity at the beginning of MIS4 implies an increase in aridity and/or a more variable climate. Rainforests are often composed of highly fire sensitive species with limited survival during, and regeneration ability following, fire (Bowman, 2000). The dry notophyllopus vine rainforests with an emergent Araucariaceae canopy of the Great Sandy Region are vulnerable to high levels of mortality and reduced regeneration for centuries following fire (Bowman, 2000; Kershaw & Wagstaff, 2001; Haberle, 2005; Haberle et al., 2010; Mooney et al., 2011). The decline in rainforest taxa at Welsby Lagoon during periods of increased fire activity suggests these taxa were fire sensitive and suffered increased mortality during fire events (Figure 7). The abundance of rainforest pollen during this period varies with Asteraceae pollen. Species in the Asteraceae family are commonly fast growing and opportunistic shrubs and/or herbs that are favoured by disturbance (Luly, 1997; Thompson, 2006). The increase in Asteraceae during periods of

greater fire activity and rainforest decline indicate an opening of the forest canopy allowing proliferation by opportunistic Asteraceae species (Thompson, 2006).

The end of MIS4 and beginning of MIS3 is characterised by lower macroscopic charcoal values. Peaks in fire activity during MIS3 are also associated with changes in vegetation composition, however the relationship during this period is less clear than during MIS4. Time series analysis of the data indicates recurrent fire activity at Welsby Lagoon, with numerous significant charcoal peaks occurring between ca. 60 – 40 ka (Figure 2, 6). The relatively low charcoal deposition during this period in comparison to early MIS4 and the Holocene may be a result of low biomass availability and vegetation type (Chapter 3, this thesis). The presence of dense rainforest and wet eucalypt forest with a heathy understory in early MIS4 provides sufficient fuel to sustain large wildfires (Figure 6). In contrast, the open grass landscapes that dominate the majority of MIS3 contain substantially less, and possibly unconnected, biomass resulting in limited ability to sustain extensive wildfires and produce substantial macroscopic charcoal (Chapter 3, this thesis). The lack of macroscopic charcoal, during a period of Poaceae dominance could perhaps be explained by a change in charcoal taphonomy in response to finer, more easily macerated fuel types (Crawford & Belcher, 2014; Belcher, 2016).

The complex relationship between charcoal and vegetation composition during MIS3 may indicate the contribution of additional factors in driving these vegetation changes. A rapid increase in Poaceae and Haloragaceae pollen occured at ca. 54 ka. This shift in vegetation is recorded as the largest change in the terrestrial pollen spectra identified by CONISS (Figure 3). Whilst this shift occurred immediately following a significant charcoal peak identified by CHARanalysis, the frequency of fire in the context of the entire record is unremarkable throughout this period (Figure 3, 7). The persistence of an open landscape could be due to an extended period of drier or more variable climates promoting opportunistic species. The interpretation is supported by an increase in Haloragaceae during the same time interval. Haloragaceae is often considered a wetland indicator as many species from this family grow on exposed moist margins of wetlands or wet soils. Aside from *Gonocarpus chinensis* and *Myriophyllum* spp., species from the Haloragaceae family found on NSI and south-east Queensland more broadly, are commonly found in open forests and heathland vegetation (Clifford & Specht, 1979; Leiper et al., 2008; Stephens & Sharp, 2009). The peak in Haloragaceae may therefore either indicate a fluctuating water level, frequently exposing saturated wetland soils or an increase in landscape openness. The dominance of Poaceae and Haloragaceae from ca. 54 ka both indicate an opening of the landscape and increased competitive ability of fast growing, perennial species driven by a drier or more variable climate.

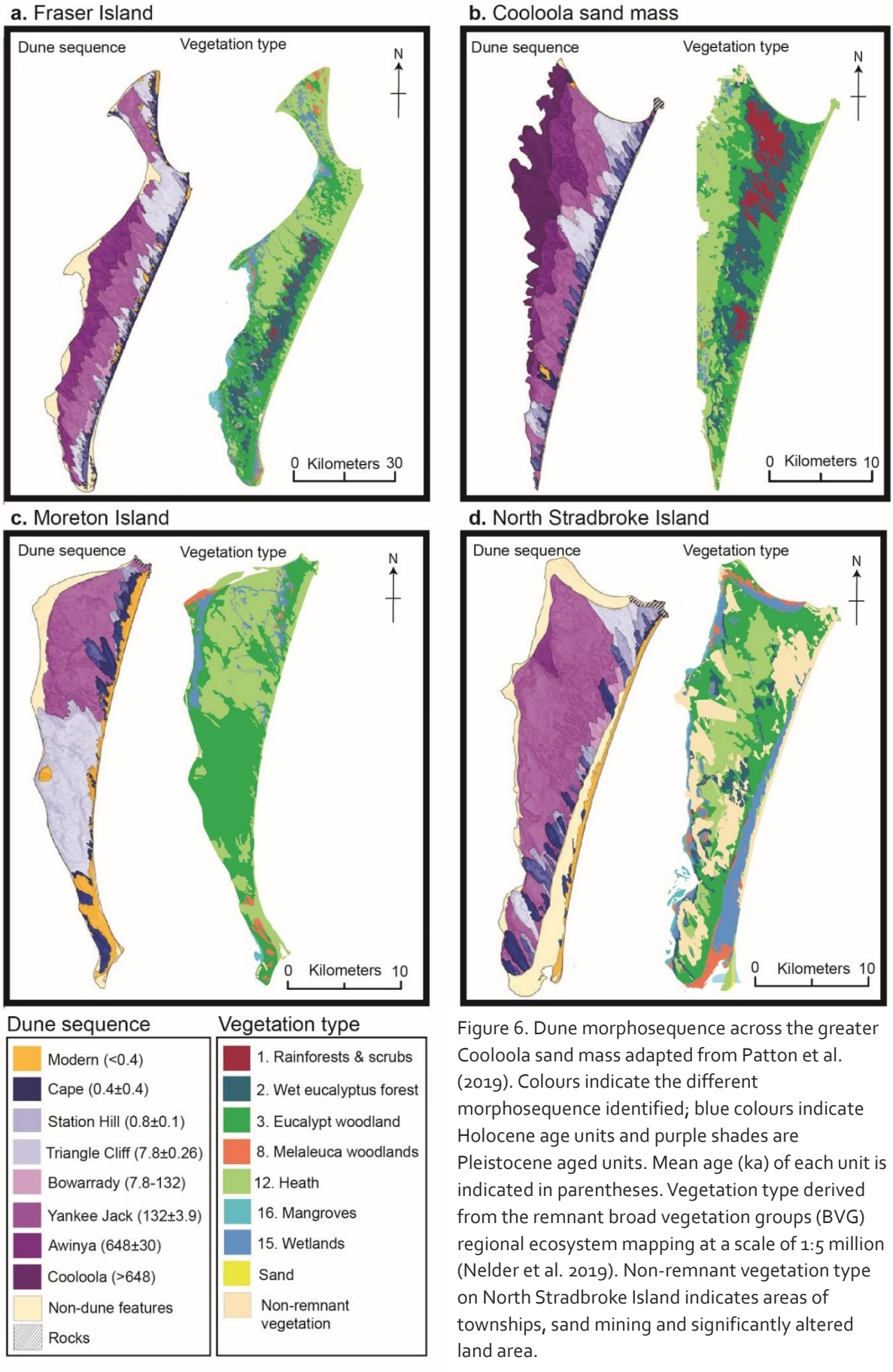

Figure 6. Dune morphosequence across the greater Cooloola sand mass adapted from Patton et al. (2019). Colours indicate the different morphosequence identified; blue colours indicate Holocene age units and purple shades are Pleistocene aged units. Mean age (ka) of each unit is indicated in parentheses. Vegetation type derived from the remnant broad vegetation groups (BVG) regional ecosystem mapping at a scale of 1:5 million (Nelder et al. 2019). Non-remnant vegetation type on North Stradbroke Island indicates areas of townships, sand mining and significantly altered land area.

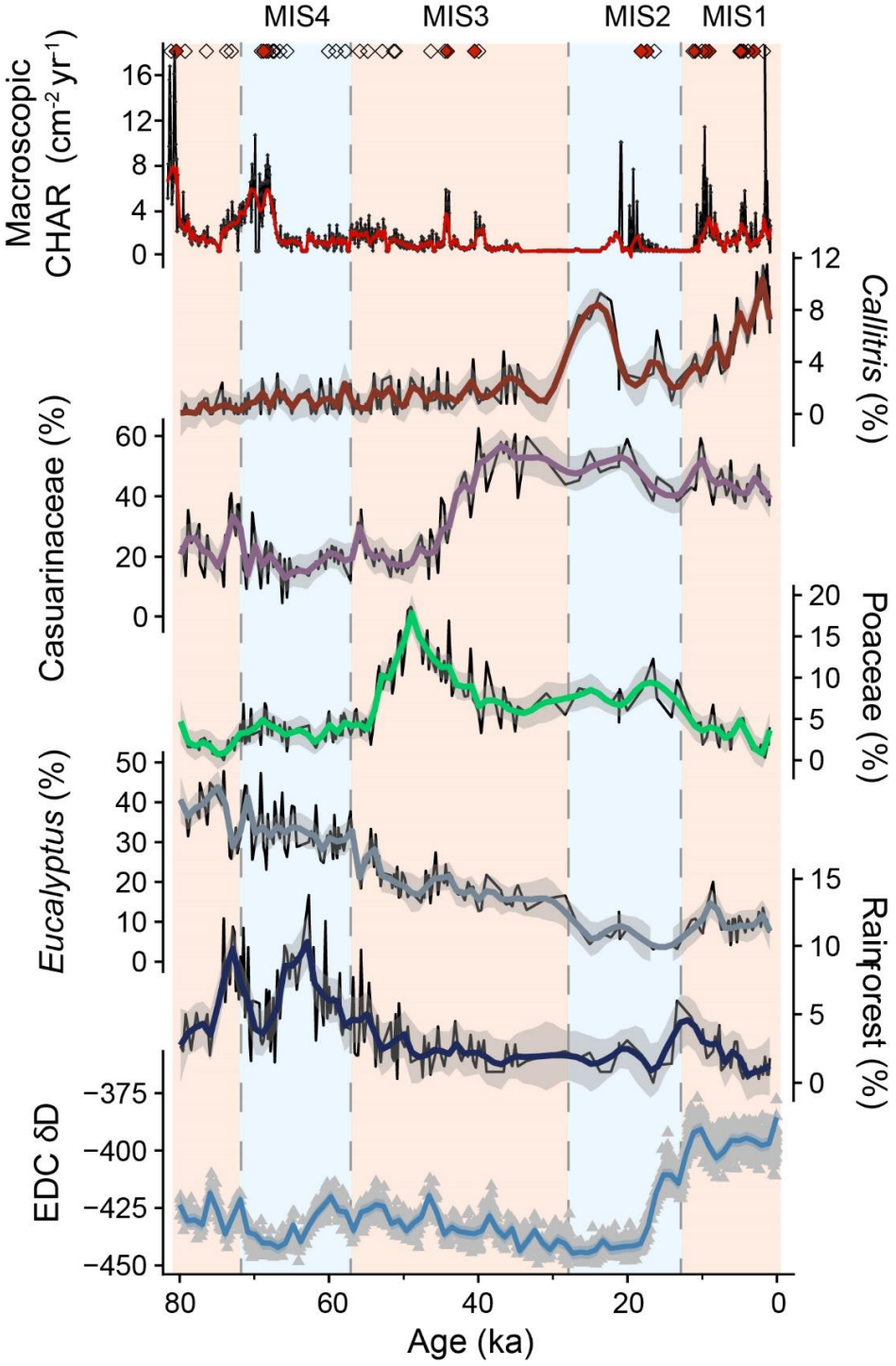

Figure 7. A summary plot of important Welsby Lagoon taxa. Macroscopic charcoal accumulation rate (CHAR cm^2 yr^{-1}) (black line) fitted with a smooth spline (span 0.01). Open diamonds are statistically significant charcoal peaks > 20 cm^{-2} $peak^{-1}$ and filled diamonds peaks > 200 cm^{-2} $peak^{-1}$ identified in timeseries analysis. *Callitris*, Casuarinaceae, Poaceae, *Eucalyptus,* Rainforest taxa and Epica Dome C (EDC) δ Deuterium fitted with a smooth spline (span 0.01). Pollen percentage data (black lines) fitted with smooth spline (span 0.05; coloured lines).Refer to Table 1 and supplimentary information for pollen group details. Chronology from Lewis et al. (Accepted).

The rapid increase in Poaceae pollen and shift in vegetation composition coincides with the hypothesised spread of humans throughout the Australian continent (Hamm et al., 2016; Tobler et al., 2017). The maintenance of an open, Poaceae dominated, landscape may be alternatively explained by the application of low intensity mosaic burning by early indigenous Australians. The low values of macroscopic charcoal during this period suggest that fire is not maintaining this open understory, however the complex relationship between macroscopic charcoal production, fine fuels and fire intensity may mask signals of burning (Roos et al., 2019). Low production and transport of macroscopic charcoal may occur as a result of frequent and low intensity burning designed to restrict reestablishment of woody vegetation. Production and preservation of microscopic charcoal fragments may provide more accurate records of low intensity burning of fine fuels (Crawford & Belcher, 2014; Belcher, 2016). Peaks of microscopic charcoal match closely to those of macroscopic charcoal, and whilst peaks occured during this period, they are not sustained throughout the entire period of Poaceae dominance, further indicating the presence of a climatic driver (Figure 3).

The elevated levels of Poaceae begin to decline after ca. 49 ka, being replaced by increasing Casuarinaceae pollen which reaches peak values after ca. 43 ka. The shift from high Poaceae values to a dominance of Casuarinaceae is accompanied by two peaks in macroscopic charcoal at ca. 44 ka and ca. 40 ka. Fire occurrence is strongly related to biomass availability, which is in turn governed by long-term changes in climate. There is strong relationship between climate driven biomass availability and fire occurrence in subtropical Australia, with higher incidences of fire occurring following periods of increased rainfall that initiate the build-up of biomass (Mariani et al., 2019b). The occurrence of two peaks in macroscopic charcoal abundance at ca. 44 and 40 ka, as Casuarinaceae increases, is likely a result of increased biomass providing sufficient fuels to support high intensity fire. An increase in biomass may have occurred due to an amelioration of regional climate allowing the development of more dense woodlands. Both peaks in charcoal are associated with sharp declines in Casuarinaceae abundance, however Casuarinaceae rapidly recovers. The relationship between fire and Casuarinaceae is complex, with the family including species that are both fire sensitive and those that rely on fire for regeneration. The rapid recovery of Casuarinaceae and persistence through the Holocene, during the period of highest firer occurrence, indicates that the species present at or around Welsby Lagoon were able to recover following fire (Figure 7).

The LGM (18 – 23 ka) is characterised by a sharp increase in the pollen of aquatic macrophyte taxa. Shallower water levels would have allowed the colonisation of rooted aquatic taxa across the wetland surface, possibly due to reduced moisture availability during the global LGM. The LGM sediments also contain the highest macroscopic charcoal values of the entire record. This period represents the slowest level of sediment accumulation in the record (Lewis et al., Accepted), possibly the result of reduced surface water and increased decomposition of organic material in a shallow, oxygenated water body. The abundance of highly resistant charcoal may indicated reduced preservation of

labile organic matter through this period or increased incidence of fire burning across the wetland surface. Reduced accumulation of sediments during dry phases or enhanced decomposition would favour the preservation of more recalcitrant forms of carbon, such as charcoal (Chapter 3, this thesis). The increase in aquatic macrophyte abundance and macroscopic charcoal may indicate that fire regularly burnt across the wetland surface during the LGM. Therefore, the increase in charcoal deposition between 18 – 23 ka is not necessarily the result of an increase in fire frequency, but likely a representation of more local fire occurrence across the wetland surface and preferential preservation of charcoal.

The Holocene portion of the record is characterised by a substantial increase in both macroscopic and microscopic charcoal abundance (Figure 3). The increase in charcoal, concurrent with the onset of the Holocene, likely reflects an increase in biomass availability and intensification of human land use in response to climate changes (Turney & Hobbs, 2006) or as a result of social change (Williams et al., 2015b). A recent study from NSI highlights the climate related biomass limitations of fire activity in subtropical sclerophyllous forests (Mariani et al., 2019b). Although there is a clear increase in fire activity at the site, Casuarinaceae continues to dominate the arboreal pollen spectra. This trend is consistent with the other late Quaternary records from across the island, where Casuarinaceae attains values in excess of 80% at some sites (Moss et al., 2013). Whilst Casuarinaceae continues to contribute >40% of the pollen spectra, there is an increasing importance of *Callitris* during the late Holocene at Welsby Lagoon. The abundance of *Callitris* pollen varies with macroscopic charcoal, indicating that *Callitris* is only able to become dominant during periods of low fire activity. This relationship between *Callitris* and fire displays the same pattern as nearby Swallow Lagoon, where a decline in rainfall and fire activity results in an increase in *Callitris* sp. (Mariani et al., 2019b).

Disentangling the role of fire, climate and succession in the vegetation communities across Great Sandy Region is difficult. The current vegetation distribution across the region display some relationship with dune morphosequence, however there is marked variations in vegetation in the same dune morphosequences (Figure 6). It can be assumed that changes in climate across the region have been broadly similar throughout the last glacial cycle, although local changes in climate cannot be discounted. Based on the evidence from Welsby Lagoon we suggest that variations in the frequency of fire are the most likely cause of the divergent vegetation patterns. Fire results in acceleration of nutrient loss from the system and may accelerate or exacerbate successional processes (Raison, 1980; Sawyer et al., 2018). Many of the longer pollen records across the Great Sandy Region do not include reconstructions of local fire activity, making inferences of the role of fire in driving the vegetation divergences difficult (Longmore, 1997; Longmore & Heijnis, 1999; Donders et al., 2006; Atahan et al., 2014). Notophyllopus vine rainforests currently found on Fraser Island and the Cooloola sand mass occur on inland dune swales, areas that are likely afforded the greatest topographic protection from fire. The greater elevation and deeper dune swales of these regions may provide increased protection from fire, therefore reducing both fire induced mortality and leaching of important nutrients.

To fully untangle the role of fire in altering successional patterns will require more records with coupled high resolution fire and vegetation histories.

5 Conclusions

Vegetation communities on similar dunal substrates in south-eastern Queensland exhibit divergent patterns both spatially and through time. The temporal progression of vegetation types and aquatic environment at Welsby Lagoon can be explained by a combination of succession, fire and climate. The Welsby Lagoon pollen spectra demonstrate evidence for a progressive long-term successional processes resulting in shifts from rainforest and *Eucalyptus* dominated to Casuarinaceae dominated vegetation communities. Along with successional processes, there is clear evidence for the role of fire in changing vegetation communities. However, succession alone is not able to explain the changes in vegetation at Welsby Lagoon, as similar late stage vegetation communities characterised by reduced plant stature and nutrient availability are not present across all dunes of the Yankee Jack morphosequence (Walker et al., 1981; Longmore & Heijnis, 1999; Bokhorst et al., 2017).

It is likely that retrogressive vegetation stages were accelerated by fire. Fire mobilises nutrients by combusting foliage and litter and promoting leaching or atmospheric removal. These processes, on an ageing dunal system, can exacerbate the long-term leaching of nutrients through the permeable sand substrates. In addition to changing nutrient conditions, the combined influence of fire disturbance and climatic change can undermine the resilience of vegetation types, resulting in contraction of fire sensitive vegetation communities (Cadd et al., 2019; Mariani et al., 2019a). Successive fire events (Figure 2, 6) and decline in nutrient availability at Welsby Lagoon during MIS3 may have resulted in reduced resilience of rainforest and *Eucalyptus* vegetation triggering a switch to an alternate vegetation state dominated by Casuarinaceae. The combination of factors, including local changes in fire occurrence and climate can help explain the divergent vegetation types found on the same dune units across the Great Sandy Region (Figure 6; Patton et al., 2019).

References

APSA Members (2007) The Australasian Pollen and Spore Atlas. *http://apsa.anu.edu.au/*, **1**, .

Atahan, P., Heijnis, H., Dodson, J., Grice, K., Le Métayer, P., Taffs, K., Hembrow, S., Woltering, M., & Zawadzki, A. (2014) Pollen, biomarker and stable isotope evidence of late Quaternary environmental change at Lake McKenzie, southeast Queensland. *Journal of Paleolimnology*, **53**, 139–156.

Belcher, C.M. (2016) The influence of leaf morphology on litter flammability and its utility for interpreting palaeofire. *Philosophical Transactions of the Royal Society B*, **371**, 1–9.

Bennett, K.D. (1996) Determination of the number of zones in a biostratigraphical sequence. *New Phytologist*, **132**, 155–170.

Black, M.P., Mooney, S.D., & Martin, H.A. (2006) A 43,000-year vegetation and fire history from Lake Baraba, New South Wales, Australia. *Quaternary Science Reviews*, **25**, 3003–3016.

Bliege Bird, R., Bird, D.W., Codding, B.F., Parker, C.H., & Jones, J.H. (2008) The "fire stick farming" hypothesis: Australian Aboriginal foraging strategies, biodiversity, and anthropogenic fire mosaics. *Proceedings of the National Academy of Sciences*, **105**, 14796–14801.

Bokhorst, S., Kardol, P., Bellingham, P.J., Kooyman, R.M., Richardson, S.J., Schmidt, S., & Wardle, D.A. (2017) Responses of communities of soil organisms and plants to soil aging at two contrasting long-term chronosequences. *Soil Biology and Biochemistry*, **106**, 69–79.

BOM & BOM, (Australian Bureau of Meterology) (2018) Available at: http://www.bom.gov.au/climate/averages/tables/cw_040209.shtml.

Bowman, D.M.J.S. (2000) *Australian Rainforests: Islands of Green in a Land of Fire.* Cambridge University Press, New York.

Bowman, D.M.J.S., Balch, J.K., Artaxo, P., et al. (2009) Fire in the Earth System. *Science*, **324**, 481–484.

Bradstock, R.A., Hammill, K.A., Collins, L., & Price, O. (2010) Effects of weather, fuel and terrain on fire severity in topographically diverse landscapes of south-eastern Australia. *Landscape Ecology*, **25**, 607–619.

Builth, H., Kershaw, A.P., White, C., Roach, A., Hartney, L., McKenzie, M., Lewis, T., & Jacobsen, G. (2008) Environmental and cultural change on the Mt Eccles lava-flow landscapes of southwest Victoria, Australia. *Holocene*, **18**, 413–424.

Cadd, H.R., Fletcher, M.-S., Mariani, M., Heijnis, H., & Gadd, P.S. (2019) The influence of fine-scale topography on the impacts of Holocene fire in a Tasmanian montane landscape. *Journal of Quaternary Science*, 1–8.

Cadd, H.R., Tibby, J., Barr, C., Tyler, J., Unger, L., Leng, M.J., Marshall, J.C., McGregor, G., Lewis, R., Arnold, L.J., Lewis, T., & Baldock, J. (2018) Development of a southern hemisphere subtropical wetland (Welsby Lagoon, south-east Queensland, Australia) through the last glacial cycle. *Quaternary Science Reviews*, **202**, 53–65.

Clarkson, C., Jacobs, Z., Marwick, B., et al. (2017) Human occupation of northern Australia by 65,000 years ago. *Nature*, **547**, 306–310.

Clifford, H.T. & Specht, R.L. (1979) *The vegetation of North Stradbroke Island, Queensland.* University of Queensland Press, St. Lucia, Q.

Crawford, A.J. & Belcher, C.M. (2014) Charcoal morphometry for paleoecological analysis: The effects of fuel type and transportation on morphological parameters. *Applications in Plant Sciences*, **2**, 1–10.

D'Costa, D.M., Grindrod, J., & Ogden, R. (1993) Preliminary environmental reconstructions from late Quaternary pollen and mollusc assemblages at Egg Lagoon, King Island, Bass Strait. *Australian Journal of Ecology*, **18**, 351–366.

Daniau, A.L., Bartlein, P.J., Harrison, S.P., et al. (2012) Predictability of biomass burning in response to climate changes. *Global Biogeochemical Cycles*, **26**, 1–12.

Daniau, A.L., Harrison, S.P., & Bartlein, P.J. (2010) Fire regimes during the Last Glacial. *Quaternary Science Reviews*, **29**, 2918–2930.

Diem, H.G., Duhoux, E., Zaid, H., & Arahou, M. (2000) Cluster roots in Casuarinaceae: Role and relationship to soil nutrient factors. *Annals of Botany*, **85**, 929–936.

Donders, T.H., Wagner, F., & Visscher, H. (2006) Late Pleistocene and Holocene subtropical vegetation dynamics recorded in perched lake deposits on Fraser Island, Queensland, Australia. *Palaeogeography, Palaeoclimatology, Palaeoecology*, **241**, 417–439.

Fægri, K. & Iverson, J. (1989) *Textbook of Pollen Analysis.* Wiley, New York.

Gillson, L. (2009) Landscapes in Time and Space. *Landscape Ecology*, **24**, 149–155.

Gontz, A.M., Moss, P.T., Sloss, C.R., Petherick, L.M., McCallum, A., & Shapland, F. (2015) Understanding past climate variation and environmental change for the future of an iconic landscape - K'gari Fraser Island, Queensland, Australia. *Australasian Journal of Environmental Management*, **22**, 105–123.

Grimm, E.C. (1987) CONISS: a FORTRAN 77 program for stratigraphically constrained cluster analysis by the method of incremental sum of squares. *Computers and Geosciences*, **13**, 13–35.

Haberle, S.G. (2005) A 23,000-yr pollen record from Lake Euramoo, Wet Tropics of NE Queensland, Australia. *Quaternary Research*, **64**, 343–356.

Haberle, S.G., Rule, S., Roberts, P., Heijnis, H., Jacobsen, G., Turney, C., Cosgrove, R., Ferrier, A., Moss, P., Mooney, S., & P., K. (2010) Paleofire in the wet tropics of northeast Queensland, Australia. *PAGES News*, **18**, 78–80.

Hamm, G., Mitchell, P., Arnold, L.J., Prideaux, G.J., Questiaux, D., Spooner, N.A., Levchenko, V.A., Foley, E.C., Worthy, T.H., Stephenson, B., Coulthard, V., Coulthard, C., Wilton, S., & Johnston, D. (2016) Cultural innovation and megafauna interaction in the early settlement of arid Australia. *Nature*, **539**, 280–283.

Harle, K.J., Kershaw, A.P., & Heijnis, H. (1999) The contributions of uranium/thorium and marine palynology to the dating of the Lake Wangoom pollen record, western plains of Victoria, Australia. *Quaternary International*, **57–58**, 25–34.

Harrison, S.P. & Sanchez Goñi, M.F. (2010) Global patterns of vegetation response to millennial-scale variability and rapid climate change during the last glacial period. *Quaternary Science Reviews*, **29**, 2957–2980.

Higuera, P.E., Brubaker, L.B., Anderson, P.M., Hu, F.S., & Brown, T. a (2009) Vegetation mediated the impacts of postglacial climate change on fire regimes in the south-central Brooks Range, Alaska. *Ecological Monographs*, **79**, 201–219.

Higuera, P.E., Gavin, D.G., Patrick J Bartlein, & Douglas J Hallett (2010) Peak detection in sediment–charcoal records: impacts of alternative data analysis methods on fire-history interpretations. *International Journal of Wildland Fire*, **19**, 996–1014.

Hofmann, H., Newborn, D., Cartwright, I., Cendón, D.I., & Raiber, M. (2019) Groundwater mean residence time of a sub-tropical barrier sand island. .

Juggins, S. (2015) rioja: Anlaysis of Quaternary science data. *R package ver. 0.9-5*, 1–58.

Kershaw, A.P., Bretherton, S.C., & van der Kaars, S. (2007) A complete pollen record of the last 230 ka from Lynch's Crater, north-eastern Australia. *Palaeogeography, Palaeoclimatology, Palaeoecology*, **251**, 23–45.

Kershaw, A.P., Clark, J.S., Gill, A.M., & D'Costa, D.M. (2002) A history of fire in Australia. *Flammable Australia: The fire regimes and biodiversity of a continent* pp. 3–25. Cambridge University Press,

Kershaw, A.P., D'Costa, D.M., McEwen Mason, J.R.C., & Wagstaff, B.E. (1991) Palynological evidence

for Quaternary vegetation and environments of mainland southeastern Australia. *Quaternary Science Reviews*, **10**, 391–404.

Kershaw, P. & Wagstaff, B. (2001) The Southern Conifer Family Araucariaceae: History, Status, and Value for Paleoenvironmental Reconstruction. *Annual Review of Ecology and Systematics*, **32**, 397–414.

Krawchuk, M.A., Haire, S.L., Coop, J., Parisien, M.A., Whitman, E., Chong, G., & Miller, C. (2016) Topographic and fire weather controls of fire refugia in forested ecosystems of northwestern North America. *Ecosphere*, **7**, 1–18.

Leiper, G., Glazebrook, J., Cox, D., & Rathie, K. (2008) *Mangroves to Mountains: a field guide to the native plants of south-east Queensland.* Logan River Branch, Society for Growing Australian Plants (Qld Region), Brisbane.

Lewis, R., Tibby, J., Arnold, L.J., Gadd, P.S., Marshall, J.C., Barr, C., & Yokoyama, Y. (Accepted) Bayesian deposition model of the Welsby Lagoon sediment sequence. *Quaternary Science Reviews*.

Longmore, M.E. (1997) Quaternary palynological records from perched lake sediments, Fraser Island, Queensland, Australia: Rainforest, forest history and climatic control. *Australian Journal of Botany*, **45**, 507–526.

Longmore, M.E. & Heijnis, H. (1999) Aridity in Australia: Pleistocene records of palaeohydrological and palaeoecological change from the perched lake sediments of Fraser Island, Queensland, Australia. *Quaternary International*, **57/58**, 35–47.

Luly, J.G. (1997) Modern pollen dynamics and surficial sedimentary processes at Lake Tyrrell, semi-arid northwestern Victoria, Australia. *Review of Palaeobotany and Palynology*, **97**, 301–318.

Lynch, A.H., Beringer, J., Kershaw, P., Marshall, A., Mooney, S., Tapper, N., Turney, C., & Van Der Kaars, S. (2007) Using the Paleorecord to Evaluate Climate and Fire Interactions in Australia. *Annual Review of Earth and Planetary Sciences*, **35**, 215–239.

Mariani, M., Fletcher, M., Haberle, S., Chin, H., Zawadzki, A., & Jacobsen, G. (2019a) Climate change reduces resilience to fire in subalpine rainforests. *Global Change Biology*, **25**, 2030–2042.

Mariani, M., Tibby, J., Barr, C., Moss, P., Marshall, J.C., & McGregor, G.B. (2019b) Reduced rainfall drives biomass limitation of long-term fire activity in Australia's subtropical sclerophyll forests. *Journal of Biogeography*, 1974–1987.

Mooney, S.D., Harrison, S.P., Bartlein, P.J., Daniau, A.L., Stevenson, J., Brownlie, K.C., Buckman, S., Cupper, M., Luly, J., Black, M., Colhoun, E., D'Costa, D., Dodson, J., Haberle, S., Hope, G.S., Kershaw, P., Kenyon, C., McKenzie, M., & Williams, N. (2011) Late Quaternary fire regimes of Australasia. *Quaternary Science Reviews*, **30**, 28–46.

Moss, P., Tibby, J., Shapland, F., Fairfax, R., Stewart, P., Barr, C., Petherick, L., Gontz, A., & Sloss, C. (2016) Patterned fen formation and development from the Great Sandy Region, south-east Queensland, Australia. *Marine and Freshwater Research*, **67**, 816–827.

Moss, P.T., Tibby, J., Petherick, L., McGowan, H., & Barr, C. (2013) Late Quaternary vegetation history of North Stradbroke Island, Queensland, eastern Australia. *Quaternary Science Reviews*, **74**, 257–272.

Nelder, V.J., Niehus, R.E., Wilson, B.A., Ford, W.J.F., & Accad, A. (2019) The Vegetation of Queensland. Descriptions of Broad Vegetation Groups. Version 4.0. .

Oksanen, J., Blanchet, F.G., Kindt, R., Legendre, P., Minchin, P.R., O'Hara, R.B., Simpson, G.L., Solymos, P., Stevens, M.H.H., & Wagner, H. (2013) Package 'vegan.' *R package ver. 2.0–8*, 254.

Patton, N.R., Ellerton, D., & Shulmeister, J. (2019) High-resolution remapping of the coastal dune fields of south east Queensland, Australia: a morphometric approach. *Journal of Maps*, **15**, 578–589.

Pausas, J.G. & Ribeiro, E. (2013) The global fire-productivity relationship. *Global Ecology and*

Biogeography, **22**, 728–736.

Petherick, L.M., Moss, P.T., & McGowan, H.A. (2011) Climatic and environmental variability during the termination of the Last Glacial Stage in coastal eastern Australia: a review. *Australian Journal of Earth Sciences*, **58**, 563–577.

R Core Team (2017) R: A Language and Environment for Statistical Computing. *R Foundation for Statistical Computing, Vienna, Austria*, **0**, {ISBN} 3-900051-07-0.

Raison, R.J. (1980) A review of the role of fire in nutrient cycling in Australian native forests, and of methodology for studying the fire-nutrient interaction. *Australian Journal of Ecology*, **5**, 15–21.

Roos, Williamson, & Bowman (2019) Is Anthropogenic Pyrodiversity Invisible in Paleofire Records? *Fire*, **2**, 42.

Sawyer, R., Bradstock, R., Bedward, M., & Morrison, R.J. (2018) Fire intensity drives post-fire temporal pattern of soil carbon accumulation in Australian fire-prone forests. *Science of the Total Environment*, **610–611**, 1113–1124.

Scheffer, M., Carpenter, S., Foley, J.A., Folke, C., & Walker, B. (2001) Catastrophic shifts in ecosystems. *Nature*, **413**, 591–596.

Seddon, A.W.R., Macias-Fauria, M., Long, P.R., Benz, D., & Willis, K.J. (2016) Sensitivity of global terrestrial ecosystems to climate variability. *Nature*, **531**, 229–232.

Simpson, G.L. & Oksanen, J. (2019) analouge: Analogue matching and Modern Analogue Technique transfer function models. .

Stephens, K.M. & Sharp, D. (2009) *The flora of North Stradbroke Island.* State of Queensland, Environmental Protection Agency,

Thompson, C.H. (1981) Podzol chronosequences on coastal dunes of eastern Australia. *Nature*, **291**, 59–61.

Thompson, C.H. (1992) Genesis of podzols on coastal dimes in southern queensland. I. field relationships and profile morphology. *Australian Journal of Soil Research*, **30**, 593–613.

Thompson, I.R. (2006) A taxonomic treatment of tribe Senecioneae (Asteraceae) in Australia. *Muelleria*, **24**, 51–110.

Timms, B. (1986) The coastal dune lakes of eastern Australia. *Limnology in Australia* (ed. by P. Deckker and W.D. Williams), pp. 688. Springer Netherlands,

Tobler, R., Rohrlach, A., Soubrier, J., et al. (2017) Aboriginal mitogenomes reveal 50,000 years of regionalism in Australia. *Nature*, **544**, 180–184.

Turney, C.S.M. & Hobbs, D. (2006) ENSO influence on Holocene Aboriginal populations in Queensland, Australia. *Journal of Archaeological Science*, **33**, 1744–1748.

Walker, J., Lees, B., Olley, J., & Thompson, C. (2018) Dating the Cooloola coastal dunes of South-Eastern Queensland, Australia. *Marine Geology*, **398**, 73–85.

Walker, J., Thompson, C.H., Fergus, I.F., & Tunstall, B.R. (1981) Plant Succession and Soil Development in Coastal Sand Dunes of Subtropical Eastern Australia. *Forest Succession: concepts and application* (ed. by D.C. West, H.H. Shugart, and D.F. Botkin), pp. 107–131. Springer, New York.

Walker, J., Thompson, C.H., & Jehne, W. (1983) Soil Weathering Stage, Vegetation Succession, and Canopy Dieback. *Pacific Science*, **37**, 471–481.

Walker, L.R., Wardle, D.A., Bardgett, R.D., & Clarkson, B.D. (2010) The use of chronosequences in studies of ecological succession and soil development. *Journal of Ecology*, **98**, 725–736.

Ward, W.T. (2016) Coastal dunes and strandplains in southeast Queensland: Sequence and chronology. *Australian Journal of Earth Sciences*, **53**, 363–373.

Williams, A.N., Veth, P., Steffen, W., Ulm, S., Turney, C.S.M., Reeves, J.M., Phipps, S.J., & Smith, M. (2015) A continental narrative: Human settlement patterns and Australian climate change over the last 35,000 years. *Quaternary Science Reviews*, **123**, 91–112.

Williams, J.W., Blois, J.L., & Shuman, B.N. (2011) Extrinsic and intrinsic forcing of abrupt ecological change: Case studies from the late Quaternary. *Journal of Ecology*, **99**, 664–677.

Williams, N.J., Harle, K.J., Gale, S.J., & Heijnis, H. (2006) The vegetation history of the last glacial–interglacial cycle in eastern New South Wales, Australia. *Journal of Quaternary Science*, **21**, 735–750.

Wood, S.W., Murphy, B.P., & Bowman, D.M.J.S. (2011) Firescape ecology: How topography determines the contrasting distribution of fire and rain forest in the south-west of the Tasmanian Wilderness World Heritage Area. *Journal of Biogeography*, **38**, 1807–1820.

6 Supplementary Information

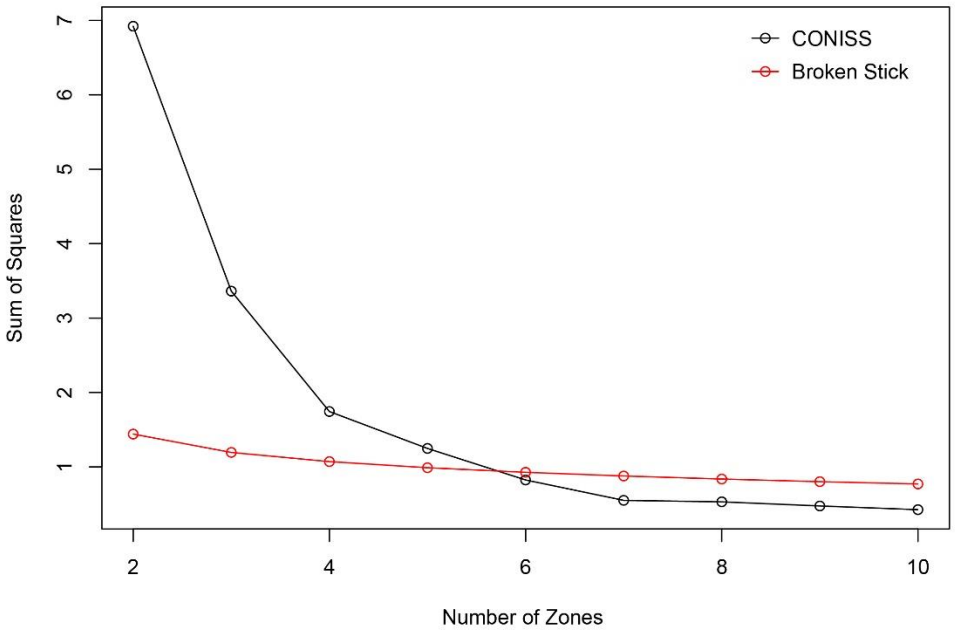

Figure S1. Broken stick test performed on the terrestrial pollen CONISS, indicating five significant zones within the dataset.

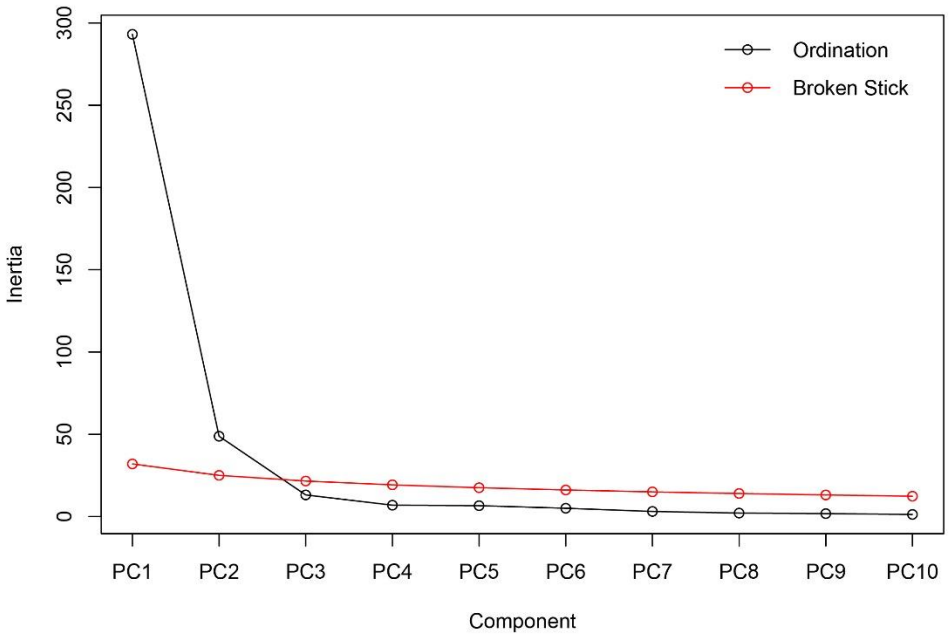

Figure S2. Broken stick test performed on the terrestrial pollen PCA, indicating the significance of the first two PC axes.

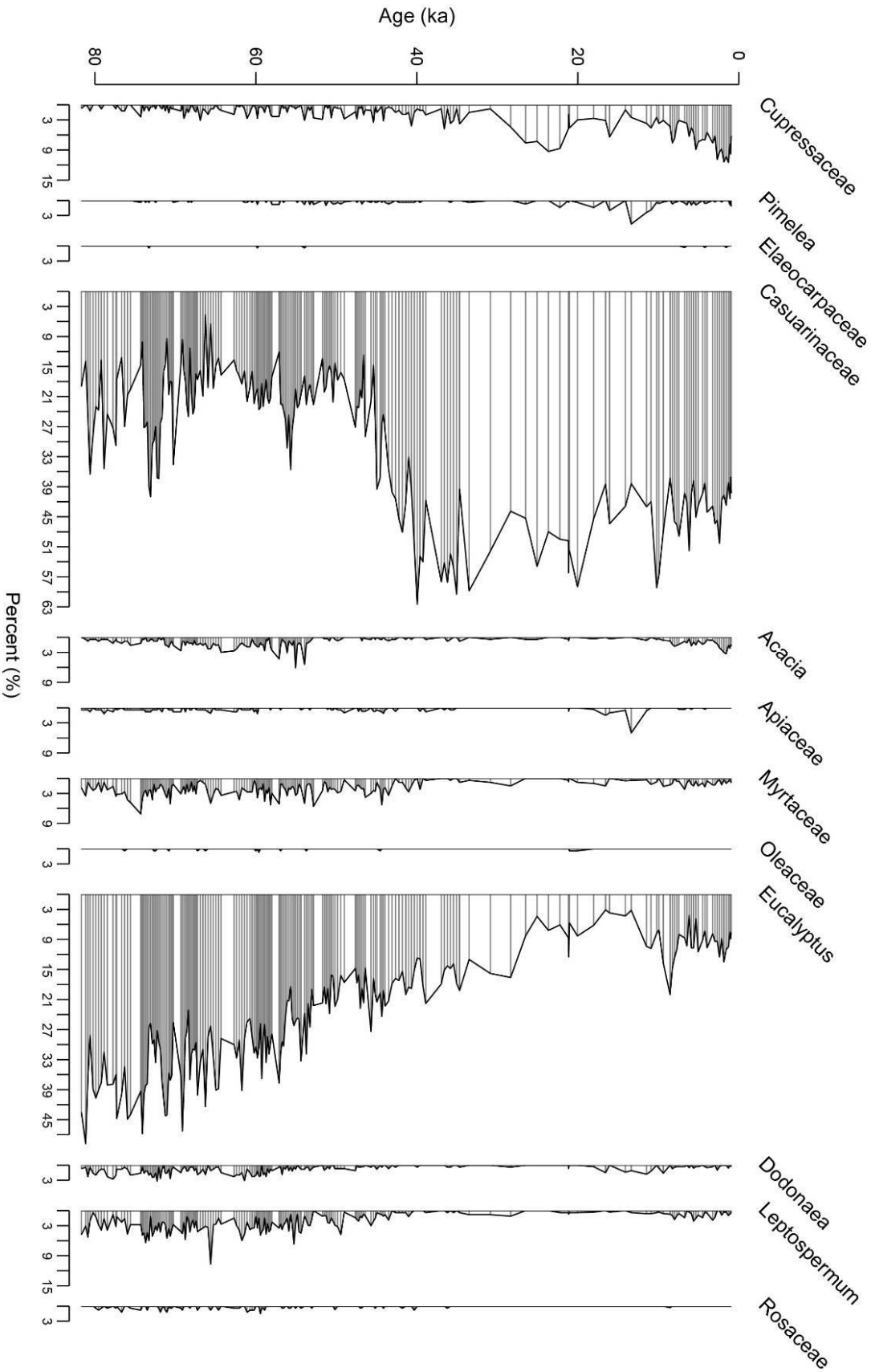

Figure S3. Stratigraphic pollen diagram of species commonly found in open forest communities on NSI as determined from Clifford and Specht (1979) and Stephens and Sharp (2009). All taxa are included in the terrestrial pollen sum. Chronology from Lewis et al. (submitted).

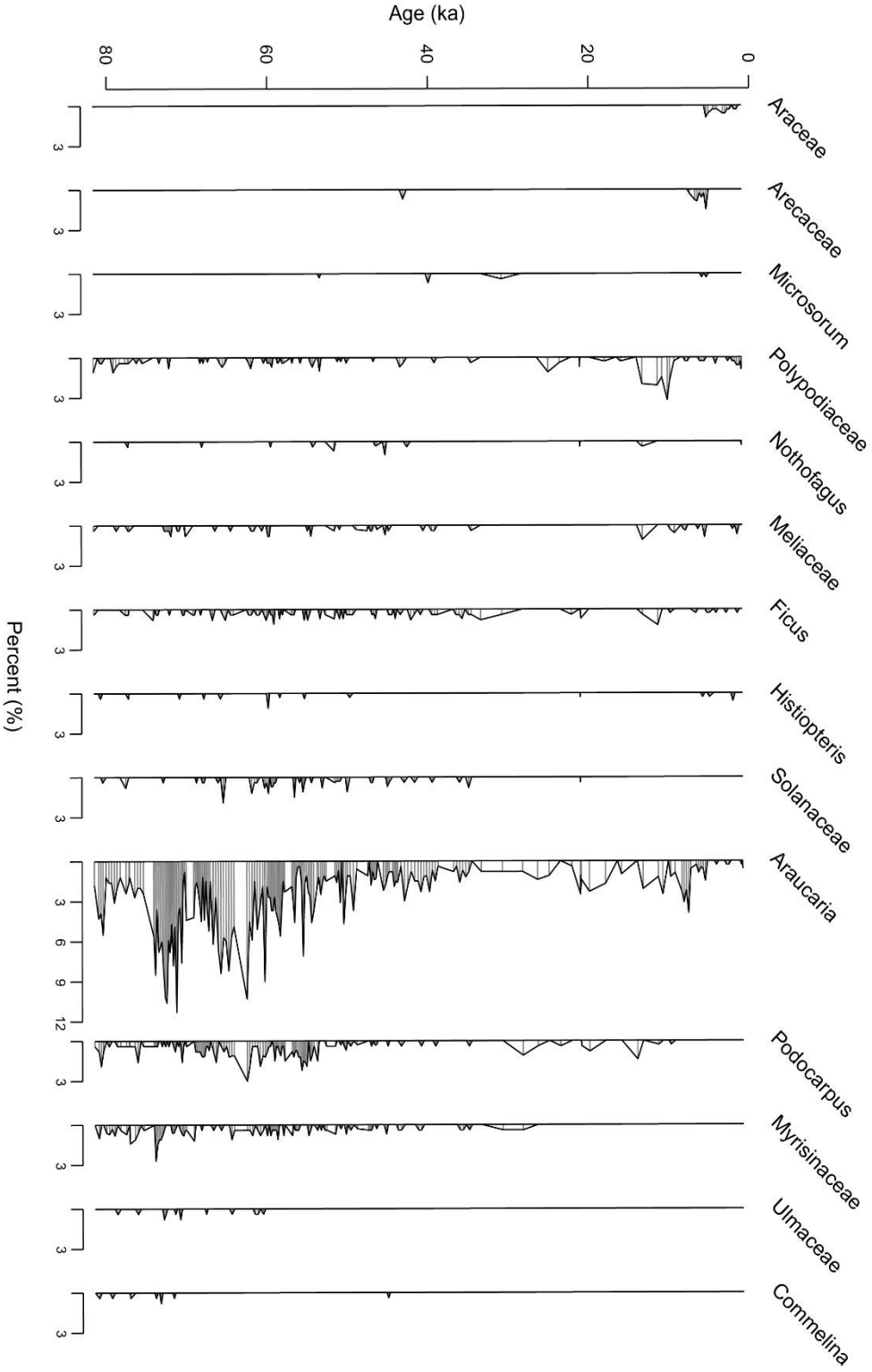

Figure S4. Stratigraphic pollen diagram of species commonly found in closed rainforest communities on NSI and south east Queensland as determined from Leiper et al. (2008), Clifford and Specht (1979) and Stephens and Sharp (2009). All taxa are included in the terrestrial pollen sum. Chronology from Lewis et al. (submitted).

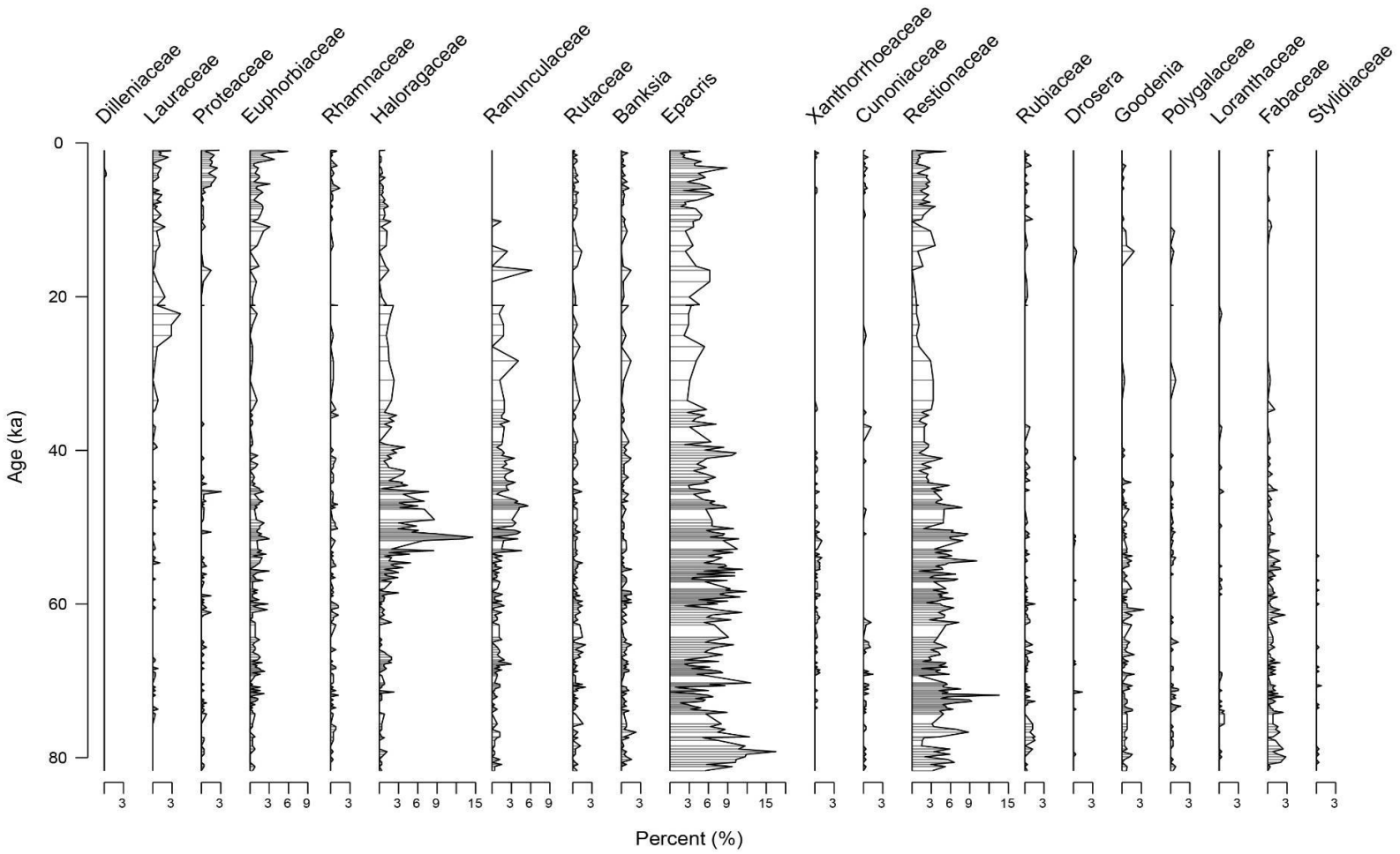

Figure S5. Stratigraphic pollen diagram of species commonly found in heath vegetation communities on NSI as determined from(Clifford and Specht, 1979; Leiper et al., 2008; Stephens and Sharp, 2009; Nelder et al., 2019)(Clifford and Specht, 1979; Leiper et al., 2008; Stephens and Sharp, 2009; Nelder et al., 2019)(Clifford & Specht, 1979; Leiper et al., 2008; Stephens & Sharp, 2009; Nelder et al., 2019)(Clifford & Specht, 1979; Leiper et al., 2008; Stephens & Sharp, 2009; Nelder et al., 2019)(Clifford & Specht, 1979; Leiper et al., 2008; Stephens & Sharp, 2009; Nelder et al., 2019). Taxa shown are all included in the calculation of heath vegetation used in Figure 3.All taxa are included in the terrestrial pollen sum. Chronology from Lewis et al. (submitted)

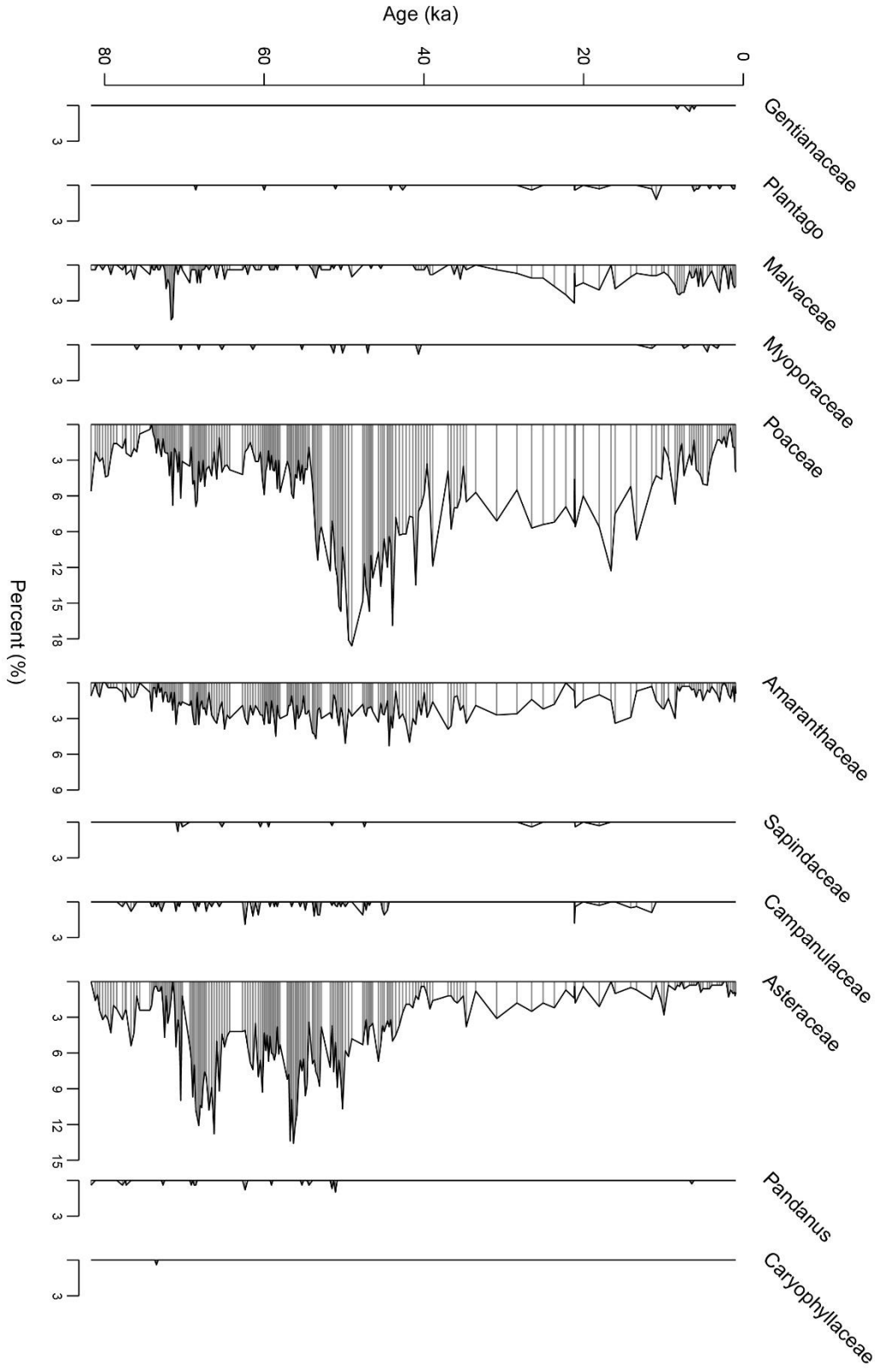

Figure S6. Stratigraphic pollen diagram of disturbance adapted and other species not classified. Disturbance taxa identified from Clifford and Specht (1979) and Stephens and Sharp (2009). All taxa are included in the terrestrial pollen sum. Chronology from Lewis et al. (submitted).

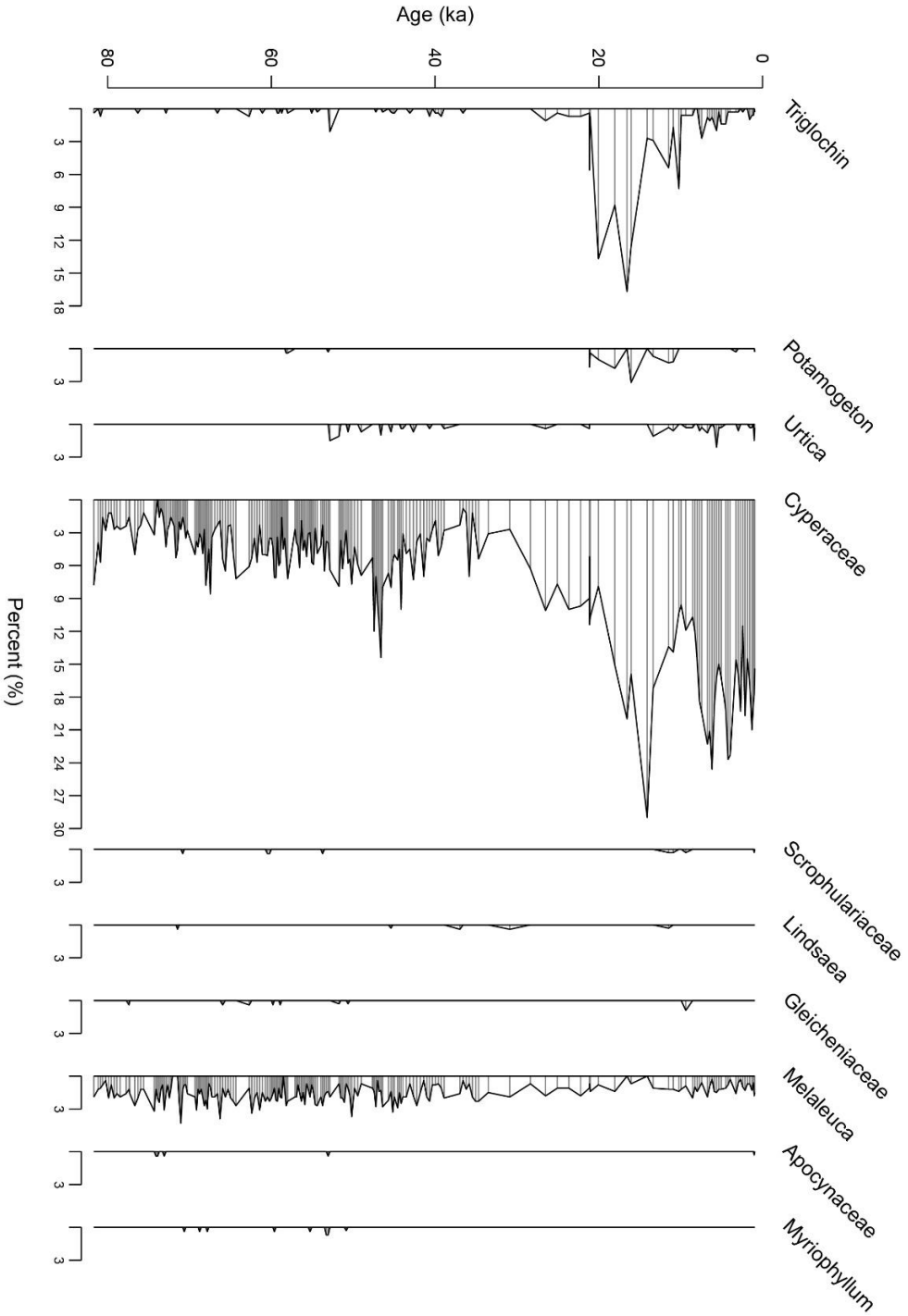

Figure S7 .Stratigraphic pollen diagram of species commonly found in marsh and aquatic environments on NSI as determined from Clifford and Specht (1979) and Stephens and Sharp (2009). Taxa are not included in the terrestrial pollen sum and are calculated from an aquatic pollen sum. Chronology from Lewis et al. (submitted).

Statement of Authorship

Title of Paper	Drivers of eastern Australia climates during MIS3 and MIS4
Publication Status	☐ Published ☐ Accepted for Publication ☐ Submitted for Publication ☑ Unpublished and Unsubmitted w ork w ritten in manuscript style
Publication Details	Cadd, H.R., Barr, C., Tyler, J., Tibby, Leng, M.J. (2019) Drivers of eastern Australia climates during MIS3 and MIS4

Principal Author

Name of Principal Author (Candidate)	Haidee Cadd		
Contribution to the Paper	Conceptualisation of the work, development of ideas and conclusions, carried out analytical work, carried out statistical analysis, interpretation of the data, wrote manuscript.		
Overall percentage (%)	80		
Certification:	This paper reports on original research I conducted during the period of my Higher Degree by Research candidature and is not subject to any obligations or contractual agreements with a third party that would constrain its inclusion in this thesis. I am the primary author of this paper.		
Signature		Date	29/09/19

Co-Author Contributions

By signing the Statement of Authorship, each author certifies that:

i. the candidate's stated contribution to the publication is accurate (as detailed above);
ii. permission is granted for the candidate in include the publication in the thesis; and
iii. the sum of all co-author contributions is equal to 100% less the candidate's stated contribution.

Name of Co-Author	Cameron Barr		
Contribution to the Paper	Carried out analytical work for oxygen isotopes, provided conceptual and interpretation guidance, edited manuscript		
Signature		Date	12/09/19

Name of Co-Author	Jonathan Tyler		
Contribution to the Paper	Provided conceptual and interpretation guidance, edited manuscript		
Signature		Date	28/09/19

Name of Co-Author	John Tibby		
Contribution to the Paper	Provided conceptual and interpretation guidance, edited manuscript		
Signature		Date	12/09/19

Name of Co-Author	Melanie Leng		
Contribution to the Paper	Assisted with acquisition and processing of isotope data, edited manuscript.		
Signature		Date	12/09/19

5

Drivers of eastern Australian climates during MIS3 and MIS4

In preparation as:

Cadd, H.R., Barr, C., Tyler, J., Tibby, J., Leng, M.J. Drivers of eastern Australian climates during MIS3 and MIS4.*Earth and Planetary Science Letters*

Abstract

Understanding Australia's climate during the last glacial period, a key time period in the environmental and cultural history of the continent, is important when considering the landscape encountered by early human migrants and the potential influence of climate on the extinction of Australia's megafauna. Determining the drivers of Australian climate during the last glacial period has remained elusive, in part due to the limited number of continuous high-resolution records and the difficulties in establishing robust, independent age constraints. In particular, in light of the bi-polar seesaw hypothesis for contrasting millennial scale climate variability between hemispheres, determining the links between Northern or Southern Hemisphere high-latitude drivers on Australian terrestrial climate has proved challenging. Here, we present a high-resolution palaeoclimate record from Welsby Lagoon, subtropical eastern Australia, constrained by an independent age-depth model, to examine drivers of changes in sediment $\delta^{13}C$ during MIS4 and MIS3 (80 – 30 ka). First-order variations in $\delta^{13}C$ occurred in concert with orbitally forced Antarctic δD and global CO_2 variation. Superimposed upon the major pattern is a second order fluctuation in $\delta^{13}C$ which corresponds to local palaeohydrology, also reflected in the $\delta^{18}O$ of lake water ($\delta^{18}O_{LW}$), and Antarctic Isotope Maxima (AIM) warming events. During AIM events, $\delta^{18}O_{LW}$ in Welsby Lagoon increased, indicating more evaporative conditions and lower lake levels. This corresponds to increases in $\delta^{13}C$, which indicate high aquatic productivity in response to a warmer, and possibly shallower lake. The tight coupling of the $\delta^{13}C$ record to Antarctic climate on both long and short time scales indicates a dominant Southern Hemisphere climate driver of east Australian climate during MIS3 and MIS4. This finding reinforces the strong connection between Pacific climates and the Southern Hemisphere high latitudes.

1 Introduction

In Australia, palaeoclimate records of the last glacial period are sparse and often rely on discontinuous fluvial archives (Hesse et al., 2018; Mueller et al., 2018), offshore sediments (Moss & Kershaw, 2000; Lopes dos Santos et al., 2013; Bayon et al., 2017; van der Kaars et al., 2017) or a limited number of continuous terrestrial records (Colhoun et al., 1999; Longmore & Heijnis, 1999; Harle et al., 2002; Turney et al., 2004; Kershaw et al., 2007b, 2007a). Furthermore, disentangling the primary climate signals from palynological records that dominate the literature has proved difficult due to interactions between vegetation, climate, fire, herbivory, nutrients and succession (Longmore & Heijnis, 1999; Murphy et al., 2012; Rule et al., 2012). The limited number of records is further confounded by challenges associated with creating accurate chronologies over the last glacial period that do not rely on correlation to benthic marine oxygen isotope records. The relative influences of Northern or Southern Hemisphere drivers of terrestrial Australian climate have, thus, remained ambiguous and often contradictory (Turney et al., 2004; Muller et al., 2008). Additionally, there is a substantial spatial gap in terrestrial records in the

subtropics, which is an important region that combines influence from both monsoonal and southern ocean climates (Murphy & Timbal, 2008; Chiang, 2009; Kajikawa et al., 2010; Ummenhofer et al., 2011; Chiang & Friedman, 2012).

The last glacial period in Australia represents an important time in the environmental and cultural history of the continent. This period encompasses both the arrival of modern humans between 65 ka and 50 ka (Hamm et al., 2016; Clarkson et al., 2017; Tobler et al., 2017) and the widespread extinction of a variety of large animals – collectively known as megafauna – concentrated around ca. 46 ka (Roberts et al., 2001; Saltré et al., 2016). Understanding the climates of Australia during this period is an essential element in attempting to untangle the relative drivers of megafauna extinctions, as well as determining the potential anthropogenic effects of early humans on the landscape, either in contrast to, or in concert with, climatic variations.

Stable isotope characterisation of bulk lacustrine organic material can provide valuable insights into the environmental and climatic conditions during carbon fixation and subsequent incorporation into the sediment record (Leng, 2006). The carbon isotope composition of autochthonous organic matter has been used to trace biogeochemical cycling, productivity and atmospheric pCO_2 concentration (Prokopenko et al., 1999; Lücke & Brauer, 2004; Street-Perrott et al., 2004; Heyng et al., 2012; Woodward et al., 2012; De Kluijver et al., 2014). The interpretation of the carbon isotope composition of bulk lacustrine organic material is difficult because of the complex combinations of primary allochthonous and autochthonous material, living organisms, detritus and diagenetic material (Leng & Marshall, 2004). Disentangling the various contributions of each component to the final sedimented organic material is thus imperative in understanding the relative importance of drivers.

Organic material derived from autochthonous primary productivity is typically characterised by low carbon to nitrogen ratios (C:N; Meyers and Lallier-Vergés, 1999). The carbon rich polymeric material required to produce structural support in terrestrial plants is not present in aquatic organisms that are typically more nitrogen and aliphatic rich (Hedges & Oades, 1997). The relationship observed by Meyers (1994) indicates that autochthonous material typically possesses C:N ratios <10. This threshold has commonly been used to quantify the proportion of autochthonous and allochthonous material contributing to bulk organic matter (Meyers & Teranes, 2001; Stephens et al., 2012). Insights into the complex processes of carbon cycling in lacustrine systems has demonstrated that this simplistic measure is not universally applicable (Hecky et al., 1993; Heyng et al., 2012; Cadd et al., 2018). High C:N ratios (C:N > 36) have been documented from cellulose-producing green algae, *Botryococcus braunii* (Maxwell et al., 1968; Street-Perrott et al., 1997; Heyng et al., 2012). High C:N ratios may also occur in aquatic organic matter from lake waters that are nitrogen deficient (Hecky et al., 1993; Talbot & Lærdal, 2000; Cadd et al., 2018) or as a result of diagenetic effects on organic matter (Meyers & Ishiwatari, 1993; Tyson, 1995).

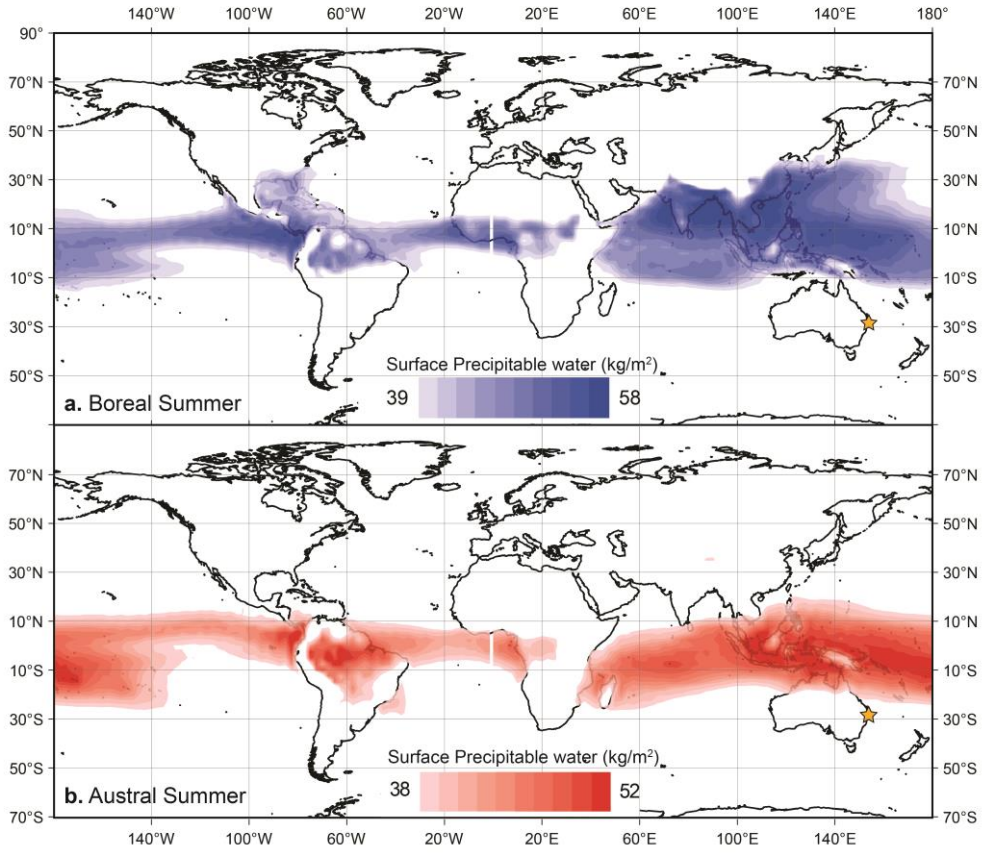

Figure 1. Global position of Intertropical Convergence Zone (ITCZ) during a. Boreal summer (JJA) and b. Austral summer (DJF). Data for precipitable water content at the earth surface from NCEP Reanalysis (https://www.esrl.noaa.gov/psd/cgi-bin/data/composites/printpage.pl; Kalnay et al. (1996). Orange star represents the location of the study site on North Stradbroke Island.

Additional indicators of the source of sedimentary organic material may be required to definitively attribute the origin of organic carbon and are complementary to C:N ratios (Dickens et al., 2006). The presence of different classes of carbon compounds, including lignin or polyphenol concentration, lignin (or polyphenol) / nitrogen ratios and protein, lipid or aliphatic concentrations can provide important additional information on the origin of carbon in lacustrine systems (Baldock et al., 2004; Dickens et al., 2011; Rodríguez-Murillo et al., 2011). If the source of sedimented carbon can adequately be identified, then sedimentary carbon isotopes can be used to track responses of lacustrine systems to environmental changes.

Carbon isotope ratio of sediments derived from predominantly aquatic sources are often interpreted in the context of aquatic primary productivity. The carbon isotope ratio of primary producers varies in response to the availability of dissolved inorganic carbon (DIC). In turn temporal DIC fluctuations depend upon the alkalinity-determined water storage capacity of DIC, biological assimilation, subsequent release of DIC and exchange of water-atmospheric CO_2 (Cole et al., 1994; Myrbo, 2012). Under present day CO_2

concentrations, there is a prevalence of CO_2 supersaturation in oligotrophic and mesotrophic systems due to low primary productivity (Cole et al., 1994; Sobek et al., 2005). High rates of primary productivity result in the increased draw down of aqueous CO_2 during photosynthesis (Sobek et al., 2005). Algae (broadly defined here to include cyanoprokaryotes) discriminate against ^{13}C during photosynthesis, preferentially removing ^{12}C from the surrounding waters. Consequently, the $\delta^{13}C$ in the waters increases, causing an increase in the $\delta^{13}C$ of newly produced organic matter and a productivity-driven increase in the $\delta^{13}C$ of sedimented organic matter (Leng, 2006). DIC limitation arising from interactions between alkalinity, pH, aquatic productivity or changing pCO_2, leads to an increase in $\delta^{13}C$ of autochonous organic matter (Leng, 2006). Incorporation of HCO_3^- during periods of aqueous CO_2 depletion, plankton growth rate and cell geometry can all influence water-cell carbon isotope fractionation, further enhancing the positive correlation between productivity and $\delta^{13}C$ (Laws et al., 1995; Leng, 2006).

Productivity-related drivers of $\delta^{13}C$, on timescales of years to centuries, include nutrient availability, water balance, temperature and competition (Boynton et al., 1983). Stable isotope analysis of aquatic carbon can therefore be used to reconstruct local climate and hydrological change through time. These drivers are also important on longer millennial to multi-millennial timescales, though may be secondary to variations in atmospheric pCO_2, solar radiation and changing basin morphology (Fontugne & Calvert, 1992; Prokopenko et al., 1999).

Here we present a high-resolution $\delta^{13}C$ record of bulk organic material from Welsby Lagoon, North Stradbroke Island (Minjerribah), subtropical eastern Australia. These data are interpreted as a record of aquatic productivity, which is an indirect tracer of climate and hydrological change. This interpretation is aided by a new cellulose- derived record of lake water oxygen isotope composition ($\delta^{18}O_{LW}$) developed by Barr et al., (in prep.). An independent age-model (Lewis et al., Accepted) allows investigation of millennial scale drivers of terrestrial climate in subtropical Australia during MIS3 and MIS4.

1.1. Study Site

North Stradbroke Island (NSI; 27°27'S, 153°28'E; Figure 1), the second largest sand island in the world, is situated in the subtropical climate zone in southeast Queensland, Australia. NSI is the southernmost island of the Great Sandy Region and was isolated from mainland Australia by rising seas during the mid-Holocene, ca. 6000 years ago (Pye, 1993). The subtropical location results in warm, wet summers (mean 26°C) and mild, dry winters (mean 19°C), with the majority of ~1670 mm mean annual precipitation falling in the Austral autumn and summer (Klingaman et al., 2013).

Intra-annual hydrological variability on the island is primarily driven by moisture bearing south-easterly trade winds, cut-off lows and extra-tropical cyclones. The broader south-east Queensland climate is modulated by the zonal migration of the Inter-Tropical Convergence Zone (ITCZ), the El Niño-Southern Oscillation (ENSO) and the Inter-

decadal Pacific Oscillation (IPO) (Risbey et al., 2009; Klingaman et al., 2013).

Welsby Lagoon (27°26'12"S, 153°26'56"E; 29 m.a.s.l) is a hydrologically closed, oligotrophic, shallow and acidic (pH 4.3 – 6.8; total alkalinity as $CaCO_3$ 2 – 3 mg/L) wetland. Welsby Lagoon reflects the surface expression of the perched freshwater aquifer of the Welsby Lagoon catchment, with a 5.38 km^2 drainage basin (Leach, 2011). A wider study by Tyler et al. (in prep) investigating the modern hydrology of NSI wetlands, shows variable water depths from Welsby Lagoon ranging from 0 – 1 m in response to the balance between precipitation and evaporation (P/E). Monitoring of the $\delta^{18}O$ composition of present day surface waters from Welsby Lagoon range from -7.2 to +6.6‰ (supplementary information Figure S1; Tyler et al. in prep).

2 Methods

2.1. Core collection

A complete sediment profile was extracted from the deepest sediments as two offset parallel cores, WL-15/1 (0–1280 cm) and WL-15/2 (50 – 1277 cm). The two sediment sequences were extracted in 1 m sections of black PVC pipe using a 60 mm Bolivia corer. Core sections were encased in black plastic to minimise light exposure before being split under filtered red LED light conditions in the OSL laboratory at the University of Adelaide. The two sediment profiles were aligned using ITRAX core scanning profiles to create a composite record (Lewis et al., Accepted).

2.2. Stable isotope analysis

A total of 568 sediment samples were collected from the composite record and sampled for total organic carbon (TOC), total nitrogen (TN) and carbon isotopes ($\delta^{13}C$). All samples were dried at 40°C and ground before being treated with 10% HCl to remove carbonates. Samples were rinsed with distilled water until a neutral pH was achieved. Dried sediment samples were weighed into tin capsules and analysed on a Costech ECS4010 Elemental Analyser coupled to a VG TripleTrap and Optima duel-inlet Isotope Ratio Mass Spectrometer at the British Geological Survey, Keyworth, Nottingham. $^{13}C/^{12}C$ isotope ratios are reported as per mille (‰), relative to NBS18, NBS-19, NBS-22, using the standard delta notation. Replicate analysis of samples had a precision of ±<0.1‰. Carbon:Nitrogn (C:N) ratios were calibrated against in house broccoli standard (BROC2). Analytical precision for replicate measurement of in house standards (BROC and SOIL) was ±<0.1.

A total of 134 sediment samples were extracted from the Welsby Lagoon core for oxygen isotope analysis of aquatic cellulose. Cellulose was extracted from bulk sediment using the CUAM method outlined by Wissel et al. (2008). Sediment samples were sieved at 250 µm

prior to the process of cellulose extraction to remove larger particles of higher plant material. Oxygen isotopes from cellulose were analysed by Dr. Cameron Barr (University of Adelaide) and Prof. Melanie Leng (British Geological Survey), and these data are examined here for the purpose of comparison. For further details of sediment cellulose oxygen isotopes see Barr et al. (in prep).

2.3. Nuclear magnetic resonance (NMR) spectroscopy

The proportions of different carbon biomolecules were determined using solid-state ^{13}C nuclear magnetic resonance (NMR) spectroscopy on 50 sediment samples sub-sampled throughout the sediment sequence. Spectra were acquired on a Bruker 200 Avance spectrometer equipped with a 4.7 T wide-bore superconducting magnet operating at a resonance frequency of 50.33 MHz at CSIRO Land and Water Adelaide, Australia. Sediment samples (150 – 600 mg) were loaded into 7 mm diameter zirconia rotors with Kel-F end caps and spun at 5 kHz. Calibration of chemical shifts was performed using the methyl resonance of hexamethylbenzene at 17.36 ppm. A 50 Hz Lorentzian line broadening was applied to all samples after calibration. Phasing and baseline corrections were conducted in the Bruker TopSpin 3.2 software. Absolute NMR signal intensities acquired for each sample were divided by the number of transients collected, corrected for the empty rotor background signal intensity and integrated over a series of chemical shift limits.

The molecular mixing model (MMM) of Baldock et al. (2004) was used to assign the molecular composition of sediment samples into 6 groups: carbohydrate, protein, lipid, lignin, resistant organic carbon (charcoal-like compounds) and pure carbonyl. Carbon rich polymeric material required to produce structural support in terrestrial plants, such as lignin and structural carbohydrates, are not required by aquatic organisms. Phytoplankton, algae and bacteria are typically more protein, lipid and aliphatic rich than terrestrial carbon (Hedges & Oades, 1997).

2.4. Palynology

A total of 197 samples were processed for pollen and spores from 0.5 cm^2 of sediment using a modified version of the standard protocols of Fægri and Iverson (1989). The base pollen sum consists of 250 grains of terrestrial origin (excluding fern spores). Algal spore abundances are expressed as a proportion of a super sum inclusive of all terrestrial and aquatic pollen and spores.

2.5. Data analysis

In order to objectively identify the low frequency variability in the Welsby Lagoon and Antarctic records, a smooth spline was fitted to the $\delta^{13}C$ (span: 0.8), $\delta^{18}O_{LW}$ (span: 0.9) and δD (span: 0.7) records. Span size reflects difference in relation to the resolution of each

record. The residuals of the long-term trend were subsequently extracted to highlight the millennial scale variability in each record. The detrended records were used for millennial scale comparisons between the $\delta^{13}C$, $\delta^{18}O_{LW}$ and δD records.

To assess the coherency between the $\delta^{13}C$ and δD records wavelet coherence analysis was performed on un-filtered time series data, binned at 500 year intervals, using the WaveletComp package (Rösch & Schmidbauer, 2018) in R (R Core Team, 2017). Lomb-Scargle periodograms were derived from raw $\delta^{13}C$ and δD data in the 'lomb' package (Ruf, 1999) in R (R Core Team, 2017) to investigate shared periodicities. Lomb-Scargle analysis allows identification of periodicities in unevenly spaced time series data, thus negating the need for interpolation of data to even time steps which can introduce artefacts into the analysis (Munteanu et al., 2016). The lower resolution of the $\delta^{18}O_{LW}$ record precluded statistical comparison with the $\delta^{13}C$ and δD records.

3 Results

In a multi-proxy study documenting the development of Welsby Lagoon, Cadd et al. (2018) demonstrated that the sediment sequence can be separated in to 3 distinct depositional phases (1270 – 1230 cm, 143 – 83 ka; 1230 – 500 cm, 83 – 30 ka; 500 – 0 cm, ca. 30 ka – present). Lewis et al. (Accepted) demonstrated that the three phases are bounded by a depositional hiatus between MIS5 and MIS4 and a marked change in sedimentation rate during MIS2. The clear changes in depositional environment between the three phases requires interpretation of each phase independently, whereby changes in ecosystem type may result in different processes affecting the mechanisms through which the geochemical data reflect environmental change. As a consequence, this study focusses on the lacustrine phase of the Welsby Lagoon sediment sequence from ca. 80 – 30 ka (1215 – 500 cm).

3.1. Stable isotope analysis

The section of Welsby Lagoon dated between ca. 80 – 30 ka is highly organic, with total organic carbon ranging between 11.8% to 59.8% (mean 38.3%). Total nitrogen ranges from 0.3% to 1.5% (mean 1.0%) and carbon to nitrogen (C:N) ratios range from 29.7 to 56.8 (mean 37.5). The $\delta^{13}C$ values range between -30.2‰ and -26.5‰ (mean -28.4‰).

Lake water $\delta^{18}O$ ($\delta^{18}O_{LW}$) was inferred from the $\delta^{18}O$ of sediment cellulose ($\delta^{18}O_{CELL}$) by assuming a constant cellulose-water isotope fractionation factor of 28‰ (Wolfe et al., 2007; Street-Perrott et al., 2018). Inferred $\delta^{18}O_{LW}$ ranges from -5.3 to +8.2‰. The reconstructed $\delta^{18}O_{LW}$ has a range of 13.5‰, which may be considered large, though is similar to the range of modern lake water data (13.8‰; supplementary information Figure S1). For further information on oxygen isotope results see Barr et al. (in prep).

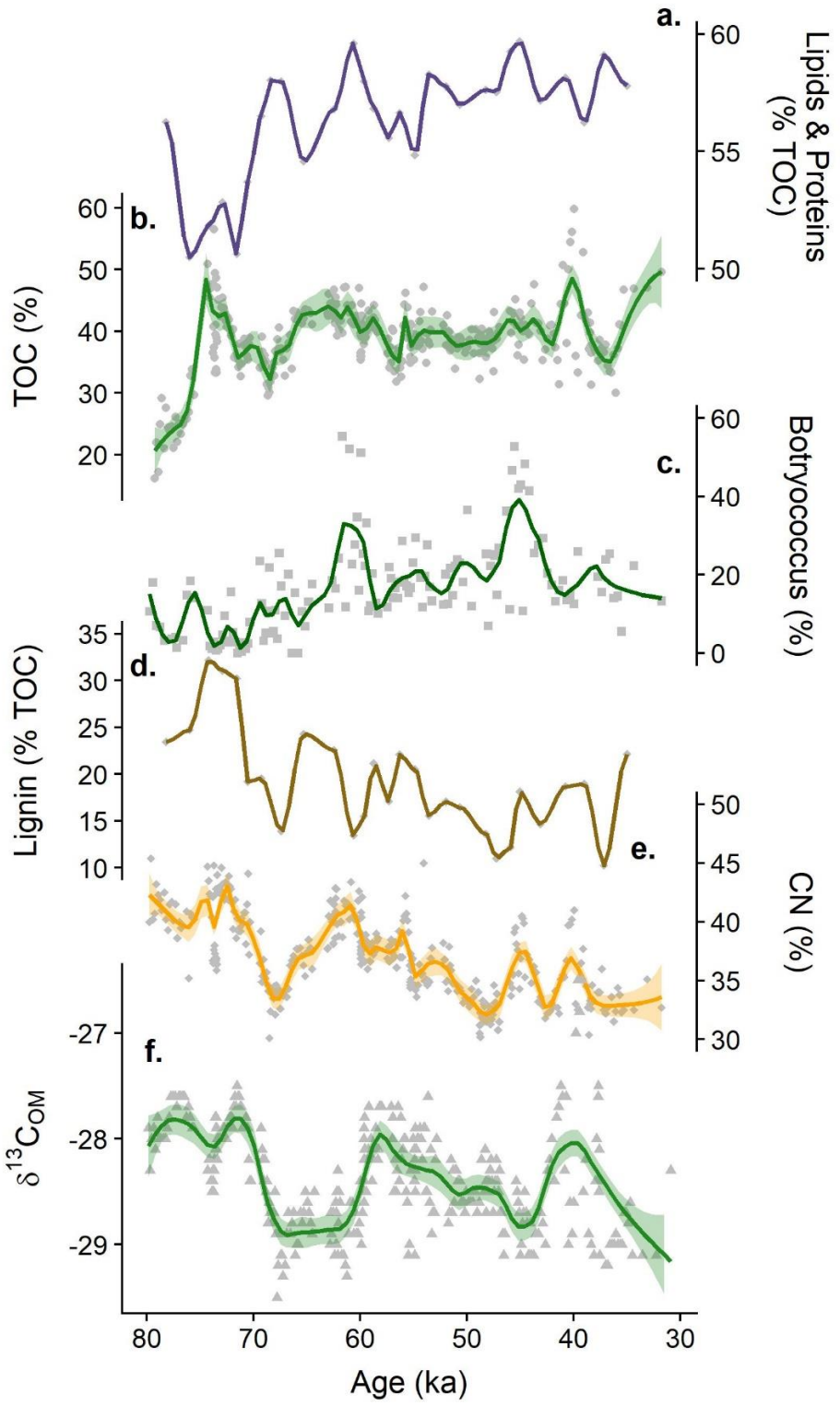

Figure 2. Multi-proxy data from Welsby Lagoon for 80 – 30 ka. a. NMR-derived percentage of protein and lipid components of the total organic carbon (TOC) content of bulk sediment; b. Total organic carbon content of bulk sediment; c. Percentage abundance of *Botryococcus* remains from pollen slides; d. NMR-derived percentage of lignin components of the TOC content of bulk sediment; e. Carbon:Nitrogen (C/N) content of bulk sediment; f. Carbon isotope composition ($\delta^{13}C$) of bulk organic matter (OM). Chronology from Lewis et al. (Accepted).

3.2. NMR

From 1230 – 500 cm of the core (ca. 80 – 30 ka) organic carbon is dominated by protein and lipid compounds (55.9 – 71.9%; mean 66.1%), consistent with the composition of aquatic algae and bacteria (Hedges & Oades, 1997; Sanderman et al., 2015). In the top 500 cm of the core (ca. 30 ka – present) the organic carbon compounds are dominated by lignin and carbohydrate material (28.6% – 71.5%; mean 51.5%) indicative of terrestrial structural carbon compounds.

3.3. Palynology

Full details of terrestrial pollen taxa, grouped according to morphology and habitat types, are presented in Chapter 4, this thesis. Algal spore abundances of the colonial green alga *Botryococcus* appear consistently throughout the ca. 80 – 30 ka portion of the record. Two distinct peaks *Botryococcus* occur at ca. 44 – 45 ka and ca. 60 – 61.5 ka. During these time periods values of *Botryococcus* make up over 50% of the palynomorphs

3.4. Statistical Analysis

Cross-wavelet coherence analysis between the $\delta^{13}C$ and δD records found significant frequency patterns through the entire 80 – 30 ka time window at a ca. 6 – 7 ka periodicity. The Lomb Scargle periodigram analysis identified a strong and significant 22.4 ka periodicity in both records. An additional significant periodicity was identified in both records, peaking between 6.4 and 7.5 ka. The Antarctica δD record displayed a third significant periodicity at 3.7 ka that was not present in the Welsby Lagoon $\delta^{13}C$.

4 Discussion

4.1. Sedimentary carbon in Welsby Lagoon

We interpret the 80 – 30 ka $\delta^{13}C$ record from Welsby Lagoon to be primarily a reflection of autochthonous organic material that escaped remineralisation. Organic material derived from autochthonous primary productivity is typically characterised by low carbon to nitrogen ratios (Meyers, 2003), however in the nitrogen poor environment of NSI, algae can have C:N ratios in excess of 20 (Cadd et al., 2018). We therefore use the presence of different classes of carbon compounds predominantly found in aquatic algae and bacteria (i.e. proteins and lipid/aliphatic material; Hedges and Oades, 1997; Sanderman et al., 2015) to further clarify the sources of sedimentary carbon through in the Welsby Lagoon sediments. Between 80 – 30 ka, the proportion of sedimentary carbon compounds of proteins and lipids associated with aquatic organisms range from 45 – 64 %, while lignin compounds associated with terrestrial carbon sources range from 16 – 32 % (Figure 2). Along with the data presented by Cadd et al. (2018), this provides further evidence for the

dominance of algal-derived carbon sources during a lacustrine depositional phase at Welsby Lagoon between 80 – 30 ka.

Changes in algal productivity at Welsby Lagoon are inferred from the $\delta^{13}C$ of organic carbon, which reflect changes in nutrient supply, mediated by lake water depth. Organic matter derived from autochthonous sources reflects changes in algal primary productivity, with elevated $\delta^{13}C$ occurring when the $^{13}C/^{12}C$ ratio of both DIC and cellular tissue increases as a result of progressive carbon uptake. Algal productivity varies as a result of climate and environmental change and in response to changing catchment conditions (i.e. nutrient availability). Water column nutrient availability in North Stradbroke Island lakes is dominated by internal recycling from the sediments, due to negligible external nutrient input associated with rapid water percolation through a nutrient deficient, quartz-dominated sandy substrate. The predominant source of nutrients in NSI wetlands is therefore thought to be from either aeolian continental inputs (Petherick et al., 2009) or by remineralisation of terrestrial or aquatic organic matter (Katz, 2001; Winder et al., 2012). Nutrient supply from the remineralisation of organic matter is strongly influenced by water level and associated hydrographic behaviour of the water column (Boynton et al., 1983; Huszar & Reynolds, 1997; Winder et al., 2012). Relatively deep, stratified lakes limit the transfer of nutrients from the hypolimnion to the epilimnion, thus restricting productivity (Katz, 2001). As lakes diminish to a shallow, continuously mixed systems, vertical exchange and recycling of nutrients occurs, enhancing nutrient availability in the photic zone, thus increasing productivity (Huszar & Reynolds, 1997). Therefore, it is reasonable to infer that changes in water depth at Welsby Lagoon would be linked to nutrient remobilisation, aquatic productivity and $\delta^{13}C$. The hydrologically closed nature of the wetland, and sensitivity of the site to changes in the balance between precipitation and evaporation, therefore provides a strong link between climate and productivity.

Low C:N, $\delta^{13}C$ values, relatively low TOC and reduced concentration of photosynthetic algal pigments at the beginning of MIS4 suggest a low productivity lake system (Cadd et al., 2018). A shift to higher C:N and slight increase in TOC after 63 ka could be interpreted to indicate an increased input of terrestrial carbon. However, the increase in C:N also coincides with declining proportions of lignin, suggesting that the increase in C:N was not driven by increased input of terrestrial carbon. The increase in C:N is mirrored by an increase in the colonial green algae *Botryococcus*. *Botryococcus* species can form dense floating mats and are widely dispersed in temperate and tropical freshwater and brackish lakes, wetlands and bogs, favouring oligotrophic waters (Metzger & Largeau, 2005; Heyng et al., 2014). The hydrocarbon rich membrane of *Botryococcus* results in high C:N ratios (Huang et al., 1999). Peaks in *Botryococcus* and C:N occurred in concert at 63 – 59 ka and again at 46 – 43 ka (Figure 2). The concurrent timing of increases in C:N and *Botryococcus* and decreases in lignin suggest that variability in C:N ratios occurred independently of terrestrial carbon inputs and was instead associated with the high carbon content of *Botryococcus* (Heyng et al., 2014).

Low $\delta^{13}C$ values persist until the end of MIS4 (ca. 59 ka), implying that the increased TOC

and presence of *Botryococcus* was not associated with an overall increase in productivity (Figure 2). *Botryococcus* can be outcompeted by faster growing species in waters with increasing nutrient availability (Metzger & Largeau, 2005). Hence, reduction in external nutrient input, or an increase in thermal stratification restricting nutrient resuspension into the epilimnion, may favour the replacement of faster growing taxa by *Botryococcus* (Tyson, 1995; Huszar & Reynolds, 1997). The increase in *Botryococcus* and decline in $\delta^{13}C$ between 63 – 59 ka and 46 – 43 ka (Figure 2) may indicate a decrease in productivity in response to low nutrient levels and/or deeper water (Widayat et al., 2016). The low productivity lacustrine conditions during MIS4 may have resulted from glacial conditions more regionally (De Deckker et al., 2019).

The beginning of MIS3 (59 ka) was characterised by a rapid increase in $\delta^{13}C$, a slight decline in C:N and a drop in *Botryococcus* (Figure 2). Between 59 – 46 ka C:N and $\delta^{13}C$ values remained relatively stable, with a variable, but reduced abundance of *Botryococcus*. After 43 ka the Welsby Lagoon record is characterised by a series of rapid oscillations in organic proxies (Figure 2). These variations in C:N, $\delta^{13}C$ and TOC, in conjunction with a decrease in *Botryococcus* and an increase in cyanobacterial photosynthetic pigments (Cadd et al., 2018), are likely an ecosystem response to shallowing water, resulting in changes in nutrient cycling and sources of organic matter.

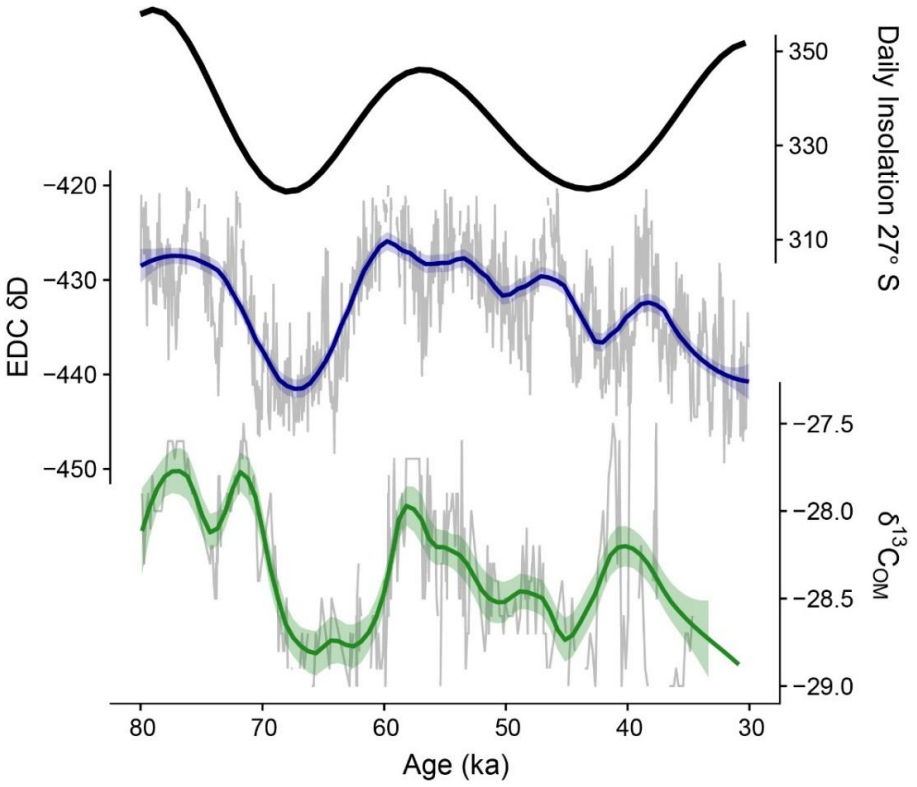

Figure 3 Daily insolation (Wm-2) at 27°S resulting from orbital forcing, EPICA Dome C (EDC) δD and carbon isotope composition (δ13C) of bulk organic matter (OM) from Welsby Lagoon from 80 – 30 ka. Smooth splines (coloured lines) were fitted to each record to highlight the long-term trends in each dataset. EDC δD is plotted using the AIC2012 chronology (Veres et al., 2013). Chronology from Lewis et al. (Accepted).

4.2. Welsby Lagoon productivity and climate

The Welsby Lagoon $\delta^{13}C$ record displays both long-term (orbital) and short-term (millennial) patterns (Figure 3, Figure 4). The long-term trend in $\delta^{13}C$, and thus productivity, shows strong cyclic variations which co-vary with Antarctic δD and global CO_2 (Figure 3; EPICA Community Members et al., 2006; Jouzel et al., 2007; Lüthi et al., 2008; Veres et al., 2013).

Covariance between atmospheric *p*CO2 and organic matter $\delta^{13}C$ could be interpreted to reflect the influence of pCO2 on carbon cycling in the aquatic system. However, lower atmospheric pCO_2 would be expected to decrease the availability of dissolved CO_2 in wetland systems, which in turn would increase $\delta^{13}C$ (Prokopenko et al., 1999). By contrast, the apparent correlation between Welsby Lagoon $\delta^{13}C$ and *p*CO2 is positive, suggesting that other processes influence this pattern. DIC limitation and utilisation of HCO_3^- are unlikely to occur at Welsby Lagoon, even during low pCO_2 of glacial periods, due to the decomposition of highly organic sediments, low alkalinity and low pH. It is therefore either possible that Welsby Lagoon continued to experience relatively high CO_2 saturation, even during glacial periods, or that CO_2 availability was not the limiting factor on aquatic productivity through this period. The low nutrient status of wetlands on NSI and across the dunes of the Great Sandy region make it likely that nutrients are more consistently the limiting factor for aquatic productivity within this ecosystem.

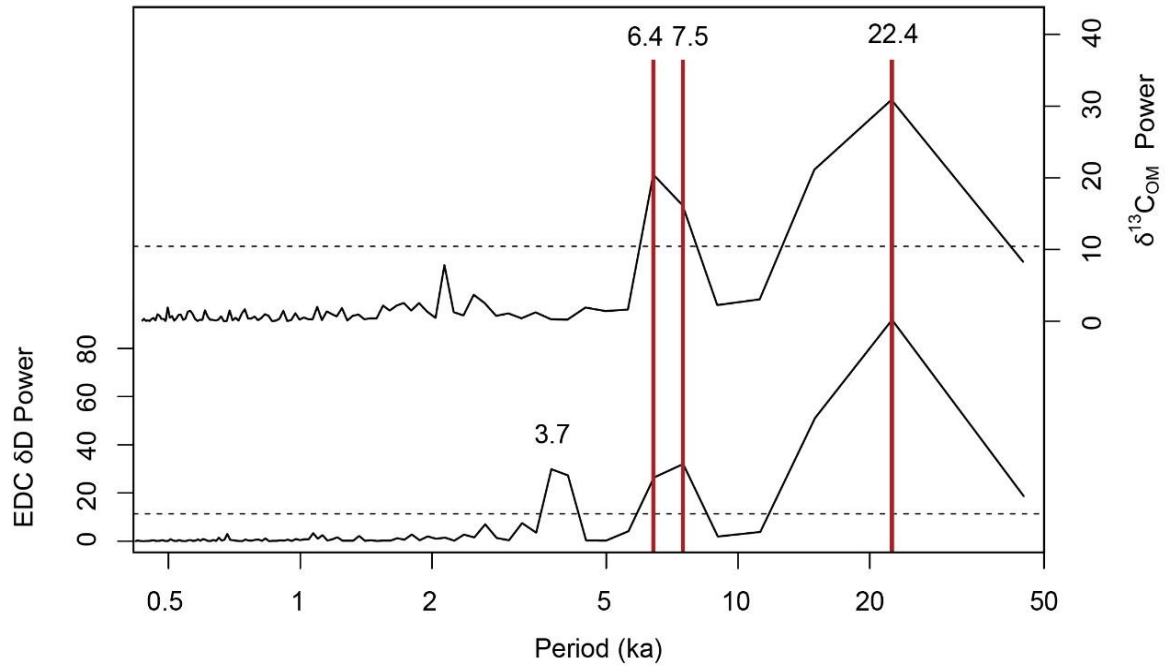

Figure 5. Lomb-Scargle periodograms for carbon isotope composition (δ13C) of bulk organic matter (OM) from Welsby Lagoon and EPICA Dome C (EDC) δD for the period 80 – 30 ka. Dashed line represents the significance level (0.01). Significant periodogram peaks occur in both data sets at 6.4, 7.5 and 22.4 ka. An additional significant peak occurs in the EDC δD dataset at 3.7 ka.

A strong 22.4 ka signal occurs in both the Welsby Lagoon $\delta^{13}C$ and the Antarctic δD records (Figure 5) indicating a dominant influence of low-frequency precession-driven climate over both regions. Analyses of Antarctic ice core records demonstrate that glacial-interglacial changes in isotope data are orbitally paced (Petit et al., 1999; Timmermann et al., 2009; Laepple et al., 2011). Photosynthetically driven increases in productivity are also typically predicted to occur during periods of high local insolation (Colman et al., 1995). In addition to an increase in local solar radiation, increases in temperature also lead to an increase in aquatic productivity, either through direct increases in growth rate or limitations on thermal stratification (Boynton et al., 1983; Katz, 2001). The correlation between long term changes in productivity at Welsby Lagoon and local daily insolation suggests that insolation, in conjunction with variations Antarctic and Southern Ocean temperature, were important drivers of productivity changes at Welsby Lagoon.

The orbitally driven trend in the Welsby Lagoon $\delta^{13}C$ record is absent from the $\delta^{18}O_{LW}$ record (supplementary information Figure S2). The absence of an orbital signal in $\delta^{18}O_{LW}$ at Welsby Lagoon may indicate that changes in basin infilling and variations in water balance have a strong non-linear relationship with P/E over this time period. The availability of a larger, deep water basin during the early part of the record (Cadd et al., 2018) may have resulted in a system less responsive to variations in $\delta^{18}O$ due to higher water residence time and reduction in the variation of the $\delta^{18}O_{LW}$ signal. Whilst a precessional signal appears absent from the $\delta^{18}O_{LW}$ record, Barr et al. (in prep) suggest a long-term trend towards drier climates in the Welsby Lagoon record, in line with increasing aridity through MIS3 (Cohen et al., 2015a; Kemp et al., 2019).

Short-term variability

In addition to the orbitally-forced signal within the Welsby Lagoon and Antarctic δD records, both records also exhibit significant periodicities of ca. 6.4 and 7.5 ka, corresponding to the periodicity of Antarctic Isotope Maxima (AIM) events (Jouzel et al., 2007). Increased SST temperatures in the mid-latitude Southern Ocean regions, occurring on a 6 – 7 ka cyclicity, have also been linked to AIM events (Barrows et al., 2007). In contrast to the orbital scale variability, the millennial scale variability in $\delta^{13}C$ is also expressed in $\delta^{18}O_{LW}$ (Figure 7). This similarity between $\delta^{13}C$ and $\delta^{18}O_{LW}$ over millennial timescales supports the hypothesised link between hydrological variability and lake productivity. The $\delta^{18}O$ of lake water is interpreted to reflect changes in the balance between evaporation and precipitation, whereby an increase in $\delta^{18}O_{LW}$ reflects a dominance of evaporation over a wetland's water balance (Gat, 1996; Gibson et al., 2016, Tyler et al. in prep). As discussed above, changes in aquatic productivity and $\delta^{13}C$ are also interpreted to be linked to wetland hydrological balance, via internal nutrient loading, resulting from continual water mixing, vertical exchange and recycling from the sediment-water interface (Huszar & Reynolds, 1997; De Senerpont Domis et al., 2013).

The coherent millennial scale cyclicity between detrended $\delta^{13}C$, $\delta^{18}O_{LW}$, Southern Ocean SST and detrended Antarctic δD strongly suggest that all records responded to the same

large scale forcing. The $\delta^{18}O_{LW}$ displays higher values during periods of warmer SST and lower Antarctic ice volume. Whilst warmer oceans typically lead to enhanced convection and increased precipitation, the balance between evaporation and precipitation at Welsby Lagoon during periods of warmer SST, indicates a predominance of evaporative conditions. The increase in evaporation may be a function of higher air temperatures, negating any potential increase in precipitation resulting from warmer SST. The coupling between Antarctic δD, Southern Ocean SSTs and Welsby Lagoon $\delta^{13}C$ and $\delta^{18}O_{LW}$ suggests that direct temperature effects may be the dominant influence on the hydrology of Welsby Lagoon during MIS4 and MIS3. This reinforces the link between Southern Hemisphere oceans and Antarctic temperatures and east coast Australian climate.

Several Australian palaeoclimate records have suggested Northern Hemisphere Dansgaard-Oeschger (D-O) and Heinrich events influenced the hydroclimate of Australia during the last glacial cycle (Turney et al., 2004; Kershaw et al., 2007b; Muller et al., 2008; Mooney et al., 2011; Kaal et al., 2014; Bayon et al., 2017), although some studies suggest a Southern Hemisphere origin for individual Heinrich events (Turney et al., 2017). The thermal bipolar seesaw hypothesis links climates of the northern and southern high latitude climates through the cross equatorial ocean heat transport in the Atlantic. Through the bipolar seesaw, D-O events are inversely coupled to AIM events, with abrupt D-O cooling events corresponding gradual warming in the Southern Hemisphere high latitudes expressed as AIM events (EPICA Community Members, 2006). The largest influence of a northern hemisphere climate signal in driving Australian hydroclimate likely manifests in latitudinal changes in the Inter Tropical Convergence Zone (ITCZ). The ITCZ is sensitive to variations in the cross-equatorial temperature gradient, with the mean position of the ITCZ in the warmer hemisphere (Donohoe et al., 2013; McGee et al., 2014). A southward shift of the mean ITCZ position in response to cooler NH temperatures during Heinrich events and warm AIM events has previously been reported from both the tropical Northern and Southern Hemispheres (Wang et al., 2001, 2007; Peterson et al., 2007; Muller et al., 2008; Denniston et al., 2013; Chiang et al., 2014; Fornace et al., 2014).

Welsby Lagoon record shows no evidence of high frequency D-O events in subtropical Australia during MIS3 and MIS4. Heinrich events are only manifest in the Welsby Lagoon record to the extent that they are inversely correlated with AIM events (EPICA Community Members, 2006). As such, our data do not support the hypothesis of an atmospheric teleconnection between the North Atlantic region and the subtropical east coast of Australia. Therefore, any influence of the NH on the subtropical latitudes of Australia are likely restricted to the established oceanographic teleconnection between the Northern and Southern Hemispheres (EPICA Community Members et al., 2006; WAIS Members et al., 2015). The absence of a Northern Hemisphere signal at Welsby Lagoon indicates that the limit of any atmospheric Northern Hemisphere influence on Australia is located to the north of NSI.

The suggested southerly shift in the latitudinal position of the ITCZ and associated changes in precipitation during warm Southern Hemisphere AIM events during MIS4 and

MIS3 (Bayon et al., 2017) do not appear to have led to an increase in precipitation on NSI. Presently, the ITCZ does not penetrate further than 20°S over Australia, however it has been suggested that it reached as far as 32°S during MIS3 and MIS4 (Bayon et al., 2017). A positional shift to 32°S would place the core of the ITCZ cloud band firmly over NSI, which would result in an increase in precipitation and more tropical climate conditions. The $\delta^{18}O_{LW}$ record from Welsby Lagoon indicates drier conditions during warm AIM events, suggesting that the southward movement of the ITCZ did not penetrate as far south as NSI (27°S) during the Heinrich and AIM events. Drier conditions on NSI, as indicated by the $\delta^{18}O_{LW}$, despite a southward migration of the ITCZ in response to warming in the SH, may be related to an associated reduction in trade wind strength (McGee et al., 2018). Southern Queensland rainfall is strongly driven by fluctuations in east-coast cyclone numbers and the strength of onshore trade winds (Klingaman et al., 2013). Proxy and modelled data suggest a clear pattern of weakened trade winds in SH ocean basins in association with a southward shift in the ITCZ (McGee et al., 2018). Weaker south easterly trade winds would reduce the moisture laden trade winds crossing NSI and reduce potential precipitation (Klingaman et al., 2013). Whilst we find no evidence within the Welsby Lagoon dataset for a southward migration of the ITCZ to 27°S, the hydroclimate of Australia is spatially diverse (Kemp et al., 2019), and influence of the ITCZ rain belt in more northern other regions of Australia during the last glacial period cannot be ruled out (Bayon et al., 2017).

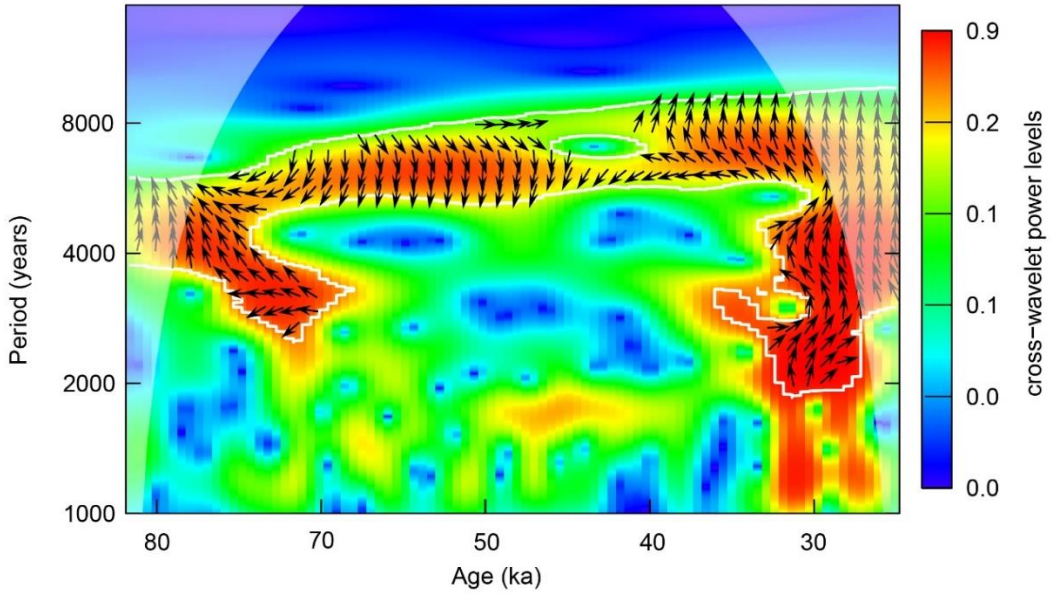

Figure 6. A cross-wavelet of carbon isotope composition (δ13C) of bulk organic matter (OM) from Welsby Lagoon and EPICA Dome C (EDC) δD data for the period 80 – 30 ka. The cross-wavelet power levels indicate the coherency between the two datasets. The white outline highlights the periods of significance. Arrows within this border indicate the direction of the correlation between the datasets. White shading indicates the location of the cone of influence. EDC δD and δ13C were binned to 500 year intervals. Where the δ13C record did not have sufficient data to create 500 year bins, data was linearly interpolated between neighbouring values.

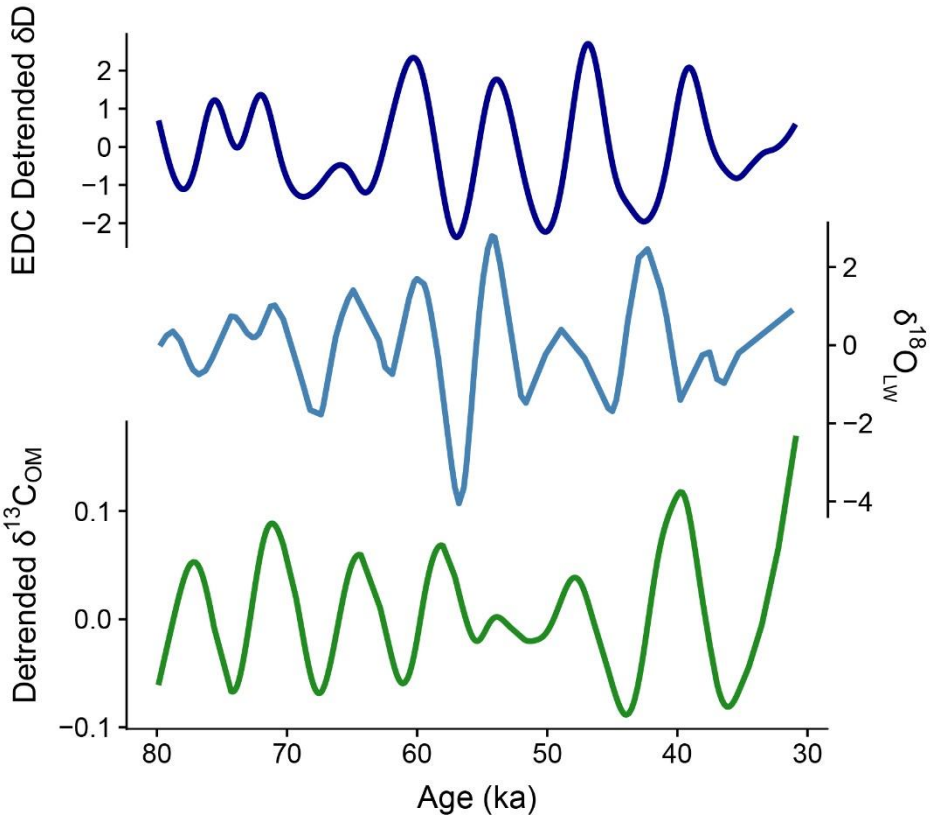

Figure 7. Extracted smooth spline of detrended EDC δD and $\delta^{13}C$ data from figure 4. Extracted smooth spline of detrended oxygen isotope ($\delta^{18}O_{LW}$) composition of aquatic cellulose (light blue). $\delta^{18}O$ and $\delta^{13}C$ chronology from Lewis et al. (Accepted).

5 Conclusions

Changes in aquatic productivity at Welsby Lagoon, as inferred from the $\delta^{13}C$ of organic matter, exhibited a marked similarity to Antarctic ice core δD during MIS3 and MIS4. This similarity persisted both through orbital-scale variability at a common ~22.4 ka periodicity in both Welsby Lagoon $\delta^{13}C$ and the δD of EDC Antarctic ice, in addition to a shorter ~7 ka oscillation with similar periodicity to Antarctic Isotope Maxima. During warm AIM events, the Welsby Lagoon $\delta^{18}O_{LW}$ record indicates that NSI experienced a drier and/or a warmer climate which promoted evaporation of lake water. The $\delta^{13}C$ record indicates that productivity was enhanced during these warm/dry climate phases, as a result of both direct temperatures effects and indirect effects of increased nutrient availability in a shallower water body. The dry conditions observed at Welsby Lagoon during warmer Southern Hemisphere AIM events may be a result of southward movement of the ITCZ restricting onshore trade wind strength or a direct influence of higher evaporative potential under warmer temperatures, or a combination of both. The relationship between $\delta^{13}C$ and Antarctic temperature, CO_2 and Southern Ocean SST reveals a link between eastern Australian climate and the Southern Hemisphere high-latitudes.

Acknowledgments.

We acknowledge Minjerribah (NSI) and the surrounding waters as Quandamooka Country. The study was funded by Australian Research Council project DP150103875. We thank Jie Chang, Jacinta Greer, Matthew Jones, Richard Lewis, Patrick Moss and Cameron Schulz for assistance in the field. We thank Chris Kendrick and the team at the British Geological Survey Stable Isotope Facility, Keyworth, for running carbon isotope analysis.

References

Baldock, J.A., Masiello, C.A., Gélinas, Y., & Hedges, J.I. (2004) Cycling and composition of organic matter in terrestrial and marine ecosystems. *Marine Chemistry*, **92**, 39–64.

Barr, C., Cadd, H.R., Tibby, J., Leng, M.J., Tyler, Jonathan J.McInerney, F.A., Henderson, A.C.G., Arnold, L.J., Marshall, J.C., & Mcgregor, G.B. Hydrological change in subtropical Australia from 80 - 40 kyr. .

Barrows, T.T., Juggins, S., De Deckker, P., Calvo, E., & Pelejero, C. (2007) Long-term sea surface temperature and climate change in the Australian-New Zealand region. *Paleoceanography*, **22**, 1–17.

Bayon, G., De Deckker, P., Magee, J.W., Germain, Y., Bermell, S., Tachikawa, K., & Norman, M.D. (2017) Extensive wet episodes in Late Glacial Australia resulting from high-latitude forcings. *Scientific Reports*, **7**, 1–7.

Boynton, W.R., Hall, C.A., Falkowski, P.G., Keefe, C.W., & Kemp, W.M. (1983) Phytoplankton Productivity in Aquatic Ecosystems. *Physiological Plant Ecology IV: Ecosystem Processes: Mineral Cycling, Productivity and Man's Influence* (ed. by O.L. Lange, P.S. Nobel, C.B. Osmond, and H. Ziegler), pp. 305–327. Springer Berlin Heidelberg, Berlin, Heidelberg.

Cadd, H.R., Tibby, J., Barr, C., Tyler, J., Unger, L., Leng, M.J., Marshall, J.C., McGregor, G., Lewis, R., Arnold, L.J., Lewis, T., & Baldock, J. (2018) Development of a southern hemisphere subtropical wetland (Welsby Lagoon, south-east Queensland, Australia) through the last glacial cycle. *Quaternary Science Reviews*, **202**, 53–65.

Chiang, J.C.H. (2009) The Tropics in Paleoclimate. *Annual Review of Earth and Planetary Sciences*, **37**, 263–297.

Chiang, J.C.H. & Friedman, A.R. (2012) Extratropical Cooling, Interhemispheric Thermal Gradients, and Tropical Climate Change. *Annual Review of Earth and Planetary Sciences*, **40**, 383–412.

Chiang, J.C.H., Lee, S.Y., Putnam, A.E., & Wang, X. (2014) South Pacific Split Jet, ITCZ shifts, and atmospheric North-South linkages during abrupt climate changes of the last glacial period. *Earth and Planetary Science Letters*, **406**, 233–246.

Clarkson, C., Jacobs, Z., Marwick, B., et al. (2017) Human occupation of northern Australia by 65,000 years ago. *Nature*, **547**, 306–310.

Cohen, T.J., Jansen, J.D., Gliganic, L.A., Larsen, J.R., Nanson, G.C., May, J.-H., Jones, B.G., & Price, D.M. (2015) Hydrological transformation coincided with megafaunal extinction in central Australia. *Geology*, **43**, 195–198.

Cole, J.J., Caraco, N.F., Kling, G.W., & Kratz, T.K. (1994) Carbon Dioxide Supersaturation in the Surface Waters of Lakes. *Science*, **265**, 1568–1570.

Colhoun, E.A., Pola, J.S., Barton, C.E., & Heijnis, H. (1999) Late Pleistocene vegetation and climate history of Lake Selina, western Tasmania. *Quaternary International*, **57–58**, 5–23.

Colman, S.M., Peck, J.A., Karabanov, E.B., Carter, S.J., Bradbury, J.P., King, J.W., & Williams, D.F.

(1995) Continental climate response to orbital forcing from biogenic silica records in lake baikal. *Nature*, **378**, 769–771.

De Deckker, P., Arnold, L.J., van der Kaars, S., Bayon, G., Stuut, J.B.W., Perner, K., Lopes dos Santos, R., Uemura, R., & Demuro, M. (2019) Marine Isotope Stage 4 in Australasia: A full glacial culminating 65,000 years ago – Global connections and implications for human dispersal. *Quaternary Science Reviews*, **204**, 187–207.

Denniston, R.F., Wyrwoll, K.H., Asmerom, Y., Polyak, V.J., Humphreys, W.F., Cugley, J., Woods, D., LaPointe, Z., Peota, J., & Greaves, E. (2013) North Atlantic forcing of millennial-scale Indo-Australian monsoon dynamics during the Last Glacial period. *Quaternary Science Reviews*, **72**, 159–168.

Dickens, A.F., Baldock, J., Kenna, T.C., & Eglinton, T.I. (2011) A depositional history of particulate organic carbon in a floodplain lake from the lower Ob' River, Siberia. *Geochimica et Cosmochimica Acta*, **75**, 4796–4815.

Dickens, A.F., Baldock, J.A., Smernik, R.J., Wakeham, S.G., Arnarson, T.S., Gélinas, Y., & Hedges, J.I. (2006) Solid-state 13C NMR analysis of size and density fractions of marine sediments: Insight into organic carbon sources and preservation mechanisms. *Geochimica et Cosmochimica Acta*, **70**, 666–686.

Donohoe, A., Marshall, J., Ferreira, D., & Mcgee, D. (2013) The relationship between ITCZ location and cross-equatorial atmospheric heat transport: From the seasonal cycle to the last glacial maximum. *Journal of Climate*, **26**, 3597–3618.

EPICA Community Members, Barbante, C., Barnola, J.M., et al. (2006) One-to-one coupling of glacial climate variability in Greenland and Antarctica. *Nature*, **444**, 195–198.

Fægri, K. & Iverson, J. (1989) *Textbook of Pollen Analysis.* Wiley, New York.

Fontugne, M.R. & Calvert, S.E. (1992) Late Pleistocene variability of the carbon isotope composition of organic matter in the eastern Mediterranean: monitor of changes in carbon sources and atmospheric CO2 concentrations. *Paleoceanography*, **7**, 1–20.

Fornace, K.L., Hughen, K.A., Shanahan, T.M., Fritz, S.C., Baker, P.A., & Sylva, S.P. (2014) A 60,000-year record of hydrologic variability in the Central Andes from the hydrogen isotopic composition of leaf waxes in Lake Titicaca sediments. *Earth and Planetary Science Letters*, **408**, 263–271.

Gat, J.R. (1996) Oxygen and Hydrogen Isotopes in the Hydrologic Cycle. *Annual Review of Earth and Planetary Sciences*, **24**, 225–262.

Gibson, J.J., Birks, S.J., & Yi, Y. (2016) Stable isotope mass balance of lakes: A contemporary perspective. *Quaternary Science Reviews*, **131**, 316–328.

Hamm, G., Mitchell, P., Arnold, L.J., Prideaux, G.J., Questiaux, D., Spooner, N.A., Levchenko, V.A., Foley, E.C., Worthy, T.H., Stephenson, B., Coulthard, V., Coulthard, C., Wilton, S., & Johnston, D. (2016) Cultural innovation and megafauna interaction in the early settlement of arid Australia. *Nature*, **539**, 280–283.

Harle, K.J., Heijnis, H., Chisari, R., Kershaw, A.P., Zoppi, U., & Jacobsen, G. (2002) A chronology for the long pollen record from Lake Wangoom, western Victoria (Australia) as derived from uranium/thorium disequilibrium dating. *Journal of Quaternary Science*, **17**, 707–720.

Hecky, R.E., Campbell, P., & Hendzel, L.L. (1993) The stoichiometry of carbon, nitrogen, and phosphorus in particulate matter of lakes and oceans. *Limnology and Oceanography*, **38**, 709–724.

Hedges, J.. & Oades, J.. (1997) Comparative organic geochemistries of soils and marine sediments. *Organic Geochemistry*, **27**, 319–361.

Hesse, P.P., Williams, R., Ralph, T.J., Fryirs, K.A., Larkin, Z.T., Westaway, K.E., & Farebrother, W. (2018) Palaeohydrology of lowland rivers in the Murray-Darling Basin, Australia. *Quaternary Science*

Reviews, **200**, 85–105.

Heyng, A.M., Mayr, C., Lücke, A., Striewski, B., Wastegård, S., & Wissel, H. (2012) Environmental changes in northern New Zealand since the Middle Holocene inferred from stable isotope records (δ15N, δ13C) of Lake Pupuke. *Journal of Paleolimnology*, **48**, 351–366.

Heyng, A.M., Mayr, C., Lücke, A., Wissel, H., & Striewski, B. (2014) Late Holocene hydrologic changes in northern New Zealand inferred from stable isotope values of aquatic cellulose in sediments from Lake Pupuke. *Journal of Paleolimnology*, **51**, 485–497.

Huang, Y., Street-Perrott, F.A., Perrott, R.A., Metzger, P., & Eglinton, G. (1999) Glacial-interglacial environmental changes inferred from molecular and compound-specific δ13C analyses of sediments from Sacred Lake, Mt. Kenya. *Geochimica et Cosmochimica Acta*, **63**, 1383–1404.

Huszar, V.L. de M. & Reynolds, C.S. (1997) Phytoplankton periodicity and sequences of dominance in an Amazonian flood-plain lake (Lago Batata , Para, Brazil): responses to gradual environmental change. *Hydrobiologia*, **346**, 169–181.

Jouzel, A.J., Cattani, O., Dreyfus, G., et al. (2007) Orbital and Millennial Antarctic Climate Variability of the Past 800,000 Yeasr. *Science*, **317**, 793–796.

Kaal, J., Schellekens, J., Nierop, K.G.J., Martı´nez Cortizas, A., & Muller, J. (2014) Contribution of organic matter molecular proxies to interpretation of the last 55ka of the Lynch's Crater record (NE Australia). *Palaeogeography, Palaeoclimatology, Palaeoecology*, **414**, 20–31.

van der Kaars, S., Miller, G.H., Turney, C.S.M., Cook, E.J., Nürnberg, D., Schönfeld, J., Kershaw, A.P., & Lehman, S.J. (2017) Humans rather than climate the primary cause of Pleistocene megafaunal extinction in Australia. *Nature Communications*, **8**, 1–6.

Kajikawa, Y., Wang, B., & Yang, J. (2010) A multi-time scale Australian monsoon index. *International Journal of Climatology*, **30**, 1114–1120.

Kalnay, E., Kanamitsu, M., Kistler, R., Collins, W., Deaven, D., Gandin, L., Iredell, M., Jenne, R., & Joseph, D. (1996) The NCEP NCAR 40-Year Reanalysis Project. *Bulletin of the American Meteorological Society*, **77**, 437–472.

Katz, B.J. (2001) Lacustrine basin hydrocarbon exploration - Current thoughts. *Journal of Paleolimnology*, **26**, 161–179.

Kemp, C.W., Tibby, J., Arnold, L.J., & Barr, C. (2019) Australian hydroclimate during Marine Isotope Stage 3: A synthesis and review. *Quaternary Science Reviews*, **204**, 94–104.

Kershaw, A.P., Bretherton, S.C., & van der Kaars, S. (2007a) A complete pollen record of the last 230 ka from Lynch's Crater, north-eastern Australia. *Palaeogeography, Palaeoclimatology, Palaeoecology*, **251**, 23–45.

Kershaw, A.P., McKenzie, G.M., Porch, N., Roberts, R.G., Brown, J., Heijnis, H., & Orr, M.. (2007b) A high-resolution record of vegetation and climate through the last glacial cycle from Caledonia Fen, southeastern highlands of Australia. *Journal of Quaternary Science*, **22**, 801–815.

Klingaman, N.P., Woolnough, S.J., & Syktus, J. (2013) On the drivers of inter-annual and decadal rainfall variability in Queensland, Australia. *International Journal of Climatology*, **33**, 2413–2430.

De Kluijver, A., Schoon, P.L., Downing, J.A., Schouten, S., & Middelburg, J.J. (2014) Stable carbon isotope biogeochemistry of lakes along a trophic gradient. *Biogeosciences*, **11**, 6265–6276.

Laepple, T., Werner, M., & Lohmann, G. (2011) Synchronicity of Antarctic temperatures and local solar insolation on orbital timescales. *Nature*, **471**, 91–94.

Laws, E.A., Popp, B.N., Bidigare, R.R., Kennicutt, M.C., & Macko, S.A. (1995) Dependence of phytoplankton carbon isotopic composition on growth rate and [CO2)aq: Theoretical considerations and experimental results. *Geochimica et Cosmochimica Acta*, **59**, 1131–1138.

Leach, L.M. (2011) Hydrological and physical setting of North Stradbroke Island. *Proceedings of the Royal Society of Queensland*, **117**, 21–46.

Leng, M.J. (2006) *Isotopes in Palaeoenvironmental Research.* Kluwer Academic Publishers, Dordrecht.

Leng, M.J. & Marshall, J.D. (2004) Palaeoclimate interpretation of stable isotope data from lake sediment archives. *Quaternary Science Reviews*, **23**, 811–831.

Lewis, R., Tibby, J., Arnold, L.J., Gadd, P.S., Marshall, J.C., Barr, C., & Yokoyama, Y. (Accepted) Bayesian deposition model of the Welsby Lagoon sediment sequence. *Quaternary Science Reviews*.

Longmore, M.E. & Heijnis, H. (1999) Aridity in Australia: Pleistocene records of palaeohydrological and palaeoecological change from the perched lake sediments of Fraser Island, Queensland, Australia. *Quaternary International*, **57/58**, 35–47.

Lopes dos Santos, R.A., De Deckker, P., Hopmans, E.C., Magee, J.W., Mets, A., Sinninghe Damsté, J.S., & Schouten, S. (2013) Abrupt vegetation change after the Late Quaternary megafaunal extinction in southeastern Australia. *Nature Geoscience*, **6**, 627–631.

Lücke, A. & Brauer, A. (2004) Biogeochemical and micro-facial fingerprints of ecosystem response to rapid Late Glacial climatic changes in varved sediments of Meerfelder Maar (Germany). *Palaeogeography, Palaeoclimatology, Palaeoecology*, **211**, 139–155.

Lüthi, D., Le Floch, M., Bereiter, B., Blunier, T., Barnola, J.M., Siegenthaler, U., Raynaud, D., Jouzel, J., Fischer, H., Kawamura, K., & Stocker, T.F. (2008) High-resolution carbon dioxide concentration record 650,000-800,000 years before present. *Nature*, **453**, 379–382.

Maxwell, J.R., Douglas, A.G., Eglinton, G., & McCormick, A. (1968) The Botryococcenes-hydrocarbons of novel structure from the alga Botryococcus braunii, Kützing. *Phytochemistry*, **7**, 2157–2171.

McGee, D., Donohoe, A., Marshall, J., & Ferreira, D. (2014) Changes in ITCZ location and cross-equatorial heat transport at the Last Glacial Maximum, Heinrich Stadial 1, and the mid-Holocene. *Earth and Planetary Science Letters*, **390**, 69–79.

McGee, D., Moreno-Chamarro, E., Green, B., Marshall, J., Galbraith, E., & Bradtmiller, L. (2018) Hemispherically asymmetric trade wind changes as signatures of past ITCZ shifts. *Quaternary Science Reviews*, **180**, 214–228.

Metzger, P. & Largeau, C. (2005) Botryococcus braunii: A rich source for hydrocarbons and related ether lipids. *Applied Microbiology and Biotechnology*, **66**, 486–496.

Meyers, P. a (2003) Application of organic geochemistry to paleolimnological reconstruction: a summary of examples from the Laurention Great Lakes. *Organic Geochemistry*, **34**, 261–289.

Meyers, P.A. (1994) Preservation of elemental and isotopic source identification of sedimentary organic matter. *Chemical Geology*, **114**, 289–302.

Meyers, P.A. & Ishiwatari, R. (1993) Lacustrine organic geochemistry—an overview of indicators of organic matter sources and diagenesis in lake sediments. *Organic Geochemistry*, **20**, 867–900.

Meyers, P.A. & Lallier-Vergés, E. (1999) Lacustrine sedimentary organic matter records of Late Quaternary paleoclimates. *Journal of Paleolimnology*, **21**, 345–372.

Meyers, P.A. & Teranes, J.L. (2001) Sediment Organic Matter. *Tracking Environmental Change Using Lake Sediments: Physical and Geochemical Methods* (ed. by W.M. Last and J.P. Smol), pp. 239–269. Springer Netherlands, Dordrecht.

Mooney, S.D., Harrison, S.P., Bartlein, P.J., Daniau, A.L., Stevenson, J., Brownlie, K.C., Buckman, S., Cupper, M., Luly, J., Black, M., Colhoun, E., D'Costa, D., Dodson, J., Haberle, S., Hope, G.S., Kershaw, P., Kenyon, C., McKenzie, M., & Williams, N. (2011) Late Quaternary fire regimes of Australasia. *Quaternary Science Reviews*, **30**, 28–46.

Moss, P.T. & Kershaw, A.P. (2000) The last glacial cycle from the humid tropics of northeastern Australia: Comparison of a terrestrial and a marine record. *Palaeogeography, Palaeoclimatology, Palaeoecology*, **155**, 155–176.

Mueller, D., Jacobs, Z., Cohen, T.J., Price, D.M., Reinfelds, I. V., & Shulmeister, J. (2018) Revisiting an

arid LGM using fluvial archives: a luminescence chronology for palaeochannels of the Murrumbidgee River, south-eastern Australia. *Journal of Quaternary Science*, .

Muller, J., Kylander, M., Wüst, R.A.J., Weiss, D., Martinez-Cortizas, A., LeGrande, A.N., Jennerjahn, T., Behling, H., Anderson, W.T., & Jacobson, G. (2008) Possible evidence for wet Heinrich phases in tropical NE Australia: the Lynch's Crater deposit. *Quaternary Science Reviews*, **27**, 468–475.

Munteanu, C., Negrea, C., Echim, M., & Mursula, K. (2016) Effect of data gaps: Comparison of different spectral analysis methods. *Annales Geophysicae*, **34**, 437–449.

Murphy, B.F. & Timbal, B. (2008) A review of recent climate variability and climate change in southeastern Australia. *International Journal of Climatology*, **28**, 859–879.

Murphy, B.P., Williamson, G.J., & Bowman, D.M.J.S. (2012) Did central Australian megafaunal extinction coincide with abrupt ecosystem collapse or gradual climate change? *Global Ecology and Biogeography*, **21**, 142–151.

Myrbo, A. (2012) Carbon cycle in lakes. *Encyclopedia of lakes and reservoirs* (ed. by L. Bengtsson, R.W. Herschy, and R.W. Fairbridge), pp. 121–175. Springer,

Peterson, L.C., Haug, G.H., & Hughen, K.A. (2007) Tropical Atlantic During the Last Glacial Rapid Changes in the Hydrologic Cycle of the Tropical Atlantic During the Last Glacial. *Science (New York, N.Y.)*, **1947**, 1947–1952.

Petherick, L.M., McGowan, H.A., & Kamber, B.S. (2009) Reconstructing transport pathways for late Quaternary dust from eastern Australia using the composition of trace elements of long traveled dusts. *Geomorphology*, **105**, 67–79.

Petit, J.R., Raynaud, D., Basile, I., Chappellaz, J., Ritz, C., Delmotte, M., Legrand, M., Lorius, C., Jouzel, J., Barkov, N.I., Barnola, J.-M., Bender, M., Davis, M., Delaygue, G., Kotlyakov, V.M., Lipenkov, V.Y., Pepin, L., Saltzman, E., & Stievenard, M. (1999) Climate and atmospheric history of the past 420,000 years from the Vostok ice core, Antarctica. *Nature*, **399**, 429–413.

Prokopenko, A.A., Williams, D.F., Karabanov, E.B., & Khursevich, G.K. (1999) Response of Lake Baikal ecosystem to climate forcing and pCO2 change over the last glacial/interglacial transition. *Earth and Planetary Science Letters*, **172**, 239–253.

Pye, K. (1993) Late Quaternary development of coastal parabolic megadune complexes in northeastern Australia. *Aeolian sediments : Ancient and modern* (ed. by K. Pye and N. Lancaster), pp. 167. Blackwell Scientific Publications,

R Core Team (2017) R: A Language and Environment for Statistical Computing. *R Foundation for Statistical Computing, Vienna, Austria*, **0**, {ISBN} 3-900051-07-0.

Risbey, J.S., Pook, M.J., McIntosh, P.C., Wheeler, M.C., & Hendon, H.H. (2009) On the Remote Drivers of Rainfall Variability in Australia. *Monthly Weather Review*, **137**, 3233–3253.

Roberts, R.G., Flannery, T.F., Ayliffe, L.K., Yoshida, H., Olley, J.M., Prideaux, G.J., Laslett, G.M., Baynes, A., Smith, M.A., Jones, R., & Smith, B.L. (2001) New ages for the last Australian megafauna: continent-wide extinction about 46,000 years ago. *Science (New York, N.Y.)*, **292**, 1888–1892.

Rodríguez-Murillo, J.C., Almendros, G., & Knicker, H. (2011) Wetland soil organic matter composition in a Mediterranean semiarid wetland (Las Tablas de Daimiel, Central Spain): Insight into different carbon sequestration pathways. *Organic Geochemistry*, **42**, 762–773.

Rösch, A. & Schmidbauer, H. (2018) WaveletComp: Computational Wavelet Analysis. 1–38.

Ruf, T. (1999) The Lomb-Scargle Periodogram in Biological Rhythm Research: Analysis of Incomplete and Unequally Spaced Time-Series. *Biological Rhythm Research*, **30**, 178–201.

Rule, S., Brook, B.W., Haberle, S.G., Turney, C.S.M., Kershaw, A.P., & Johnson, C.N. (2012) The Aftermath of Megafaunal Extinction: Ecosystem Transformation in Pleistocene Australia. *Science*, **335**, 1483–1486.

Saltré, F., Rodríguez-Rey, M., Brook, B.W., Johnson, C.N., Turney, C.S.M., Alroy, J., Cooper, A., Beeton, N., Bird, M.I., Fordham, D.A., Gillespie, R., Herrando-Pérez, S., Jacobs, Z., Miller, G.H., Nogués-Bravo, D., Prideaux, G.J., Roberts, R.G., & Bradshaw, C.J.A. (2016) Climate change not to blame for late Quaternary megafauna extinctions in Australia. *Nature Communications*, **7**, 1–7.

Sanderman, J., Krull, E., Kuhn, T., Hancock, G., Mcgowan, J., Maddern, T., Fallon, S., & Steven, A. (2015) Deciphering sedimentary organic matter sources: Insights from radiocarbon measurements and NMR spectroscopy. *Limnology and Oceanography*, **60**, 739–753.

De Senerpont Domis, L.N., Elser, J.J., Gsell, A.S., Huszar, V.L.M., Ibelings, B.W., Jeppesen, E., Kosten, S., Mooij, W.M., Roland, F., Sommer, U., Van Donk, E., Winder, M., & Lürling, M. (2013) Plankton dynamics under different climatic conditions in space and time. *Freshwater Biology*, **58**, 463–482.

Sobek, S., Tranvik, L.J., & Cole, J.J. (2005) Temperature independence of carbon dioxide supersaturation in global lakes. *Global Biogeochemical Cycles*, **19**, 1–10.

Stephens, T., Atkin, D., Augustinus, P., Shane, P., Lorrey, A., Street-Perrott, A., Nilsson, A., & Snowball, I. (2012) A late glacial Antarctic climate teleconnection and variable Holocene seasonality at Lake Pupuke, Auckland, New Zealand. *Journal of Paleolimnology*, **48**, 785–800.

Street-Perrott, F.A., Ficken, K.J., Huang, Y., & Eglinton, G. (2004) Late Quaternary changes in carbon cycling on Mt. Kenya, East Africa: An overview of the δ13C record in lacustrine organic matter. *Quaternary Science Reviews*, **23**, 861–879.

Street-Perrott, F.A., Holmes, J.A., Robertson, I., Ficken, K.J., Koff, T., Loader, N.J., Marshall, J.D., & Martma, T. (2018) The Holocene isotopic record of aquatic cellulose from Lake Äntu Sinijärv, Estonia: Influence of changing climate and organic-matter sources. *Quaternary Science Reviews*, **193**, 68–83.

Street-Perrott, F.A., Huang, Y., Perrott, R.A., Eglinton, G., Barker, P.A., Khelifa, L.B., Harkness, D.D., & Olga, D.O. (1997) Impact of Lower Atmospheric Carbon Dioxide on Tropical. *Science*, **278**, 1422–1426.

Talbot, M.R. & Lærdal, T. (2000) The Late Pleistocene - Holocene palaeolimnology of Lake Victoria, East Africa, based upon elemental and isotopic analyses of sedimentary organic matter. *Journal of Paleolimnology*, **23**, 141–164.

Timmermann, A., Timm, O., Stott, L., & Menviel, L. (2009) The roles of CO2 and orbital forcing in driving Southern Hemispheric temperature variations during the last 21 000 Yr. *Journal of Climate*, **22**, 1626–1640.

Tobler, R., Rohrlach, A., Soubrier, J., et al. (2017) Aboriginal mitogenomes reveal 50,000 years of regionalism in Australia. *Nature*, **544**, 180–184.

Turney, C.S.M., Jones, R.T., Phipps, S.J., et al. (2017) Rapid global ocean-atmosphere response to Southern Ocean freshening during the last glacial. *Nature Communications*, **8**, 520.

Turney, C.S.M., Kershaw, a P., Clemens, S.C., Branch, N., Moss, P.T., & Fifield, L.K. (2004) Millennial and orbital variations of El Niño/Southern Oscillation and high-latitude climate in the last glacial period. *Nature*, **428**, 306–10.

Tyler, J.J., Barr, C., Tibby, J., Hoffmann, H., Marshall, J.C., Shultz, C., & Mcgregor, G.B. Subtropical wetland isotope hydrological responses to climate: a case study on North Stradbroke Island, Queensland, Australia. *Journal of Hydrogeology*, .

Tyson, R. V (1995) *Sedimentary Organic Matter.* Springer Netherlands, Dordrecht.

Ummenhofer, C.C., Gupta, A. Sen, Briggs, P.R., England, M.H., McIntosh, P.C., Meyers, G.A., Pook, M.J., Raupach, M.R., & Risbey, J.S. (2011) Indian and Pacific Ocean influences on southeast Australian drought and soil moisture. *Journal of Climate*, **24**, 1313–1336.

Veres, D., Bazin, L., Landais, A., Toyé Mahamadou Kele, H., Lemieux-Dudon, B., Parrenin, F., Martinerie, P., Blayo, E., Blunier, T., Capron, E., Chappellaz, J., Rasmussen, S.O., Severi, M.,

Svensson, A., Vinther, B., & Wolff, E.W. (2013) The Antarctic ice core chronology (AICC2012): An optimized multi-parameter and multi-site dating approach for the last 120 thousand years. *Climate of the Past*, **9**, 1733–1748.

WAIS Members, Buizert, C., Adrian, B., et al. (2015) Precise interpolar phasing of abrupt climate change during the last ice age. *Nature*, **520**, 661–665.

Wang, X., Auler, A.S., Edwards, R.L., Cheng, H., Ito, E., Wang, Y., Kong, X., & Solheid, M. (2007) Millennial-scale precipitation changes in southern Brazil over the past 90,000 years. *Geophysical Research Letters*, **34**, 1–5.

Wang, Y.J., Cheng, H., Edwards, R.L., An, Z.S., Wu, J.Y., Shen, C.-C., & Dorale, J.A. (2001) A High-Resolution Absolute-Dated Late Pleistocene Monsoon Record from Hulu Cave, China. *Science*, **294**, 2345–2348.

Widayat, A.H., van de Schootbrugge, B., Oschmann, W., Anggayana, K., & Püttmann, W. (2016) Climatic control on primary productivity changes during development of the Late Eocene Kiliran Jao lake, Central Sumatra Basin, Indonesia. *International Journal of Coal Geology*, **165**, 133–141.

Winder, M., Berger, S.A., Lewandowska, A., Aberle, N., Lengfellner, K., Sommer, U., & Diehl, S. (2012) Spring phenological responses of marine and freshwater plankton to changing temperature and light conditions. *Marine Biology*, **159**, 2491–2501.

Wolfe, B.B., Falcone, M.D., Clogg-Wright, K.P., Mongeon, C.L., Yi, Y., Brock, B.E., Amour, N.A.S., Mark, W.A., & Edwards, T.W.D. (2007) Progress in isotope paleohydrology using lake sediment cellulose. *Journal of Paleolimnology*, **37**, 221–231.

Woodward, C.A., Potito, A.P., & Beilman, D.W. (2012) Carbon and nitrogen stable isotope ratios in surface sediments from lakes of western Ireland: Implications for inferring past lake productivity and nitrogen loading. *Journal of Paleolimnology*, **47**, 167–184.

6 Supplementary Information

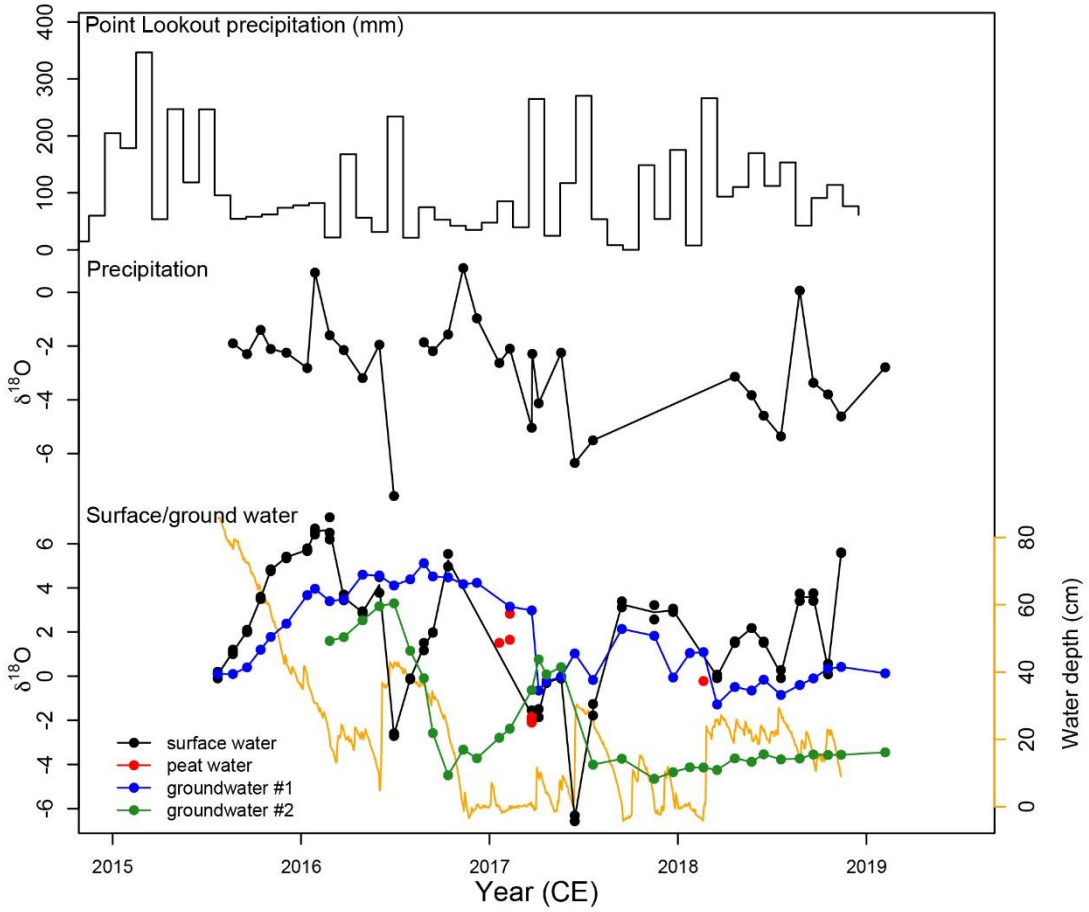

Figure S1. Modern monitoring data from North Stradbroke Island from Tyler et al. (in prep). Top: Monthly precipitation from Point Lookout (NSI), Middle: d18O of precipitation from Point Lookout, Bottom: d18O of surface, peat and groundwater from Welsby Lagoon.

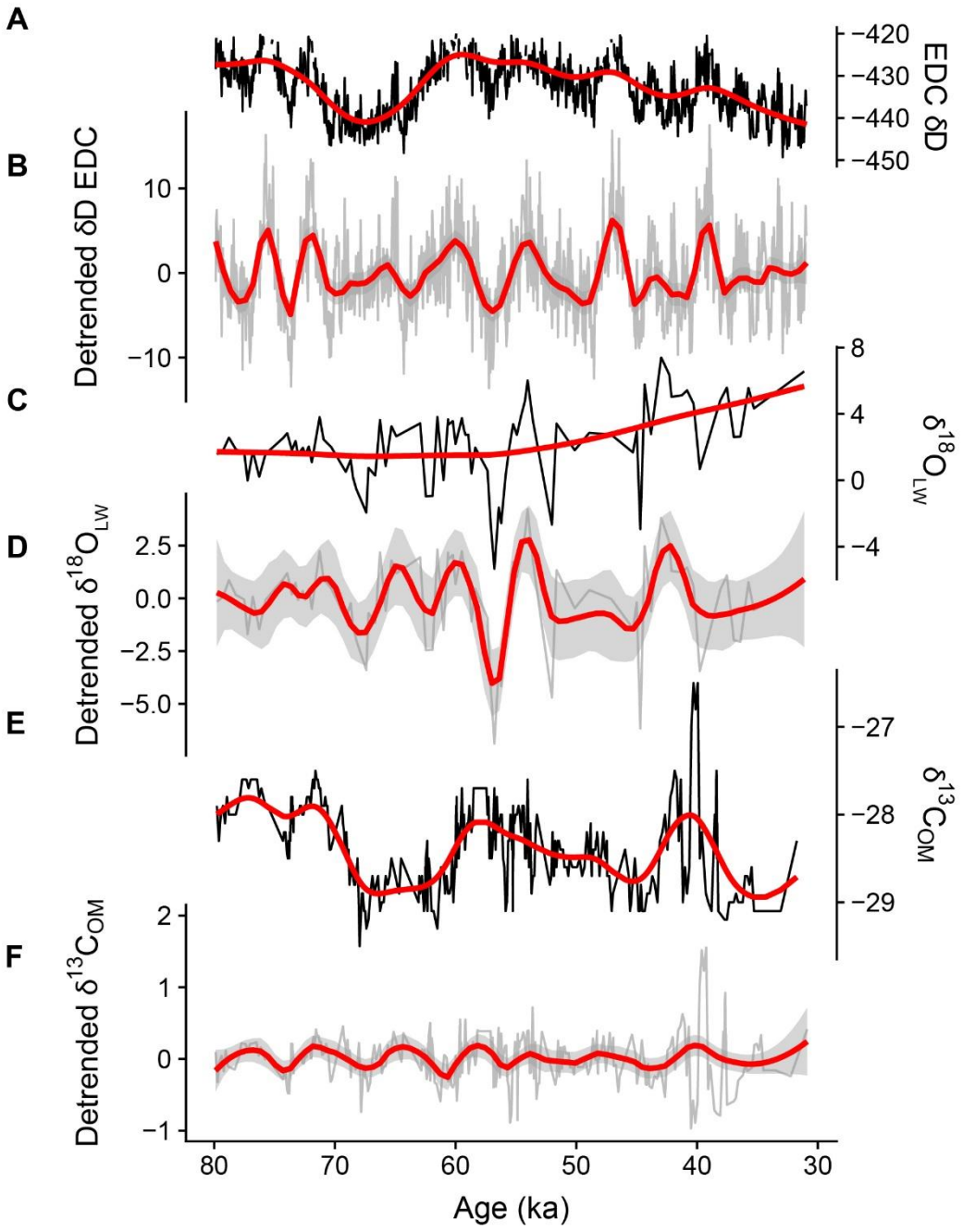

Figure S2. A. EPICA Dome C (EDC) δD, B. Detrended EDC δD, C. Inferred oxygen isotope composition of lake water ($\delta^{18}O_{LW}$) from Welsby Lagoon. D. Detrended $\delta^{18}O_{LW}$, E. Carbon isotope composition ($\delta^{13}C$) of bulk organic matter (OM) from Welsby Lagoon, D. Detrended $\delta^{13}C_{OM}$ Datasets were detrended to highlight the millennial scale variability in each record. Smooth splines (red lines) were fitted to detrended data sets to highlight the millennial scale trends in each dataset. Lower (higher) δD values represent periods of greater (lower) Antarctic ice volume and cooler (warmer) temperatures. Lower (higher) $\delta^{18}O_{LW}$ represent reduced (increased) evaporative conditions Lower (higher) $\delta^{13}C_{OM}$ values represent lower (higher) productivity at Welsby Lagoon. EDC δD is plotted using the AIC2012 chronology $\delta^{18}O$ and $\delta^{13}C$ chronology from Lewis et al. (Accepted).

Statement of Authorship

Title of Paper	Climatic changes proceed ecosystem change and megafauna extinction in Australia
Publication Status	☐ Published ☐ Accepted for Publication ☐ Submitted for Publication ☑ Unpublished and Unsubmitted w ork w ritten in manuscript style
Publication Details	Cadd, H.R., Tibby, J, Tyler, J., Barr, C., Climatic changes proceed ecosystem change and megafauna extinction in Australia

Principal Author

Name of Principal Author (Candidate)	Haidee Cadd		
Contribution to the Paper	Conceptualisation of the work, development of ideas and conclusions, carried out analytical work, carried out statistical analysis, interpretation of the data, wrote manuscript.		
Overall percentage (%)	90		
Certification:	This paper reports on original research I conducted during the period of my Higher Degree by Research candidature and is not subject to any obligations or contractual agreements with a third party that would constrain its inclusion in this thesis. I am the primary author of this paper.		
Signature		Date	29/09/19

Co-Author Contributions

By signing the Statement of Authorship, each author certifies that:

i. the candidate's stated contribution to the publication is accurate (as detailed above);
ii. permission is granted for the candidate in include the publication in the thesis; and
iii. the sum of all co-author contributions is equal to 100% less the candidate's stated contribution.

Name of Co-Author	John Tibby		
Contribution to the Paper	Provided conceptual and interpretation guidance, edited manuscript		
Signature		Date	12/09/19

Name of Co-Author	Jonathan Tyler		
Contribution to the Paper	Provided conceptual and interpretation guidance, edited manuscript		
Signature		Date	28/09/19

Name of Co-Author	Cameron Barr		
Contribution to the Paper	Provided conceptual and interpretation guidance, edited manuscript		
Signature		Date	12/09/19

6

Climatic changes proceed ecosystem change and megafauna extinction in Australia

In preparation as:

Cadd, H.R., Tibby, J., Barr, C., Tyler, J., In Prep. Climatic changes proceed ecosystem change and megafauna extinction in Australia. *Geology*

Abstract

The cause(s) of the extinction of Australia's megafauna is a highly contested topic. Recently, much of the evidence presented has been interpreted to indicate that Australia's megafauna were extirpated by humans shortly after their arrival. However, this evidence is often confounded by a variety of factors. Here we present, for the first time at a single location, Welsby Lagoon, records of inferred megafauna presence, local fire occurrence, vegetation change and climate variability. The largest changes in the Welsby Lagoon record occur between 55 – 40 ka, coincident with the timing of human arrival and megafauna extinction. A carbon and oxygen isotope based climate reconstruction indicates that the major vegetation shifts occurring at ca. 55 and 44 ka were driven by changes in hydroclimate and a shift to increasingly drier climates. A decline in the abundance of *Sporormiella* spores – a proxy for the presence of megafauna - occurred after a change in vegetation, directly following the largest drying event at the site. We compare the record from Welsby Lagoon with palaeoecological and palaeoclimate records from a variety of ecosystems across the Australian continent to examine the extent to which the changes at Welsby Lagoon were synchronous with similarly abrupt changes at other Australian sites. Within chronological uncertainty, the vegetation and hydrological changes at Welsby Lagoon at ca. 44 ka coincide with changes in the Darling River region and central Australia as well as five vegetation records from across the central and eastern regions of Australia. These data suggest that a ubiquitous climatic change was major contributor to megafauna and vegetation change during Marine Isotope Stage 3, at least several thousand years after the first arrival of humans in Australia.

1 Introduction

In Australia, Marine Isotope Stage 3 (MIS3; 59 – 29 ka) was marked by substantial environmental and cultural change, including the extinction of 21 genera of megafauna – animals greater than 45 kg in weight (Roberts et al., 2001; Barnosky et al., 2004) and the arrival of *Homo Sapiens* (Hamm et al., 2016; Saltré et al., 2016; Clarkson et al., 2017). Hypothesised mechanisms to explain the widespread disappearance of Australia's megafauna include human overkill, fire induced habitat modification and an increasingly inhospitable climate (Miller, 2005; Price & Webb, 2006; Wroe & Field, 2006; Rule et al., 2012; Webb, 2013; Johnson et al., 2016b; Miller et al., 2016b; Saltré et al., 2016; van der Kaars et al., 2017). It has previously been argued that the extinction of Australia's megafauna followed rapidly on the heels of human occupation (Roberts et al., 2001; Miller, 2005; Turney et al., 2008; Gillespie et al., 2012; Brook et al., 2013). However, recent evidence extending the timing of first human arrival (Clarkson et al., 2017) and the late survival of some megafauna species (Jankowski et al., 2016; Westaway et al., 2017) suggests a larger temporal overlap than previously recognized.

Examination of the response of Australian ecosystems to megafauna extinction has

suggested that substantial habitat transformation and an increase in biomass burning occurred as a consequence of mega-herbivore removal (Miller, 2005; Rule et al., 2012; Lopes dos Santos et al., 2013). The removal of mega-herbivore browsers from contemporary ecosystems has been observed to cause an increase in woody biomass abundance due to relaxed herbivory pressure and decreasing mortality of seedling and shrubs from trampling (Maron & Crone, 2006; Bakker et al., 2016; Malhi et al., 2016). Exclusion experiments have demonstrated the influence of megafauna on vegetation communities through edaphic disturbance, herbivory, seed dispersal and fuel load suppression (Bakker et al., 2016).

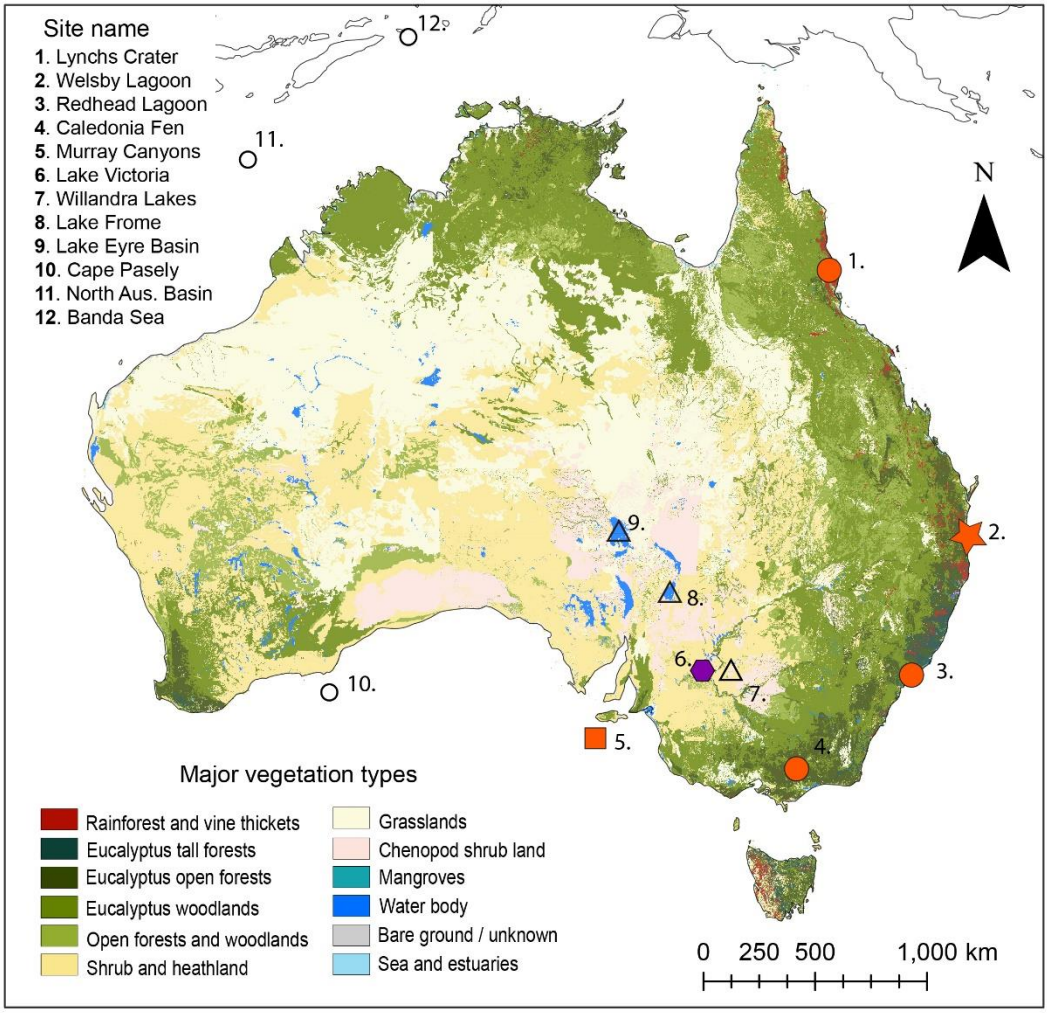

Figure 1. Map of Australia showing location of Welsby Lagoon (star) and sites discussed in text. Map layer shows continental composite of pre-1750 major vegetation types across Australia (NVIS Version 5.1). Differential vegetation surveying results in slight variations in predicted vegetation across states. Open symbols represent sites discussed in text and closed symbols represent sites used in analyses. Symbol shape represents proxy type; pollen (circle), OSL dating of shorelines (triangle), $\delta^{13}C$ leaf wax n-alkanes (square) and $\delta^{18}O$ of *Dromaius* eggshells (octagon). Site numbers on map; 1. Lynchs Crater, 2. Welsby Lagoon, 3. Redhead Lagoon, 4. Caledonia Fen, 5. Murray Canyons core MD03-2607, 6. Lake Victoria, 7. Willandra Lakes, 8. Lake Frome, 9. Lake Eyre Basin, 10. Core MD03-2614G, 11. North Australia Basin core MD98-2167, 12. Banda Sea core SHI-9014

In Australia, shifts in vegetation composition and an increase in fire occurrence have been attributed to the combined influence of human arrival and megafauna extinction, resulting in changes in ecosystem state (Miller, 2005; Rule et al., 2012; Lopes dos Santos et al., 2013). However, there are substantial uncertainties associated with determining the primary cause of vegetation change, due to the multitude and changing nature of potential drivers across diverse ecosystems (Bond & Keeley, 2005; Murphy & Bowman, 2007; Higgins & Scheiter, 2012; Lehmann et al., 2014). The lack of information regarding potential climate changes in association with these shifts restricts the inference of definitive causal relationships. For example, fire occurrence is a product of both incidence of ignition and biomass availability (Bowman et al., 2009). Climate mediates fire occurrence by controlling long term biomass availability, while the presence/absence of 'fire weather' determines the probability of fire on daily to weekly timescales (Bowman et al., 2009). The arrival of modern humans in Australia is hypothesised to have increased the likelihood of fire ignition, however the ability for an ecosystem to carry fire would have been contingent upon proceeding and current climate conditions. Although the relationships are complex, in arid to semi-arid environments, an increase in precipitation is required to create significant connected biomass for burning, whereas in temperate and tropical regions a reduction in precipitation is required to allow usually moist forest to burn (Flannigan et al., 2009; Pausas & Ribeiro, 2013).

Testing causal hypotheses of extinctions in Australia has been hampered by difficulties in establishing the precise sequence of events during the period of human arrival and megafaunal extinction. The paucity of both well-dated fossil sites and palaeoclimate records, that are often both temporally and spatially discrete, hinders elucidation of primary drivers of extinctions. The timing of both human arrival and megafauna extinction at, or beyond, the limit of radiocarbon dating has restricted the ability to obtain robust and comparable chronologies. Inherent uncertainties associated with dating of fossil and palaeoenvironmental records impedes precise cross-site comparisons and identification of drivers.

In wetland sediments, the spores of the coprophilous fungi *Sporormiella* can be used to infer the presence of large animals in the catchment (Davis & Shafer, 2006; Baker et al. 2013). In conjunction with multi-proxy environmental and climate reconstructions from a single sedimentary sequence, this can facilitate direct comparisons between vegetation, fire, climate and megafauna avoiding the challenges of comparing multiple time-uncertain records (Gill et al., 2009; Swift et al., 2019). Understanding how climate has altered faunal abundances and vegetation changes prior to, and following, extinction events is necessary to understand the relative role of climate as a potential extinction driver and the influence of megafauna on ecosystem dynamics. More robust conclusions about the relative role of drivers can be determined if sedimentary sequences are coupled with independent and comprehensive chronologies. Accounting for inherent uncertainties in the dating methods and development of age-depth models can then allow for a more realistic appraisal of synchronicity/non-synchronicity between records.

Here we present, for the first time, an independent climate record coupled with records of vegetation, fire and inferred megafaunal presence underpinned by a robust and independent chronology (Lewis et al., Accepted). We compare pollen and *Sporormiella* abundances, microscopic and macroscopic charcoal concentrations with the $\delta^{13}C$ of bulk sediment and $\delta^{18}O$ of aquatic cellulose (Barr et al. in prep) from a continuous, independently dated sedimentary sequence (Lewis et al., Accepted) from subtropical eastern Australia. Welsby Lagoon is a hydrologically perched, permanent freshwater wetland on North Stradbroke Island (NSI) off the coast from Brisbane, Queensland, Australia. The nature of Welsby Lagoon, isolated from the regional groundwater table by an impermeable perching layer, makes it an ideal location to reconstruct past hydroclimate as the $\delta^{18}O$ of lagoonal waters are sensitive to the local balance between precipitation and evaporation (P/E) (Barr et al. in prep). By combining this oxygen isotope record with evidence for catchment vegetation and fire we are able to independently assess the role of climate in influencing megafauna abundance and regional scale environmental change.

2 Results and discussion

The vegetation record from Welsby Lagoon shows a complex relationship with fire, succession and climate (Chapter 4, this thesis). Declines in rainforest abundance between 80 – 60 ka occurred predominantly in response to fire, driving declines in fire sensitive rainforest species and an increase in disturbance adapted Asteraceae species (Figure 2; Chapter 4, this thesis). Re-establishment of fire sensitive rainforest communities occurred during periods of increased moisture availability and low fire frequency. The high values of macroscopic charcoal and associated changes in vegetation (ca. 71 – 68 ka) occurred independently of a likely human presence, even if the oldest known date of human arrival in northern Australia is adopted (ca. 65 ka, Clarkson et al. 2017).

Macroscopic charcoal abundance is strongly related to biomass availability, which is in turn governed by long-term changes in climate. There is strong relationship between climate driven biomass availability and fire occurrence in subtropical Australia, with higher incidences of fire occurring during dry conditions, preceded by periods of increased rainfall that promote an increase in biomass (Mariani et al., 2019b). Increased fire activity during early MIS3 coincides with a period of wetter climate between ca. 57 – 55 ka (Figure 2). Peaks in macroscopic charcoal at 44 and 40 ka also correspond to minima in $\delta^{18}O_{LW}$, further supporting the inference that fire occurrence is related to the increased availability of biomass, in response to increased precipitation (Figure 2). The Welsby Lagoon sediments therefore suggest that climate variability played an overarching role in controlling fire dynamics, without the need to invoke human agency.

The $\delta^{18}O_{LW}$ record displays substantial fluctuations in water balance between ca. 55 – 40 ka. The increased variation occurs in addition to a distinct long term drying trend (Chapter 5, this thesis). The period of high moisture between 57 – 55 ka is followed by

rapidly drying climate between ca. 55 – 51 ka and a shift to a drier mean climate state. The rapid increase in Poaceae from ca. 54 ka is associated with an 11.35 ‰ increase in the inferred $\delta^{18}O$ of lake water, indicating a major change in hydrology. Low levels of macroscopic charcoal from 52 – 45 ka indicate low fire frequency, however the initial increase in Poaceae pollen was marked by a peak in fire activity (Chapter 4, this thesis). This event may have paved the way for the increase in Poaceae by opening the canopy vegetation, giving opportunistic Poaceae species a competitive advantage through their ability to survive dryer conditions. The dominance of Poaceae continued until 49 ka, after which point it began to decline. The protracted decline in Poaceae was mirrored by an increase in Casuarinaceae (Figure 2). This replacement of Poaceae by Casuarinaceae may indicate a thickening of the woodland canopy in response to a brief increase in moisture availability, as indicated by the $\delta^{18}O_{LW}$. Whilst a brief return to higher moisture conditions may have facilitated the expansion of Casuarinaceae woodlands, the $\delta^{18}O_{LW}$ indicates a further shift to a drier mean climate state from ca. 44 ka.

Sporormiella values at Welsby Lagoon are low throughout the entire record. Low values of *Sporormiella* are likely related to the nature of the Welsby Lagoon wetland and its catchment. The low relief topography and sandy substrates result in limited overland flow and rapid infiltration of precipitation, likely reducing transport of spores to the wetland. Furthermore, the location of the core from the centre of the large, shallow wetland potentially restricted sediment focusing of spores to the core site, in contrast to other wetland sites (Johnson et al., 2015; Dodson & Field, 2018). Despite the uncertainty of taphonomic processes, including transport and preservation, the continued presence of *Sporormiella* between 75 – 50 ka indicates that megafauna were at least intermittently present locally (Davis & Shafer, 2006). Proportions of *Sporormiella* are highest in the record between 75 – 60 ka, possibly reflecting the largest presence of megafauna populations at the site. Two stepwise reductions in the mean proportion of *Sporormiella* occurred at ca. 60 ka and ca. 50 ka (Figure 2). *Sporormiella* does not exhibit a consistent presence after 50 ka, potentially indicating the extirpation of the local megafauna population at or around this time. However, the relationship between the life cycle, transport and preservation of *Sporormiella* in relation to changing hydrological conditions may suggest that the disappearance of *Sporormiella* could also be related to the shift to drier conditions after 55 ka (Baker et al., 2013; Johnson et al., 2015; Dodson & Field, 2018).

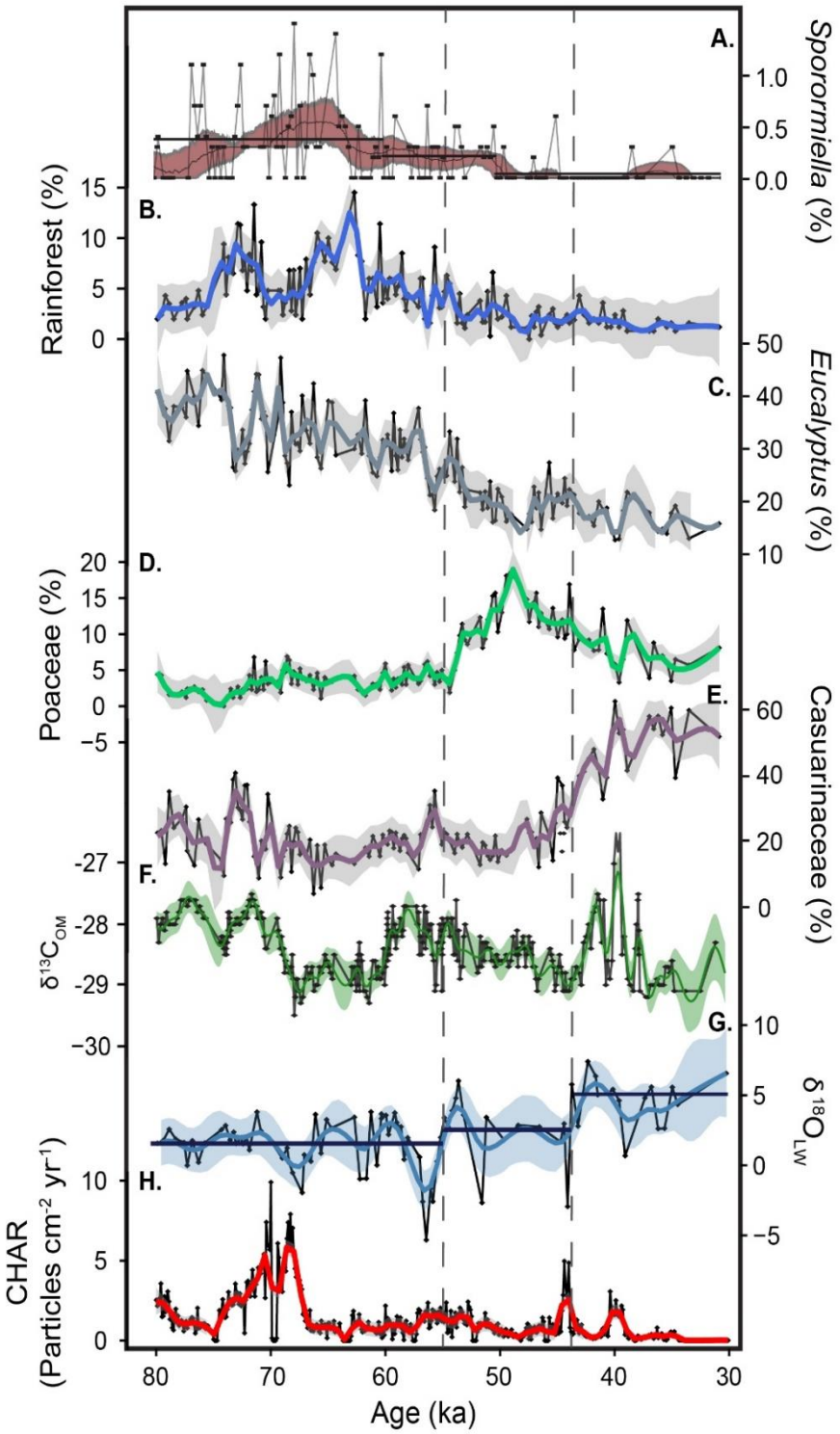

Figure 2. Summary plot of Welsby Lagoon data. *Sporormiella* (%), Rainforest pollen taxa (%), *Eucalyptus* pollen (%), Poaceae pollen (%), Casuarinaceae pollen (%), Inferred lake water $\delta^{18}O$ based on $\delta^{18}O$ of cellulose (Barr et al., in prep) fitted with a generalized additive model (GAM), Macroscopic CHAR (particles $cm^{-2}\,yr^{-1}$). Black lines on pollen and *Sporormiella* data are percentage values and coloured lines are smooth spline (span 0.2). Black line of macroscopic charcoal are charcoal accumulation rates (CHAR; particles $cm^{-2}\,yr^{-1}$) fitted with smooth spline (span 0.05). Horizontal lines on *Sporormiella* and $\delta^{18}O_{LW}$ indicate the timeseries mean between change points, as identified using the *changepoint* package in R (Killick, 2014). Chronology from Lewis et al. (submitted).

Similar changes as those seen at Welsby Lagoon have been observed in other palaeoecological records from across Australia (Figure 1). A compilation was made of all available records spanning a time window from 60 – 30 ka (Figure 3). Seven records were identified with sufficient sample resolution and chronological control to compare vegetation and climate changes across a variety of ecosystem and climate regions (Figure 1). The timing of changes in the dominant vegetation taxon at these seven sites was objectively determined using a Monte-Carlo change point approach (following Tibby et al., 2018). The most abundant single taxon from each pollen record was selected as representative of that record, or in the case of Lynchs Crater, a ratio between the two dominant arboreal vegetation types. For the Murray Canyons record, the stable carbon isotopic composition of higher plant leaf wax *n*-alkanes was used (Lopes dos Santos 2013; Figure 3).

A significant change point was identified in all timeseries at 43 ± 2.3 ka (Figures 3 and 4). At Lynchs Crater in northern Queensland a shift from rainforest to sclerophyllous arboreal taxa and an increase in fire occurred at ~41.2 ka (35.7 – 46.4 ka; 95% Confidence Interval). In the Lake Eyre Basin in central Australia a shift in the diet of *Dromaius* from predominantly C_4 to mixed C_4-C_3 vegetation occurred at ~45.5 ka (39.9 – 49.8 ka; 95% CI) (Miller et al., 2016; Miller, 2005). At Caledonia Fen in the highlands of southern temperate Australia, a decline in the dominant species, Asteraceae, occurs at ~43.6 ka (36.1 – 47.8 ka; 95% CI). At Murray Canyons a transient shift from C_4 dominated to C_3 dominated vegetation within the Murray-Darling catchment occurred at ~42.2 ka (35.7 – 48 ka; 95% CI).

In addition to the timeseries data analysed here, several other records report changes in vegetation composition at approximately the same time. Records from the Banda Sea (van der Kaars et al., 2000) and the North Australian Basin (Kershaw et al., 2011) indicate marked vegetation changes at around 40 ka. Based on a newly developed age model from Redhead Lagoon, Casuarinaceae open woodlands begin to dominate at ~39.5 ka (36.8 – 41.8 ka; 95% CI) before a substantial hiatus beginning at ~37 ka (supplementary information Figure S2; Williams et al., 2006). In south-western Australia no change in vegetation from pollen spectra is indicated in the Cape Pasley marine core at this time, however a decline in *Sporormiella* occurred between 45 – 43.1 ka (van der Kaars et al., 2017). The low resolution nature of Cape Pasley record after ca. 43 ka precludes examining whether a transitional shift in vegetation composition occurred (Lopes dos Santos et al., 2013; van der Kaars et al., 2017). The limited taxonomic resolution of pollen data may obscure changes in vegetation functional types (e.g. within the family Poaceae). The two nearest palaeoecological records to Cape Pasley, Murray Canyons *n*-alkane $\delta^{13}C$ and $\delta^{13}C$ of *Dromaius* eggshells from Port Augusta, indicate a shift in vegetation functional types from C_4 dominated to mixed C_3-C_4 vegetation dominance at this time (Lopes dos Santos et al., 2013; Miller et al., 2016a). It is therefore possible that the decline in *Sporormiella* between 45 – 43.1 ka is associated with a shift in functional vegetation types that is not captured in the pollen spectra.

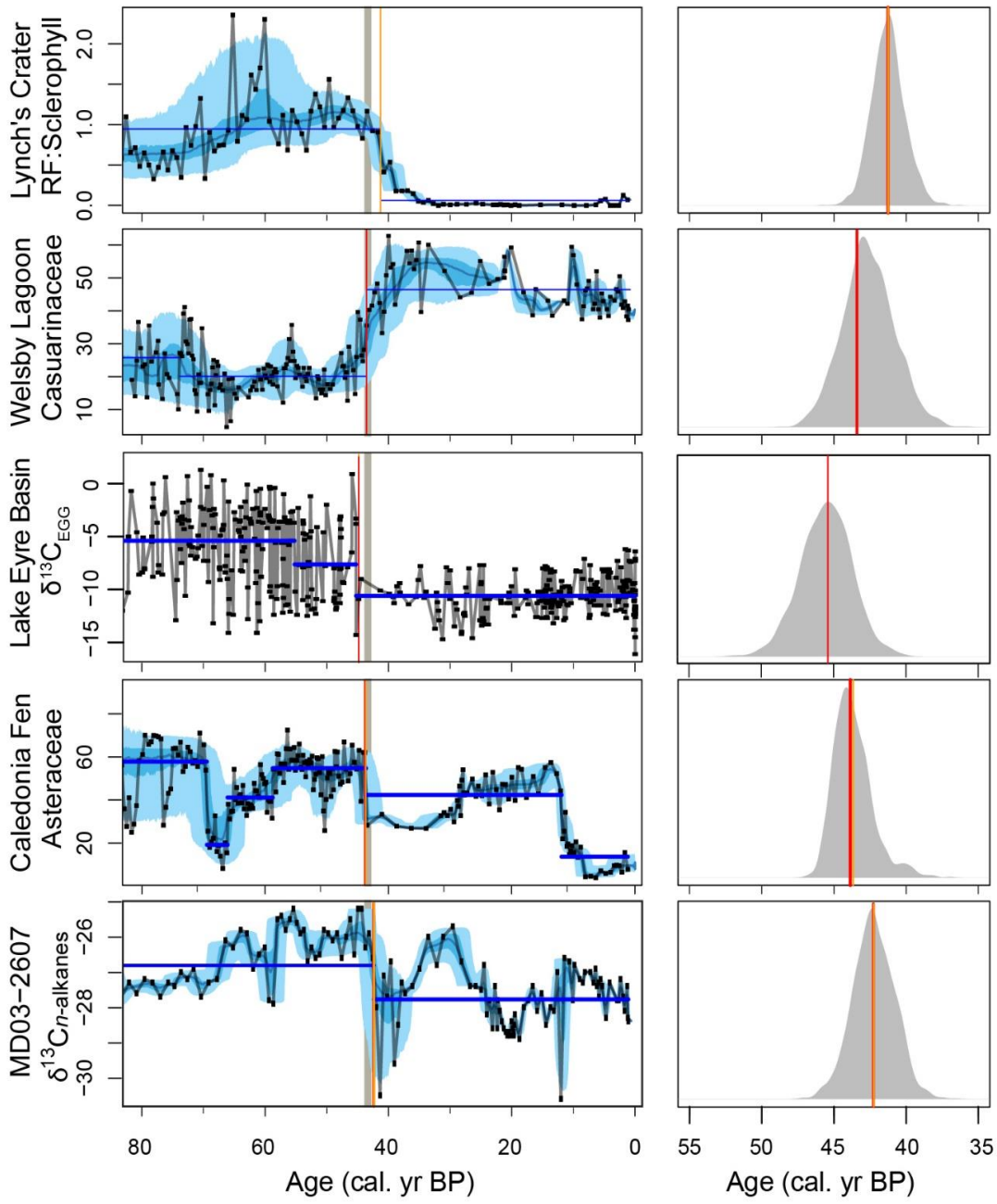

Figure 3. Timeseries analysis of vegetation records from five eastern Australian records: Lynchs Crater (Kershaw et al., 2007a), Welsby Lagoon (Chapter 5, this thesis), Lake Eyre Basin (Miller et al., 2016; Miller, 2005), Caledonia Fen (Kershaw et al., 2007b) and core MD03-2607 (Lopes dos Santos et al., 2013). Left Panel: Light blue shading represents the 95% confidence intervals of the age uncertainty and dark blue shading represents the 68% confidence intervals of the 2000 age model iterations. Black lines are timeseries plotted on the weighted mean of 2000 age model iterations derived from Bacon age models, re-calibrated for all secondary data. Mean age model for Welsby Lagoon from Lewis et al. (submitted), Monte-Carlo age uncertainty iterations from 2000 Bacon age model iterations developed in this study. Horizontal blue lines idicate indicate the mean values of each timeseries between change points. Vertical red lines are the median and orange lines are the weighted mean of the 2000 Monte Carlo iterations of the change points. Vertical grey shaded bars is the mean $\delta^{18}O$ change points identified in figure 4. Right panel: Grey polygons are probability density functions of 2000 age model iterations at change points identified in left panel.

Prior interpretation of records from Lynchs Crater, Murray Canyons and the Lake Eyre Basin have suggested a human-mediated ecosystem shift (Miller, 2005; Rule et al., 2012; Lopes dos Santos et al., 2013; van der Kaars et al., 2017). Human agency, either through direct habitat modification or as a consequence of the extinction of megafauna, has been suggested, while explicitly ruling out the influence of climate (Miller, 2005; van der Kaars et al., 2017). The assertion that anthropogenic influences were the primary driver of the extinction of Australia's megafauna largely hinges on the assumption that there was no widespread, considerable, or persistent climate changes during the hypothesised extinction window (Miller, 2005; Rule et al., 2012; van der Kaars et al., 2017). To date, this argument has been supported by the use of distal climate records and climate models, due to the dearth of regional climate data, which suggest that no marked change in either the mean or variance of climate occurred during the extinction window (Johnson et al., 2016b; Saltré et al., 2016). However, palaeoclimate data from within Australia suggest that this interpretation may not be entirely robust (Cohen et al., 2011, 2015).

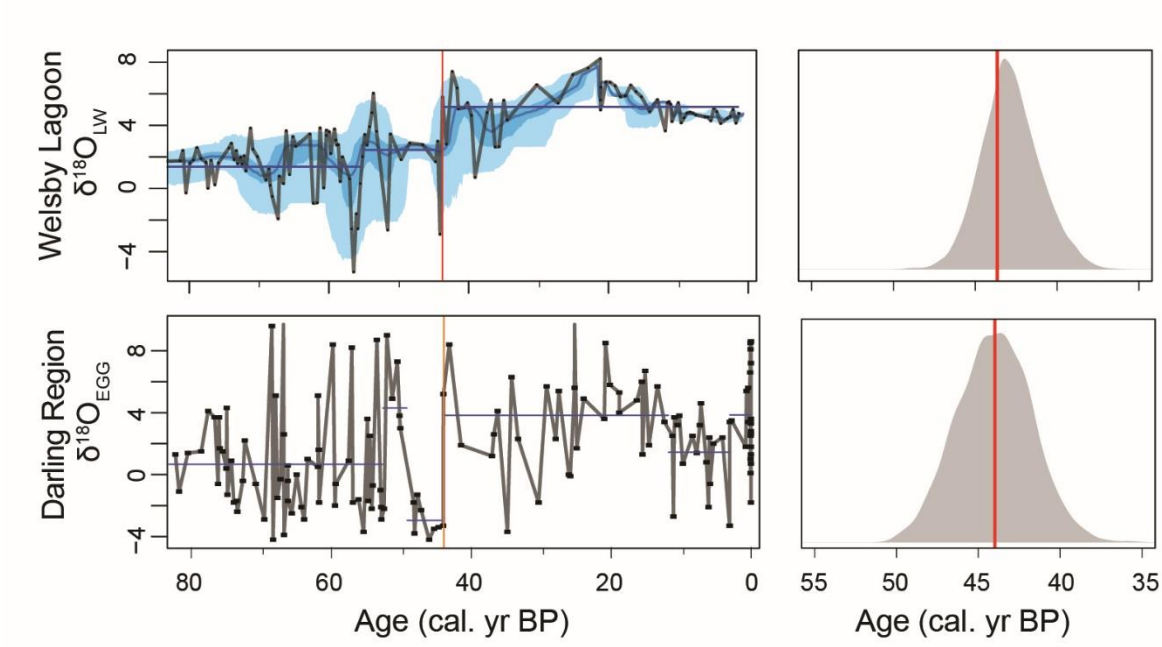

Figure 4. Hydroclimate timeseries from Welsby Lagoon inferred $\delta^{18}O$ of lake water ($\delta^{18}O_{LW}$) and lower Darling River $\delta^{18}O$ *Dromaius* eggshells ($\delta^{18}O_{EGG}$). Left Panel: Light blue shading represents the 95% confidence intervals of the age uncertainty and dark blue shading represents the 68% confidence intervals of the 2000 age iterations for the Welsby Lagoon $\delta^{18}O_{LW}$. Mean age model for Welsby Lagoon from Lewis et al. (Accepted), Monte-Carlo age uncertainty iterations from 2000 Bacon age model iterations developed in this study. Darling Region *Dromaius* timeseries plotted on the age-depth model of Miller et al. (2016a). Horizontal blue lines idicate indicate the mean values of each timeseries between change points. Vertical red lines are the mean change points for each record. Right panel: Grey polygon for Welsby Lagoon is probability density functions of 2000 age model iterations at change point identified in left panel. Grey polygon for *Dromaius* is a caluclated normal distribution using change point mean and reported errors in Miller et al. (2016a).

In addition to the oxygen isotope record from Welsby Lagoon, geomorphology and oxygen isotope data from inland arid Australia tentatively support the observation of substantial

climatic change coincident with the extinction of the Australian megafauna (Cohen et al., 2011, 2015; Miller et al. 2016a). The $\delta^{18}O$ of *Dromaius* eggshells ($\delta^{18}O_{EGG}$) from the lower Darling River region in southwest NSW displays similar patterns to the $\delta^{18}O_{LW}$ of Welsby Lagoon (Figure 4). A shift in the mean $\delta^{18}O$ to higher values, indicative of more evaporative conditions, occurred at both Welsby Lagoon and the Darling River region at 55.2 ka and 55.3 ka, respectively. In the Darling River region this was followed by a 4 ka period of negative $\delta^{18}O$ values between ca. 48 – 44 ka. Although this period of negative $\delta^{18}O_{EGG}$ values may indicate a phase of more amenable conditions, it was followed by a shift to considerably more enriched $\delta^{18}O_{EGG}$ at 43.9 ka. This change is again coincident with an additional shift to drier conditions at Welsby Lagoon at 43.7 ka. A shift in regional hydrology between 45 – 40 ka is further supported by climate reconstructions from the Willandra Lakes (Bowler et al., 2003). Moreover, Cohen et al. (2015, 2011) demonstrate a similar shift to drier climates occurred within the Lake Eyre Basin, which entered a major drying phase at 48±2 ka. *Dromaius* eggshell $\delta^{18}O$ from the Lake Eyre Basin and Lake Frome during this period are too few to draw confident conclusions of a potential change in hydrology, however the $\delta^{18}O_{EGG}$ that have been analysed from these sites and dated between 45 – 40 ka (n=6) all display $\delta^{18}O$ values indicative of evaporative conditions (mean=8±3.5‰; supplementary figure S2).

The new record from Welsby Lagoon, in addition to the revised analysis of the timing of major environmental changes in published records, facilitates a new perspective on the causes of megafauna extinction in Australia. Human predation of megafauna cannot be discounted, and in fact, is implied by the deliberate burning of *Genyornis* and *Dromaius* eggshells (Miller et al., 2016). However, evidence of substantial human predation leading to the extinction of the megafauna or precipitating ecosystem collapse is lacking. The extended overlap between the timing of human occupation and the extinction of megafauna makes a concurrent extinction 'event' at ca. 43 ka on a pan Australian scale unlikely (Figure 5). If human agency was the sole driver, patterns of megafauna extinctions and ecosystem change would be expected to follow a geographic gradient as humans migrated across the continent (Hamm et al., 2016; Tobler et al., 2017). The change point analysis presented here demonstrates no evidence of systematic geographic patterns suggests that ecosystems across all regions changed within a window 43.7 – 39.5 ka and when factoring age uncertainty in each record, with no significant difference in timing between sites. While we cannot discount the potential impact of humans in hastening localised extinctions and driving shifts in vegetation, it is unlikely that humans can be invoked as the sole driver. The presence of humans may have introduced additional pressures on megafauna populations that reduced their resilience to increasingly arid climates, contributing to their final demise.

The coincident timing of ecosystem changes across the continent, in conjunction with the extinction of megafauna is perhaps better explained by a shift in the climate system. Welsby Lagoon provides evidence of major vegetation transitions coincident with changes in local hydroclimate at 43 ka (Figure 2). Whilst we are unable to definitively assign

climate as the primary driver of the coeval vegetation changes seen throughout the continent, the concurrent timing suggests that climate is likely to have played a significant role (Figure 3, 4, 5). Cohen et al. (2015) suggested that the catastrophic drying of the Lake Eyre Basin was caused by a weakening of the Indo-Australian monsoon. Evidence for a coincident increase in aridity from Welsby Lagoon and the Murray-Darling basin suggests a potential role of the El Niño Southern Oscillation (ENSO) in amplifying changes in the monsoon and driving increases in aridity across eastern Australia (Barr et al., in prep.; Bowler et al., 2003; Miller and Fogel, 2016). The teleconnection between the Australian monsoon and ENSO results in weakened monsoonal influence during El Niño events (Kajikawa et al., 2010; Jourdain et al., 2013). We tentatively suggest that an increase in the strength or persistence of the El Niño mode may have led to enhanced drying across eastern Australia (Barr et al., in prep; Bowler et al., 2003) and drove a weakening or reduced continental penetration of the Australian monsoon, resulting in the dry conditions evident within the Lake Eyre Basin after 48 ka (Cohen et al., 2011, 2015a).

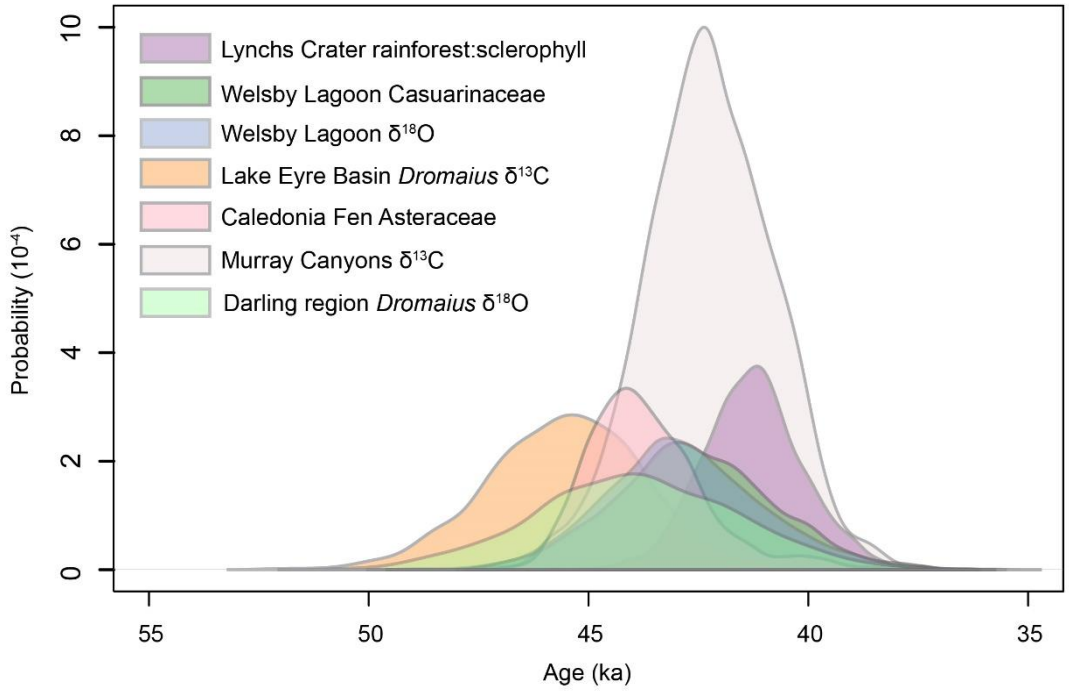

Figure 5 .Probability density functions of change points identified from Lynchs Crater rainforest: sclerophyll ratio, Welsby Lagoon Casuarinaceae and δ18OLW, Redhead Lagoon Casuarinaceae, Caledonia Fen Asteraceae, Murray Canyons n-alkane δ13C and lower Darling River Dromaius δ18OEGG. Age uncertainty for all records, except the Dromaius δ18OEGG, were determined using Bacon (Blaauw and Christen 2011). Age uncertainty for the Dromaius δ18OEGG and Dromaius δ13CEGG is based on the age model uncertainty reported by Miller et al. (2016).

The role of climate contributing to the demise of Australia's megafauna needs to be re-evaluated. The timing of substantial climate change, coincident with the extinction of Australia's megafauna, suggest that rather than a dominant role of humans, climatic

changes played a central role in these extinctions. The initial changes in ecosystems across Australia may have been triggered by changes in climate, but the removal of a suite of important ecosystem engineers may have produced a more long-lasting impact upon these environments. Human mediated pressures on both megafauna populations and habitat modifications may have exacerbated the effects of climate. The combined effect of drying climate conditions, substantial ecosystem changes and human pressure on populations appears to have created an increasingly inhospitable environment for megafauna survival.

3 Methods

Two overlapping 12.5 m cores were extracted from the deepest part of Welsby Lagoon. Sediment samples (0.5 cm^2) were taken approximately every 4 cm for pollen, spore and microscopic charcoal analysis for a total of 198 samples. A total of 250 grains of terrestrial origin form the base pollen sum. *Sporormiella* is expressed as the number of spores / number of Lycopodium grains per sample. Macroscopic charcoal (>125 µm) samples were subsampled every 1 cm along the entire length of the core. Approximately 2 cm^3 was submerged in 5-10% H_2O_2 for 7 days prior to sieving. Charcoal fragments were tallied under a binocular microscope and normalised by dry gram. Time series analysis of the charcoal record was performed in CHARanaylsis. For further information on palynology and charcoal methods used see Chapter 4, this thesis.

Oxygen isotope values of aquatic cellulose was analysed. Further information regarding methods of cellulose extraction and analysis can be found in Chapter 5, this thesis and Barr et al. (in prep). Briefly, $\delta^{18}O$ of lake water in closed basins reflects the balance between precipitation and evaporation (P/E). Aquatic algae that incorporates oxygen from this water therefore mirrors the $\delta^{18}O$ of the lake water ($\delta^{18}O_{LW}$) with a constant offset. More negative $\delta^{18}O_{LW}$ values at Welsby Lagoon indicate an increase in water balance (P/E). More positive $\delta^{18}O_{LW}$ values indicate a decrease in available water balance and decreased (P/E). A generalised additive model (GAM) was fitted to the $\delta^{18}O_{LW}$ data to identify important trends in the timeseries using the mgcv package in R (Wood, 2013). The GAM was fitted using an additive Generalised Cross Validation (GCV.Cp) prediction error criteria (Wood, 2013).

Pollen and geochemical records analysed in this paper met the criteria of at least 40 samples between 60 – 30 ka with at least one independent age control point prior to 45 ka and one after 45 ka (supplementary information Figure S1). Change point analysis was conducted on each record using the changepoint package in R (Killick et al., 2012; Killick, 2014). Where possible (original dates and depths provided by authors) re-calibrated age-depth models were created in Bacon (Blaauw & Christen, 2011). For each timeseries record with available data, an ensemble of 2000 potential palaeoclimate timeseries and associated chronologies were extracted from the re-calibrated Bacon age-depth models (Blaauw & Christen, 2011).

The data from Welsby Lagoon used in this chapter is plotted using the mean age-depth model of Lewis et al. (Accepted), as per chapters 4 and 5 of this thesis. To enable comparison across records and assess the age uncertainty of identified change points, we developed a Bacon age-depth model using the primary data from Lewis et al. (Accepted) to facilitate the extraction of 2000 age model iterations (supplementary information Figure S1).

To identify the probability distribution of the timing of change, each ensemble member for all records was subjected to change point analysis (Killick et al., 2012; Killick, 2014). Multiple significant change points were identified for some records analysed, however a consistent feature of all timeseries was a shift in vegetation or climate proxy at 43 ± 2.3 ka (42.5 ± 3 ka when Redhead Lagoon is included, supplementary information figure S2). A probability density function (pdf) was derived from the ensemble of age iterations for each change point, along with the median and weighted average of the pdf. For records without 2000 ensemble models (*Dromaius* eggshell data), a normal distribution of the mean and standard deviation was calculated for each identified changepoint.

References

Baker, A.G., Bhagwat, S.A., & Willis, K.J. (2013) Do dung fungal spores make a good proxy for past distribution of large herbivores? *Quaternary Science Reviews*, **62**, 21–31.

Bakker, E.S., Gill, J.L., Johnson, C.N., Vera, F.W.M., Sandom, C.J., Asner, G.P., & Svenning, J.-C. (2016) Combining paleo-data and modern exclosure experiments to assess the impact of megafauna extinctions on woody vegetation. *Proceedings of the National Academy of Sciences*, **113**, 847–855.

Barnosky, A.D., Koch, P.L., Feranec, R.S., Wing, S.L., & Shaberl, A.B. (2004) Assessing the Causes of Late Pleistocene Extinctions on the Continents. *Science*, **306**, 70–75.

Barr, C., Cadd, H.R., Tibby, J., Leng, M.J., Tyler, Jonathan J.McInerney, F.A., Henderson, A.C.G., Arnold, L.J., Marshall, J.C., & Mcgregor, G.B. Hydrological change in subtropical Australia from 80 - 40 kyr. .

Blaauw, M. & Christen, J.A. (2011) Flexible paleoclimate age-depth models using an autoregressive gamma process. *Bayesian Analysis*, **6**, 457–474.

Bond, W.J. & Keeley, J.E. (2005) Fire as a global "herbivore": The ecology and evolution of flammable ecosystems. *Trends in Ecology and Evolution*, **20**, 387–394.

Bowler, J.M., Johnston, H., Olley, J.M., Prescott, J.R., Roberts, R.G., Shawcross, W., & Spooner, N.A. (2003) New ages for human occupation and climatic change at Lake Mungo, Australia. *Nature*, **421**, 837–840.

Bowman, D.M.J.S., Balch, J.K., Artaxo, P., et al. (2009) Fire in the Earth System. *Science*, **324**, 481–484.

Brook, B.W., Bradshaw, C.J.A., Cooper, A., Johnson, C.N., Worthy, T.H., Bird, M., Gillespie, R., & Roberts, R.G. (2013) Lack of chronological support for stepwise prehuman extinctions of Australian megafauna. *Proceedings of the National Academy of Sciences*, **110**, 3368–3368.

Clarkson, C., Jacobs, Z., Marwick, B., et al. (2017) Human occupation of northern Australia by 65,000 years ago. *Nature*, **547**, 306–310.

Cohen, T.J., Jansen, J.D., Gliganic, L.A., Larsen, J.R., Nanson, G.C., May, J.-H., Jones, B.G., & Price, D.M. (2015) Hydrological transformation coincided with megafaunal extinction in central Australia. *Geology*, **43**, 195–198.

Cohen, T.J., Nanson, G.C., Jansen, J.D., Jones, B.G., Jacobs, Z., Treble, P., Price, D.M., May, J.H., Smith, A.M., Ayliffe, L.K., & Hellstrom, J.C. (2011) Continental aridification and the vanishing of Australia's megalakes. *Geology*, **39**, 167–170.

Davis, O.K. & Shafer, D.S. (2006) Sporormiella fungal spores, a palynological means of detecting herbivore density. *Palaeogeography, Palaeoclimatology, Palaeoecology*, **237**, 40–50.

Dodson, J. & Field, J.H. (2018) What does the occurrence of Sporormiella (Preussia) spores mean in Australian fossil sequences? *Journal of Quaternary Science*, **33**, 380–392.

Flannigan, M.D., Krawchuk B, M.A., de Groot, W.J., Mike Wotton, B.A., Gowman, L.M., Krawchuk, M.A., de Groot, W.J., Wotton, M., Gowman, L.M., Krawchuk B, M.A., de Groot, W.J., Mike Wotton, B.A., & Gowman, L.M. (2009) Implications of changing climate for global wildland fire. *International Journal of Wildland Fire*, **18**, 483–507.

Gillespie, R., Camens, A.B., Worthy, T.H., Rawlence, N.J., Reid, C., Bertuch, F., Levchenko, V., & Cooper, A. (2012) Man and megafauna in Tasmania : closing the gap. *Quaternary Science Reviews*, **37**, 38–47.

Hamm, G., Mitchell, P., Arnold, L.J., Prideaux, G.J., Questiaux, D., Spooner, N.A., Levchenko, V.A., Foley, E.C., Worthy, T.H., Stephenson, B., Coulthard, V., Coulthard, C., Wilton, S., & Johnston, D. (2016) Cultural innovation and megafauna interaction in the early settlement of arid Australia. *Nature*, **539**, 280–283.

Higgins, S.I. & Scheiter, S. (2012) Atmospheric CO2 forces abrupt vegetation shifts locally, but not globally. *Nature*, **488**, 209–212.

Jankowski, N.R., Gully, G.A., Jacobs, Z., Roberts, R.G., & Prideaux, G.J. (2016) A late Quaternary vertebrate deposit in Kudjal Yolgah Cave, south-western Australia: refining regional late Pleistocene extinctions. *Journal of Quaternary Science*, **31**, 538–550.

Johnson, C.N., Alroy, J., Beeton, N.J., Bird, M.I., Brook, B.W., Cooper, A., Gillespie, R., Herrando-PÉrez, S., Jacobs, Z., Miller, G.H., Prideaux, G.J., Roberts, R.G., Rodríguez-Rey, M., SaltrÉ, F., Turney, C.S.M., & Bradshaw, C.J.A. (2016) What caused extinction of the pleistocene megafauna of sahul? *Proceedings of the Royal Society B: Biological Sciences*, **283**, 1–8.

Johnson, C.N., Rule, S., Haberle, S.G., Turney, C.S.M., Kershaw, A.P., & Brook, B.W. (2015) Using dung fungi to interpret decline and extinction ofmegaherbivores: Problems and solutions. *Quaternary Science Reviews*, **110**, 107–113.

Jourdain, N.C., Gupta, A. Sen, Taschetto, A.S., Ummenhofer, C.C., Moise, A.F., & Ashok, K. (2013) The Indo-Australian monsoon and its relationship to ENSO and IOD in reanalysis data and the CMIP3/CMIP5 simulations. *Climate Dynamics*, **41**, 3073–3102.

van der Kaars, S., Miller, G.H., Turney, C.S.M., Cook, E.J., Nürnberg, D., Schönfeld, J., Kershaw, A.P., & Lehman, S.J. (2017) Humans rather than climate the primary cause of Pleistocene megafaunal extinction in Australia. *Nature Communications*, **8**, 1–6.

Kaars, S. van der, Wang, X., Kershaw, P., Guichard, F., & Setiabudi, D.A. (2000) A Late Quaternary palaeoecological record from the Banda Sea, Indonesia: patterns of vegetation, climate and biomass burning in Indonesia and northern Australia. *Palaeogeography, Palaeoclimatology, Palaeoecology*, **155**, 135–153.

Kajikawa, Y., Wang, B., & Yang, J. (2010) A multi-time scale Australian monsoon index. *International Journal of Climatology*, **30**, 1114–1120.

Kershaw, A.P., Bretherton, S.C., & van der Kaars, S. (2007a) A complete pollen record of the last 230 ka from Lynch's Crater, north-eastern Australia. *Palaeogeography, Palaeoclimatology, Palaeoecology*, **251**, 23–45.

Kershaw, A.P., van der Kaars, S., & Flenley, J.R. (2011) The Quaternary history of far eastern rainforests. *Tropical rainforest responses to climate change* (ed. by M.B. Bush, J.R. Flenley, and W.D. Gosling),

pp. 85–123. Springer-Verlag, Berlin Heidelberg.

Kershaw, A.P., McKenzie, G.M., Porch, N., Roberts, R.G., Brown, J., Heijnis, H., & Orr, M.. (2007b) A high-resolution record of vegetation and climate through the last glacial cycle from Caledonia Fen, southeastern highlands of Australia. *Journal of Quaternary Science*, **22**, 801–815.

Killick, R. (2014) changepoint : An R Package for Changepoint Analysis. *Journal of Statistical Software*, **58**, 1–19.

Killick, R., Fearnhead, P., & Eckley, I.A. (2012) Optimal detection of changepoints with a linear computational cost. *Journal of the American Statistical Association*, **107**, 1590–1598.

Lehmann, C.E.R., Anderson, T.M., Sankaran, M., et al. (2014) Savanna vegetation-fire-climate relationships differ among continents. *Science*, **343**, 548–552.

Lewis, R., Tibby, J., Arnold, L.J., Gadd, P.S., Marshall, J.C., Barr, C., & Yokoyama, Y. (Accepted) Bayesian deposition model of the Welsby Lagoon sediment sequence. *Quaternary Science Reviews*

Lopes dos Santos, R.A., De Deckker, P., Hopmans, E.C., Magee, J.W., Mets, A., Sinninghe Damsté, J.S., & Schouten, S. (2013) Abrupt vegetation change after the Late Quaternary megafaunal extinction in southeastern Australia. *Nature Geoscience*, **6**, 627–631.

Malhi, Y., Doughty, C.E., Galetti, M., Smith, F.A., Svenning, J.-C., & Terborgh, J.W. (2016) Megafauna and ecosystem function from the Pleistocene to the Anthropocene. *Proceedings of the National Academy of Sciences*, **113**, 838–846.

Mariani, M., Tibby, J., Barr, C., Moss, P., Marshall, J.C., & McGregor, G.B. (2019) Reduced rainfall drives biomass limitation of long-term fire activity in Australia's subtropical sclerophyll forests. *Journal of Biogeography*, 1974–1987.

Maron, J.L. & Crone, E. (2006) Herbivory: effects on plant abundance, distribution and population growth. *Proceedings of the Royal Society B: Biological Sciences*, **273**, 2575–2584.

Miller, G.H. (2005) Ecosystem Collapse in Pleistocene Australia and a Human Role in Megafaunal Extinction. *Science*, **309**, 287–290.

Miller, G.H. & Fogel, M.L. (2016) Calibrating δ18O in Dromaius novaehollandiae (emu) eggshell calcite as a paleo-aridity proxy for the Quaternary of Australia. *Geochimica et Cosmochimica Acta*, **193**, 1–13.

Miller, G.H., Fogel, M.L., Magee, J.W., & Gagan, M.K. (2016a) Disentangling the impacts of climate and human colonization on the flora and fauna of the Australian arid zone over the past 100 ka using stable isotopes in avian eggshell. *Quaternary Science Reviews*, **151**, 27–57.

Miller, G.H., Magee, J., Smith, M., Spooner, N., Baynes, A., Lehman, S., Fogel, M., Johnston, H., Williams, D., Clark, P., Florian, C., Holst, R., & DeVogel, S. (2016b) Human predation contributed to the extinction of the Australian megafaunal bird Genyornis newtoni ~47 ka. *Nature Communications*, **7**, 1–7.

Murphy, B.P. & Bowman, D.M.J.S. (2007) Seasonal water availability predicts the relative abundance of C3 and C4 grasses in Australia. *Global Ecology and Biogeography*, **16**, 160–169.

Pausas, J.G. & Ribeiro, E. (2013) The global fire-productivity relationship. *Global Ecology and Biogeography*, **22**, 728–736.

Price, G.J. & Webb, G.E. (2006) Late Pleistocene sedimentology, taphonomy and megafauna extinction on the Darling Downs, southeastern Queensland. *Australian Journal of Earth Sciences*, **53**, 947–970.

Roberts, R.G., Flannery, T.F., Ayliffe, L.K., Yoshida, H., Olley, J.M., Prideaux, G.J., Laslett, G.M., Baynes, A., Smith, M.A., Jones, R., & Smith, B.L. (2001) New ages for the last Australian megafauna: continent-wide extinction about 46,000 years ago. *Science*, **292**, 1888–1892.

Rule, S., Brook, B.W., Haberle, S.G., Turney, C.S.M., Kershaw, A.P., & Johnson, C.N. (2012) The

Aftermath of Megafaunal Extinction: Ecosystem Transformation in Pleistocene Australia. *Science*, **335**, 1483–1486.

Saltré, F., Rodríguez-Rey, M., Brook, B.W., Johnson, C.N., Turney, C.S.M., Alroy, J., Cooper, A., Beeton, N., Bird, M.I., Fordham, D.A., Gillespie, R., Herrando-Pérez, S., Jacobs, Z., Miller, G.H., Nogués-Bravo, D., Prideaux, G.J., Roberts, R.G., & Bradshaw, C.J.A. (2016) Climate change not to blame for late Quaternary megafauna extinctions in Australia. *Nature Communications*, **7**, 1–7.

Tibby, J., Tyler, J.J., & Barr, C. (2018) Post little ice age drying of eastern Australia con fl ates understanding of early settlement impacts. *Quaternary Science Reviews*, **202**, 45–52.

Tobler, R., Rohrlach, A., Soubrier, J., et al. (2017) Aboriginal mitogenomes reveal 50,000 years of regionalism in Australia. *Nature*, **544**, 180–184.

Turney, C.S.M., Flannery, T.F., Roberts, R.G., Reid, C., Fifield, L.K., Higham, T.F.G., Jacobs, Z., Kemp, N., Colhoun, E.A., Kalin, R.M., & Ogle, N. (2008) implicate human involvement in their extinction. .

Webb, S. (2013) Australia's Megafauna Extinction Drivers. *Corridors to Extinction and the Australian Megafauna*, 217–242.

Westaway, M.C., Olley, J., & Grün, R. (2017) At least 17,000 years of coexistence: Modern humans and megafauna at the Willandra Lakes, South-Eastern Australia. *Quaternary Science Reviews*, **157**, 206–211.

Williams, N.J., Harle, K.J., Gale, S.J., & Heijnis, H. (2006) The vegetation history of the last glacial–interglacial cycle in eastern New South Wales, Australia. *Journal of Quaternary Science*, **21**, 735–750.

Wood, S. (2013) Package ' mgcv .' *http://cran.r-project.org/web/packages/mgcv/mgcv.pdf.*, .

Wroe, S. & Field, J. (2006) A review of the evidence for a human role in the extinction of Australian megafauna and an alternative interpretation. *Quaternary Science Reviews*, **25**, 2692–2703.

4 Supplementary Information

Extracted age iterations used in the uncertainty plots from Welsby Lagoon in this chapter largely fall within the uncertainty of the model developed by Lewis et al. (Accepted).

Recalibrated age-depth models were created for each record analysed in this paper using Bacon (Blaauw & Christen, 2011). Updates in calibration curves and Bayesian age-depth modelling since publication by the original authors has resulted in some anomalies from the original models. The recalibrated age-depth models are largely within uncertainty of models published by the original authors, where age-depth models had previously been determined. The presence of dates in many of these records at the limit of radiocarbon dating (at the time of measurement) have additional uncertainty associated with them and can only be considered as minimum ages. This is consistent with the original papers where these radiocarbon ages have been reported as minimum estimates. The method used here take in to account the age uncertainty from the concentration and spread of dates, however cannot capture additional uncertainty associated with the dates themselves.

The uncertainties for each of the records presented are likely an underrepresentation of the true error surrounding the time period between 50 – 35 ka. The Redhead Lagoon age-depth model indicates relatively low levels of uncertainty at ca. 40 ka. The large cluster of radiocarbon dates ca. 40ka make the model appear more certain during this time period, however the sedimentation rates based on this section of the age model are much slower than at any other point in the record. The 'flattening' of the age model through this period is likely driven by the fact that a number of these ages represent minimum ages at the limit of radiocarbon dating. In addition, the large hiatus in the record, beginning at ca. 37 ka adding further unquantified uncertainty into the model at this point.

The Caledonia Fen model is also likely to have substantial unquantified uncertainty within the model. The oldest two radiocarbon dates within this record are again flattening the model and reducing the uncertainty during this period. These two date were considered minimum ages by the original authors and the tight model fit around these dates has led to artificial confidence in the model. The age model for Lynch's Crater has more realistic uncertainty as the radiocarbon dates at the limit of dating have been identified by the model as outliers, therefore they do not result in a more certain model. The age model from MD03-2607 is the most reliable of all the models due to the high density of dates and multiple dating methods used. Perhaps some level of increased uncertainty is introduced as we correlated this model, as the original authors did, to stacked isotope records. Therefore in each of these records we suggest the uncertainty to be considered as minimum uncertainty.

The chronologies from *Dromaius* egg shells used in this paper are those produced by the original authors due to the records being non-traditional sedimentary sequences and

complications in adapting amino acid racemization ratios to absolute ages. The uncertainties of the lower Darling River data presented in this paper use the reported uncertainty of Miller et al. (2016). The *Dromaius* d13C data of Miller does not age uncertainties and therefore no uncertainty is able to be reported in this paper. It is difficult to compare this record accurately to the other records due to this.

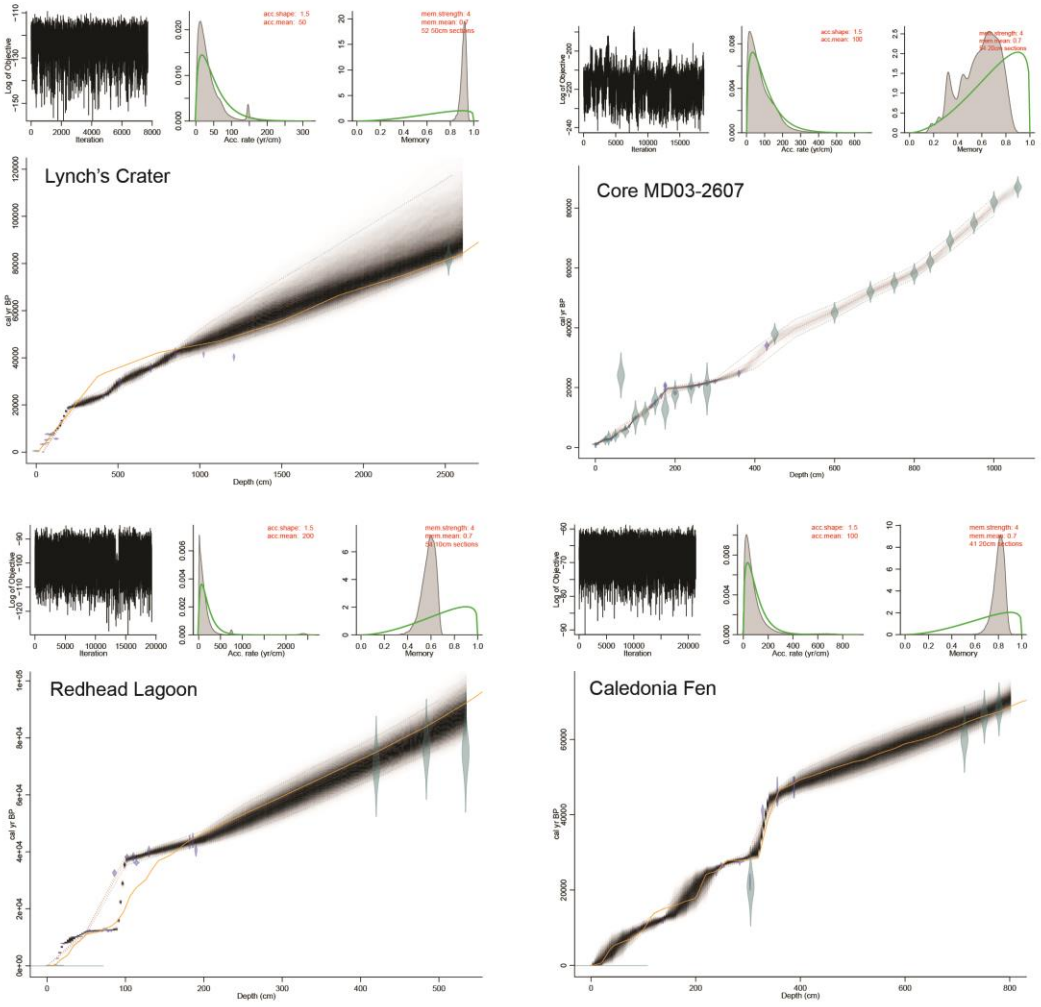

Figure 1. Recalibrated Bacon age-depth models from Lynch's Crater, Redhead Lagoon, Caledonia Fen and MDO3-2607. Origional age-depth models are shown as orange lines.

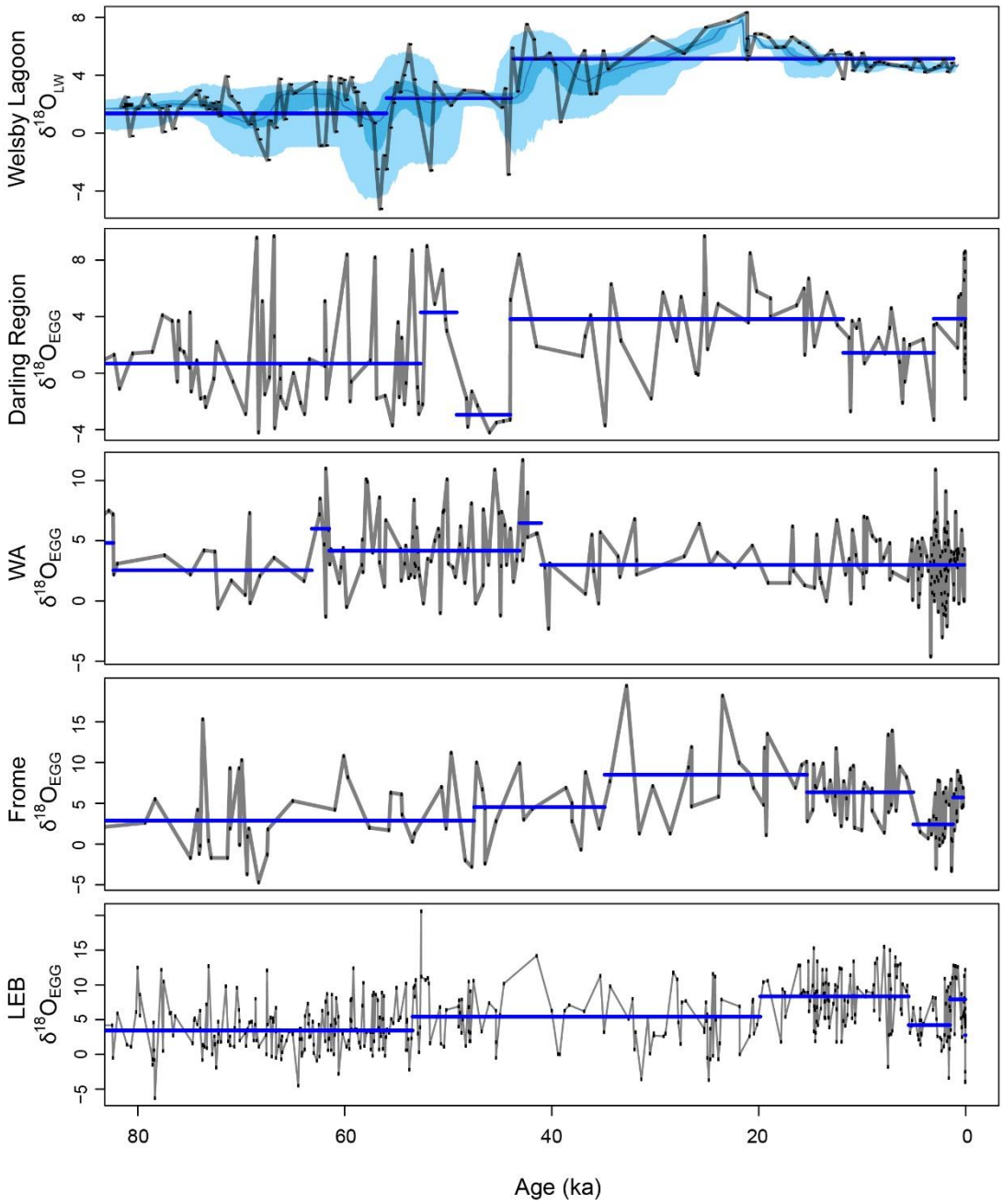

Figure S2. Welsby Lagoon $\delta^{18}O$ lake water and *Dromaius* eggshell $\delta^{18}O$ from the Darling Region, Western Australia, Lake Frome region and Lake Eyre Basin (Miller et al. 2016a). Horizontal blue lines idicate indicate the mean values of each timeseries between change points. Changepoints were identified using the changepoint package in R.

7

Key outcomes and suggestions for future research

Through this high resolution, multi-proxy PhD, valuable progress has been made toward understanding the interaction between climate, fire, megafauna and vegetation through the last glacial cycle in subtropical Australia. This thesis had an overarching goal to examine the impact of megafauna extinction and climate on the fire and vegetation dynamics in a subtropical landscape. Each chapter of this thesis contributes to this goal. The primary aims of this research were:

1. To understand the evolution of the Welsby Lagoon wetland and taphonomic processes.
2. To reconstruct the vegetation and fire history of subtropical eastern Australia.
3. To reconstruct the climate and determine the primary drivers of hydrological variability in subtropical eastern Australia.
4. To examine the role of climate, fire and megafauna in driving vegetation changes and Welsby Lagoon and investigate potential drivers of megafauna extinctions.

1 Key outcomes

The thesis brought together a wide variety of ecological and climate proxies to understand changes in ecosystem function and climate drivers through the last glacial cycle. The second chapter of this thesis documents the development of Welsby Lagoon wetland from its inception ca. 130 ka and provided a robust basis for interpretation of palaeoecological and palaeoclimatological proxies examined in this thesis. Defining the source of sedimentary organic carbon and extreme nutrient limitation from Welsby Lagoon in chapter 2 was key to this outcome. In doing so, it highlighted the unusual organic composition of plants and algae on North Stradbroke Island.

The high resolution $\delta^{13}C$ record permitted the reconstruction of millennial scale climate variations through time. The long-term pattern in Welsby Lagoon $\delta^{13}C$ demonstrates the

orbital controls on long term productivity. Millennial scale variations in productivity are related to changes in hydroclimate an inference supported by the reconstructed $\delta^{18}O$ of lake water. Millennial scale climate variations occur in concert with Antarctic Isotope Maximum (AIM) events. The close association between Welsby Lagoon productivity and Antarctic temperature highlights the substantial influence of the Southern Hemisphere high latitudes on subtropical east Australian climates. The findings of this chapter and Barr et al. (in prep) provide a strong climatological foundation to examine the role of climate in driving vegetation changes at Welsby Lagoon.

The high-resolution vegetation and fire record from Welsby Lagoon demonstrates the complex interplay between climate, fire and succession on the nutrient poor sand dunes of North Stradbroke Island. The inclusion of an independent climate reconstruction indicates that climate is the primary driver of fire occurrence, through its influence on biomass accumulation, and vegetation change through the last glacial cycle. Millennial scale climate variations result in substantial reorganisation of the vegetation system. The interaction between climate, fire and succession are fundamental to the present day vegetation composition of North Stradbroke Island.

The primary influence of climate on the vegetation composition at Welsby Lagoon is evident throughout the entire last glacial cycle and, in particular, the timing of megafauna extinctions through a shift to drier climates. The shift in vegetation composition at Welsby Lagoon, in response to drier climates at 43 ka, as indicated by the $\delta^{13}C$ and $\delta^{18}O_{LW}$, occurred within uncertainty of ecosystem changes recorded at a number of geographically dispersed sites, in conjunction with the extinction of megafauna. The synchronism of this change (within uncertainty) with drying seen in central Australia, suggests a wide-ranging change in climate. A synthesis of the data collected in this thesis and comparison to palaeoclimate and palaeoecological records from across Australia provides evidence for the important role of climate in both driving widespread vegetation changes and megafauna extinctions. We suggest that climate change was an important driver of these widespread vegetation changes and concur with the conclusions of previous studies that propose climatic change may have played a role in the extinction of Australian megafauna.

2 Suggestions for future research

This thesis has provided new data and tools to understand the nature of climate, fire and vegetation variability in Australia over the last glacial cycle. To fully understand the nature of climate in driving ecosystem change requires the development of more high-resolution, multi-proxy reconstructions underpinned by robust chronologies, across a broader range of climatological and ecological regions. Coupling records of fire and vegetation change with independent records of climate can reduce some of the ambiguity in interpreting palynological (and indeed other palaeoecological) records and elucidate key drivers of vegetation change.

Uncertainty surrounding interpretations of sedimentary charcoal deposits continues to restrict the understanding of past variations in fire regimes and anthropogenic burning in Australia. In particular, fundamental studies of charcoal production, transport and preservation from Australia are lacking. As the most fire prone continent on earth, with a long history of human occupation, it is important to understand how variations in charcoal taphonomy, resulting from factors including changing source area, fuel type and fire intensity may be represented in the sedimentary charcoal record. This thesis presented a new method to examine the charcoal content of wetland sediments. Further method development and calibration with modern taphonomic studies would likely resolve some of the uncertainty in interpretations of fire history from sedimentary charcoal.

Determining regional patterns of environmental change is difficult due to taphonomic variations in individual sites and the influences of local scale dynamics. Identifying spatial and temporal variability in palaeoenvironmental records is further challenged due to the inherent time uncertainty of individual records. By comparing changes in palaeoenvironmental records using appropriate measures of change and accounting for inherent time uncertainty, facilitates rigorous examination of regional scale trends from individual palaeoenvironmental reconstructions. Rigorous application of statistical methods and time uncertain techniques is recommended for future studies attempting to infer regional scale trends from palaeoenvironmental reconstructions.

The key drivers of megafauna extinctions in Australia have remained elusive. The limited number of palaeoclimate and palaeoecological records from this time period have made determining causal factors difficult. Models attempting to address this issue have previously incorporated data from distal locations due to the lack of palaeoclimate data from Australia. Incorporation of local palaeoclimate and palaeoenvironmental records, such as those presented in chapter 6 of this thesis, could provide a more nuanced assessment of local patterns in climate and extinction models.